SEPT. – DEC. 1995
Volume I Number III

ISSN 0859 144X

THE ASEAN JOURNAL OF RADIOLOGY

Published by The Radiological Society and
the College of Radiologists of Thailand,
Bangkok, Thailand

Supported through an educational grant from

Have you really considered the importance of open MRI on patient comfort?

- for your patients who will return to you?
- for your technicians, who will improve throughput?
- for your radiologists, who will not have to read patient movement artifacts?
- for your administrator, who will see better return on investment?

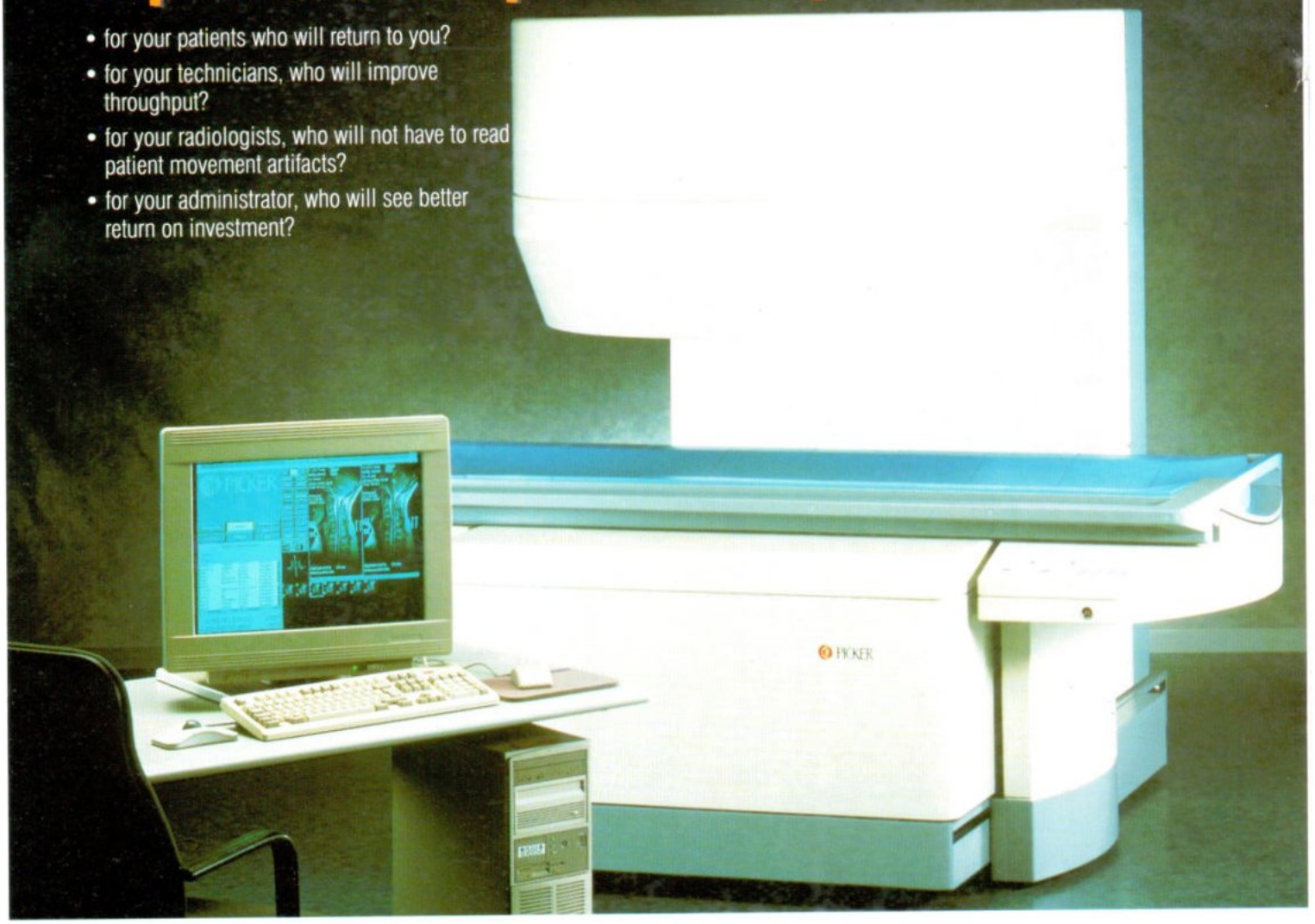

The new OUTLOOK™ in MRI...

Picker's new, really open, state-of-the-art, whole body MRI scanner.

Features include: 46 cm free vertical opening, freedom of patient handling in horizontal plane, easy access to the patient, CP phased array coils, powerful and fast gradients, high quality MR angio with MT, integrated MPR and MIP, and very fast 233 MHz Digital AlphaStation™ 400 console. The most modern open MRI scanner available.

OUTLOOK™ is Picker's newest addition to its impressive line of MRI scanners.
For more information, please contact your nearest Picker representative.

PICKER

Picker International, Inc.
World Headquarters
595 Miner Road
Cleveland, Ohio 44143
U.S.A.
Tel: 1-216-473-3000
Fax: 1-216-473-2413

Picker International, France
GEC S.A.
2, rue Henri Bergson
92600 Asnières
France
Tel: 33-1-46-13-52-54
Fax: 33-1-47-33-11-31

Picker International GmbH
Robert-Bosch-Strasse 11
6238 Hofheim 4 Wallau
Germany
Tel: 49-6122-9140
Fax: 49-6122-8536

Picker International Canada, Inc.
7956 Torbram Road
Brampton, Ontario L6T 5A2
Canada
Tel: 1-960-791-1494
Fax: 1-960-791-7297

Picker International, Inc.
Room 1303
C.C. Wu Building
302-308 Hennessy Road
G.P.O. Box 15
Wanchai, Hong Kong
Tel: 852-892-1238
Fax: 852-838-4302

Picker International Latin America
110 Merrick Way
Suite 3A
Coral Gables, Florida
33134 U.S.A.
Tel: 1-305-444-9993
Fax: 1-305-445-0545

Picker International GmbH
Mosettgasse 1
4th floor, A-1232 Vienna
Austria
Tel: (43) 1-66107
Fax: (43) 1-6610760

Picker International Ltd.
Kemble House
Kemble Street
London, WC2B 4AJ
England
Tel: +44-71-489-4044
Fax: +44-71-489-4043

Picker Singapore
101 Thomson Road,
#10-01 United Square,
Singapore 1130
Tel: (65) 250-9866
Fax: (65) 254-0020

Picker International GmbH
European/Middle East Distribution
Headquarters
Robert-Bosch-Str. 11
65719 Hofheim
Tel: +49-6122-9140
Fax: +49-6122-914-460

Picker Italia SpA
Vicolo Carloni, 4
I-22055 Merate (Lecco)
Tel: (39)39-9900169
Fax: (39)39-9901016

SEPT. – DEC. 1995

Volume I Number III

ISSN 0859 144X

THE ASEAN JOURNAL OF RADIOLOGY

Published by The Radiological Society and the College of Radiologists of Thailand, Bangkok, Thailand

Supported through an educational grant from

BRACCO INTERNATIONAL

1. The AAR Journal of Radiology publishes the papers on Radiological Sciences, such as research work, review articles, case reports, innovations in Medical Sciences related to all branches of Radiology, and letters to the editor. The aforementioned materials can be written in English only.

2. The authors have to submit 2 copies of the manuscript and a diskette: **to Prof. Dr. Kawee Tungsubutra,** 318 Kaweevej Hospital, Tarksin Road, Dhonburi, Bangkok 10600, Thailand.
or to the Associate Editors at the Radiological Society of Malaysia, Indonesia, Phillippine, Singapore and Brunei. The names and addresses of the Associate Editors in each country were published in the front page of this Journal.

3. The original copy to be submitted must be typed in a double space on one side of the page of 8" × 11" paper.

4. The format of the article must include:

   a. Title page and address of the author (s)

   b. Abstract

   c. Introduction (Background)

   d. Material and Method

   e. Results and discussion (Tables and Illustrations)

   f. Acknowledgement (it any)

   g. References (Follow the Vancouver style developed by ICMJE)

5. We will provide 25 copies of reprints for the author (s) who submit (s) and article for publication in the AAR Journal.

6. The illustrations and tables must be clearly prepared with legends in English as they are the art works to be reproduced.

7. The authors are responsible for the contents of the article as to its facts and findings.

8. Ethics.

Paper reporting studies which might be interpreated as human experimentation (e.g. controlled trials) should conform to the standards of the Declaration of Helsinki (see British Medical Journal 1964:2:177) and should indicate that approval that such studies may proceed has been granted by the local or hospital Ethics Committee.

When reporting experiments on animals indicate whether the institution's or the National Research Council's guide for, or any national law on, the care and use of laboratory animals was followed.

Message from Prof. Dr. Kawee Tungsubutra
Editor-in-Chief, The Asean Journal of Radiology

This is the third issue of the Asean Journal of Radiology. (Asean J.R.) In this issue, we have the articles from the President of Nuclear Medicine Society of Thailand, Dr. M. Poshyachinda. So give her the honour of printing her article in the first section of this issue No III. The second section is the articles about CT., Interventional Radiology, Ultrasound, etc. The third section is, of course, Radiation Oncology. Also in this issue, we have an article from the very famous members of Radiological Society of Singapore headed by Dr. Francis Hui of the Tan Tock Seng Hospital. We already have in hand the manuscripts from Singapore, and different University hospitals from Malaysia. We are expecting more articles from Indonesia and Phillippine. The Asean Journal of Radiology Vol II, No I 1996 will be published and ready for distribution as the New Year gift to every member of the AAR countries. So I would like to let you know that the dead-line for the receive of the manuscripts will be the 30th of November 1995. Articles received after November 30, 1995 will be considered to be published in the Vol II, No II 1996. I have changed the names and addresses of the associate editors according to the informations I received from the member countries.

With best wishes

Kawee Tungsubutra

Prof. Dr. Kawee Tungsubutra

19 October 1995

THE ASEAN JOURNAL OF RADIOLOGY

Volume I Number III SEPT.-DEC. 1995

CONTENTS

Volume I Number III SEPT.-DEC. 1995

CONTENTS

DETECTION OF INFLAMMATORY LESIONS WITH ^{99m}Tc HMPAO LABELLED LEUKOCYTES

M. POSHYACHINDA
S. MEKAREEYA

ABSTRACT

This study was undertaken to evaluate the usefulness of ^{99m}Tc HMPAO leukocyte imaging in the detection of inflammatory lesions. A group of 35 patients with suspected infection or inflammatory lesions was studied. Leukocytes from 45 millilitres of blood from each patient were labelled with ^{99m}Tc HMPAO. The mean labelling efficiency was 44%. After dynamic image, the static images were taken at 30-60 minute, 4 and 24 hour after injection of labelled leukocytes. Most of the positive scans were best seen at 4 hour and lasted till 24 hour. The overall sensitivity, specificity and accuracy was 92%, 95% and 94% respectively.

It is concluded that ^{99m}Tc HMPAO leukocyted imaging is a very helpful diagnostic investigation for infection or inflammatory lesions.

Key Words : Leukocytc imaging, Inflammatory lesion, Radionuclide imaging

INTRODUCTION

Gallium-67 (^{67}Ga) citrate has been use routinely in the detection of inflammation (1-4). Since 1976 ^{111}In labelled leukocytes scans have been shown to be useful in the detection of infections and inflammatory lesions (5-10). ^{99m}Tc-hexamethylpropylene-amineoxime (HMPAO) has been reported as an alternative agent to ^{111}In oxime for labelling leukocytes (11). ^{99m}Tc HMPAO labelled leukocytes has many advantages over ^{111}In oxime with respect to radiation dose to the patient, image quality, acquisition time, availability and expense, therefore ^{99m}Tc HMPAO has become the preferred agent for labelling leukocytes for imaging of various inflammatory conditions (12-14).

This work reports our clinical experience with the use of ^{99m}Tc HMPAO to label leukocytes in patients suspected of having various inflammatory conditions.

MATERIALS AND METHODS

Patients

The study included 35 patients, 18 males and 17 females, with an age range from 11 to 77 years (mean age 40.4 yr). Of these, 6 had suspected intraabdominal sepsis, 10 suspected brain abscess, 3 suspected bone infection, 3 suspected polycystic kidneys, 10 had fever of unknown origin and one each had suspected inflammatory bowel disease, splenic abscess and cellulitis of leg. The final diagnosis was confirmed with surgery in 14 patients, histologic and/or microbiologic findings in 12, endoscopy in one and autopsy in one. The diagosis was based on computed tomography and/or ultrasonography and clinical findings in 4 patients. Final diagnosis was not achieved in 3 patients with fever of unknown origin.

Division of Nuclear Medicine, Department of Radiology, Chulalongkorn Hospital, Faculty of Medicine, Chulalongkorn University, Rama IV Road, Bangkok 10330 Thailand.

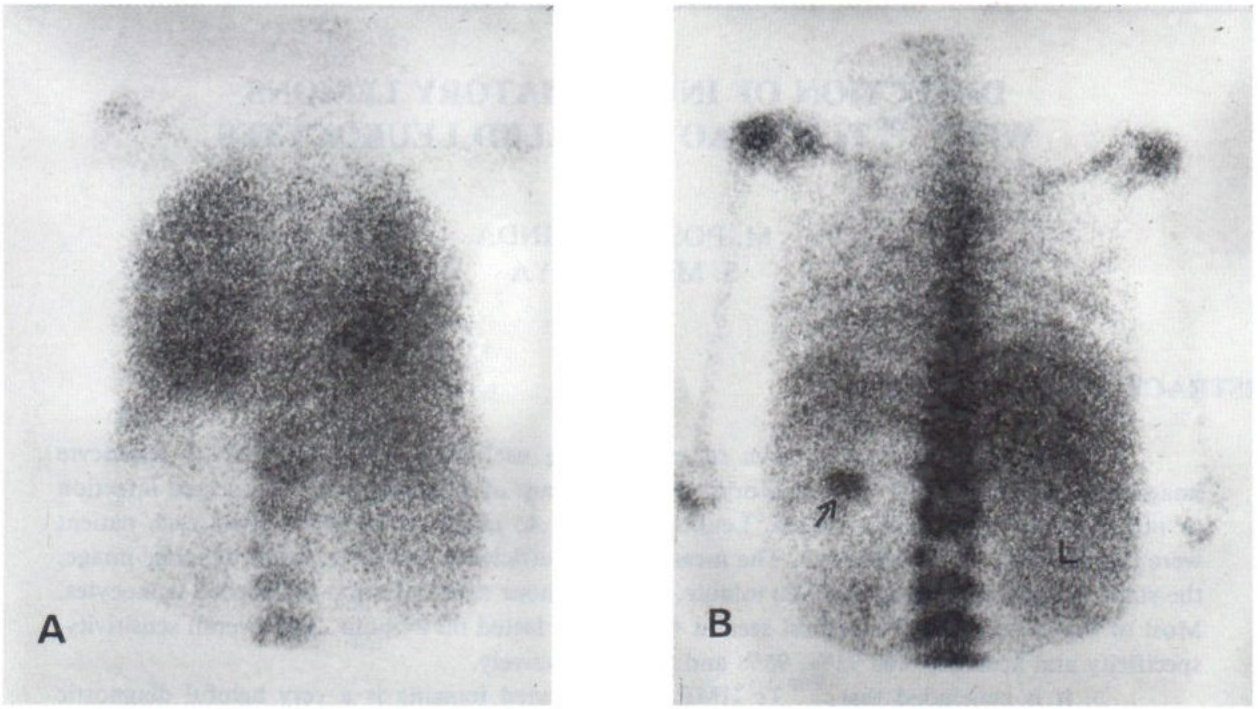

Fig 1 Abnormal uptake of ^{99m}Tc HMPAO labelled leukocytes at splenic bed (arrow) in a patient with abdominal sepsis post splenectomy, (A) 1 hour and (B) 4 hours after injection of labelled leukocytes. Both images are posterior view. L = liver

White blood cell labelling with ^{99m}Tc HMPAO

Fourty five ml of venous blood was collected from patient into 8 ml of acid citrate dextrose (ACD) solution. Mixed leukocytes were separated and labelled with ^{99m}Tc HMPAO according to method described by Costa et al. (13). After reconstitution, ^{99m}Tc HMPAO leukocytes was injected intravenously to the patient with the average activity of 300 MBq (8.1 mCi).

An intravenous blood sample was taken about 45 minutes after injection for the calculation of labelled leukocyte recovery. The cell labelling efficiency was 42.8 ± 15.7% (Mean ± S.D).

Imaging protocol

Patients underwent planar imaging at 30-60 min, 4-6 h and 18-24 h after injection. Initial dynamic acquisition of 20 × 60 seconds frames, 64 × 64 matrix resolution, immediately post injection were carried out whenever appropriated at the suspected site. A Phillip's gamma camera was used in the initial period of study, then the IGE 400 AC/STARCAM system was used instead. A low energy, general purpose collimator was employed and 500 k counts per image were recorded in the ^{99m}Tc energy window (140 KeV with 20% window).

RESULTS

The results of studies are shown in Table 1. All patients with true positive findings in inflammatory or infectious disease showed intense activity in the affected sites at 4 hour or even earlier with further increased or persisted activity at 24 hour image. Three of 6 patients with suspected intra-abdominal abscess were true positive, 2 of these, the diagnosis were confirmed at surgery while the other patient with suspected abdominal sepsis after splenectomy was subsequently improved after antibiotic therapy (Fig. 1). The remaining 3 patients were true negative (one hematoma, one recurrent cancer of distal ureter, one loculated ascites). Two of the 3 patients with suspected infected polycystic kidneys demonstrated multiple hot rim lesions in both kidneys which were better seen at 24 hour images (Fig. 2). The other patient with false negative scan demonstrated only multiple big cold lesions in enlarged liver while ultrasound revealed multiple cysts in the liver and the kidneys. But this patient had received antibiotic treatment one week before ^{99m}Tc HMPAO leukocytes imaging.

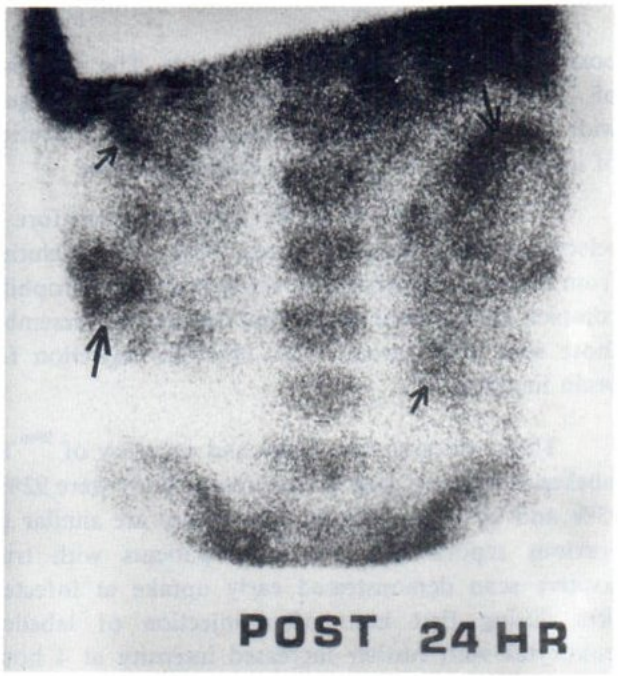

Fig 2 Posterior view of 24 hour image of a patient with polycystic renal disease shows multiple areas of abnormal uptake in both enlarged polycystic kidneys (arrows). Ultrasound and CT scan did not reveal a source of infection.

In the suspected brain abscess group, 2 patients had abnormal uptake at 4 hours and 24 hours images and were proved later to be brain abscesses (Fig. 3). One patient in this group yielded false positive scan, this patient showed a big focal uptake at left thalamus region at 1 hour image but was virtually disappeared at 4 hour and 24 hour images, germinoma of left thalamus was found at surgery (Fig. 4). The remaining 7 patients were subsequently proved to have brain tumours in 6 patients and meningitis in one patient.

In bone infection group, 2 patients with suspected infected hip prostheses had positive images (Fig. 5) and the diagnosis was confirmed at surgery in both patients. The remaining patient with negative scan was finally proved to have no infection of lumbar spine.

Of the 10 patients with fever of unknown origin, 7 patients were true negative with ^{99m}Tc leukocytes scan. Final diagnosis was not achieved in the remaining 3 patients.

One of each patient with ulcerative colitis and splenic abscess was correctly diagnosed with ^{99m}Tc HMPAO leukocytes imaging. The ulcerative colitis was better diagnosed by 4 hour image (Fig. 6) while the splenic abscess was better diagnosed by 4 hour and 24 hour images (Fig. 7). One patient with suspected cellulitis of leg who had negative scan was finally diagnosed to have cardiomyopathy.

The overall sensitivity, specificity and accuracy of labelled leukocyte imaging was 92%, 95% and 94% respectively.

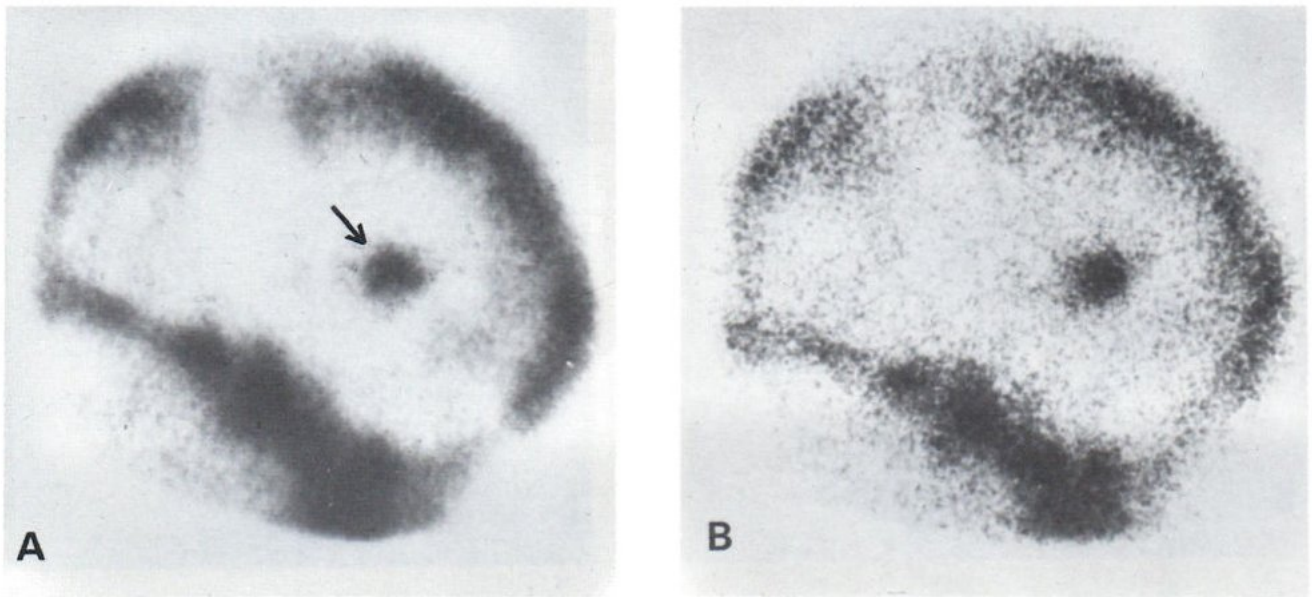

Fig 3 Left lateral view of brain show a focal abnormal activity at temporal lobe region (arrow), (A) 4 hours and (B) 24 hours after injection. Brain abscess was found at surgery in this patient.

DISCUSSION

^{67}Ga citrate has been used in the determination of abscesses but it is difficult to differentiate the uptake of ^{67}Ga in infection from uptake in a tumour, therefore it lacks specificity.[111] In labelling of leukocytes has been proved to be more useful in detection of infection and inflammatory lesions (8-10). Apart from some undesirable properties of ^{111}In, its use is not possible for developing country like us. The invention of ^{99m}Tc HMPAO in labelling leukocytes has gain wide interests in study of its reliability in the detection of inflammatory or infectious diseases (11-14).

^{99m}Tc HMPAO is highly lipophilic therefore it selectively labels the leukocytes. Free activity eluting from the cells is probably in the form of a hydrophilic complex, thus there is no cerebral radioactivity resemble those seen after direct ^{99m}Tc HMPAO injection for brain imaging (12).

The sensitivity, specificity and accuracy of ^{99m}Tc labelled leukocytes scan in the present study were 92%, 95% and 94% respectively. The values are similar to previous reports (12, 14). Most patients with true positive scan demonstrated early uptake at infected sites during first hour after injection of labelled leukocytes with further increased intensity at 4 hour image and persisted or even further increased intensity at 24 hour image. One patient with infected polycystic kidney had negative scan at 1 hour image but was positive at 4 hour and 24 hour. The patient with splenic abscess demonstrated a big cold lesion in early image with decreased in size of the lesion in the late images which indicated increase accumulation of labelled leukocytes with time around the lesion. Hence three phase scan provided better diagnostic validity as shown in this and other studies (10).

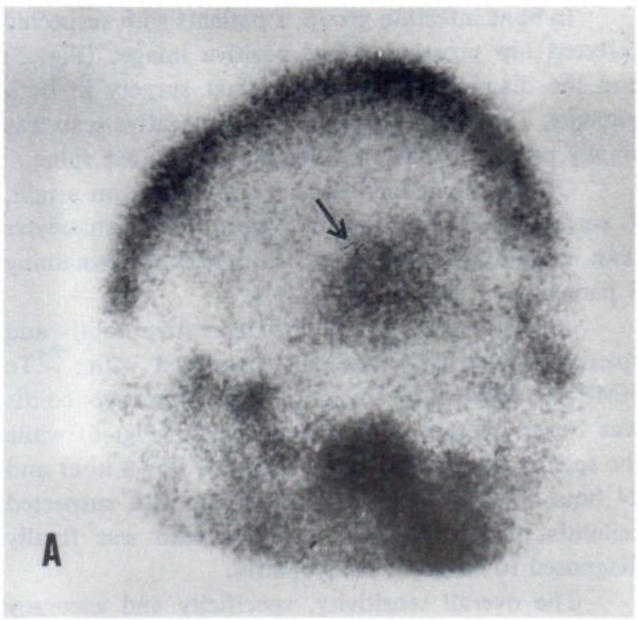

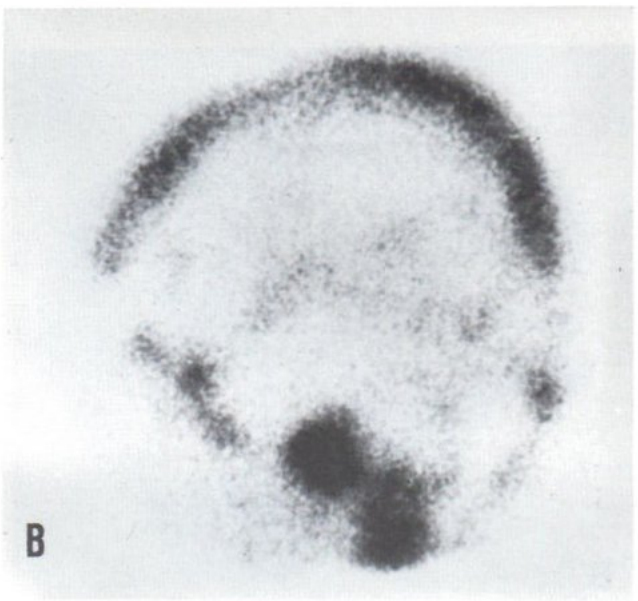

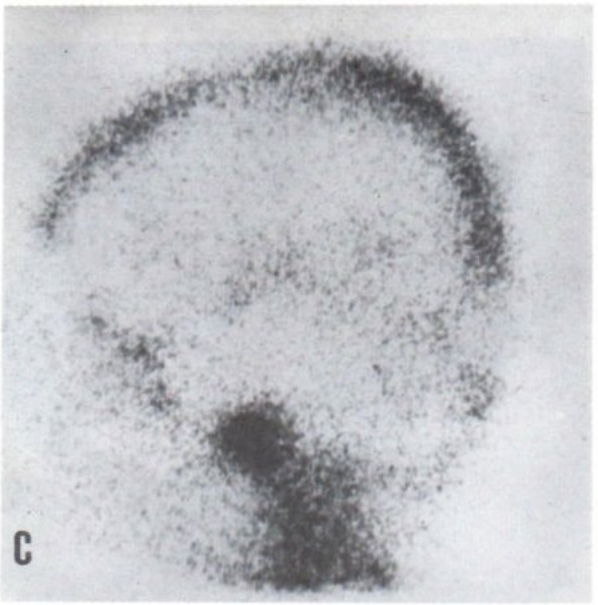

Fig 4 Left lateral view of brain in a patient shows a big abnormal uptake at temporal region (arrow) at 1 hour after injection (A), the activity was virtually faded away at 4 hour (B) and 24 hours (C). Germinoma of left thalamus was found at surgery.

Our findings agree with other reports that patients with suspected inflammation in the abdominal region should be imaged during the first 4 hour after administration of ^{99m}Tc leukocytes to avoid false positive findings resulted from nonspecific bowel activity which was always at least weakly visualized at 18-24 hour and in some patients in the 6 hour image (10, 12, 14).

The only one false positive finding found in this study was in a patient with brain tumour. However the intense activity at the lesion was seen only at 1 hour image which may represent high vascularity at the lesion. Thus the late image at 4 hour and 24 hour are more specific to diagnose brain abscess. However positive findings of ^{111}In-leukocytes scan in some malignancies have been reported (15, 16).

The only one false negative finding in this study was found in a patient with suspected polycystic kidney, but this patient had on antibiotic therapy one week prior to the study. It is possible that the infective process had already subsided. CT and Ultrasonography, although highly sensitive in diagnosis of polycystic renal disease, are not able to specifically indicate the presence of infection while labelled leukocyte imaging are highly sensitive and specific for the detection of infection as demonstrated in this study and other studies (17, 18).

It has been reported that labelled leukocyte imaging as well as immunoscintigraphy (IS) using antigranulocyte monoclonal antibodies are sensitive and accurate imaging modality for detection of infected joint protheses (14, 19, 20). Our results were also good in patients with infected prosthetic hip. However it is necessary to correlate the finding of labelled leukocyte imaging or IS with ^{99m}Tc MDP bone imaging in the detection of periprosthetic infection (19, 20).

All 7 patients with fever of unknown origin were true negative with ^{99m}Tc leukocytes. It has been shown previously that there is very low frequency of detectable infection in these patients (21).

In conclusion, our results with ^{99m}Tc HMPAO labelled leukocytes imaging exhibit the usefulness of this technique in the diagnosis or exclusion of various infectious and inflammatory processes. Although most of the lesions were better demonstrated at 4 hour after injection of labelled leukocytes, 1 hour and 24 hour images are also recommended for better sensitivity and specificity in the diagnosis. The readily available ^{99m}Tc and HMPAO kits are more suitable in developing countries than ^{111}In for labelling leukocytes.

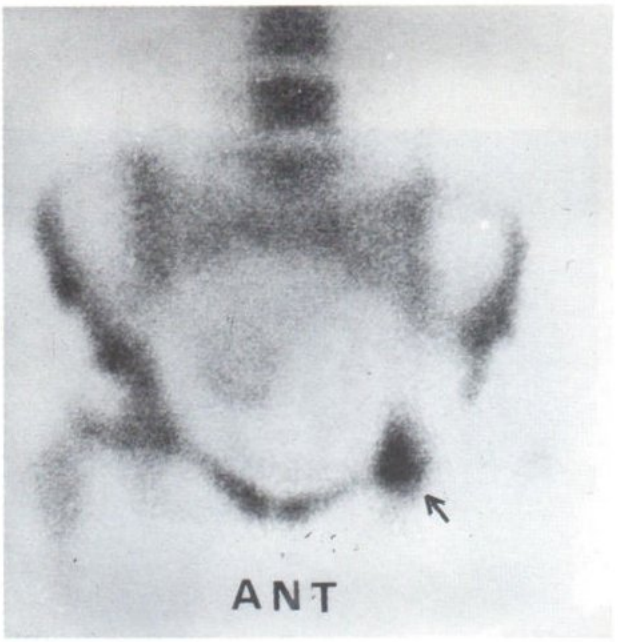

Fig 5 Anterior pelvis of a patient with infected prosthetic hip joint shows marked abnormal uptake (arrow) at 4 hour image.

Fig 6 Anterior abdomen of a patient with ulcerative colitis at 4 hours after injection shows abnormal accumulation of ^{99m}Tc HMPAO labelled leukocytes in the entire colon.

Table 1 RESULTS OF STUDIES WITH Tc-99m LABELLED LEUKOCYTES

INITIAL DIAGNOSIS	TP	FP	TN	FN	NO DIAGNOSIS
INTRA-ABDOMINAL ABSCESS (n = 6)	3	—	3	—	
INFECTED POLYCYSTIC KIDNEYS (n = 3)	2	—	—	1	
BRAIN ABSCESS (n = 10)	2	1	7	—	
BONE INFECTION (n = 3)	2	—	1	—	
ULCERATIVE COLITIS (n = 1)	1	—	—	—	
SPLENIC ABSCESS (n = 1)	1	—	—	—	
CELLULITIS (n = 1)	—	—	1	—	
FEVER OF UNKNOWN ORIGIN (n = 10)	—	—	7	—	3
TOTAL (n = 35)	11	1	19	1	3

TP = True positive FP = False positive
TN = True negative FN = False negative

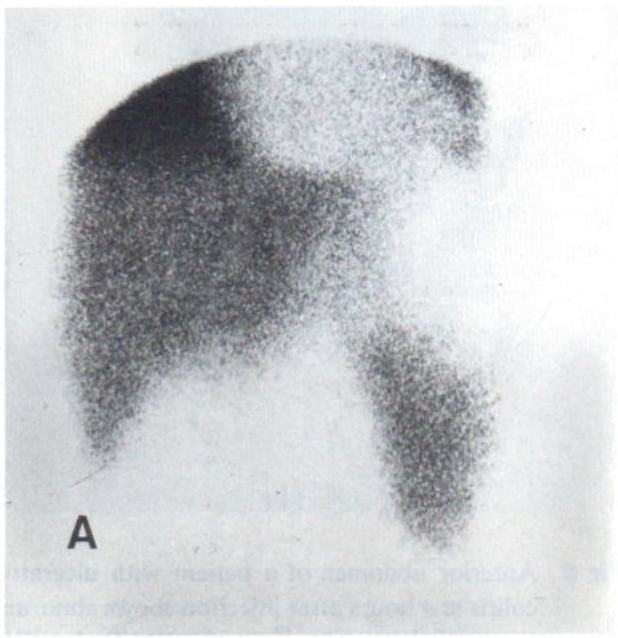

Fig 7 A

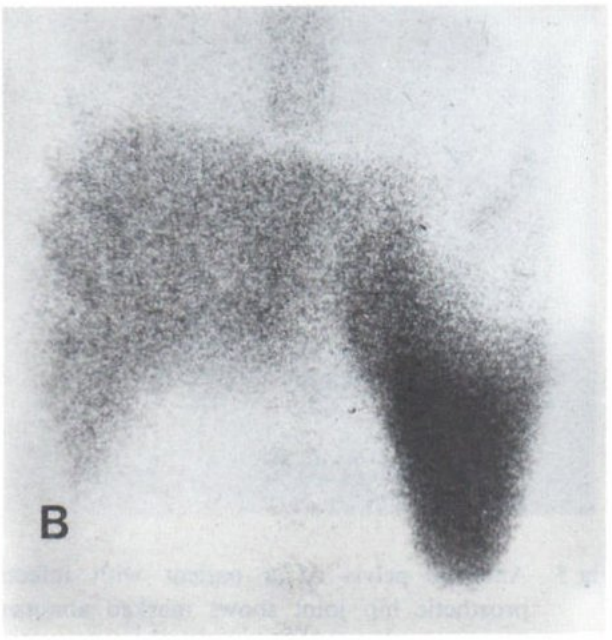

Fig 7 B

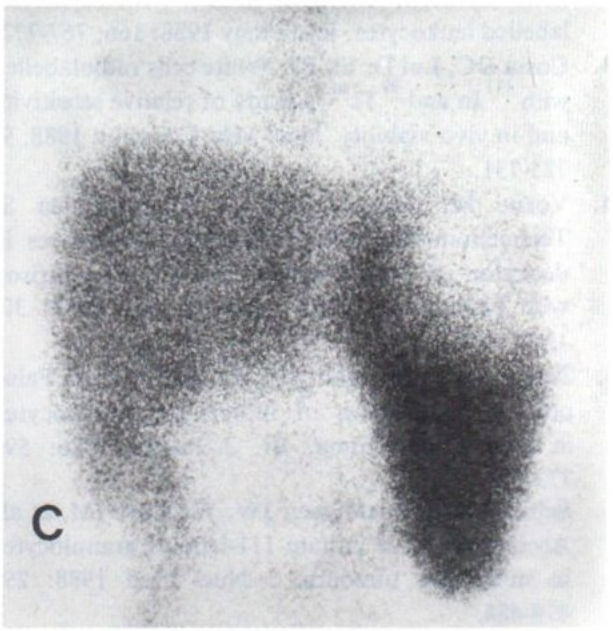

Fig 7 C

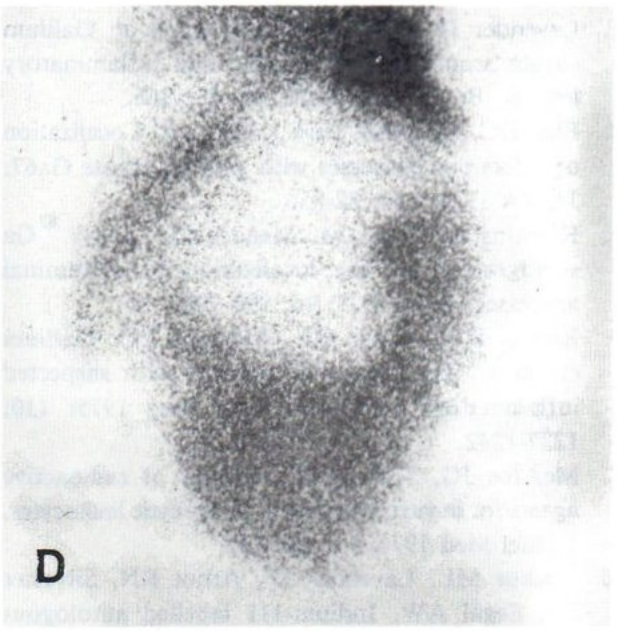

Fig 7 D

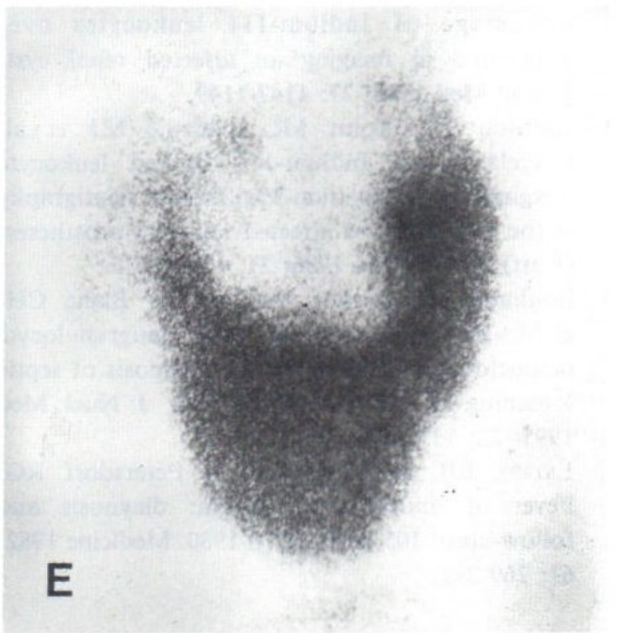

Fig 7 E

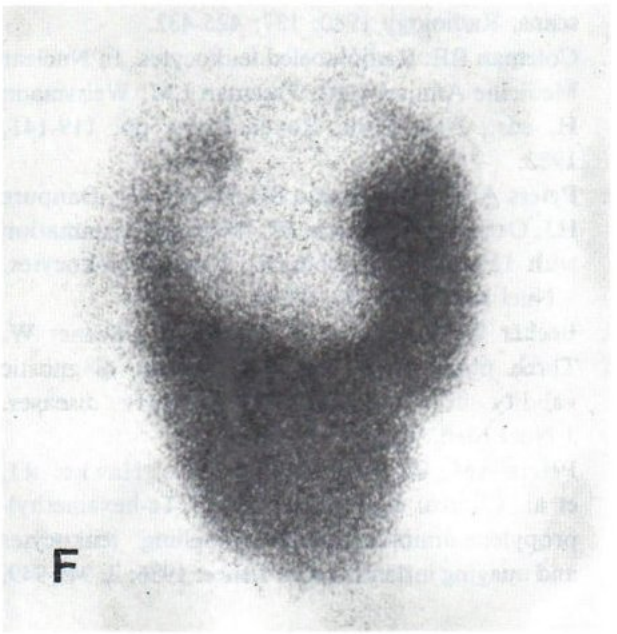

Fig 7 F

Fig 7 Anterior (upper row) and left lateral (lower row) views of abdomen in a patient with splenic abscess show a big cold lesion in enlarged spleen at 1 hour image (A and D), the focal defect is decreased in size with time according to increased accumulation of labelled leukocytes around the lesion as shown in 4 hour images (B and E) and 24 hour images (C and F).

REFERENCES

1. Lavender JP, Lowe J, Bakere Jr, et al. Gallium citrate scanning in neoplastic and inflammatory lesions. Br J Radiol 1971: 44: 361-366.
2. Blair DC, Carrol M, Silva J, Fekety R. Localization of infectious processes with gallium citrate Ga67. JAMA 1974: 230; 82-85.
3. Hopkins GA, Kan M, Mendez CQ. Early ^{67}Ga scintigraphy for the localization of abdominal abscesses. JNM 1975: 16; 990-992.
4. Kumar B, Coleman RE, Alderson PO. Gallium citrate (^{67}Ga) imaging in patients with suspected inflammatory processes. Arch Surg 1975: 110; 1237-1242.
5. McAfee JG, Thakur ML. Survey of radioactive agents for in vitro labelling of phagocytic leukocytes. J Nucl Med 1976: 17; 480-487.
6. Thakur ML, Lavender JP, Arnot RN, Silvester DJ, Segal AW. Indium-111 labelled autologous leukocytes in man. J Nucl Med 1977: 18; 1014-1021.
7. Knochel JQ, Koehler PR, Lee TG, Welch DM. Diagnosis of abdominal abscesses with computed tomography, ultrasound and In-111 leukocyte scans. Radiology 1980: 137; 425-432.
8. Coleman RE: Radiolabeled leukocytes. In Nuclear Medicine Annual 1982, Freeman LM, Weissmann H, eds., New York, Roven Press, pp. 119-141, 1982.
9. Peters AM, Saverymuttu SH, Reavy HJ, Danpure HJ, Osman S, Lavender JP. Imaging inflammation with 111-indium-tropolonate labelled leukocytes. J Nucl Med 1983: 24; 39-44.
10. Becker W, Fischbach W, Reiners C, Borner W. Three phase white blood cell scan: diagnostic validity in abdominal inflammatory diseases. J Nucl Med 1986: 27; 1109-1115.
11. Peters AM, Danpure HJ. Osman s, Hawker RJ, et al. Clinical experience with ^{99m}Tc-hexamethyl-propylene-amineoxime for labelling leukocytes and imaging inflammation. Lancet 1986: ii; 946-949.
12. Roddie ML, Peters AM, Danpure HJ, et al. Inflammation: Imaging with ^{99m}Tc-HMPAO-labelled leukocytes. Radiology 1988: 166; 767-772.
13. Costa DC, Lui D, Ell PJ. White cells radiolabelled with ^{111}In and ^{99}Tc^{m}- a study of relative sensitivity and in vivo viability. Nucl Med Commun 1988: 9; 725-731.
14. Vorne M, Soini I, Lantto T, Paakinen S. Technetium-99m HM-PAO-labeled leukocytes in detection of inflammatary lesions: Comparison with Gallium-67 citrate. J Nucl Med 1989: 30; 1332-1336.
15. Saverymuttu SH, Maltby P, Batman P, et al. False positive localization of indium-III granulocytes in colonic carcinoma. Br. J Radiol 1986: 59; 773-777.
16. Schmidt KG, Rosmussen JW, Wedebye IM, et al. Accumulation of indium-111-labeled granulocytes in malignant tumours. J Nucl Med 1988: 29; 479-484.
17. Gilbert BR, Gerqueira MD, Eary JF, et al. Indium-111 white blood cell scan for infectious complications of polycystic renal disease. J Nucl Med 1985: 26; 1283-1286.
18. Fortner A, Taylor A. Jr, Alazraki N, Datz FL. Advantage of Indium-111 leukocytes over ultrasound in imaging an infected renal cyst. J Nucl Med 1986: 27; 1147-1149.
19. Johnson JA, Routt ML, Christie MJ et al. Correlation of Indium-111 labeled leukocyte imaging and Technetium-99m skeletal scintigraphy in the evaluation of infected total hip prostheses. (Abst) J Nucl Med 1986: 27; 1800-1801.
20. Boubaker A, Bischof Delaloye A, Blanc CH, et al. Immunoscintigraphy with antigranulocyte monoclonal antibodies for the diagnosis of septic loosening of hip prostheses. Eur J Nucl Med 1995: 22; 139-147.
21. Larson EB, Featherstone HJ, Petersdorf RG. Fever of undetermined origin: diagnosis and follow-up of 105 cases; 1970-1980. Medicine 1982: 61; 269-292.

DIAGNOSIS OF PARATHYROID ADENOMA USING TECHNETIUM-99m-SESTAMIBI IMAGING

Molrudee EKMAHACHAI, M.D.*
Wannee OJARUSPORN, M.D.*
Sombut BOONYAPRAPA, M.D.*
Kamthorn THAMPRASERT, M.D.**

ABSTRACT

A 24-year-old female was referred for Technetium-99m-Sestamibi (^{99m}Tc-MIBI) parathyroid imaging, due to highly suspected of primary hyperparathyroidism from the clinical and biochemical findings. The early ^{99m}Tc-MIBI parathyroid imaging clearly demonstrated a focal increased uptake located just inferior to the left lobe of thyroid gland and the lesion showed significantly increased uptake on late imaging at 2 hours after ^{99m}Tc-MIBI injection, in contrast to the gradually decreased uptake of the normal thyroid tissue. The scintigraphic findings were typical for left parathyroid adenoma. Surgical finding and histopathologic examination also confirmed the diagnosis of the left parathyroid adenoma.

INTRODUCTION

Hyperparathyroidism is a disease characterized by an excess secretion of parathyroid hormone by adenomatous or hyperplastic glands. The incidence of primary hyperparathyroidism in females and males is about two to one and the disease is most prevalent in the third to fifth decades of life.[1]

The most common cause of primary hyperparathyroidism is due to a single parathyroid adenoma, which is found approximately 80-95%. The remainders are due to parathyroid hyperplasia, multiple parathyroid adenomas and rarely parathyroid carcinoma.[1,2] Adenomas are most often located in the inferior parathyroid gland, but may be found in ectopic locations in about 6-10% of patients.[1]

Different imaging techniques have been used for diagnosis and detection of abnormal parathyroid glands such as radionuclide parathyroid imaging, high resolution ultrasonography, high resolution computed tomography, selective arteriography and magnetic resonance imaging.[2-6] Among These techniques, dual radionuclide parathyroid imaging using Thallium-201 (^{201}Tl)/Technetium-99m-pertechnetate or ^{201}Tl/Iodine-123 (^{123}I) parathyroid subtraction imagings are well recognized as a useful procedure in the preoperative localization of parathyroid adenoma and hyperplasia.[2,3,7-10]

Recently, the use of Technetium-99m-Sestamibi (^{99m}Tc-MIBI) as a new agent for parathyroid imaging was initially reported by Coakley et al in 1989.[11] ^{99m}Tc-MIBI is a cationic isonitrile analog that has been introduced for myocardial perfusion imaging as an alternative to ^{201}Tl[12] and later it was applied to parathyroid imaging.[11] Subsequently, the usefulness and effectiveness of ^{99m}Tc-MIBI in parathyroid imagings have been reported in many series.[13-18]

Parathyroid imagings either with single radionuclide using ^{99m}Tc-MIBI or dual radionuclide using ^{99m}Tc-MIBI/^{123}I subtraction imaging is a promising procedure in the preoperative detection and localization of parathyroid adenoma(s) in patients with suspected of primary hyperparathyroidism.[11,13-16] Because they can

* Department of Radiology,
** Department of Pathology, Faculty of Medicine, Chiang Mai University, Chiang Mai 50200, THAILAND.

locate the lesion in both normal anatomic and ectopic locations. In addition, they are also useful for postoperative detection and localization of abnormal parathyroid glands as well, especially in patients with persistent or recurrent hyperparathyroidism.[15,17,18]

We present a case of primary hyperparathyroidism from left parathyroid adenoma, which produced the typical scintigraphic patterns from the ^{99m}Tc-MIBI parathyroid imaging.

CASE REPORT

A 24-year-old female presented with a history of back pain with kyphosis for 5 months prior to admission. Upon physical examination, no neck mass was found and thyroid gland was also normal on palpation. Complete blood count was normal. Serum creatinine and BUN were 1.5 mg% (normal 0.6-1.7) and 20 mg% (normal 7-27) respectively. Serum calcium was 9.3 mg% (normal 9-11) and parathyroid hormone level was 316 pg/ml (normal 10-65). Serum alkaline phosphatase was 289 IU/L (normal 9-35). Bone survey demonstrated collapse of the T12-L3 spines, which caused back pain and kyphosis in this patient, with generalized extensive bone change characteristic of hyperparathyroidism. First ultrasonography of the neck revealed no definite neck mass seen. She was then referred for ^{99m}Tc-MIBI parathyroid imaging, due to highly suspected of primary hyperparathyroidism. The ^{99m}Tc-MIBI parathyroid imaging was performed with intravenous injection of 15 mCi of ^{99m}Tc-MIBI and anterior cervicothoracic planar imagings were done at 10 minutes and at 2 hours after injection with the patient supine and the head and neck extended and immobilized, using the Apex-SP4 Elscint gamma camera. The parathyroid imagings were acquired with a preset-time mode of 5 minutes for each image and with the zoom factor of 1.5 in 256×256 matrix, using a large-field-of-view, low energy, general purpose parallel hole collimator. Early image at 10 minutes clearly demonstrated a focal area of increased ^{99m}Tc-MIBI uptake caudal to the left lobe of thyroid gland extending inferiorly (Fig.1). Delayed images at 2 hours revealed more intense of the tracer accumulation in the lesion (Fig.2), which was compatible with a left parathyroid adenoma. Thyroid scan of the patient was also performed in the following day with 5 mCi of ^{99m}Tc-pertechnetate, in order to outline the thyroid parenchyma and it showed no definite radiopertechnetate uptake seen in the region inferior to the lower pole of the left thyroid lobe (Fig.3). Therefore, repeated ultrasonography of the thyroid

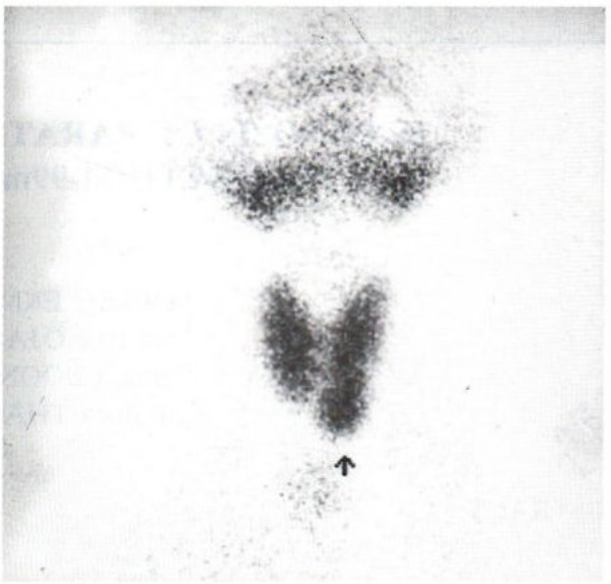

Fig.1: Parathyroid imaging with ^{99m}Tc-MIBI at 10 min reveals a focal increased uptake located adjacent to the lower pole of the left thyroid lobe extending inferiorly (arrow).

gland was performed and revealed a 2 cm hypoechoic lesion located posterior and inferior to the lower pole of left thyroid lobe, corresponding with the scintigraphic finding from ^{99m}Tc-MIBI imaging (Fig.4). The ultrasonographic lesion was located rather behind the left sternoclavicular joint. That is why it was missed from the first ultrasonography of the neck. Surgery was performed and a $2.5 \times 2 \times 1.5$ cm parathyroid adenoma located inferoposterior to the lower pole of the left thyroid lobe removed. The histopathologic findings revealed a well encapsulated mass composing of uniformed parathyroid chief cells with a delicated capillary networks seen arround the nests of the tumor cells, which was compatible with the diagnosis of left parathyroid adenoma. After surgical treatment, her serum parathyroid hormone level returned to normal value.

DISCUSSION

Hypercalcemia is the most common manifestation in primary hyperparathyroidism, either sustained or intermittent hypercalcemia. However, some cases of normocalcemic hyperparathyroidism may present and this condition may cause by coexistent vitamin D deficiency, hypoalbuminemia, severe malabsorption or acidosis.[1,19] Like this patient, her serum calcium was in normal range, but other findings included significant elevated serum parathyroid hormone level were highly suggestive of primary hyperparathyroidism.

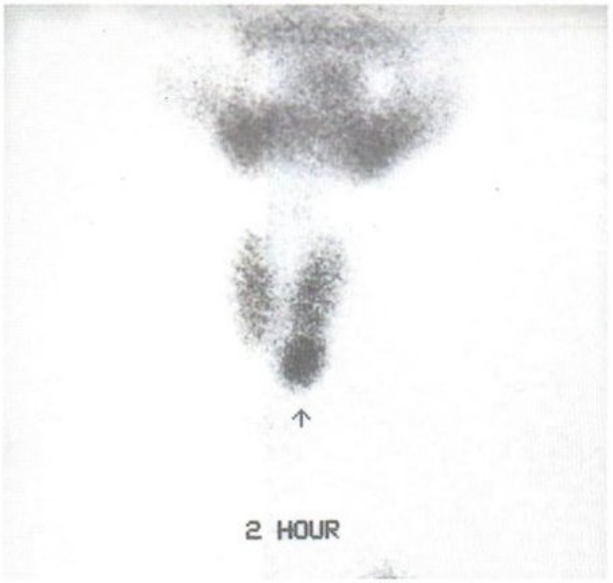

Fig.2: Delayed ^{99m}Tc-MIBI parathyroid imaging at 2 hours shows significantly increased uptake at the lesion (arrow), in contrast to the gradually decreased uptake of the normal thyroid tissue.

Fig.3: Thyroid scan with ^{99m}Tc-pertechnetate reveals no definite activity seen in the region inferior to the lower pole of the left thyroid lobe (arrow), whereas the ^{99m}Tc-MIBI imaging shows a definite focal increased uptake in that region.

It is said that surgery of primary hyperparathyroidism is successful in approximately 90-95% of patients by experienced surgeons.[1,2,15-17] However, 5-10% of cases are failed from the first operation, which may be due to ectopic locations or supernumerary glands not identified at operation.[15-18] Therefore, localization of abnormal parathyroid glands preoperatively has become a more widely used procedure in the past several years.

Preoperative localization of abnormal parathyroid glands may produce many advantages such as increase surgical successful rate, limit neck surgery with smaller incision, decrease operative and anesthesia time and also decrease the risk of surgical complications by guiding the surgeon to the site of abnormality directly.[15-17]

Parathyroid imaging using single radionuclide with ^{99m}Tc-MIBI is a promising procedure in the preoperative detection and localization of parathyroid adenomas in patients with primary hyperparathyroidism.[11,13,14] The early image at 10 minutes after injection is used as the thyroid phase of the study, because the radiotracer is rapidly concentrated in the thyroid parenchyma. The delayed image at 2-3 hours is represent the parathyroid phase, since the radioactivity will be progressively washout from the normal thyroid tissue in contrast to uptake in the parathyroid lesion, which will show progressively increased ^{99m}Tc-MIBI uptake over time.[13] The double phase ^{99m}Tc-MIBI parathyroid imaging is more simple and convenient as compared with the subtraction method using either ^{201}Tl/^{99m}Tc-pertechnetate, ^{201}Tl/^{123}I or ^{99m}Tc-MIBI/^{123}I. It is reported to have a diagnostic accuracy of more than 90% for diagnosis of parathyroid adenoma.[13,14] In addition, the superiority of this technique is using only single radiotracer, less radiation exposure, cheaper and it does not require the immobilization of the patient.[13]

Presumably, the initial ^{99m}Tc-MIBI uptake in parathyroid adenoma relates to increase perfusion or cellularity in the tumor. Furthermore, it may associate with the size of the adenoma or hyperplastic gland. The prolonged retention of ^{99m}Tc-MIBI in the parathyroid gland is hypothesized to be related to the presence and number of mitochondria-rich oxyphil cells, which is usually found in abnormal parathyroid glands.[14,20]

The typical ^{99m}Tc-MIBI parathyroid imaging for parathyroid adenoma is defined as an area of focal increased uptake which persists or reveals relatively increased uptake on delayed imaging, in contrast to the uptake in the normal thyroid tissue which progressively decreases over time.[13,14] Like this case, the scintigraphic finding was typical for left parathyroid adenoma, which was confirmed later from the surgery and histopathologic examination.

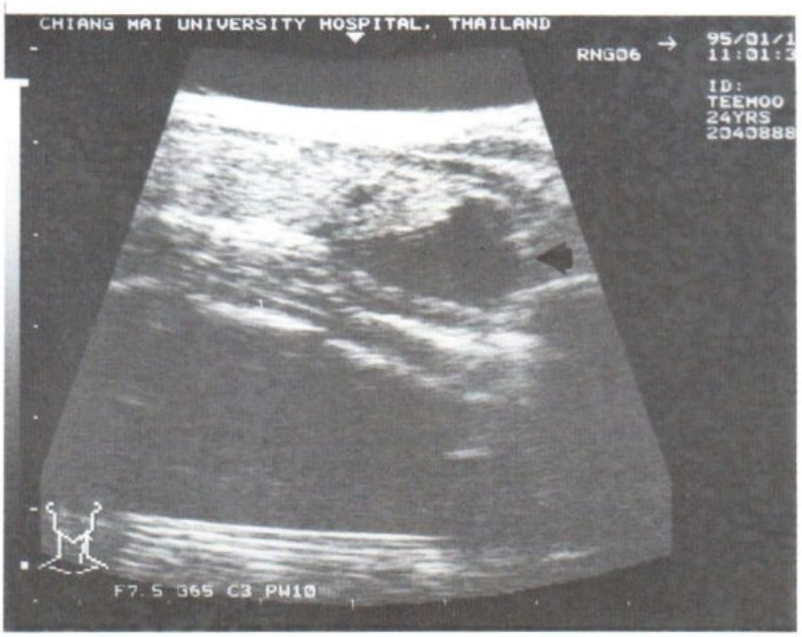

Fig.4: Longitudinal sonographic scan of the left lobe of thyroid gland demonstrates a triangular shaped hypoechoic mass (arrow) with echogenic line separating it from the inferoposterior aspect of the lower pole of thyroid gland, corresponding with the focal increased uptake from the ^{99m}Tc-MIBI imaging.

In conclusion, the double phase ^{99m}Tc-MIBI parathyroid imaging is highly recommended for both preoperative and postoperative localization of abnormal parathyroid glands in patients with suspected of primary hyperparathyroidism and in patients with persistent or recurrent hyperparathyroidism as well.

ACKNOWLEDGEMENT

The authors would like to thank Professor Dr. Sanan Simarak for his valuable suggestions and reviewing of this manuscript.

REFERENCES

1. Potts JT Jr. Diseases of the parathyroid gland and other hyper- and hypocalcemic disorders. In: Wilson JD, eds. Harrison's principles of internal medicine. 12th ed. McGraw-Hill, 1991: 1902-6.
2. Fine EJ. Parathyroid imaging: Its current status and future role. Semin Nucl Med 1987;17:350-9.
3. Gooding GAW, Oker lund MD, Stark DD. Parathyroid imaging: comparison of double-tracer (Tl-201, Tc-99m) scintigraphy and high-resolution US. Radiology 1986;161:57-64.
4. Stark DD, Gooding GAW, Moss AA, et al. Parathyroid imaging: comparison of high-resolution CT and high-resolution sonography. AJR 1983; 141:633-8.
5. Spritzer CE, Gefter WB, Hamilton R, et al. Abnormal parathyroid glands: high-resolution MR imaging. Radiology 1987;162:487-91.
6. Eisenberg H, Pallotta J, Sherwood LM. Selective arteriography, venography and venous hormone assay in diagnosis and localization of parathyroid lesions. Am J Med 1974;56:810-20.
7. Picard D, D'Amour P, Carrier L, et al. Localization of abnormal parathyroid gland(s) using thallium-201/iodine-123 subtraction scintigraphy in patients with primary hyperparathyroidism. Clin Nucl Med 1987;12:60-4.
8. Ferlin G, Borsato N, Camerani M, et al. New perspectives in localizing enlarged parathyroids by technetium-thallium subtraction scan. J Nucl Med 1983;24:438-41.
9. Young AE, Gaunt JI, Croft DN, et al. Location of parathyroid adenomas by thallium-201 and technetium-99m subtraction scanning. Br Med J 1983;286:1384-6.
10. Percival RC, Blake GH, Urwin GH, et al. Assessment of thallium pertechnetate subtraction scintigraphy in hyperparathyroidism. Br J Radiol 1985;58:131-5.

11. Coakley AJ, Kettle AG, Wells CP, et al. Technetium-99m-sestamibi-a new agent for parathyroid imaging. Nucl Med Commun 1989; 10:791-4.
12. Wackers FJ, Berman DJ, Maddahi J, et al. Technetium-99m-hexakis-2-methoxyisobutyl isonitrile: human biodistribution, dosimetry, safety and preliminary comparison to thallium-201 for myocardial perfusion imaging. J Nucl Med 1989; 30:301-11.
13. Taillefer R, Boucher Y, Potvin C, et al. Detection and localization of parathyroid adenomas in patients with hyperparathyroidism using a single radionuclide imaging procedure with Technetium-99m-Sestamibi (double-phase study). J Nucl Med 1992;33:1801-7.
14. O'Doherty MJ, Kettle AG, Wells CP, et al. Parathyroid imaging with technetium-99m-sestamibi: preoperative localization and tissue uptake studies. J nucl Med 1992;33:313-8.
15. Wei JP, Burke GJ, Mansberger AR Jr. Prospective evaluation of the efficacy of technetium-99m sestamibi and iodine-123 radionuclide imaging of abnormal parathyroid glands. Surg 1992;112:1111-7.
16. Casas AT, Burke GJ, Sathyanarayana, et al. Prospective comparison of Technetium-99m-Sestamibi/Iodine-123 radionuclide scan versus high-resolution ultrasonography for the preoperative localization of abnormal glands in patients with previously unoperated primary hyperparathyroidism. Am J Surg 1993;166:369-73.
17. Weber CJ. Vansant J, Alazraki N, et al. Value of technetium-99m sestamibi iodine-123 imaging in preoperative parathyroid surgery. Surg 1993; 114:1011-8.
18. Neumann DR, Esselstyn CB, Eastwood J, et al. Localization of mediastinal parathyroid adenoma in recurrent postoperative hyperparathyroidism with Tc-99m Sestamibi SPECT. Clin Nucl Med 1995;20:175.
19. Aurbach GD, Marx SJ, Spiegel AM. Parathyroid hormone, calcitonin and the calciferols. In: Wilson JD, Foster DW, eds. Textbook of endocrinology. 7th ed. W.B.Saunders company, 1985:1170-6.
20. Benard F, Lefebvre B, Beuvon F, et al. Rapid washout of Technetium-99m-MIBI from a large parathyroid adenoma. J Nucl Med 1995;36:241-3.

INTRAORBITAL DERMOID: CT IMAGING

Patchrin PEKANAN, Suphaneewan JAOVISIDA, Rasri VEJARAK

ABSTRACT

A case of intraorbital dermoid was reported with the findings on the CT imaging Revision of the articles on intraorbital dermoid was done

CASE REPORT

A 43-year-old female patient had the problem of left exopthalmos. CT scan of the orbits was performed with contrast enhancement. It showed a mass at the upper outer quadrant of left orbital cavity. The size of the mass was 1.5 × 1.5 × 5 cm. The mass has well defined rim without calcification. There were two densities in the mass, i.e. soft tissue density component, 41.1. H.U., as a majority and smaller area of fat component at the superior part of the mass, −143.7 H.U. The medial margin was attached to the outer margin of the eyeball and the lateral margin to the lateral rectus muscle. The globe was displaced anteriorly and medially. There was no bone changes. The degree of enhancement could not be determined due to lack of noncontrast study. The lacrimal gland was shown to be well separated from the mass.

DISCUSSION

Dermoids are the most common congenital lesions of the orbits, accounting for 2% of all orbital masses (1,2). Ten percent of orbital region dermoids are intraorbital (3). Gorve (4) classified orbital region dermoids anatomically into subconjunctival, superficial subcutaneous, and deep groups.

Orbital dermoids occur as a result of developmental sequestration of ectoderm within the suture lines of the orbital bones (4). The most common location is the superior temporal quadrant at the frontozygomatic suture. Histologically, these lesion have a well-defined wall, with the outer portion consisting of a fibrous envelope containing sebaceous glands, hair follicles and sweat glands. These dermal appendages are not present in epidermoid cysts. The inner lining is a true epidermis with stratified squamous epithelium. The central cavity contains laminated keratin and cholesterol crystals. Rupture of a dermoid lesion is a frequent event that is often clinically silent (5). Histologically, such an occurrence can induce granulomatous inflammation, as well as calcification and scar formation. Dermoids may extend in a dumbbell configuration through a bone canal to reach an extraorbital space such as the anterior or middle cranial fossa, temporal fossa, paranasal sinuses and through the orbital fissure (6).

Deep orbital dermoids typically present with proptosis in older children and adults. The posterior margins cannot be palpated (5). They have generally been described as having density similar to that of fat on CT scans (7,8). The presence of fat within an orbital mass lesion is virtually pathognomonic of a dermoid (9), especially since orbital lipomas and liposarcomas are extremely rare (2). Layering of different density components within the dermoid has been reported occasionally (10). Some dermoids had intermediate density, suggesting a cystic or partially fatty lesion (1). Lesions of muscle density, a pattern that is not very specific, represented the least common pattern (1), however, these lesions enhanced minimally or not at all. The margin is distinct with calcification. The lack of enhancement helps to differentiate dermoids from other orbital soft tissue tumors.

The bone changes with these lesions were particularly characteristic, especially the pattern of excavation. This pattern of notching reflects the origin within the suture followed by the slow erosion of bone as the lesion enlarges. Other bone changes are erosion, sclerosis and orbital enlargement. (1).

Nugent RA, et al (1) reported 13 deep lesions, the CT features are shown in the table 1.

Department of Radiology, Ramathibodi Hospital, Rama 6 Street, Bangkok 10400, Thailand.

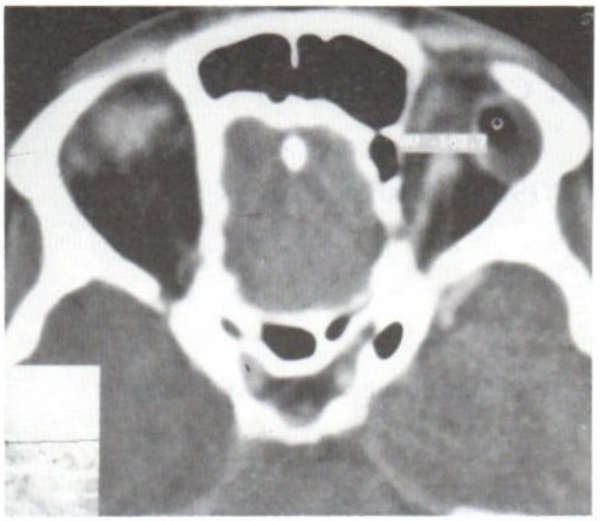

Fig.1.A Axial view of the mass showed fatty component (−143.3 H.U.)

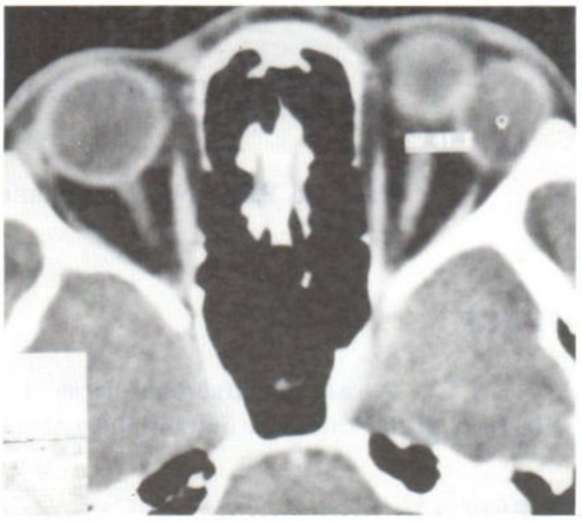

Fig.1.B Axial view of the mass showed soft tissue component (41.1 H.U.)

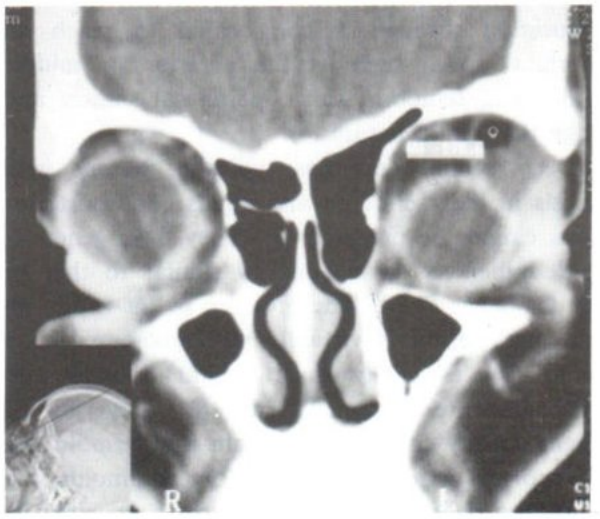

Fig.1.C Coronal view CT scan of the mass revealed fatty content (−172 H.U.)

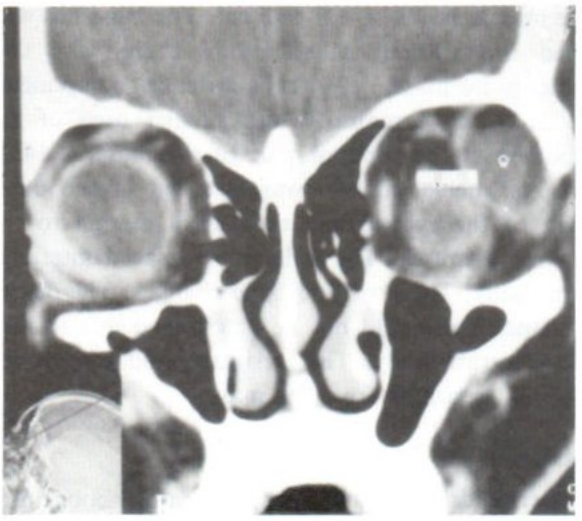

Fig.1.D Coronal view CT scan of the mass showed soft tissue content (25.5 H.U.)

REFERENCES:

1. Nugent RA, Lapointe Js, Rootman J, Roberson WD, Graeb DA. Orbital dermoids:features on CT. Radiology 1987;165:475-478.
2. Jones IS, Jakobiec FA, eds. Diseases of the orbit. New York:Harper & Row, 1979.
3. Pollard ZF, Callhoun MD. Deep orbital dermoid with draining sinuses. Am J Ophthalmol 1975; 79:310-313.
4. Grove AS Jr. Orbital disorders, diagnosis and management. In:McCord CD Jr, ed. Oculoplastic surgery. New York: Raven 1981:274-277.
5. Sherman RP, Rootman J, Lapinte JS. Orbital dermoids: clinical presentation and management. Br J Ophthalmol 1984;68:642-652.
6. Peyster RG, Hoover E. Primary orbital neoplasms. in: Peyster RG, Hoover E., eds. Computerized

Table 1. Summary of findings on CT scans in 13 patients with deep dermoid orbital lesions.

CT features	No. of cases
1. Location	
lateral	9
medial	2
inferior	1
intraconal	1
2. Density	
fat	5
muscle	4
intermediate	4
3. Rim	
no rim visible	6
rim with calcification	6
rim without calcification	1
4. Globe displacement	
none	1
downward	5
medial	2
axial	2
globe flattening	3
5. Size of lesion (mm)	
range	10-40
6. Increased orbital size	
no increase	4
general	5
focal	4
7. Bone changes	
none	2
thinning or notching	11
full thickness defect	3
linear	2
sclerosis	2
8. Contrast enhancement	2/5

tomography in orbital disease and neuro-opthalmology. Chicago: year Book Medical, 1984;23.
7. Rothfus WE. Orbital masses. In: Latchaw RE, ed. Computed tomography of the head, neck and spine. Chicago: Year Book, Medical, 1985;380.
8. Zimmerman RA, Bilaniuk LT. The orbit. In: Lee SH, Rao KCVG, eds. cranial computed tomography. New York: McGraw-Hill, 1983; 104-105.
9. Hammerschlag SB, Hesselink JR, Weber AL. Primary orbital neoplasms. In: Hammerschlag SB, Hesselink JR, Weber AL.eds. Computed tomography of the eye and orbit. Norwalk, Conn:Appleton-Century-Crofts, 1983;74.
10. Rothfus WE. Differential problems in orbital diagnosis. In: Latchaw RE, ed. Computed tomography of the head, neck and spine. Chicago: Year Book Medical, 1985:402.

APEX **Helix**

The first Slip-Ring nuclear imaging system

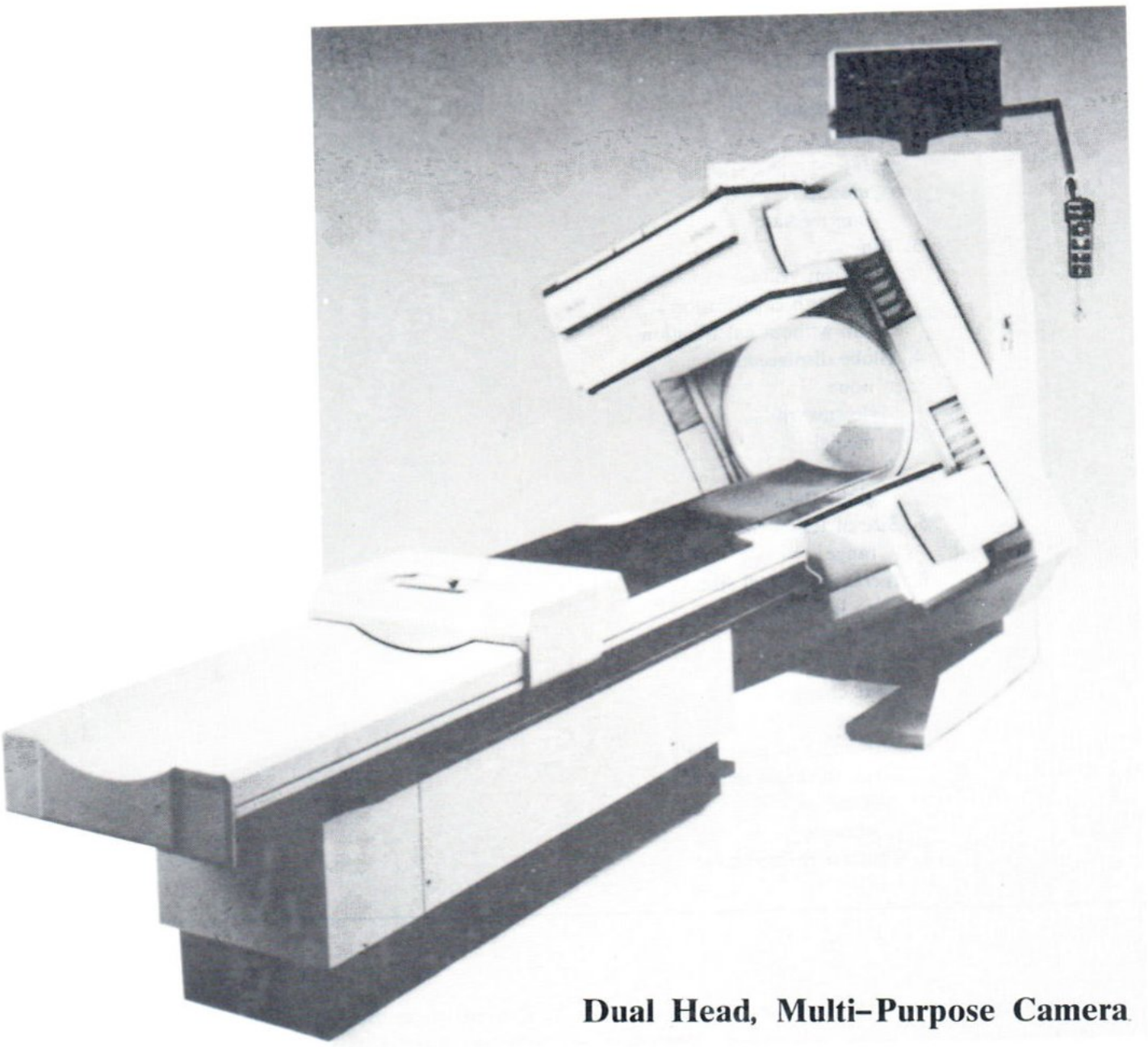

Dual Head, Multi-Purpose Camera

SOLE DISTRIBUTOR

supreme PRODUCTS CO.,LTD.

บริษัท สุพรีม โพรดักส์ จำกัด

163/81-82 PRAPINKLAO ROAD. BANGKOK 10700 THAILAND.

TEL.434-0040,434-0050 SERVICE DEPT.434-0060 FAX.433-3971

CT APPEARANCE OF THE INTRAOCULAR PROSTHETIC LENS

Patchrin PEKANAN[1],
Verat NGERNYAM[1], Chaiyasit THEPCHATRI[2]

Juvenile or adult cataract is characterized by progressive, painless loss of vision. The cause may be aging, exposure to x-rays, heat from infrared exposure, systemic disease (eg. diabetes mellitus), uveitis, or systemic medications (eg. corticosteroids).

The cardinal symtom is a progressive, painless loss of vision. The degree of loss depends on the location and extent of the opacity, when the opacity is in the central lens nucleus (nuclear cataract), myopia develops in the early stages, so that a presbyopic patient may discover that he can read without his glasses (second sight). Pain occurs if the cataract swells and produces secondary glaucoma.

Opacity beneath the posterior lens capsule (posterior subcapsular cataract) affects vision out of proportion to the degree of cloudiness, because the opacity is located at the crossing point of the light rays from the viewed object. Such cataracts are particularly troublesome in bright light.

Frequent refractions and eyeglass prescription changes help maintain useful vision during cataract development. Occasionally, chronic pupillary dilatation with phenylophrine 2.5 to 10% is helpful for small lenticular opacities. When useful vision is lost, lens extraction is necessary; it can be accomplished by removal of the lens infact or by emulsification followed by irrigation and aspiration. Age is no contraindication to surgery. Corticosteroids must be given topically and systemically when surgery is needed in the presence of uveitis. Refractive correction is accomplished by intraoperative implantation of an intraocular prosthetic lens, cataract spectacles, or contact lenses.

Figure showd CT scan of the orbits of a 78 years old female patient. Right intraocular prosthesis lens was shown and natural left intraocular lense was noted. This artificial lens is the foldable lens from Iovision and is much thinner than the natural one. This type of lens has UV filter. It is as radiopaque as the natural lens.

REFERENCES

1. The Merck manual. 16the Ed. Rahway: Merck & Co., Inc, 1992.
2. Ocular Surgery News; International edition 1994; 5:6.

[1]Department of Radiology, Ramathibodi Hospital, Rama 6 Street, Bangkok 10400 Thailand.
[2]Department of Ophthalmology, Ramathibodi Hospital

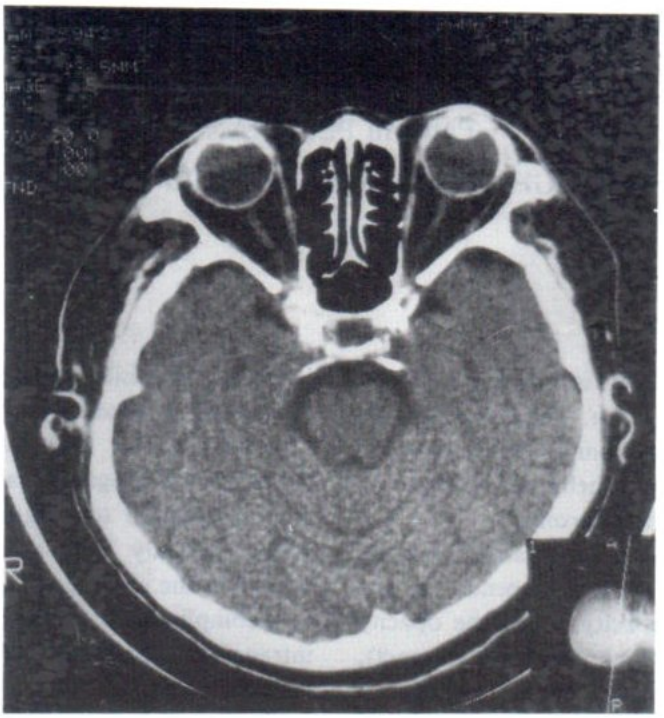

Fig.1 CT scan of the orbits showed flattened opaque artificial lens of right eye.

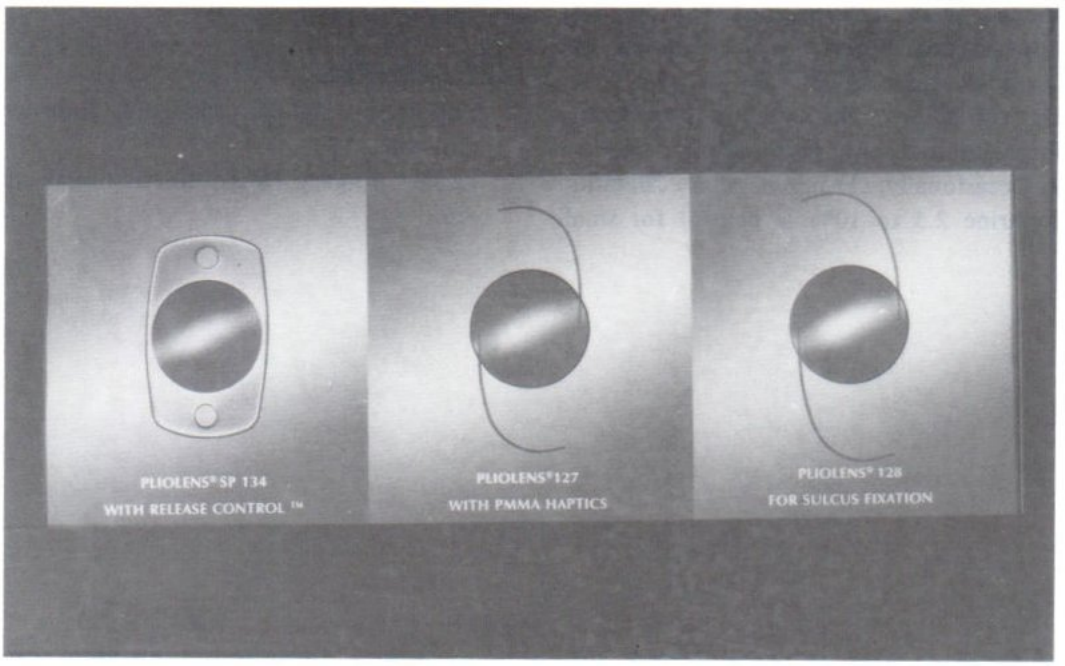

Fig.2 The foldable artificial lens from Iovision which has UV filter.

LIPOMA OF THE PAROTID GLAND: A CASE REPORT

Janjira JATCHAVALA[1], Pimjai SIRIWONGPAIRAT[1]
Patchrin PEKANAN[1], Chira SIRIBODHI[2].

ABSTRACT

Lipoma was the most common neoplasm of mesenchymal origin, about 13% of it arose in the head and neck regions. Lipoma of the parotid gland was uncommon, accounting for 1% of parotid tumors. We report a case of an ordinary lipoma in the parotid gland and review articles.

Key words: Parotid gland, lipoma

Lipoma was the most common benign neoplasm of mesenchymal origin. About 13% of it occurred in the head and neck regions, most commonly in the posterior neck.[1-3] Lipoma in the region of parotid gland was rarely found, accounting for 1% of the parotid tumor.[4,5] Complete excision is curative, thus preoperative diagnosis could help in the treatment planning.

CASE REPORT

A 47 year-old female patient, presented with intermittent swelling of left neck for 2 years. There was no tenderness nor evidence of inflammation. No facial palsy is noted. Physical examination showed a soft tissue mass at left jugulodigastric area. Indirect laryngoscope revealed fullness of the left pyriform sinus.

Post contrast CT scan demonstrated a well-circumscribed low density mass of attenuation value -129 HU.,approximately 3 X 2 x 4 cm. in size. The mass was located in the deep part of left parotid gland. The rim of the normal parotid gland overlying lateral margin was identified. The posterior facial vein and external carotid artery were well seen lying within the mass (Fig.1,A,B). Right parotid gland is normal.

DISCUSSION

Lipoma may arise in the parotid gland and periparotid area. Of the reported cases, 57% arose within the gland and 43% were of periparotid origin (4-5). About 90% of these tumors were ordinary lipomas and the remaining lesions were infiltrating lipomatosis or infiltrating lipomas.

The ordinary lipoma was a discrete lesion that usually had a homogeneous low attenuation value (-65 to -125 HU.) Although a definite capsule was not seen, the lipoma was clearly defined from the adjacent structures (5,6). The lesion varied in size from 1 to 8 cm. in diameter, more common in female by a 10:1:ratio and was not associated with lipoma elsewhere in the body (7).

Infiltrating type of lipoma was rare. The CT appearance was one of a fatty infiltration that replaced all part of the parotid gland (7,8).

In this case, the typical CT characteristic with evidence of discrete margin, the definite diagnosis of ordinary lipoma was made. The presence of blood vessels inside the tumor mass suggested that the tumor had arose in the parotid gland. The tumor could be distinguished from other low attenuation masses in the parotid space such as branchial cleft cyst, cystic Warthin's tumors, abscess and rarely lymphangioma, by the characteristic density of fat. The rim and the associated clinical findings are not present.

[1] Department of Radiology, Ramathibodi Hospital, Rama 6 Street, Bangkok, Thailand.
[2] Department of Otolaryngology, Hua Cheaw Hospital, Bumrungmeung Street, Bangkok, Thailand.

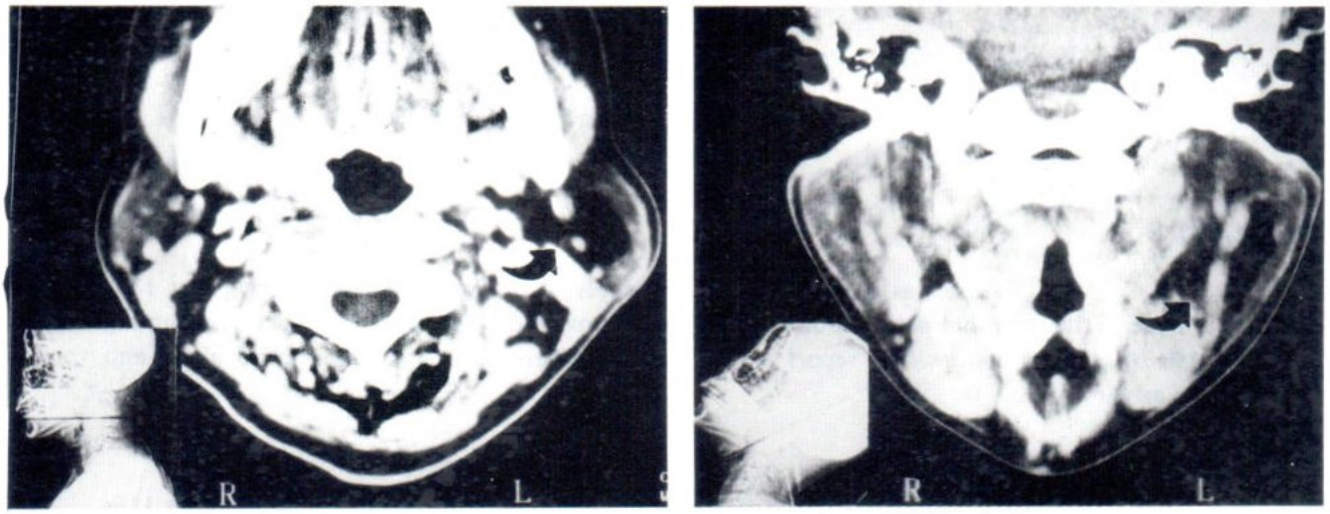

Fig.1. Post contrast (a) axial and (b) coronal CT scan showed left parotid lipoma with rim of normal parotid gland overlying lateral margin. Posterior facial vein and external carotid artery were well seen lying within the mass.

REFERENCES

1. Enzinger FM, Weiss SW. Soft tissue tumors. ST.Louis:Mosby, 1983:199-241.
2. Barnes L. Surgical pathology of the head and neck, Vol 1. New York:Dekker, 1985:747-758.
3. Batsakis JG. Tumors of the head and neck, clinical and pathological considerations, 2nd ed. Baltimore: Williams & Wilkins, 1979:360-364.
4. Janecka IP, Conley J, Perzin KH, Pitman G. Lipomas presenting as parotid tumors. Laryngoscope 1977;87:1007-1010.
5. Som PM, Bergeron TR. Head and neck imaging 2nd. St.Louis: Mosby, 1991:343.
6. Rabinov K, Weber AL. Radiology of the salivary gland, Boston: GK Hall & Co, 1985:292-367.
7. Som PM, Scherl MP, Rao VM, Biller HF. Rare presentations of Ordinary Lipomas of the Head and Neck:a review. AJNR 1986;7:657-664.
8. Godwin JT,Dew JH. Fatty infiltration of parotid gland:report of a case. Arch Surg 1958;76:525-526.

INTRAABDOMINAL RETROPERITONEAL MALIGNANT FIBROUS HISTIOCYTOMA

Sompot JITGASAMESUK, Patchrin PEKANAN, Puangtong KRAIPHIBUL

ABSTRACT

The malignant fibrous histiocytoma (MFH), a tumor also referred to as malignant fibrous xanthoma and fibroxanthosarcoma is a predominantly pleomorphic sarcoma usually occurring in the deep soft tissue of adults (1,2). This type of tumor also affects the bones (3). Most reports to date concern the soft tissues of the extremities; only 16% of the cases concern the abdominal cavity, where the retroperitoneum represents the most frequent site (1,4). Because of its highly variable morphologic pattern, this tumor has often been confused with other sarcomas such as pleomorphic rhabdomyosarcoma and liposarcoma.

This is the case report of MFH demonstrated by IVP, Barium bowel study, ultrasonography, CT scan and angiography.

CASE REPORT

A 50-year-old female patient, had weight loss of 4 kg, in one month. She had fever, anorexia. Physical examination revealed only thin woman without other abnormality. A previous history of adrenal mass, hypertension and hypokalemia 15 years ago. treated by medication. Plain KUB and IVP showed lateral displacement of left kidney and obliteration of the medial border of upper and middle pole of left kidney. The entire left psoas shadow was not seen, but there was no deviation of the left ureter, except at the proximal part (Fig. 1) UGI and small bowel series showed large LUQ mass, displacing the stomach medially and anteriorly. The DJ junction is also displaced medially; the jejunum is displaced inferiorly (Fig. 2). Pleated appearance of the splenic flexure was seen (Fig. 3). Ultrasonography showed a lobulated border solid low echoic mass, size 10 cm diameter at medioventral aspect of left kidney, obliterating ventral outline of left kidney. The echo of the mass was mildly inhomogenous, (Fig. 4) Noncontrast CT scan at the mass area showed a large isodensity mass (isodensity to the renal parenchyma). With contrast enhancement, the mass had central low density areas, in nearly entire mass. Other parts shows rather homogeneously enhancement. Invasion of the ventral part of left kidney, left psoas muscle. Left renal vein was included in the mass; however the rest of the left renal vein and inferior vena cava contained no thrombus. The left adrenal gland was displaced posteriorly. The pancreatic tail was attached to the mass. Separated enlarged nodes were not identified (Fig 5). Abdominal aortography and left renal angiography (Fig. 6) showed neovasculature to the mass from left renal artery. Retroperitoneal malignant fibrous histiocytoma, inflammatory type with invasion into the adjacent pancreatic tissue was found at surgery and pathology. The adrenal gland, left kidney and spleen were unremarkable.

DISCUSSION

In 1972, Kahn (5) reviewed a literature about retroperitoneal malignant fibrous xanthoma or xanthogranuloma, yielded 29 cases. The patient's ages ranged from 2 years to 73 years with a mean of 46 years. There were only three cases recorded in children

Department of Radiology, Ramathibodi Hospital, Rama 6 Street, Bangkok 10400, Thailand.

UGI = Upper Gastro-intestinal, LUQ = Left Upper Quadrant,
DJ = Duodeno-Jejunal

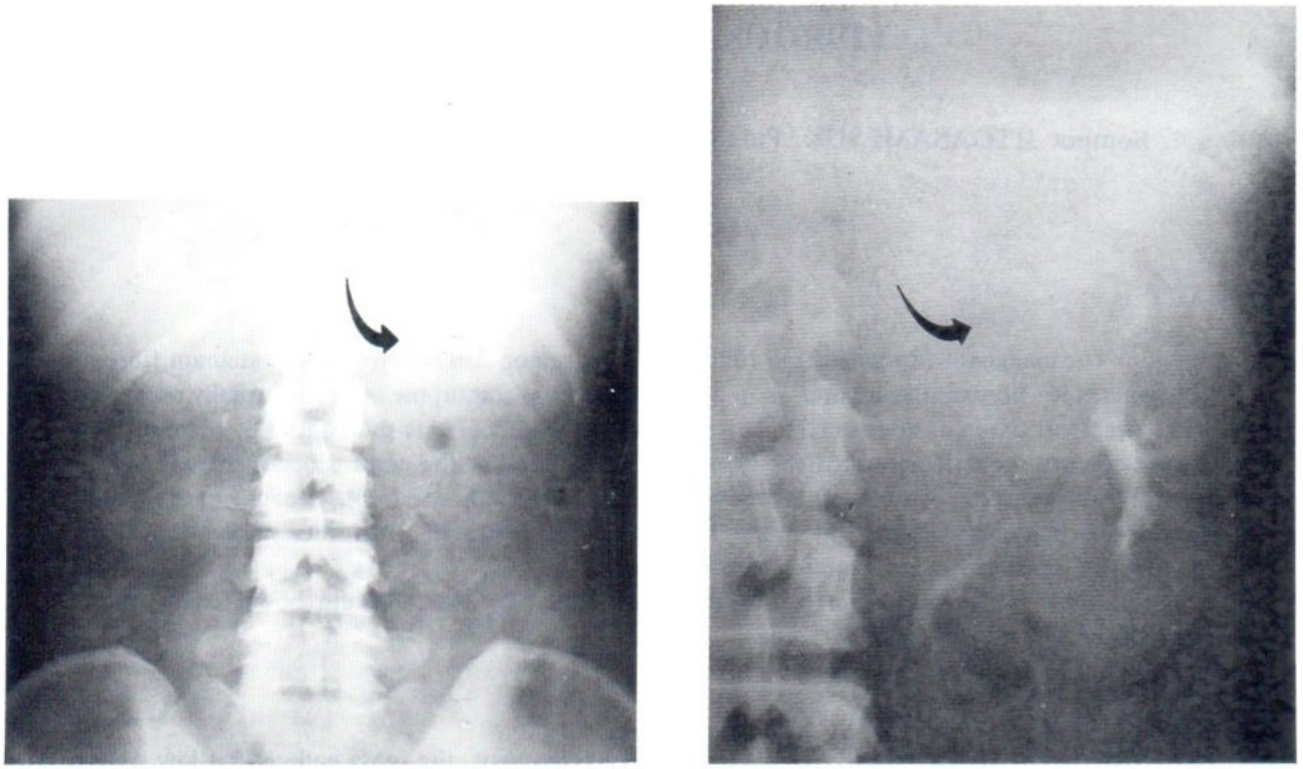

Fig. 1A,B Plain film of the kidneys showed obliteration of the upper pole-left renal outline. Lateral deviation of left kidney with loss of medial outline of upper and middle pole.

and only five cases in patients below the age of 30 years. The other cases were more or less evenly distributed over the next four decades with a peak in the sixth decade. Sixteen of the patients were males and 13 were females. Most of the lesions were circumscribed, non-encapsulated and lobulated retroperitoneal masses. In 13 cases, they were described as being large but no size was given. In the 10 cases in which the mass was measured, it varied in size from 6 to 20 cm in greatest dimension. It was occasionally adherent to adjacent retroperitoneal structures and complete excision of grossly visible tumor was not always possible.

Malignant fibrous histiocytoma is thought to originate from undifferentiated mesenchymal cells and is composed of fibroblast-like and histiocyte-like cell lines. Typically, these cells are arranged in a storiform pattern accompanied by pleomorphic giant cells and inflammatory infiltration. Fibrous, myxoid, giant-cell and inflammatory variants have been described (6).

Lane (7) described CT finding in 16 cases of retroperitoneal fibrous histiocytoma. The average tumor size on CT was 12 cm. Fifty-six per cents of the cases were seen on CT as muscle-density masses with regions of low density representing necrosis; 44 per cents showed smaller tumors with homogeneous muscle density; 25% contains areas of dystrophic calcification. From the work of various authors (8-11), it may be concluded that there are no computerized tomographic features specific for MFH or other soft tissue sarcomas except in tumors of high lipid content such as liposarcoma.

Sonographically, MFH usually presents itself as well-defined mass, the heterogeneity of the tumor giving rise to a variable echographic pattern (6). This variability seems to explain the different observations of Buecheler (12), Sarti (13) and Ros (9), who respectively describe the echographic aspects of MFH as mainly sonolucent (12), mainly solid-hyperechoic (13), and variable (9). Internal septation was also seen (6).

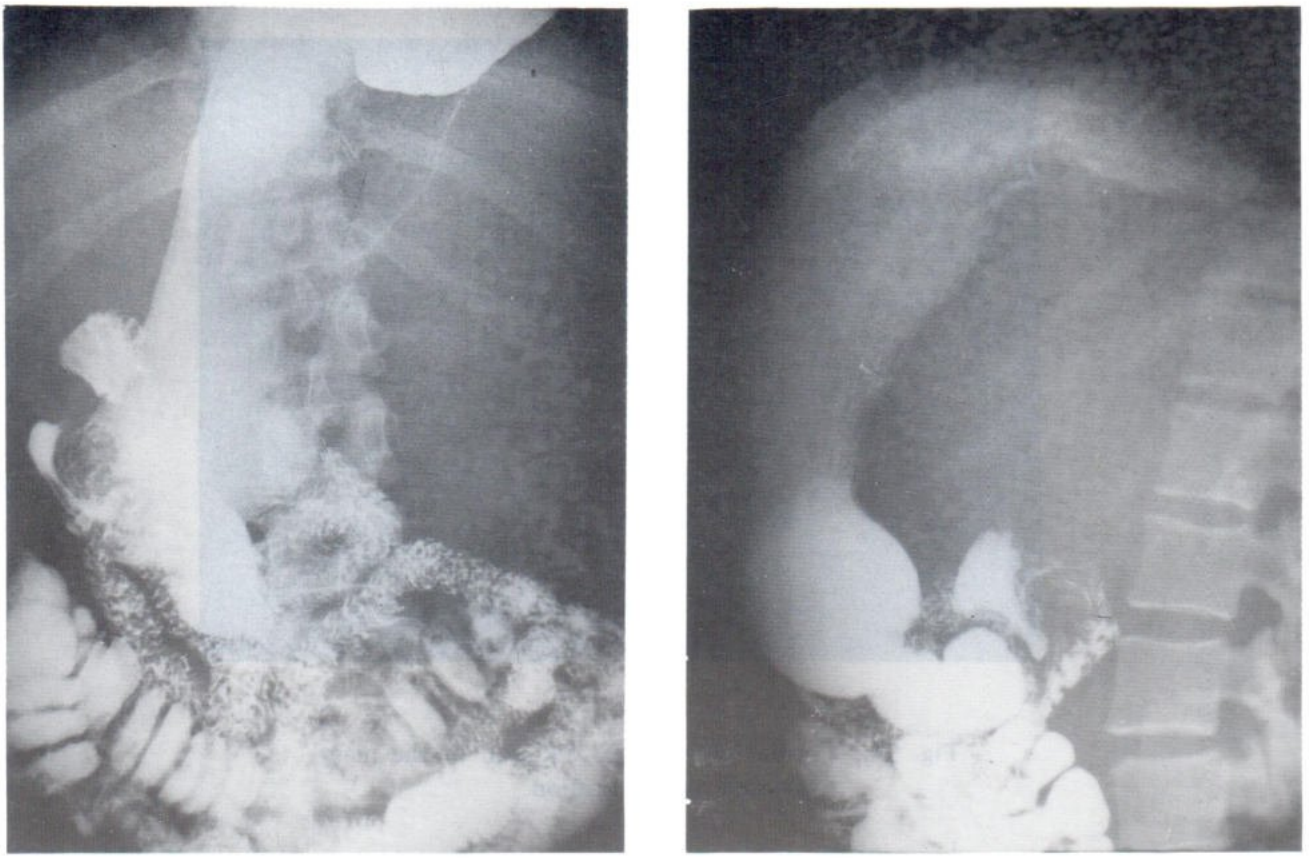

Fig. 2A,B UGI series demonstrated a large LUQ mass displacing the stomach to the right and anteriorly , indicating retroperitoneal mass.

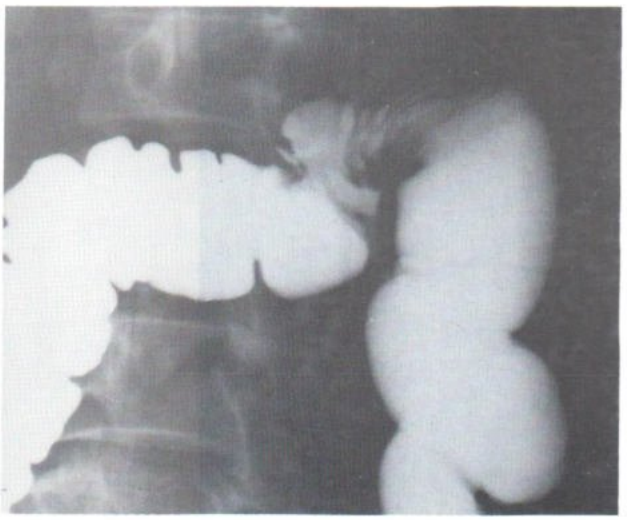

Fig. 3 Pleated appearance of splenic flexure due to infiltrated extrinsic mass was seen by Barium Enaema.

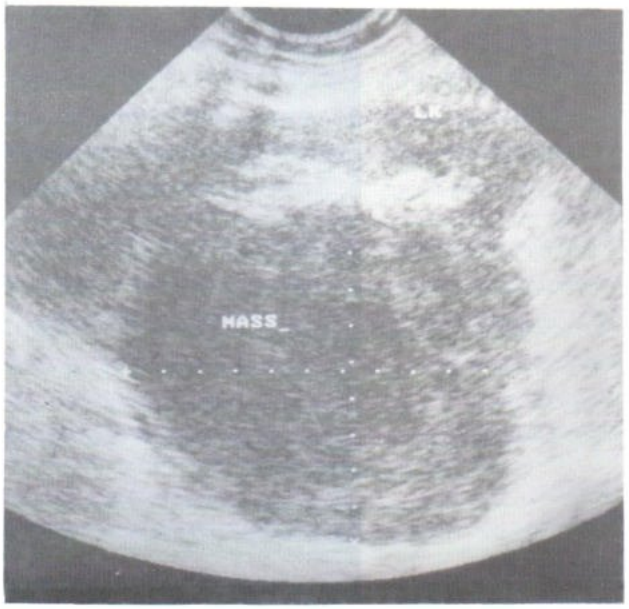

Fig. 4 An irregular border hypoechoic solid mass, ventral to left kidney was shown, obliterating ventral left renal parenchyma.

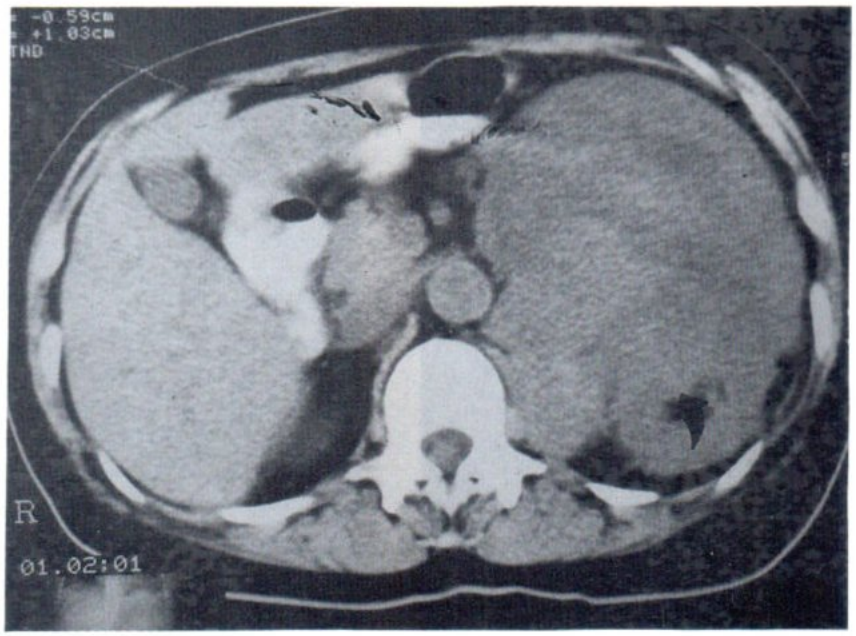

Fig. 5A. Non i.v. contrast CT scan of the mass showed no calcification.

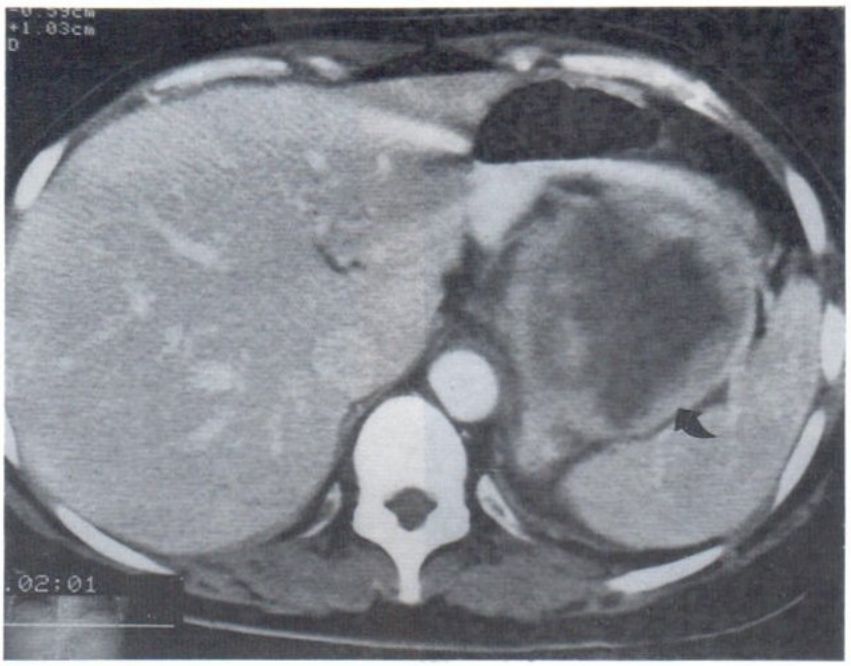

Fig. 5B. I.V. contrast CT scan of the mass showed rim enhancement, central necrosis and enhanced non-necrotic part.

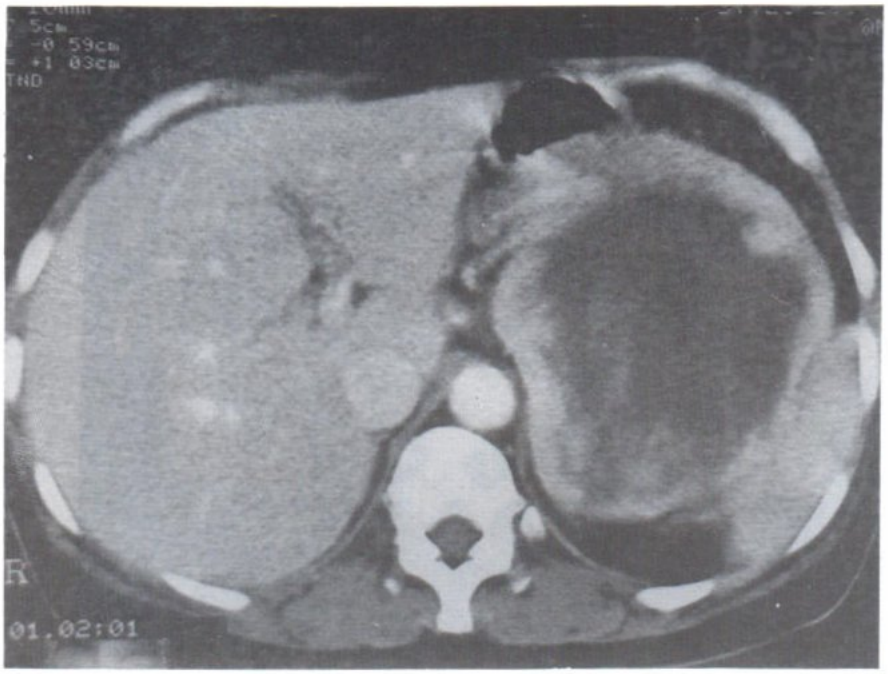

Fig. 5C. The unenhanced portion of the mass was at the central part.

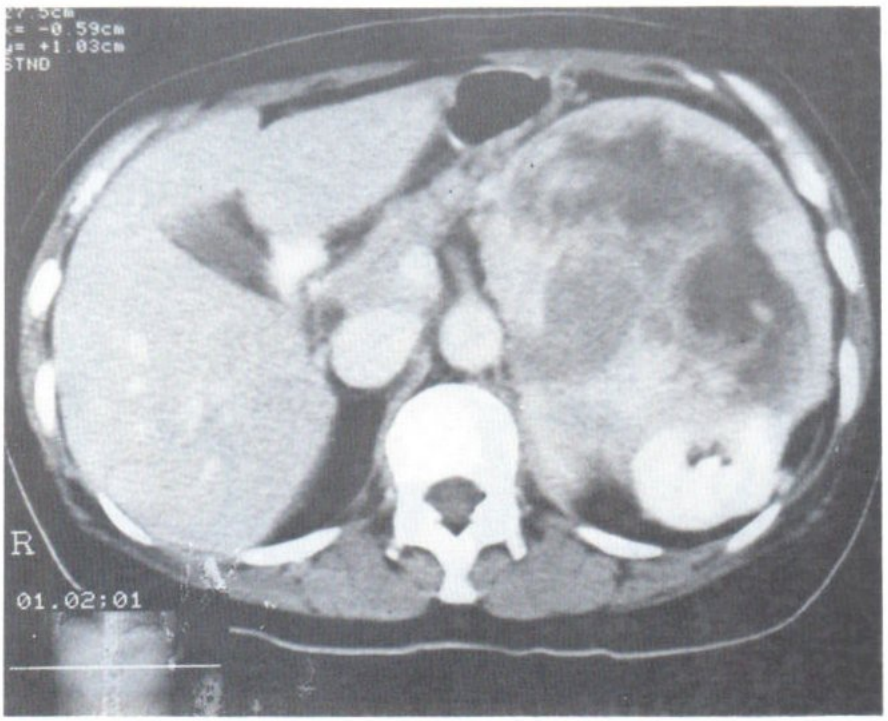

Fig. 5D. Left crus of the diaphragm, the pancreatic tail and ventral border of left kidney was infiltrated.

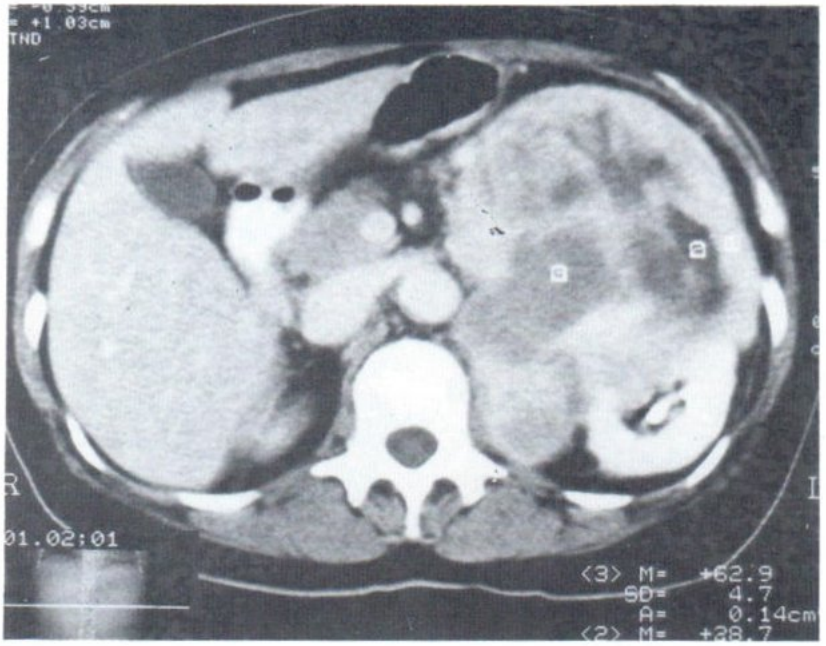

Fig. 5E. Inhomogeneity of tissue enhancement was shown.

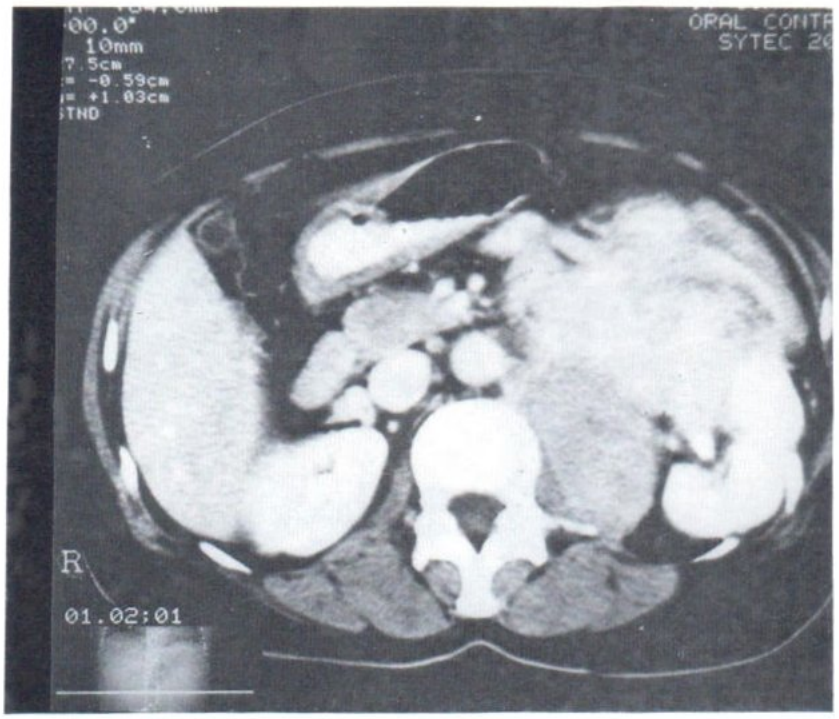

Fig. 5F. The mass extended to the anterior part of the abdominal cavity.

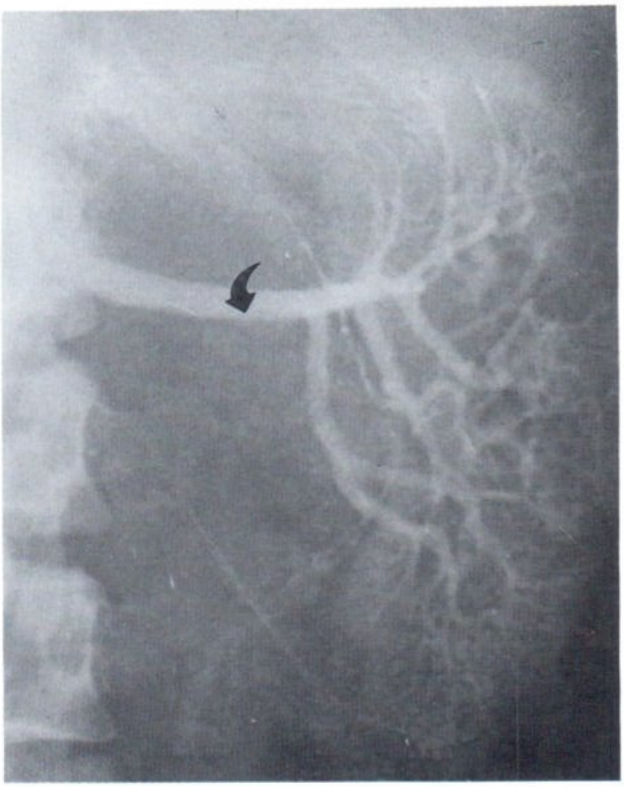

Fig. 6 Left renal angiography showed neovasculature arising from left renal A.

REFERENCES

1. Weiss SW, Enzinger FM. Malignant fibrous histiocytoma. An analysis of 200 cases. Cancer 1978; 41: 2250-66.
2. Kempson RL, Kyriakos M. Fibroxanthosarcoma of the soft tissue. A type of malignant fibrous histiocytoma. Cancer 1872; 29: 961-76.
3. Hudson TM, Hawkins IF Jr, Spanier SS, Enneking WF: Angiography of malignant fibrous histiocytoma of bone. Radiology 1979; 131: 9-15.
4. Bruneton JN, et al. Extraretroperitoneal abdominal malignant fibrous histiocytoma. Gastrointest Radio 1988; 13: 299-305.
5. Kahn LB, Path MM. Retroperitoneal, xanthogranuloma and xanthosarcoma (malignant fibrous xanthoma). Cancer 1973; 31: 441-22.
6. Schut JM, van Imhoff WL. Retroperitoneal malignant fibrous histiocytoma: an unusual echographic presentation. J Clin Ultrasound 1987; 15: 145-49.
7. Lane RH, Sephens DH, Reiman HM. Primary retroperitoneal neoplasm : AJR 1989; 152: 83-89.
8. Bernardino ME, Jing B, Thomas JL, et al. The extremity soft tissue lesion: A comparative study of ultrasound, computed tomography, and xeroradiography. Radiology 1981; 139: 53-59.
9. Ros PR, Viamonte M, Rywlin AM: Malignant fibrous histiocytoma: Mesenchymal tumor of ubiquitous origin. Am J Roentgenol 1984; 140: 753-59.
10. Paling MR, Hyams DM. Computed tomography in malignant fibrous histiocytoma. J Comput Assist Tomogr 1982; 6: 785-88.
11. Friedburg H, Wimmer B, Adler CP, et al. Malignes fibroeses histiocytom der weichteile: Pathologie and radiologie eigenartigen sarkoms. Fortschr Roentgenstr 1982; 137: 388-93.
12. Buecheler E, Friedmann G, Thelen M. Real-time-sonographic des koerpers. Stuttgart, New York, Georg Thieme Verlag, 1983, pp 444.
13. Sarti DA, Sample WF. Diagnostic ultrasound: Text and cases. Boston, GK Hall & Co, 1980, pp 498-99.

ACOUSTIC IMAGING
A Dornier Company

Presents...

HIGH PERFORMANCE, COST EFFECTIVE ULTRASOUND FOR:

- ABDOMINAL
- OBSTETRICS
- GYNECOLOGY
- VASCULAR
- PROSTATE
- MUSCULOSKELETAL
- SMALL PARTS
- MAMMOGRAPHY
- PEDIATRICS

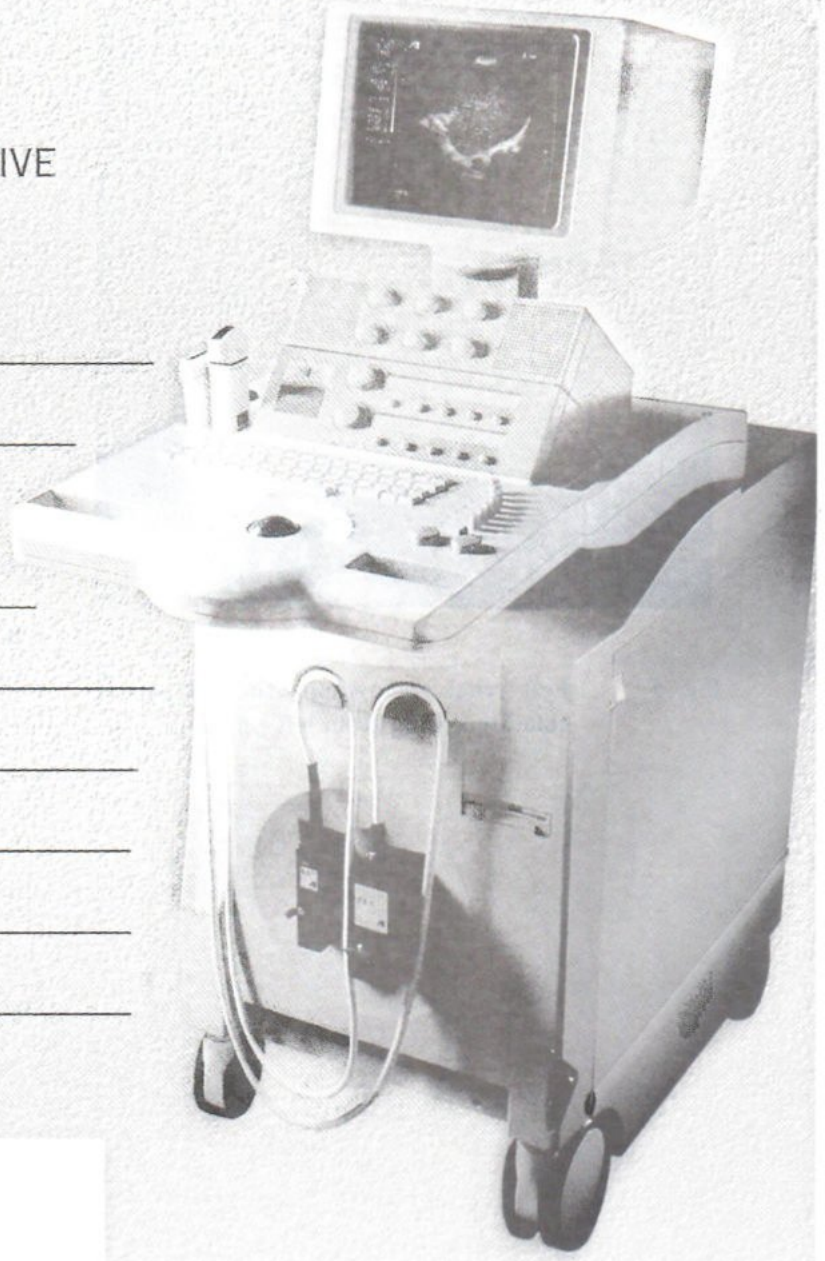

MEDICAL MEDIA PRODUCT CO., LTD.
บริษัท เมดิคอล มีเดีย โปรดักส์ จำกัด
633/14 ถนนสาธุประดิษฐ์ เขตยานนาวา กรุงเทพฯ 10120
โทร. (662) 2943364-8 โทรสาร : (662) 2943373

Performa™

High resolution ultrasound imaging scanner

ADULT WILMS' TUMOR

Patchrin PEKANAN, Chitchanok TANTIWIWAT

ABSTRACT

Wilms' tumor (nephroblastoma) is a mixed renal tumor composed of metanephric blastema and its stromal and epithelial derivatives at variable stages of differentiation. It is a disease of early childhood and 80% of patients are cured with current therapy (1,2). Wilms' tumor in adults occurs rarely and has a poorer prognosis (3). The adult patients present more often with metastases and patients who present with localized disease, relapse more frequently at follow-up (3). The chemotherapy regimens, which have been successfully used in pediatric patients, are not as effective in the adult patients (3,4,5,6).

We report a case of adult Wilms' tumor in a 60-year-old female patient, studied by IVP, ultrasonography and CT scan.

CASE REPORT

A 60 year-old female patient had an abdominal discomfort and a palpable mass at LUQ. Physical examination showed left upper quadrant mass. Plain film of the abdomen showed a large soft tissue mass at left upper and mid abdomen. The mass did not obliterate the shadow of left psoas muscle or left kidney. The stomach was displaced superiorly. Intravenous pyelography showed enlarged left kidney with preserved outline, mild hydropelvis and separation of the upper and middle pole calyceal system. The right kidney appeared normal. CT scan of the mass showed a large solid mass with lobulated superior border and rim enhanced border at the other part of the mass. The ventral parenchyma of the upper pole, middle pole and lower pole of left kidney was invaded. The lateral part of the parenchyma of the middle pole seemed to stretch around the lateral aspect of the mass. There is large area of central necrosis. The proximal half of left renal vein was compressed, the distal half and the inferior vena cava contained no thrombus. The mass sat on the left psoas muscle with preserved the fat plane which could explain the unobliteration of the muscle on plain film. The surrounding organs were not invaded. The enlarged nodes were also not seen. Ultrasonography revealed the hyperechoic mass (compared with the echo of the renal parenchyma; however less echoic compared with the central renal fat). The hyperechoic area was intervened by the low echoic septa-like areas. Surgery was performed and left kidney was removed. Histology revealed a nephroblastoma.

DISCUSSION

Wilms' tumor occurs primarily in infants. Klapproth in 1959 reviewed 1351 cases of Wilms' tumors reported in the literature and added 45 cases of the his own (7). Four point four per cent occurred in adults, 13.4 per cent were in children below the age of one, and 82.2 per cent were in children above the age of 1 year. The peak incidence in children was between the ages of 1 and 2 years. In adults, the highest peak of occurrence of Wilms' tumor in reported cases appears to be in the fifth decade. The oldest patient was an 80 year-old woman. Wilms' tumor appears to occur in both sexes with approximately the same frequency. No predilection has been shown for either the right or the left kidney.

Wilms' tumor varies considerably in size. It may grow enormously and destroyed the kidney and the surrounding structures. Grossly the tumor is usually grayish in color, homogeneous in appearance and may appear encapsulated. The gross picture may be altered by extensive necrosis and hemorrhage. Cystic

Department of Radiology, Ramathibodi Hospital, Rama 6 Street, Bangkok 10400, Thailand.

degeneration and calcification may occur. Islands of bone and cartilage may be present.

Generally the Wilms' tumor is known to spread to neighboring organs by direct extension. Blood borne metastases also occur. Metastasis to lungs is the most common site in reported cases.

Wilms' tumor in adults is usually recognized after surgical and histologic examination or at autopsy as an incidental finding. The symptoms include abdominal pain, fever, hematuria, nausea, vomiting, constipation, secondary anemia, loss of weight, anorexia, cachexia and few reported of ascites. Hypertension is present in more than 50 per cent of cases.

Reported associated abnormalities included 1) Beckwith-Wiedemann syndrome (exophthalmos, macrosomia, macroglossia, hepatomegaly, omphalocoele, hyperglycemia from islet cell hyperplasia) 2) Sporadic aniridia 3) Hemihypertrophy; total/segmental/crossed 4) Drash syndrome (pseudohermaphroditism, glomerulonephritis, nephrotic syndrome) 5) Renal anomalies (horseshoe kidney, duplix/solitary/fused kidney) 6) Genital anomalies (cryptorchidism, hypospadia, ambiguous genitalia).

The tumor is hypervascular with enlarged tortuous vessels, coarse neovascularity, small arterial aneurysms, vascular lakes and parasitization of the vascular supply (8).

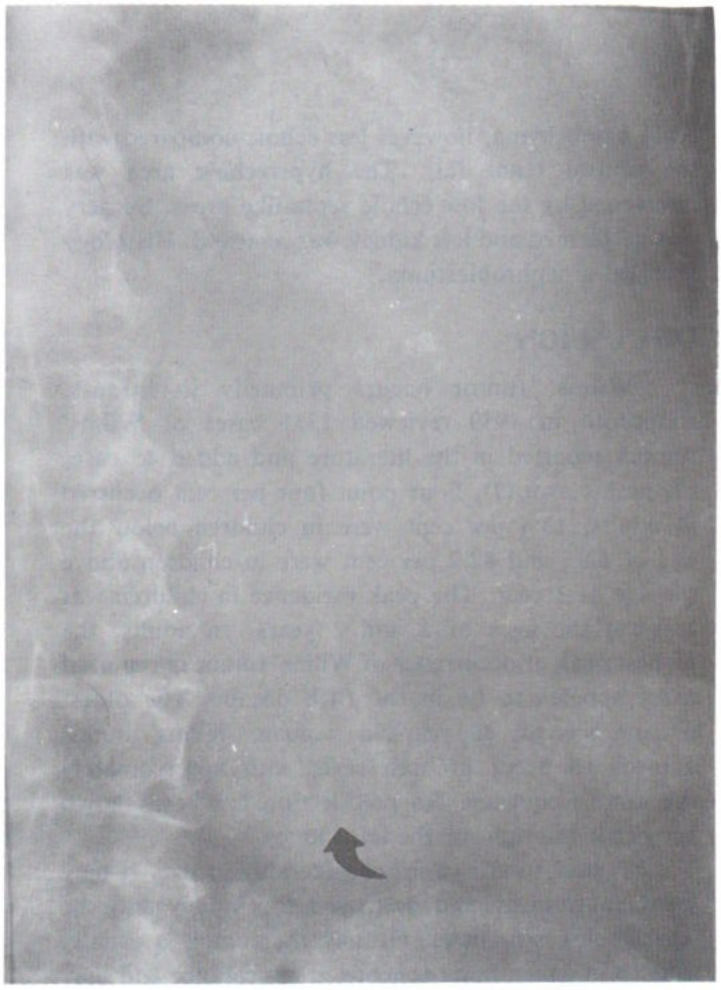

Fig.1 Plain KUB showed a large soft tissue mass at the left renal and left psoas region without obliterating them.

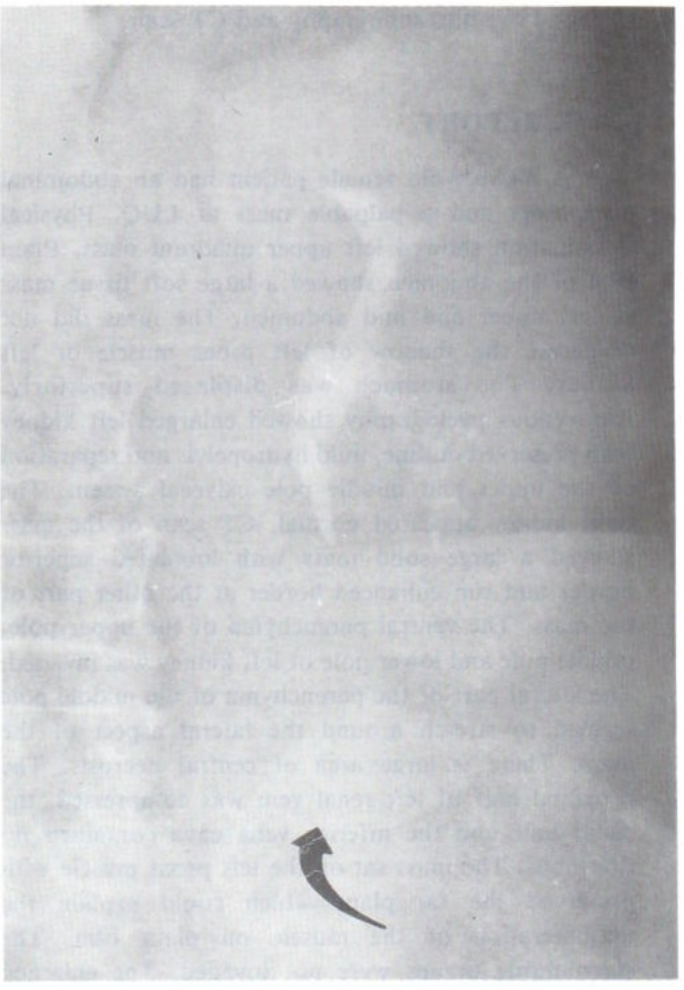

Fig.2 IVP of the left kidney showed preserved left renal outline with separation of the upper and middle pole collecting system

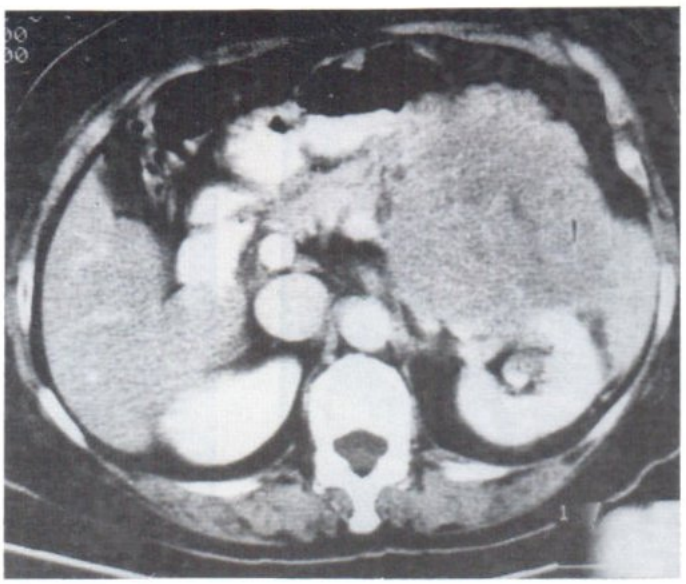

Fig.3A

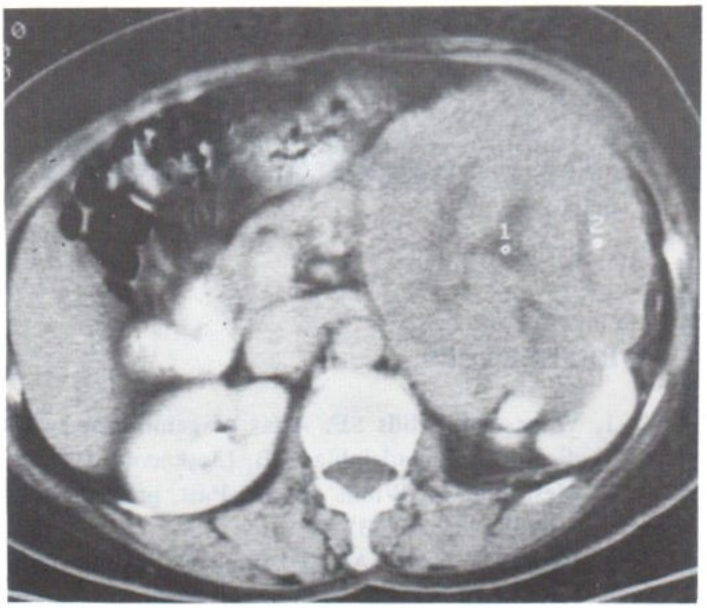

Fig.3A,B,C.

I.V. contrast CT scan showed a rim enhanced solid mass with lobulated border. Multiple necrotic areas were shown. Well defined border invasion of the renal pelvis was seen. The pancreatic body and tail was elevated and infiltrated. The psoas muscle was free from involvement.

Fig.3B

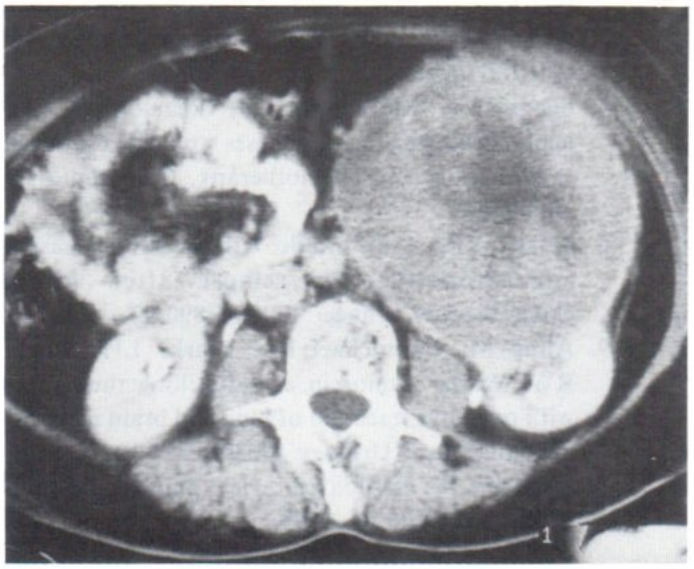

Fig.3 C

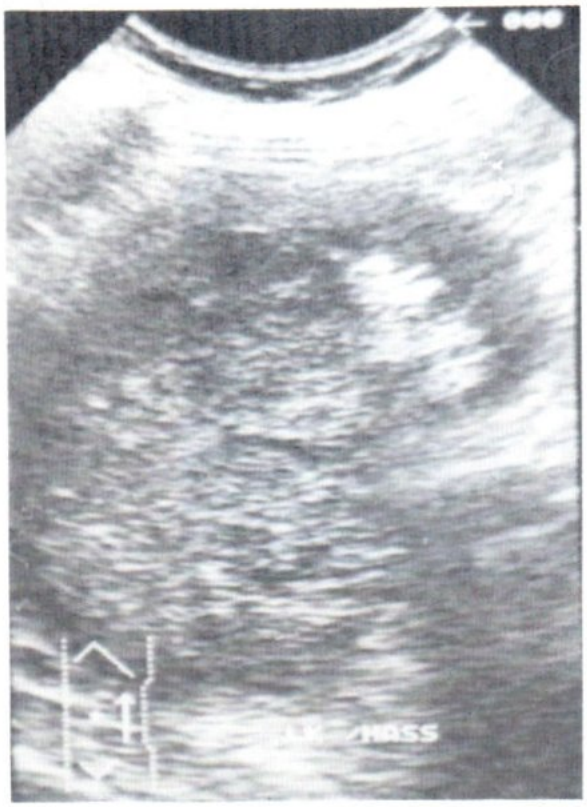

Fig.4A

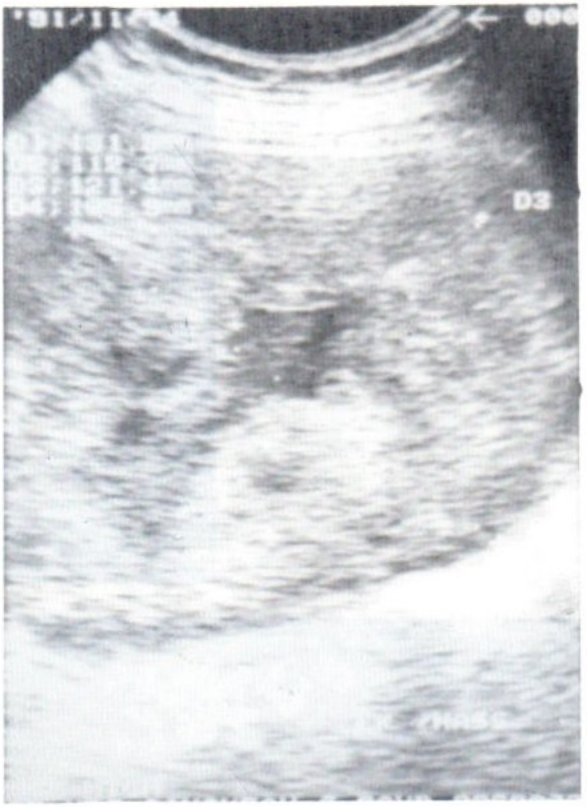

Fig.4 B

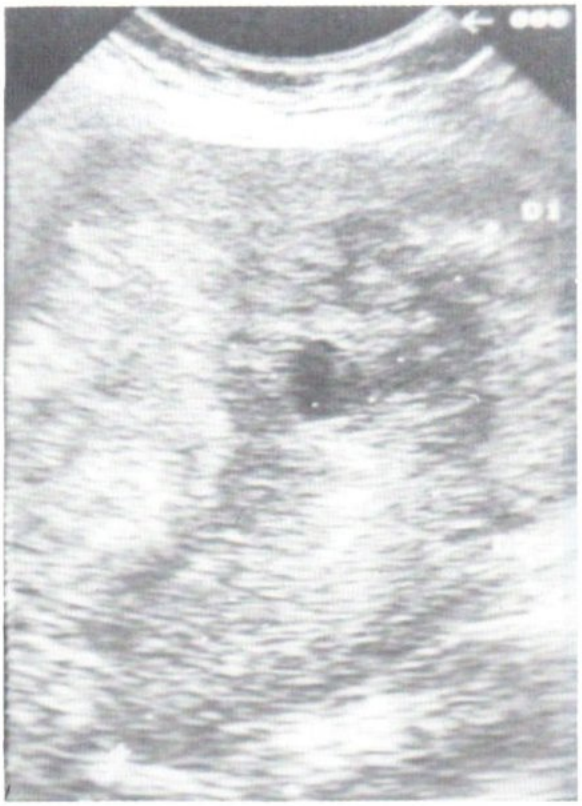

Fig.4 C

Fig.4A,B,C. Ultrasonography showed a solid mass at ventral aspect of the upper and middle pole of left kidney. The mass was hyperechoic, compared with normal renal parenchyma and contains low echoic areas of necrosis.

REFERENCES

1. Weiss MA. Mills SE. Atlas of genitourinary tract disorders. Philadelphia: J.B. Lippincott, 1988.
2. Mesrobian H. Wilms' tumor; Past, present, future. J Urol 1988;140:231-238.
3. Byrd RL, Evans AE, D'Angio GJ. Adult Wilms' tumor: Effect of combined therapy on survival. J.Urol 1982;127:648-651.
4. Dawson NA, Klein MA, Taylor G. Salvage therapy in metastatic adult Wilms' tumor. Cancer 1988; 62:1017-1021.
5. Slevin NJ, McWilliam LJ, Pearson D. Adult nephroblastoma : Five cases treated by surgery, radiotherapy and chemotherapy. Clin Radio 1987; 38:483-86.
6. Abratt RP, et al. Adult Wilms' tumor: Cisplatin and Etoposide for relapse after adjuvant chemotherapy. Cancer 1990;65:890-92.
7. Altug M, Carmichael FA, Clarke LH, Stockton RW. Wilms' tumor in an adult:long time survival with palliative resection of lung and brain metastases. The journal of Urology 1964;91:212-19.
8. Daehnert W. Radiology review manual. Baltimore: Willians & Wilkins, 1993.

GLUE EMBOLISATION OF INTRACRANIAL AND EXTRACRANIAL ARTERIOVENOUS MALFORMATIONS

Francis Hui MBBS FRCR FAMS[1]
Kheng-Hin Lee MBBS FRCS (E) FRCS (G) FAMS[2]
Peck-Leong Ong MBBS FRACS[3]
Samuel Ng MBBS FRCR FAMS[1]
Hong-Khim Boey MBBS FRCR FAMS[1]

ABSTRACT

Anteriovenous malformations of the head are formidable to treat. Embolisation with N Butyl Cyanoacrylate glue was carried out in 22 patients; 16 had cerebral AVMs, 4 had facial AVMs and 2 patients had dural AVMs. Complete obliteration of the shunt by the endovascular route was achieved in 7 patients. Altogether, 15 patients were cured by embolisation alone or in combination with surgery. Embolisation enhanced subsequent surgical or radiosurgical management by reducing nidus size, occluding intra nidal aneurysms and decreasing flow through the shunt. 3 more patients have not completed surgery or are awaiting follow up after radiosurgery. 2 permanent complications occurred, one deficit was mild and the other moderate in severity. Glue embolisation was found to be very effective in the treatment of patients with intra and extracranial AVMs.

INTRODUCTION

Arteriovenous malformations (AVMs) are always formidable lesions to treat, particularly if they occur in the head. AVMs occurring in the brain are particularly dangerous because of their propensity to cause intracerebral haemorrhage. Surgery has previously been the only modality available in the treatment of these lesions. Recently, endovascular therapy has emerged as a viable alternative in the treatment of these conditions either as a pre operative procedure or as the sole form of treatment.[1] Many types of embolic agents are available, including PVA and gelfoam particles, liquid glue, coils and balloons. This study involves the treatment of such AVMs with liquid glue in the form of N-Butyl-Cyanoacrylate (NBCA).

MATERIALS & METHODS

22 consecutive patients with intracranial and facial AVMs treated by glue embolisation were studied. All cases were done in the neuroangiographic suite at Tan Tock Seng Hospital, Singapore. The study period was from March 1994 to April 1995. Follow up period ranged from 1 to 12 months (mean = 3.5 months). 16 patients had cerebral AVMs, 2 patients had dural AVMs and 4 patients had facial AVMs. All patients were evaluated by digital subtraction

[1] Section of Neuroradiology, Department of Diagnostic Imaging, Tan Tock Seng Hospital, Moulmein Road, Singapore 1130.
[2] Consultant Neurosurgeon, Gleneagles Hospital, 6A Napier Road, Singapore 1025.
[3] Department of Neurosurgery, Tan Tock Seng Hospital, Moulmein Road, Singapore 1130.

Correspondences and reprints to: Dr. Francis Hui, Consultant In Charge, Section of Neuroradiology, Department of Diagnostic Imaging, Tan Tock Seng Hospital, Moulmein Road, Singapore 1130, Republic of Singapore.

angiography (DSA) using a General Electric Advantx® single plane fluoroscopic unit. In each case, super-selective catheterisation of the arterial pedicle was obtained with a microcatheter (Magic® Std by Balt, France or Minitorquer® , France). NBCA glue mixed with Lipiodol® and occasionally tungsten powder was injected under DSA.. An angiogram is then obtained to confirm the result of the embolisation. Glue was the sole embolic agent in 16 patients and was combined with polyvinyl alcohol and gelfoam particles in the other 6 patients. The procedures were carried out under neuroleptic analgesia or general anaesthesia. Systemic heparinisation was initiated if the guiding catheter was placed in the internal carotid or vertebral arteries. Amytal testing was carried out if embolisation was carried out at or near eloquent regions. Corticosteroids were given routinely after embolisation of a cerebral AVM. The effect of embolisation on the AVM and any complication that occurred were recorded. Patient outcome was studied immediately post embolisation and at follow up.

RESULTS

Altogether, 35 vessels were glued in 29 sessions, averaging 1.6 vessels and 1.3 sessions per patient. 11 patients had embolisation done as the sole therapeutic procedure and 9 had surgery cum embolisation and 1 patient had radiosurgery after embolisation. 1 patient is awaiting radiosurgery for a small nidus remaining after surgery and pre operative embolisation.

Among the patients who have embolisation of their AVMs as the sole therapeutic procedure, total occlusion of the AVM was achieved in 7 (32%) out of the 22 patients. Surgery after embolisation successfully eliminated the AVM completely in another 8 (36%) patients. In one case, embolisation accomplished complete obliteration of the residual nidus remaining after surgery and pre operative embolisation. Of the remaining 7 patients, 2 (8%) patients have not completed surgical treatment and 2 more are awaiting the result of radiosurgery. 2 (8%) patients had between 40 to 90% occlusion of their AVM after completing therapy. 1 (4%) patient had a large facial AVM which regrew to its original size each time after repeated episodes of embolisation.

Among the patients with cerebral AVMs, complete obliteration of the AVM was achieved in 3 (19%) of 16 patients. Embolisation combind with surgery resulted in complete occlusion of the nidus in another 8 (50%) patients. Complete obliteration of the arterio-venous shunt was achieved in 2 (50%) of the patients with facial AVMs and both (100%) of patients with dural AVMs.

One patient had a temporary complication. This was a 15 year old boy with a corpus callosal AVM. He was noted to have alexia after the embolisation but recovered fully from it within 3 days. Two patients had permanent complications. One patient with a dural AVM had a mild residual left hemiparesis at follow up but was able to lead a normal lifestyle. The other patient had an inoperable AVM in the right basal ganglia with enormous cerebral venous congestion because of venous outlet stenosis. Embolisation of the lenticulostriate feeders resulted in decrease in the flow through the AVM but the patient had worsening of the existing left hemiparesis.

At follow up, 6 (27%) patients had improvement of their clinical deficits. 9 (41%) patients who were neurologically intact remained normal. 6 (27%) patients with pre existing deficits had unchanged clinical status. 1 (5%) patient had worsening of her clinical status compared to her pre embolisation state. One patient had a rebleed 4 months after the embolisation while waiting for radiosurgery. His AVM was subsequently excised.

DISCUSSION

Management of arteriovenous malformations of the head and neck is always a challenging one. Vascular architecture of the lesion can be very complex. Previously, the only mode of treatment is surgery. However, surgery itself can be difficult particularly in lesions associated with a large nidus or a fast shunt. Proximal ligation of feeders is ineffective.[2,3] Obliteration of the nidus must remain the main aim of any form of therapy. In recent years endovascular treatment of these lesions has become an important mode of management.[1]

The need for intervention has been particularly well studied in patients with cerebral AVMs. As with any other disease, any form of therapy must be compared with the natural history of the disease. The risk of haemorrhage for an average lesion is about 2-4% a year.[4,5] The risk is increased if the haemorrhage is the presenting clinical feature. The presence of arterial ectasias, venous stenoses or intranidal aneurysms also increases the risk of haemorrhage.[6,7] The primary goal of any form of treatment of a cerebral AVM must be the prevention of subsequent haemorrhage, the most devastating complication. The risk of haemorrhage will still be present as long as the AVM is still patent. Therefore, the ultimate aim of therapy has to be the

complete elimination of any residual arteriovenous shunting. In the treatment of an extracerebral AVM, the aims are similar although the risk of cerebral haemorrhage may be less or not present.

The advent of variable stiffness microcatheter has enabled superselective catheterisation of AVM vessels. There is also a choice of different embolic agents. Initially, large particle embolisation using gelfoam or PVA through 5F catheters lodged in the internal carotid or vertebral artery was carried out. The technique and materials used in embolisation have changed over the years and presently most interventionists introduce the embolic agent through a microcatheter positioned with its tip close to the AVM nidus.

The selection of an optimal embolic agent depends on the familiarity of the operator. The 3 most common embolic agents utilised in AVM embolisation are glue such as N-butyl cyanoacrylate (NBCA), thrombogenic coils and particles like polyvinyl alcohol (PVA).

NBCA glue is a vinyl monomer which polymerises to a solid compound on contact with an ionic solution such as blood or saline.[10] When injected into any blood vessels, it will then form a cast of the vascular structure. It has the advantage of being suitable for use through any microcatheter. Being liquid initially, it has the capability of penetrating into the nidus of the AVM. In high concentrations, glue is suitable for occlusion of arteriovenous fistulae. It has also been shown to be permanent and AVMs occluded with glue do not recanalise.[11] However, it also requires considerable operator experience to master the technique so as to avoid a high rate of complications. Pulmonary complications can also occur with reflux into the venous side of the shunt.[12] Particles, on the other hand are more controllable and easier to handle. But they can be difficult to inject through a microcatheter, occasionally resulting in clogging of the catheter itself.[13] Recanalisation of occluded vessels can also occur.[14] In cases of large arteriovenous fistulae, particles may also be ineffective and will pass directly into the pulmonary circulation. Thrombogenic coils, when employed are usually delivered in the feeding artery to reduce blood flow or close the whole vessel itself. However, it tends to produce proximal occlusion and collateral circulation to the nidus results.

In a certain percentage of patients, penetration of the nidus by the glue is complete, obviating the need for any other form of treatment. In this series, this was achieved in 19% of cerebral AVMs. Unlike surgery, the size of the AVM vessels may not be an important consideration as illustrated by a 62 year old Malay man who had a left frontal AVM which had bled and resulted in subarachnoid and intraventricular haemorrhage (Fig 1). He was admitted to hospital in a coma. Embolisation of the AV shunt resulted in complete occlusion and the patient had no neurological deficit. He was discharged fully ambulant 3 days after the procedure.

Occlusion of the actual shunt and not just the arterial feeders is essential to the success of the endovascular procedure. Collateral feeders from other sources close up completely if the shunt is obliterated. An example is a 34 year old Chinese man who had a right facial AVM. After occlusion of the shunt via the right facial artery, feeders from the internal maxillary artery disappeared (Fig. 2).

To patients who had undergone complete occlusion of their AVM by endovascular techniques alone, embolisation confers obvious benefits. The patient is spared a craniotomy or facial incision, experiences less pain and scarring and eventually pays less costs for a safer procedure. Apart from this benefit to the patient, there are also advantages to the health service in the form of reduced hospital stay and less intensive care management.

Embolisation can also be used as a complementary mode of therapy in combination with surgery and radiosurgery. Spetzler[15] indicated in his classification of cerebral AVMs that the larger sized AVMs are associated with a higher operative morbidity rate. Embolisation prior to surgery can help by reducing the size of the AVM besides decreasing the flow. In this way, it can help in lessening the surgical morbidity.[16] Many of the patients in this series benefited from reduction in nidus size. In one case (Fig. 3), it allowed awake surgery, a specialised operative technique meant to decrease surgical morbidity in operations near eloquent regions of the brain. Pre operative embolisation can help in other ways. For example, it is well known that certain angiographic features such as aneurysms[6,7] predisposes to bleeding. There are points of weakness within the AVM which have a high potential for haemorrhage. Bleeding from aneurysm rupture can also complicate AVM surgery. In one patient (Fig. 4), glue filling of the aneurysmal sac helped obviate this possibility. Patients with deep periventricular AVMs can also benefit from a combination of embolisation and surgery.[17]

Embolisation followed by surgery is an effective way of treating large AVMs.[18] One patient in this series had a large inoperable right cerebellar AVM. She was treated with staged embolisation until the nidus size shrank by about 80%. This meant that the patient can then undergo surgery with potential complete excision of her AVM.

Embolisation can complement radiosurgery by reducing the size of the nidus prior to radiation.[19] It can also be used effectively to treat lesions that have not responded to initial radiosurgical treatment.[20]

Complications of glue embolisation can occur as a result of glue occluding normal arterial branches or occlusion of an important venous outlet. In one patient with a dural AVM which bled, embolisation of the feeding artery was carried out with a microcatheter positioned a short distance from its origin from the left vertebral artery (Fig. 5). Unfortunately, some reflux of glue into the main artery was noted. The fistula was closed but the patient had a left hemiplegia and hemianopia. He, however, recovered fully from his hemianopia and at follow-up, was found to have only a mild hemiparesis (Grade 4+/5 motor power) and was able to lead a normal lifestyle.

In conclusion, glue embolisation is an effective mode of therapy in the management of intra and extracranial AVMs. Careful embolisation of the AVM nidus produces efficient results and helps keep procedural complications to a minimum.

Figs. 1 (a)-(c) 62 year old man who was admitted to hospital in a coma. Enhanced CT scan (a) shows subarachnoid and intraventricular haemorrhage with large dilated vessels in left frontal lobe (arrowheads). Frontal view of left internal carotid angiogram (b) revealed the AV shunt to be supplied by the left middle cerebral artery. Post embolisation angiogram (c) showed no residual shunt and good filling of the left anterior and middle cerebral arteries (arrows). The patient had no deficit and was discharged 3 days post embolisation ambulant and neurologically intact.

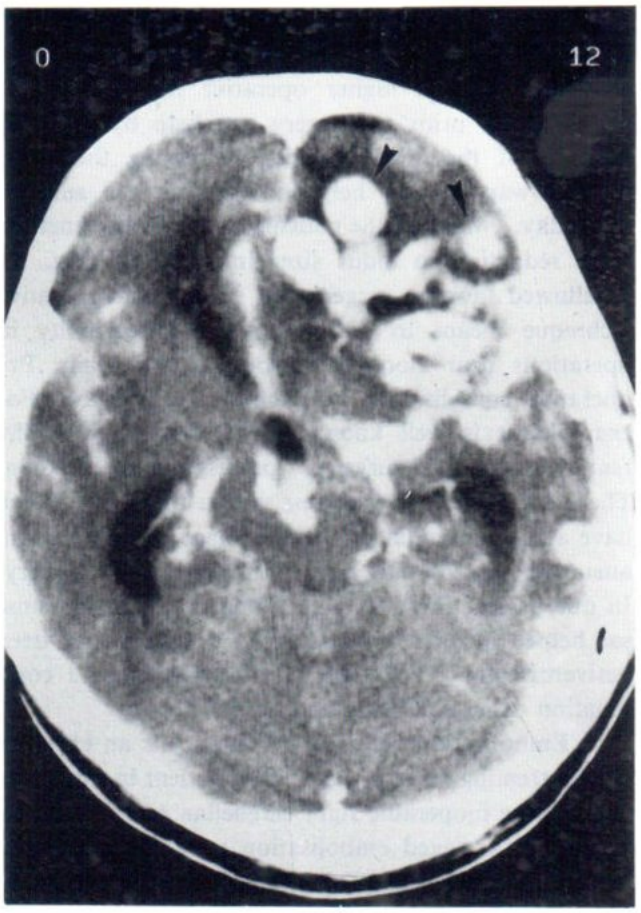

Fig. 1A.

Fig. 1B.

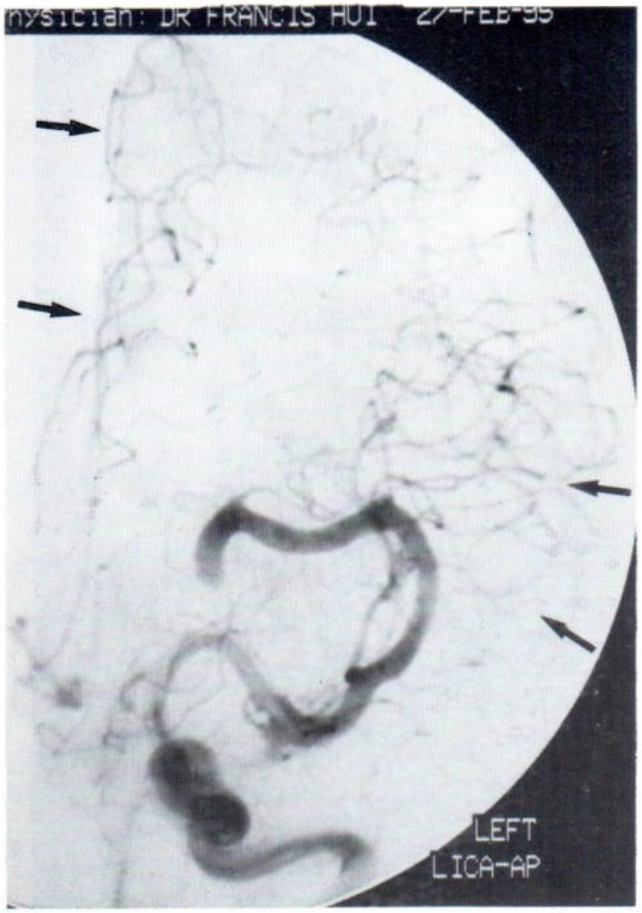

Fig. 1C.

Figs. 2 (a)-(f) 34 year old man with a right facial AVM. Diagnostic angiogram (a) showed an AV fistula in the right cheek. The angiographic catheter is in the right facial artery (arrows). Right internal maxillary angiogram (b) showed opacification of the AV shunt via collateral feeders (arrowheads). Film done after embolisation of the right facial artery feeder (c) demonstrated glue (fat arrow) in the feeding artery, fistula and in the draining vein. Post embolisation right facial angiogram (d) revealed complete occlusion of the AV fistula. The collateral feeders from the right internal maxillary artery have also disappeared even though this artery was not embolised (e). 6 month follow up angiogram (f) showed persistent obliteration of the AV shunt.

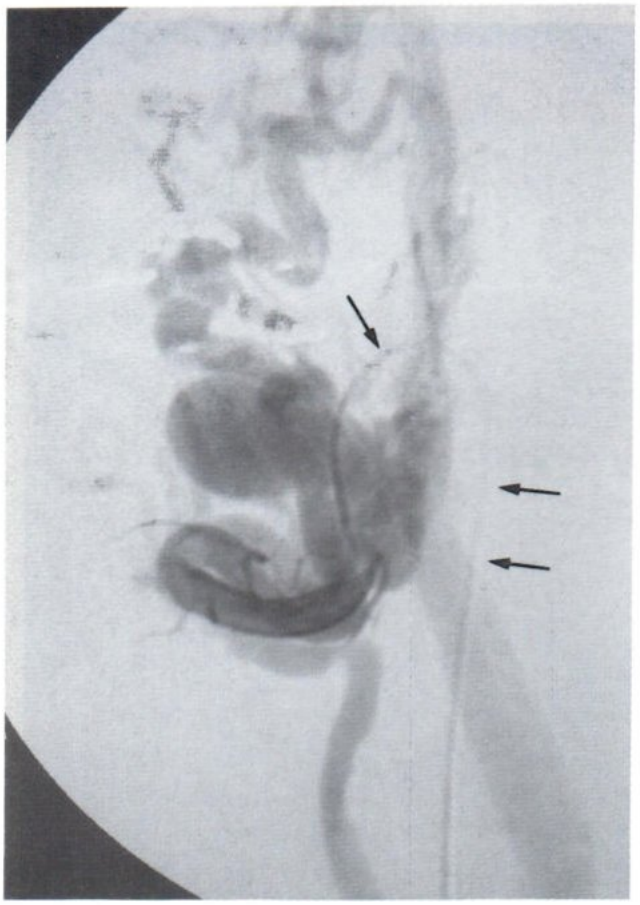

Fig.2A.

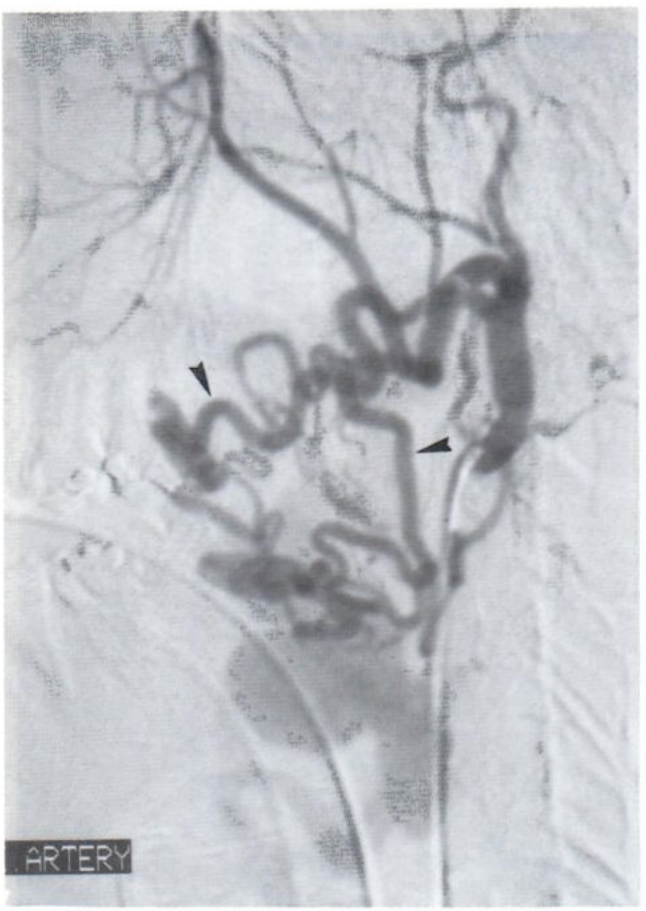

Fig.2B.

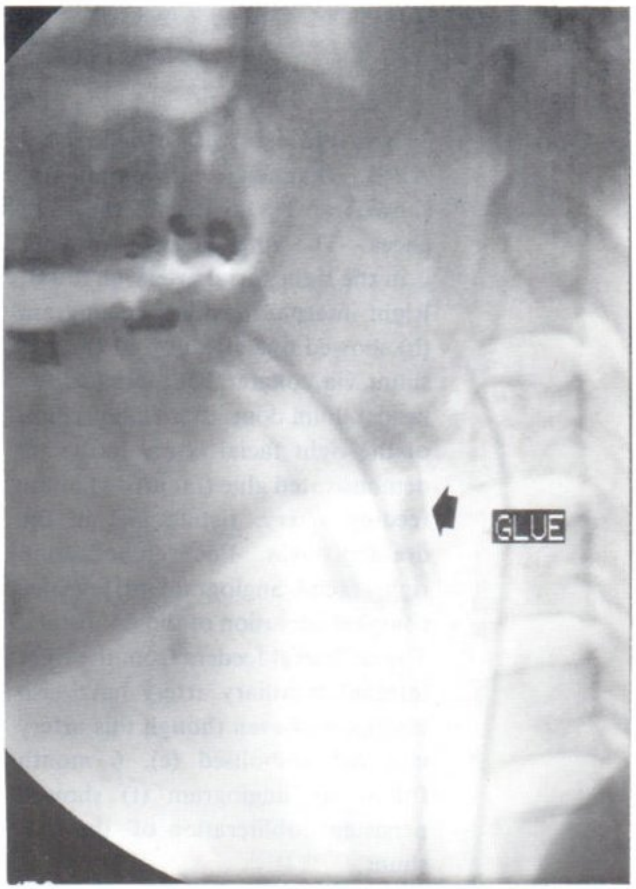

Fig.2C.

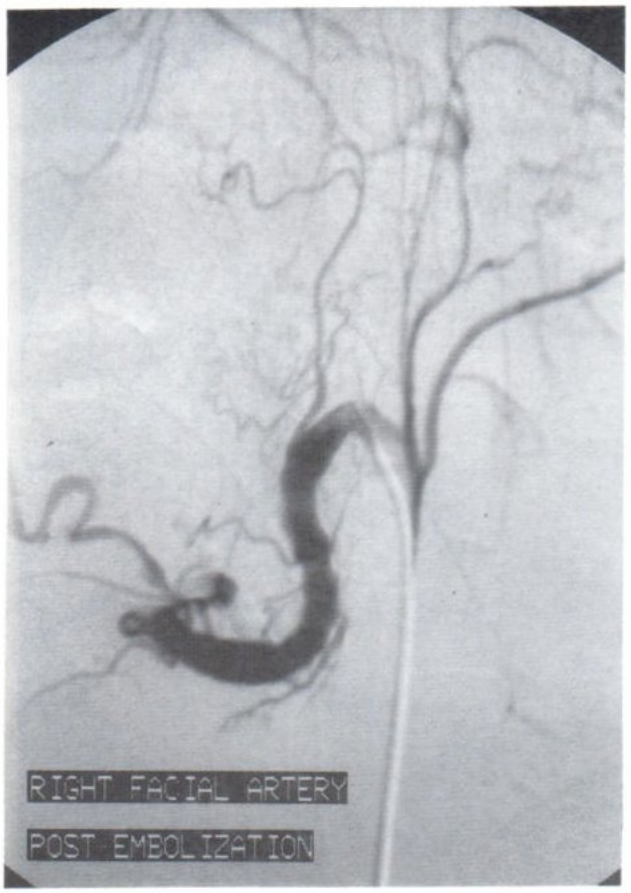

Fig.2D.

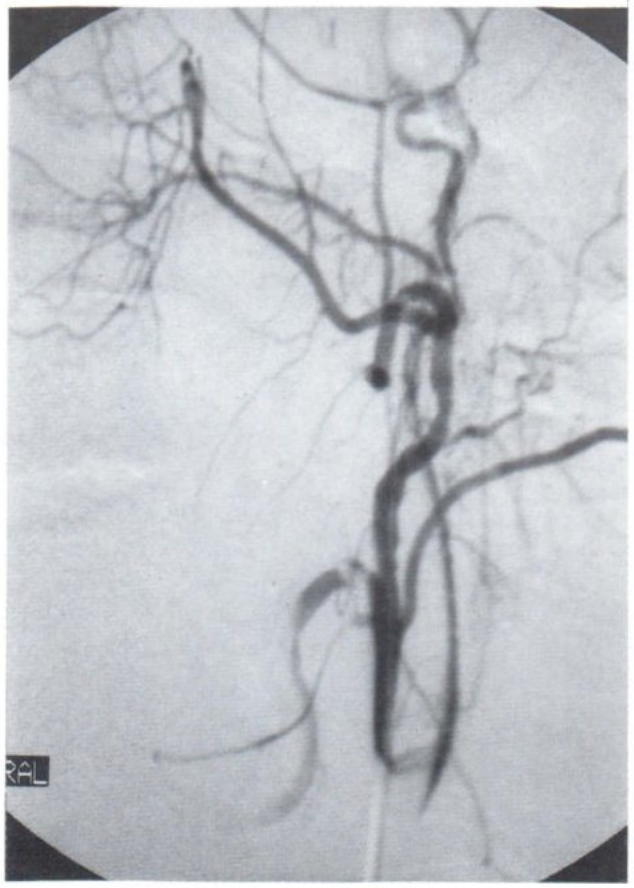

Fig. 2 E.

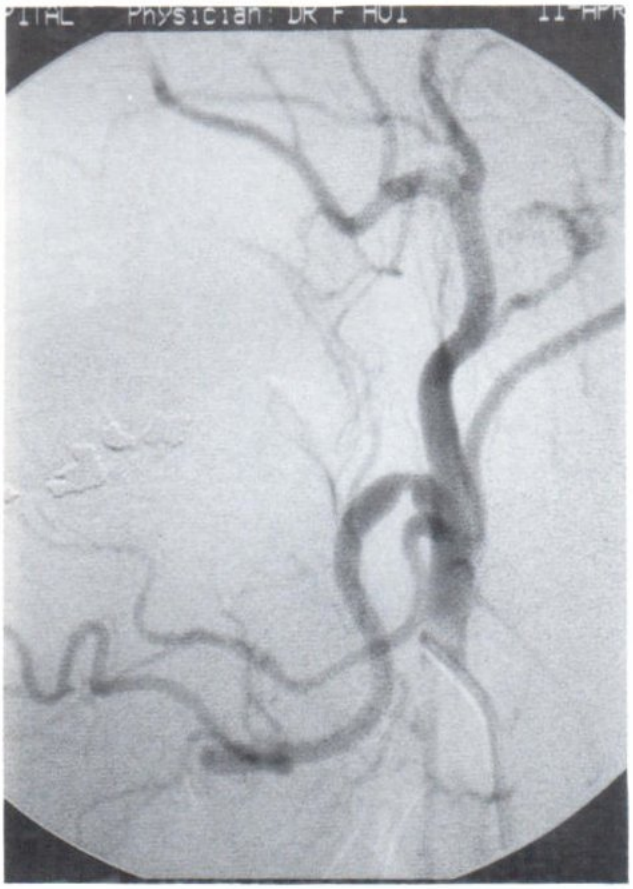

Fig. 2 F.

Figs. 3 (a)-(d) 15 year old girl with left temporal lobe AVM (fat arrow) shown on MRI (a). Pre embolisation angiogram (b) shows the AVM nidus (open arrow-head) with feeders arising from the left MCA. After 2 injections, the nidus is almost completely filled with glue (arrows in c). Post embolisation angiogram (d) indicated good occlusion of nidus. The patient remained well and underwent awake surgery at a later date with complete obliteration of the AVM.

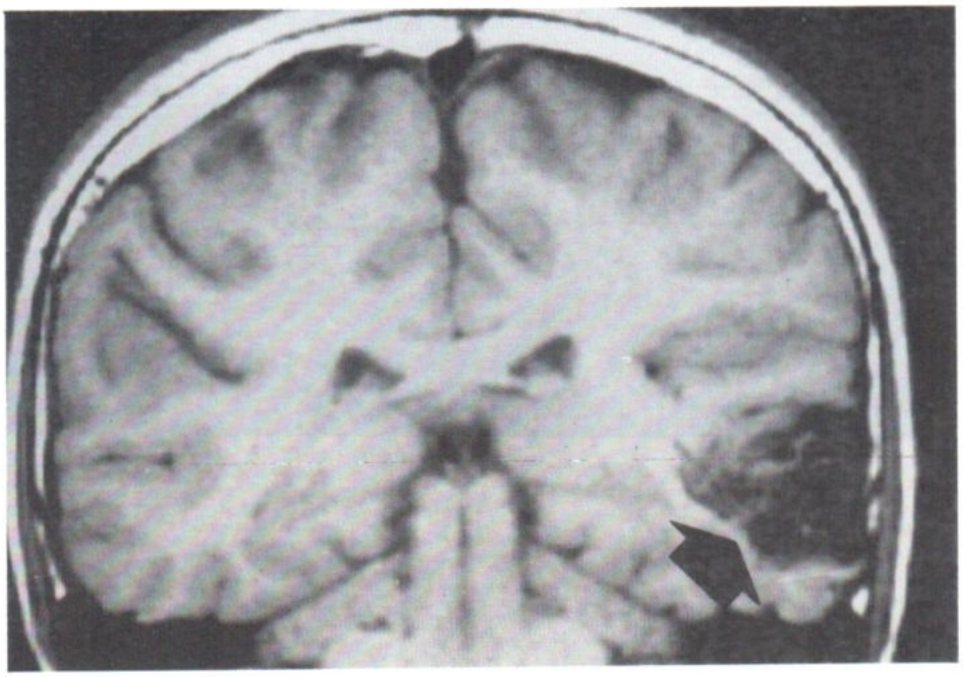

Fig.3A.

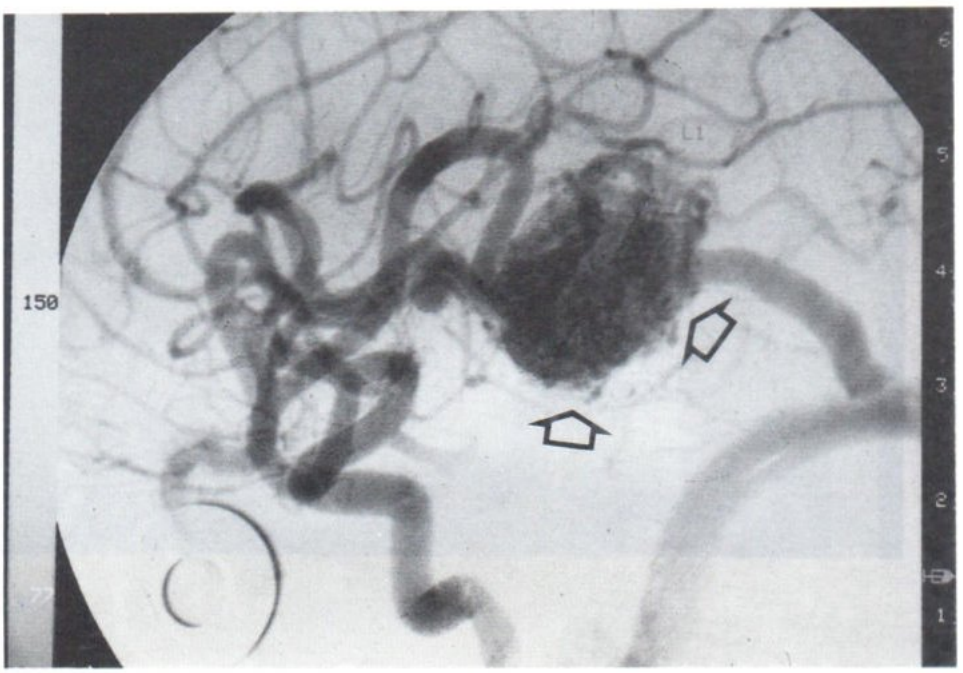

Fig. 3B.

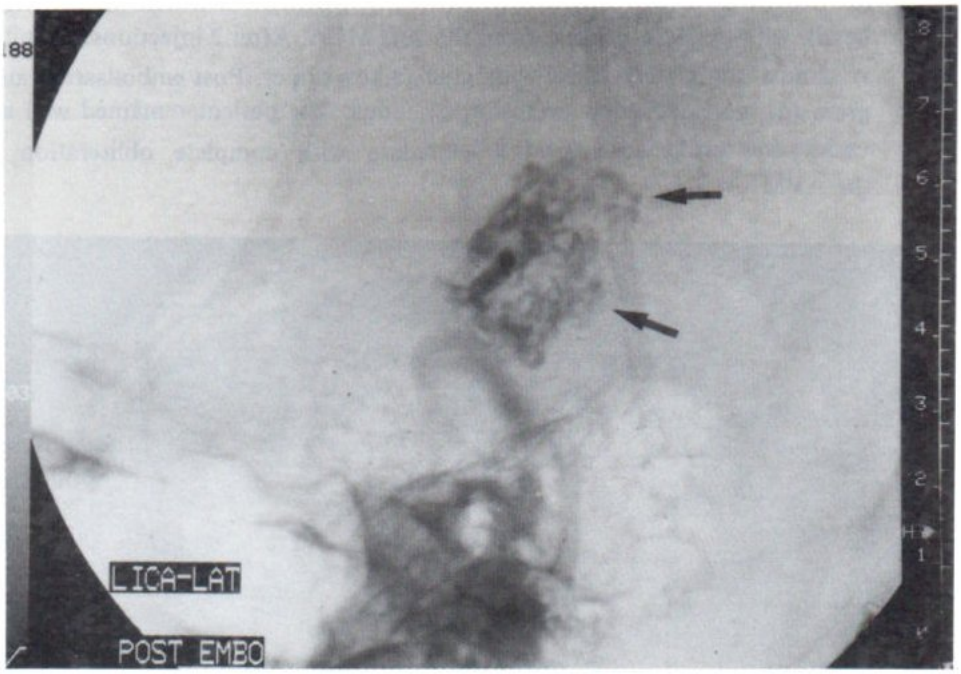

Fig. 3C.

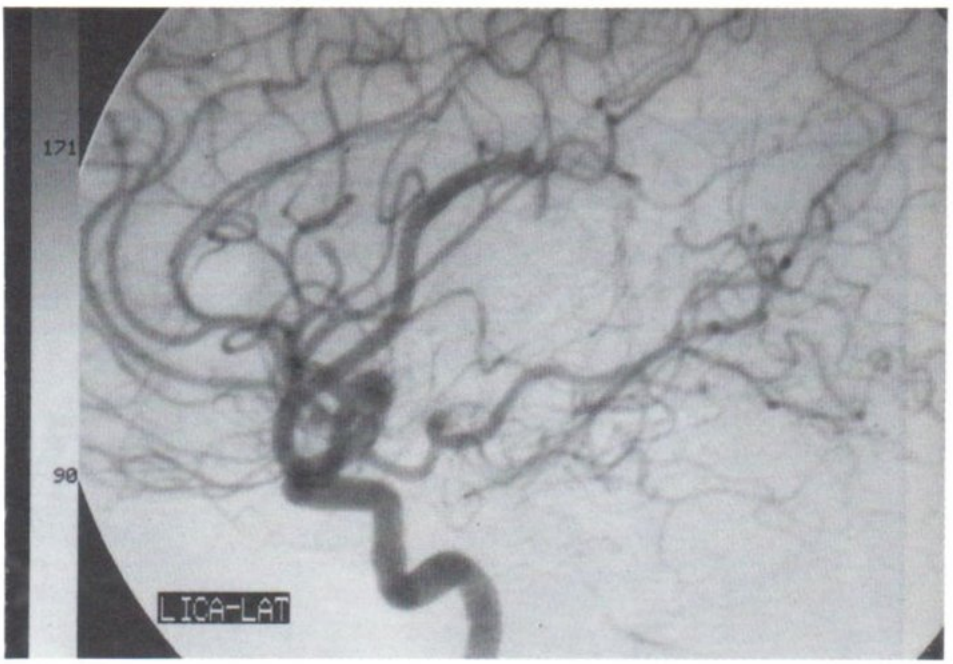

Fig. 3D.

Figs. 4 (a)-(d) 40 year old woman with right frontal AVM which bled and resulted in deep coma on presentation. The diagnostic angiogram (a) indicated the presence of an aneurysm (arrows) in a feeding pedicle from the right anterior cerebral artery. A microcatheter was manoeuvred into this pedicle and glue was then injected into it (b). Post embolisation film (c) showed glue filling the whole aneurysm (fat arrow). The angiogram thereafter (d) showed obliteration of the aneurysm and part of the nidus. The surgeon was then able to resect the whole AVM without any complication.

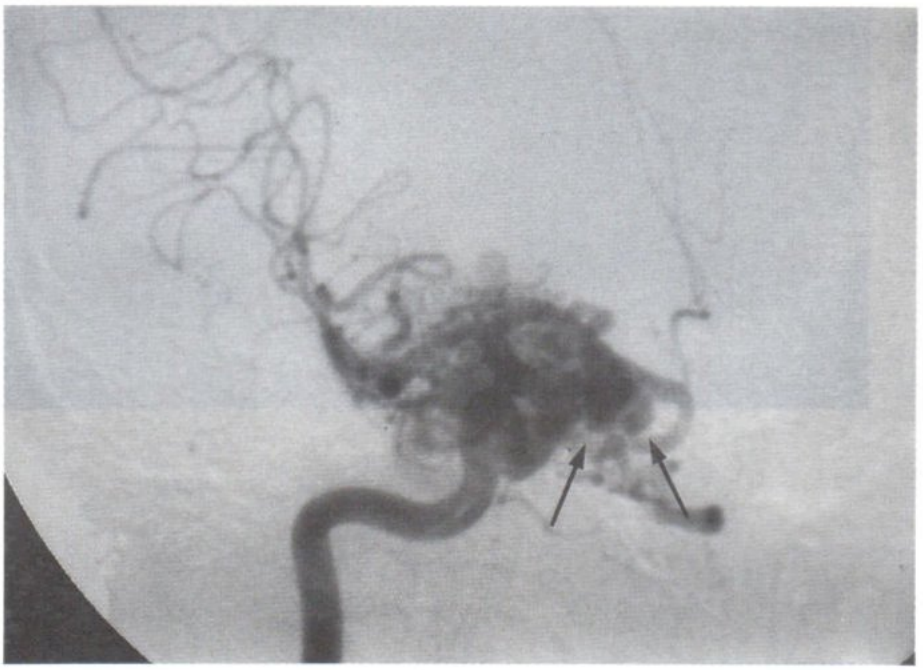

Fig. 4A.

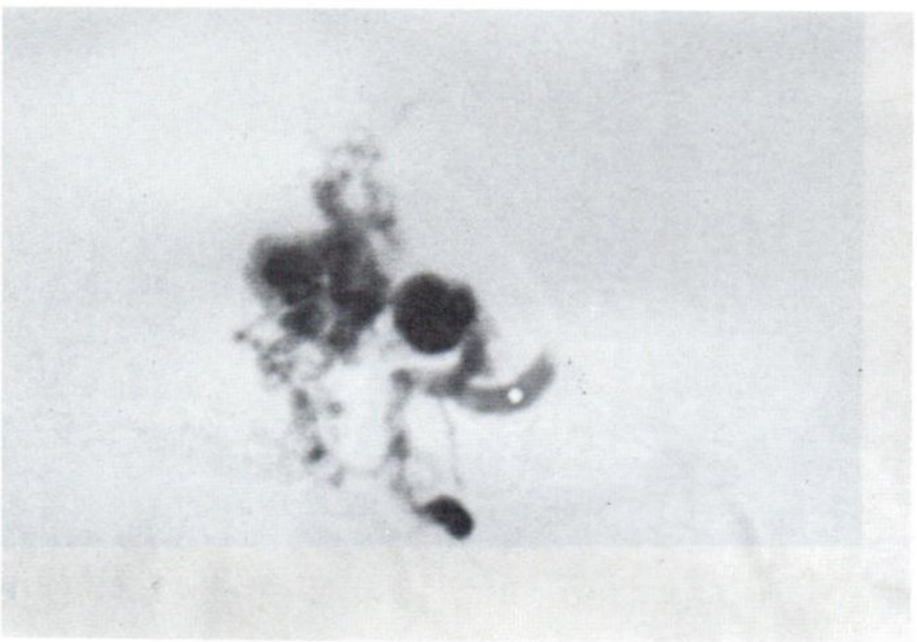

Fig.4B.

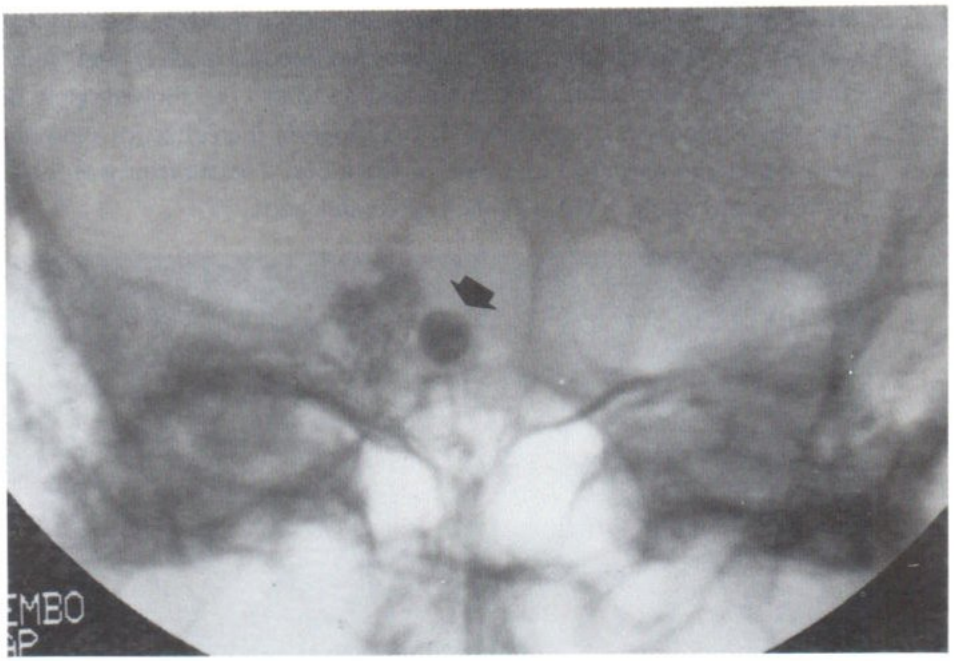

Fig.4C.

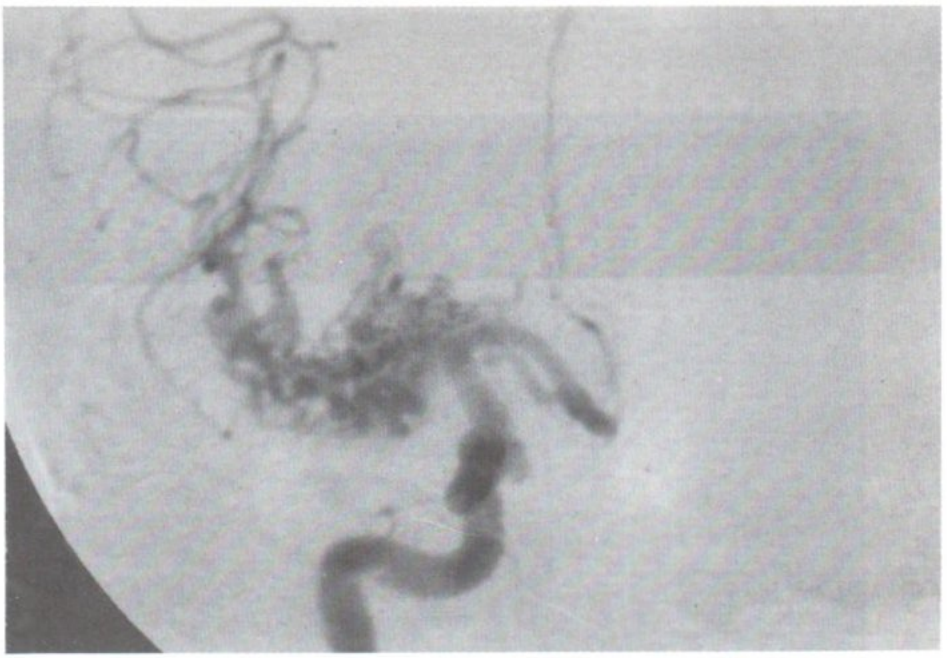

Fig 4 D.

Figs. 5 (a)-(e) 50 year old man who presented in a comatose state. Unenhanced CT scan (a) showed subarachnoid haemorrhage (arrows). Left vertebral angiogram (b) showed considerable spasm in the basilar and left vertebral artery (arrowheads) and a dural fistula (arrows) at the skull base. Superselective angiogram of meningeal feeder (c) with a microcatheter in place showed the AV shunt (arrows) and the arterial aneurysm (open arrowhead). Post embolisation angiogram (d) showed occlusion of the AV shunt but also narrowing of the right posterior cerebral artery due to reflux of glue. He was noted to have a left hemianopia and moderately severe left hemiparesis. Follow up angiogram 2 months post embolisation (e) revealed relief of the spasm in the basilar and left vertebral arteries (arrows) with no filling of the AV fistula. The proximal right posterior cerebral artery remains narrowed (open arrowhead). The patient recovered well and suffered no further haemorrhage. At 6 month post embolisation follow up, he had no visual field loss and only mild left hemiparesis (Grade 4+/5 motor power) and was able to lead a normal lifestyle.

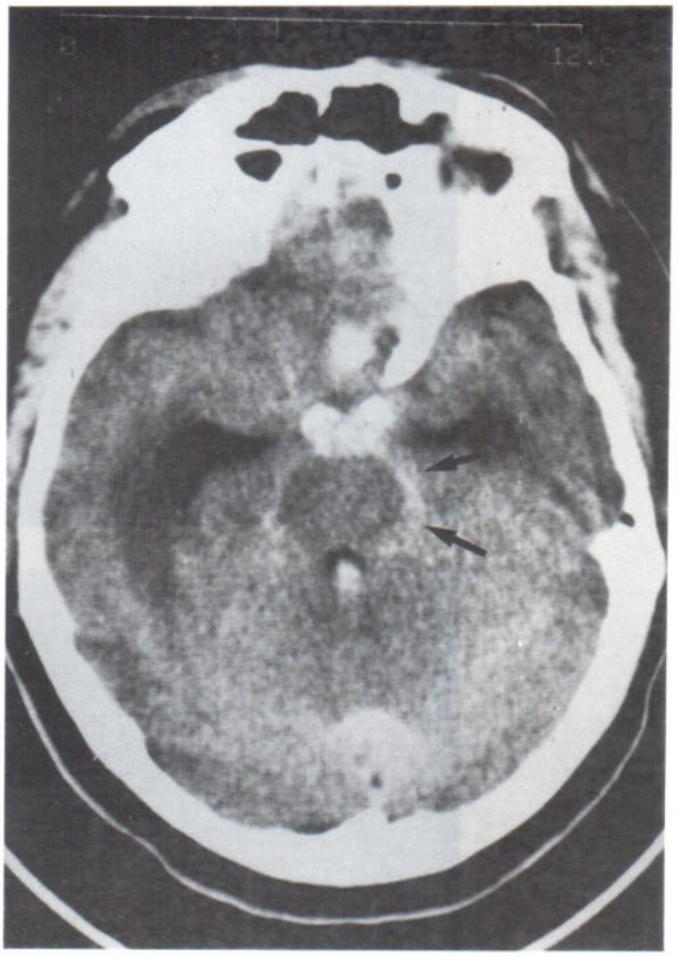

Fig. 5 A.

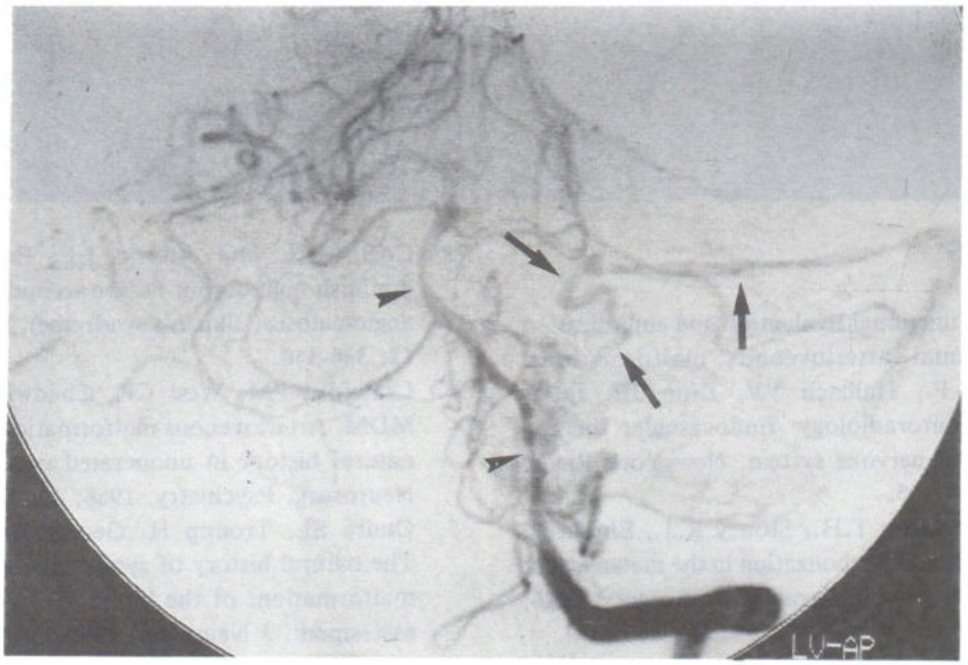

Fig. 5 B.

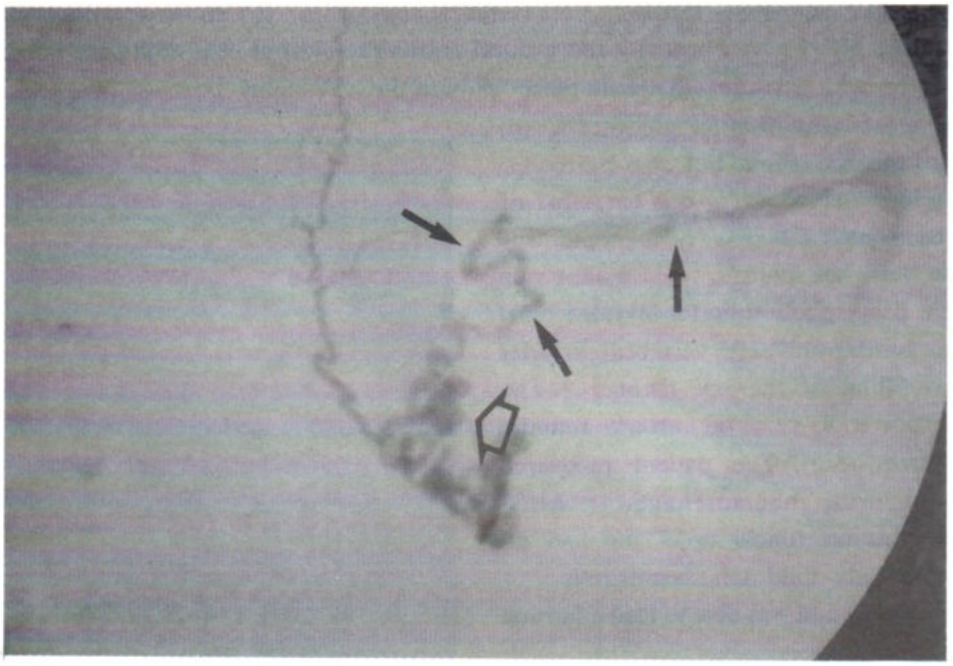

Fig. 5 C.

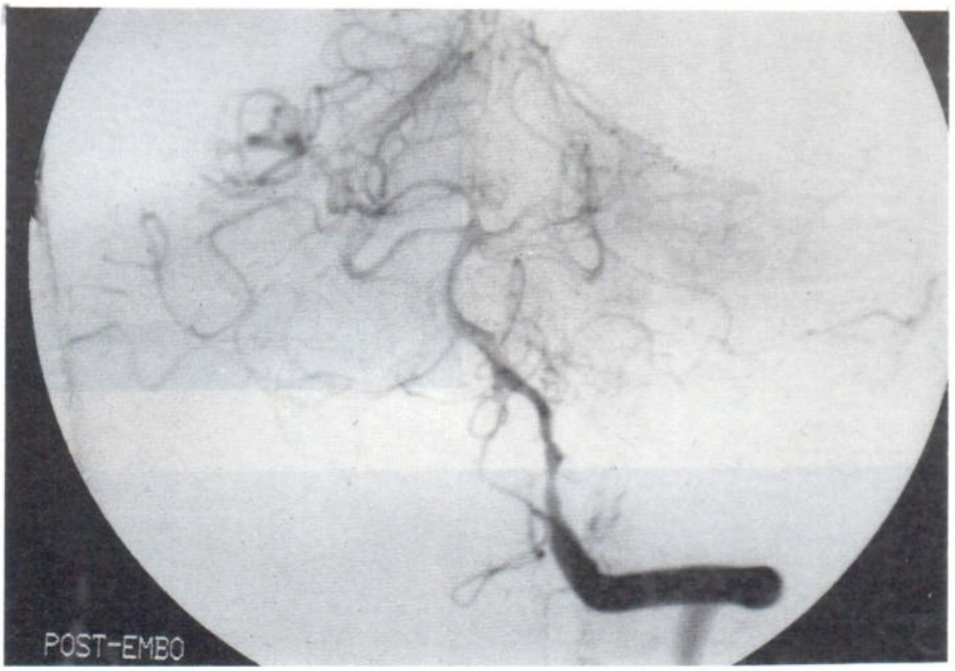

Fig 5 D.

REFERENCES

1. Vinuela F. Functional Evaluation and embolization of intracranial arteriovenous malformations. In Vinuela F., Halbach VV, Dion JE. Interventional Neuroradiology: Endovascular therapy of the central nervous system. New York Raven Press 1992; 77-86.
2. Olcott C., Newton T.H., Stoney R.J., Ehrenfeld W.K. Intra arterial embolization in the management of arteriovenous malformations. Surgery 1976; 79: 3-12.
3. Coel M.N. and Alksne J.F. Embolization to diminish high output failure secondary to systemic angiomatosis (Ullman's syndrome). Vasc Surg 1978; 12: 336-340.
4. Crawford PM, West CR, Chadwick DW, Shaw MDM. Arteriovenous malformations of the brain: natural history in unoperated patients. J Neurol Neurosurg, Psychiatry, 1986; 49: 1-10.
5. Ondra SL, Troupp H, George ED, Schwab K. The natural history of symptomatic arteriovenous malformations of the brain: A 24 year follow-up assessment. J Neurosurg 1990: 73: 387-91.

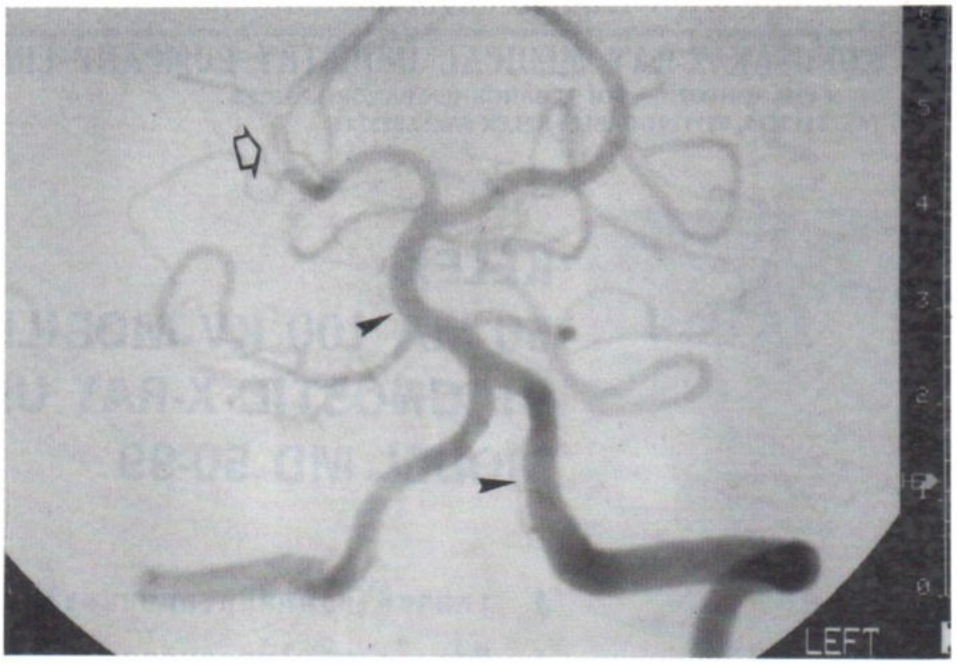

Fig. 5 E.

6. Willinsky R, Lasjaunias P, Terbrugge K, Pruvost P. Brain arteriovenous malformations: analysis of the angioarchitecture in relationship to hemorrhage (based on 152 patients explored and/or treated at the Hospital de Bicetre between 1981 and 1986) J Neuroradiol 1988; 15: 225-37.
7. Marks M, Lane B, Steinberg G, Chang P. Hemorrhage in Intracranial Arteriovenous Malformations: Angiographic determinants. Radiology 1990; 176: 807-13.
8. Wolpert SM, Stein BB. Factors governing the course of emboli in the therapeutic embolization of cerebral arteriovenous malformation. Radiology 1979; 131: 125-131).
9. Mullan S, Kawanaga H et al. Microvascular embolisation of cerebral arteriovenous malformations. J Neurosurg 1979; 51: 621-627.
10. Lasjaunias P., Berenstein A. Surgical Neuroangiography Vol 2. (1987) Springer Verlag. Heidelberg, New York.
11. Wikholm G Occlusion of cerebral arteriovenous malformations with N-Butyl Cyanoacrylate is permanent. AJNR 1995; 16: 479-83.
12. Pelz DM, Lownie SP, Fox AJ, Hutton LC. Symptomatic pulmonary complications from liquid acrylate embolisation of brain arteriovenous malformations. AJNR 1995; 16: 19- 26.
13. Derdeyn CP, Moran CJ, Cross DT, Dietrich HH, Dacey RG. Polyvinyl alcohol particle size and suspension characteristics.AJNR 1995; 1335-43.
14. Germano IM, Davis RL, Wilson CB, Hieshima GB. Histo pathological follow up study of 66 cerebral arteriovenous malformations after therapeutic embolisation with polyvinyl alcohol. J. Neurosurg 1992; 76: 607-14.
15. Spetzler RF, Martin NA. A proposed grading system for arteriovenous malformations J Neurosurg. 1986; 65: 476-83.
16. Fox AJ, Pelz DM, Lee DH. Arteriovenous malformations of the brain: Recent results of endovascular therapy. Radiology 1990; 177: 51-7.
17. U HS, Kerber CW, Todd MM. Multi modality treatment of deep periventricular cerebral AVMs. Surg Neurol 1992; 38: 192-203.
18. Spetzler RF, Martin NA, Carter P, Flom RA, Raudzens PA, Wilkinson E. Surgical management of large AVMs by staged embolisation and operative excision. J Neurosurg 1987: 67: 17-28.
19. Dawson III RC, Tarr RW, Hecht ST, Jungreis CA, Lunsford LD, Coffey R, Horton JA. Treatment of arteriovenous malformations of the brain with combined embolization and stereotactic redio-surgery: Results after 1 and 2 years AJNR 1990; 11: 857-864.
20. Marks MP, Lane B, Steinberg GK, Fabrikant JI, Levy RP, Frankel KA, Phillips MH. Endovascular treatment of cerebral arteriovenous malformations following radiosurgery. AJNR 1993; 14: 297-303.

บริษัท คงศักดิ์เอ็กซเรย์การแพทย์อุตสาหกรรม จำกัด
KONGSAK X-RAY MEDICAL INDUSTRY COMPANY LIMITED
212/1 PHAHONYOTHIN SOI 55 BANGKHEN BANGKOK 10220
TEL. 5213214, 5511794 CABLE: KELEX FAX: 5523744

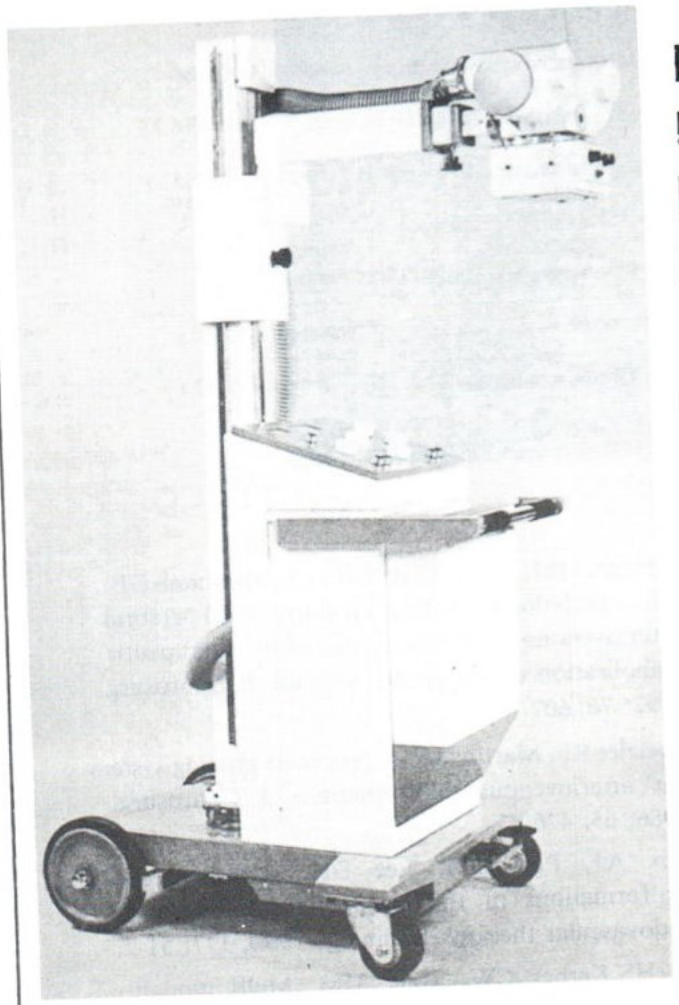

KELEX
50 mA 100 KV MOBILE TYPE DIAGNOSTIC X-RAY UNIT MODEL MD 50-99

- # เหมาะสำหรับคลินิคเอกชนและโรงพยาบาลทั่วไป
- # มีช่างผู้ชำนาญให้การบริการ ตลอดอายุการใช้งาน
- # พร้อมทั้งจำหน่ายอุปกรณ์เอ็กซเรย์

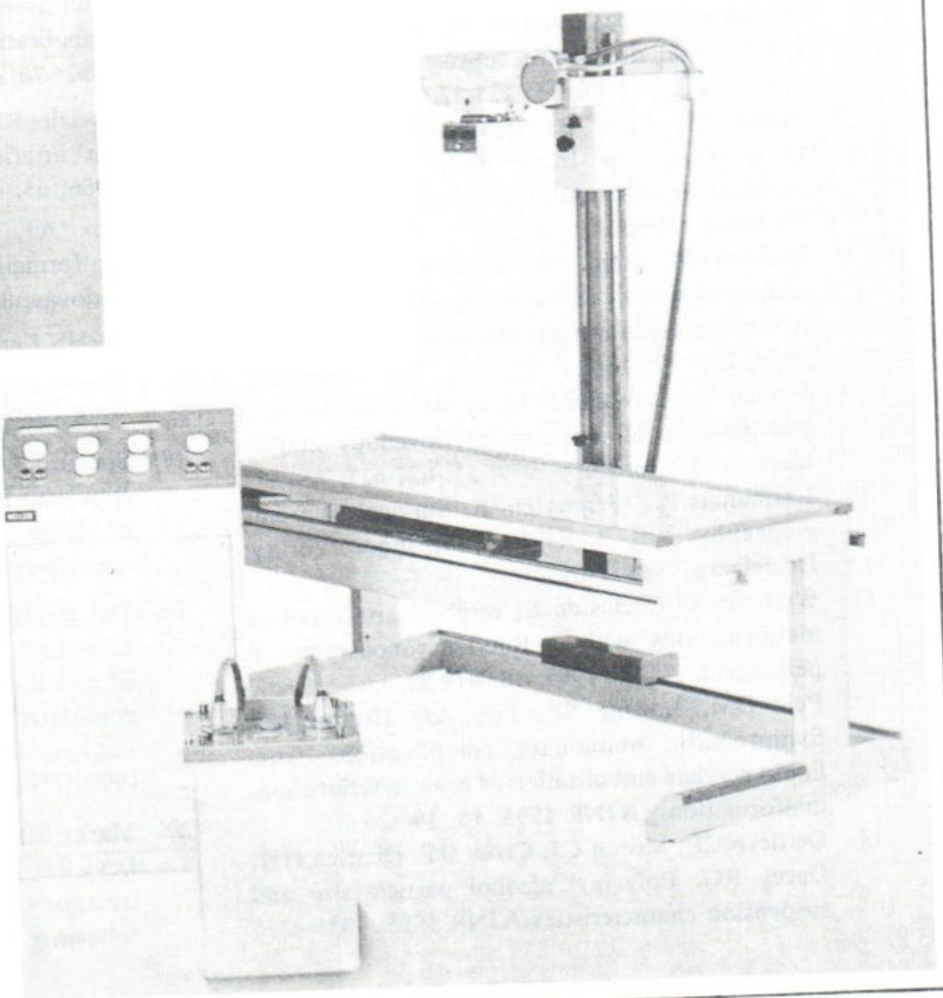

KELEX
MD 100-99 X-RAY SYSTEM
FULL WAVE 100 MA 100 KV

PULMONARY ARTERIOVENOUS MALFORMATION PRESENTNG WITH BRAIN ABSCESS : REPORT OF TWO CASES*

Suphaneewan JAOVISIDHA M.D.**
Permyot KOSOLBHAND M.D.***

ABSTRACT

Brain abscess can be an initial clinical manifestation of asymptomatic pulmonary arteriovenous malformation. Recently, we were referred with two cases of brain abscess who were found to have pulmonary arteriovenous malformation, and presenting with repeated neurological symptoms; one of them had medical treatment for bacterial meningitis, and presenting again with brain abscess at 1 month after discharged, another one had repeated episodes of brain abscesses in three-years interval. Both of them had pulmonary angiographically, surgically, and pathologically proved to have arteriovenous malformation in right middle lobe and right lower lobe of lungs. The clinical findings of hereditary hemorrhagic telangiectasia (Osler-Weber-Rendu Syndrome) were discussed.

The possible association between repeated episodes of brain abscesses and pulmonary arteriovenous malformation should be bone in mind, especially in cases with the clinical findings of hereditary haemorrhagic telangiectasia.

INTRODUCTION

Pulmonary arteriovenous malformation (PAVM) is a condition of pathologic direct communication of abnormally dilated arterial & venous vessels of the lungs. It may be congenital or acquired type. 13-56% of diseased patients may be asymptomatic (4) or presenting with pulmonary symptoms, or neurological symptoms. Brain abscess is about 9% of all neurological presentation.

Osler-Weber-Rendu Syndrome (Hereditary hemorrhagic telangiectasia) is a syndrome transmitted as autosomal dominance which increased penetrance with age, characterized by widespread vascular telangiectasia and frequently resulting in hemorrhages. Association with PAVM is found in 30-40% of diseased patients.

CASE REPORTS

CASE 1.

A 44-year-old female patient was admitted because of severe headache and vomiting.

One month earlier, there was a history of bacterial meningitis which was subsided by three-weeks medical treatment. The patient was discharged without neurological sequele.

On admission, her temperature was 37.7 C, pulse 96, respiration 20 and blood pressure 110/60 mmHg. The patient was drowsy but respond to pain. Head & neck examination showed **intra-oral and lingual telangiectasia** (Fig. 1-2). Heart, lungs & abdomen appear normal. **Clubbing of fingernails** were observed.

Neurological examination showed normal pupils & optic fundi. Motor weakness is observed; grade 4/5

* Presented in the annual meeting of The Radiological Society of Thailand; March 26-28, 1992 at Bangkok Convention Center, Central Plaza, Bangkok, Thailand.

** Department of Radiology, Faculty of Medicine, Ramathibodi Hospital, Mahidol University. Department of Radiology, Faculty of Medicine, Chulalongkorn University.

on the right and 1/5 on the left. Deep tendon reflex is 3 + in all extremities. Babinski's sign was present on the left side. Kernig's sign was positive.

The hematocrit and the hemoglobin concentration were within normal limit; the white-cell count was 10,800 cells/mm^3, with 69% neutrophils, 25% lymphocytes 2% eosinophils and 1% monocyted; platelets were adequate in number. The urine had 50 white-blood cells/high power field; with otherwise normal finding. Fasting blood sugar is 146 mg/dl. Urea nitrogen, creatinine, cholesterol, routine liver function test, & electrolytes were normal. Electrocardiogram revealed normal sinus rhythm.

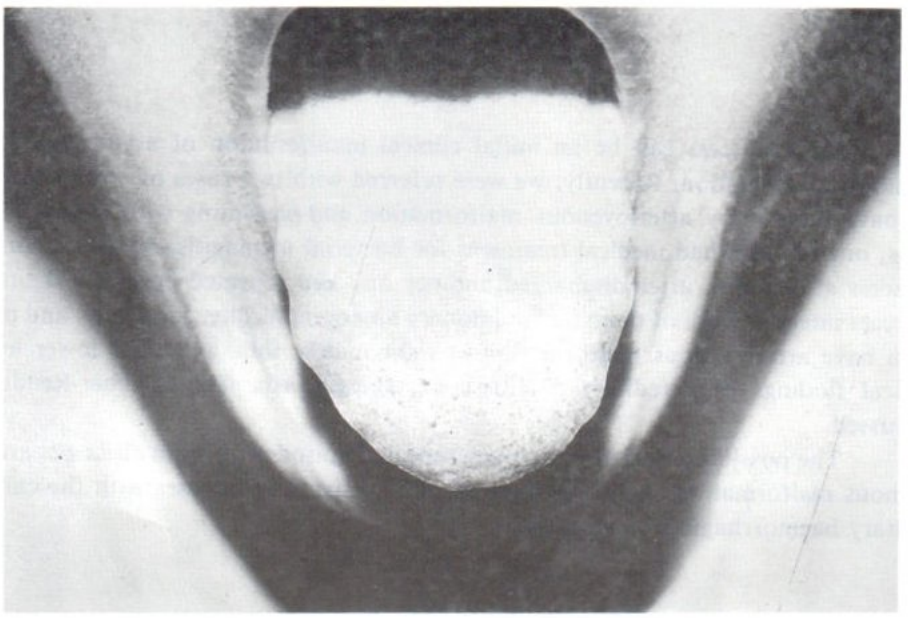

Case 1 : Fig. 1

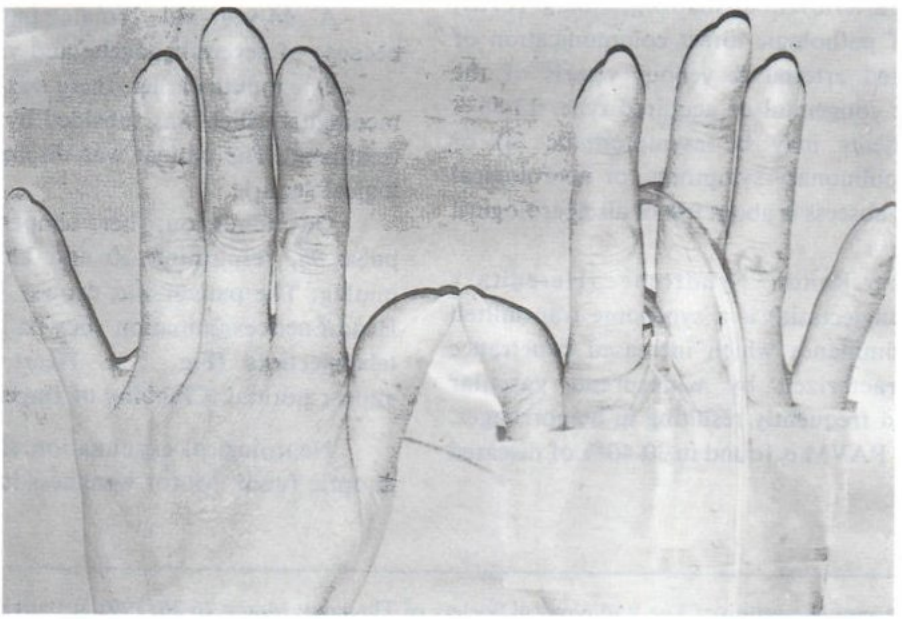

Case 1 : Fig. 2 Clubbing of fingers.

Fig. 1-2 Photograph of the patient revealed lingual telangiectasia & clubbing of fingernails

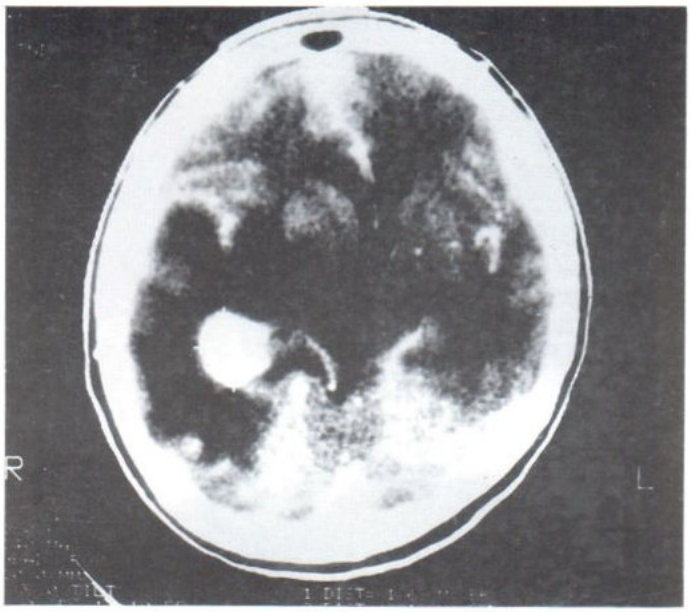

Case 1 : Fig.3 CT scan of the brain showed enhancing solid lesion in the Rt. parietal area with marked perifocal edema. According to this CT finding, tumoral process cannot be completely excluded.

The preliminary diagnosis is **brain abscess, so CT scan of the brain** was performed (Fig. 3).

The patient received conservative treatment, and developed clinical **uncal herniation** on the next day.

The final treatment is explore thoracotomy. The findings were collapsed and destruction of RUL; caseous nodule 1 cm.; & subpleural AVM in RLL with pulsation were found at surgery and RUL and RLL bilobectomy was performed.

Pathological findings showed no malignancy nor parasite. Special stains (AFB & GMS) showed no organism.

CASE 2.

A 36-year-old male patient was admitted (December 1990) because of severe headache with vomiting. He has a history of admission (March 1988) and treated for brain abscess for 6 weeks (Craniotomy + excision of abscess). Retrospective study revealed that evidence of hypoxia was shown at that time by the hemoglobin concentration of 18.4% gm/dl & hematocrit 56%. Arterial blood gas revealed low oxygen concentration. Echocardiogram was normal.

On the second admission, his temperature was 38.3 C, pulse 120, respiratory rate 20, and blood pressure 130/80 mmHg. The patient was drowsy with sluggish respond to verbal command. Head & neck examination was unremarkable. Pulmonary auscultation revealed **bruit at posterior RLL which increased on inspiration.** Heart & abdomen are normal. **Peripheral cyanosis & clubbing of fingernails** are observed, as well as focal **small telangiectasia at the back.**

Neurological examination showed **flame-shaped hemorrhage** in the right eye, including **right facial palsy.** Motor weakness was found; grade 3/5 & 4/5 at upper

After intubation of endotracheal tube and putting on respirator, **the arterial blood gases** were monitored and the results were as followed;

	PO_2 (74-108) mmHg
Day 1; T-piece 40% O_2, 6 LPM	59.6
60% O_2, 6 LPM	67.5
100% O_2, 6 LPM	75.5
Day 2; Bird's respirator 60% O_2	113.1
T-piece 60% O_2, 10 LPM	74.4
100% O_2, 10 LPM	99.6
Day 3; Mask with bag 5 LPM	60.3
Day 4; Room air	37.5

From the arterial blood gas results, the recent impression is **HYPOXIA, & congenital heart disease with R to L shunt** had to be ruled out. Echocardiogram & Pulmonary function test appear normal, and **the systemic shunt** has been searched for: (Fig. 4-8).

& lower extremities on the right respectively; grade 5/5 on the left. Deep tendon reflex was 3+ in all. Babinski's sign was presented on right side. Clonus (patella and ankle) were positive, but not sustained. Palmo-mental reflex was negative. Nuchal rigidity was found.

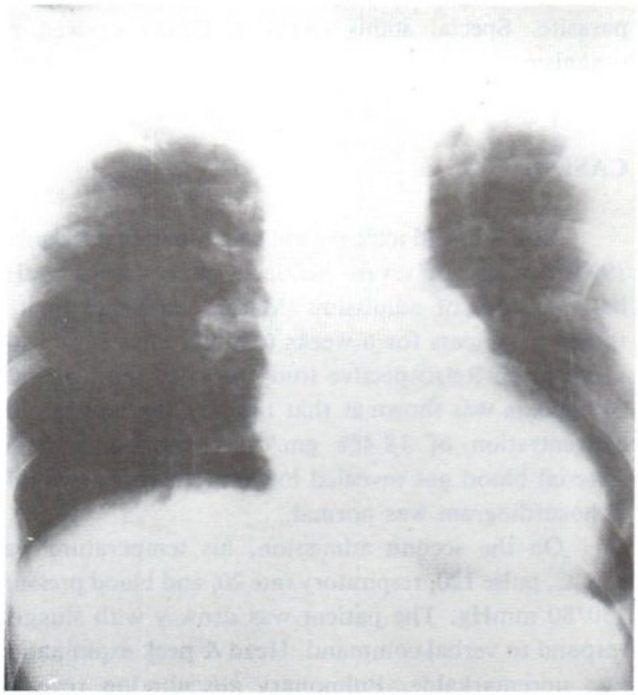

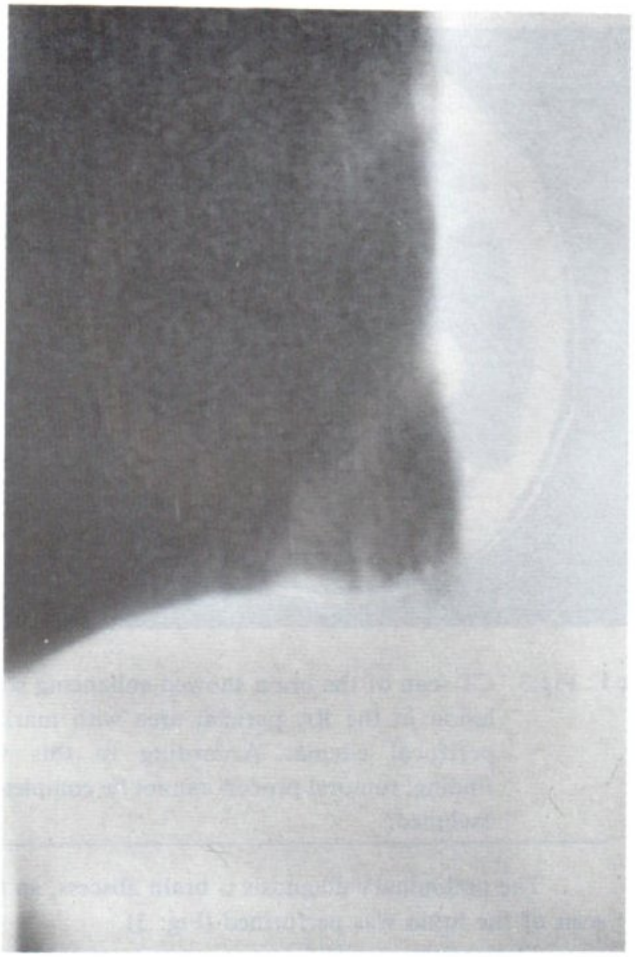

Case 1 : Fig. 4-5 Chest film & tomogram of RLL disclose abnormal vessels at Rt. lung base.

The hemoglobin concentration was 16.9 gm/dl & the hematocrit was 51%. Platelet count was normal in number. Urine analysis, blood urea nitrogen, creatinine, blood sugar, electrolytes, erythrocyte sedimentation rate, & carcino-embryonic antigen were normal.

The first impression was **recurrent brain abscess,** and **CT scan of the brain** was performed. (Fig. 9).

As his history was reveiwed, **arterial blood gas** was monitored at this time;

	PO_2 (74.108) mmHg.
Day 1; Room air	56.8
Day 2; Room air	64.0
Day 3; Room air	54.4
Day 4; Room air	56.6

The clinical hypoxia was diagnosed, and echocardiogram was normal without vegetation, myxoma, or shunt. Further investigation were as followed. (Fig. 10-17)

Gastroscopic examination showed 4-5 telangiectatic vessels within the gastric wall

The possible association between repeated episode of brain abseesses and pulmonary arteriovenous malformation should be borne in mind, especially in cases with the clinical findings of hereditary haemorhagic telangicetasia.

DISCUSSION

Osler-Weber-Rendu Syndrome (OWRD) or Hereditary hemorrhagic telangiectasia (HHT) is a syndrome of autosomal dominant transmission which increased penetrance with age, characterizing by widespread vascular telangiectasia and frequently result in bleeding in multiple organs. Skip generation may be occurred in this disease, and 30-40% of the diseased patient have pulmonary arteriovenous malformation (PAVM). PAVM in OWRD tend to have more incidence of neurologic complication (41%) as compared to 18% incidence in the PAVM-patient without this syndrome.[8,22]

Pulmonary arteriovenous malformation (PAVM) was first described in 1932 by Reading,[5] and defined

Case 1 :
Fig . 6

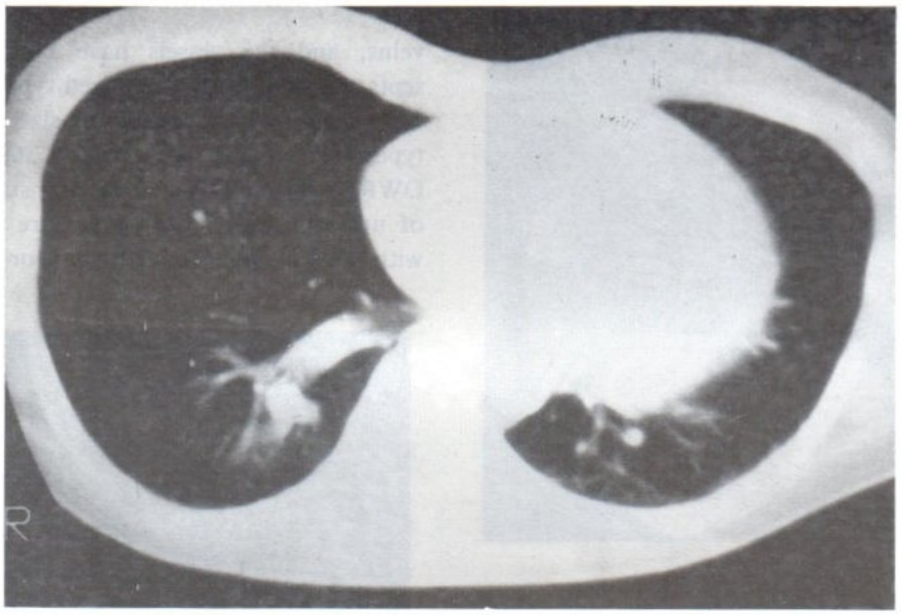

Case 1 :
Fig. 7

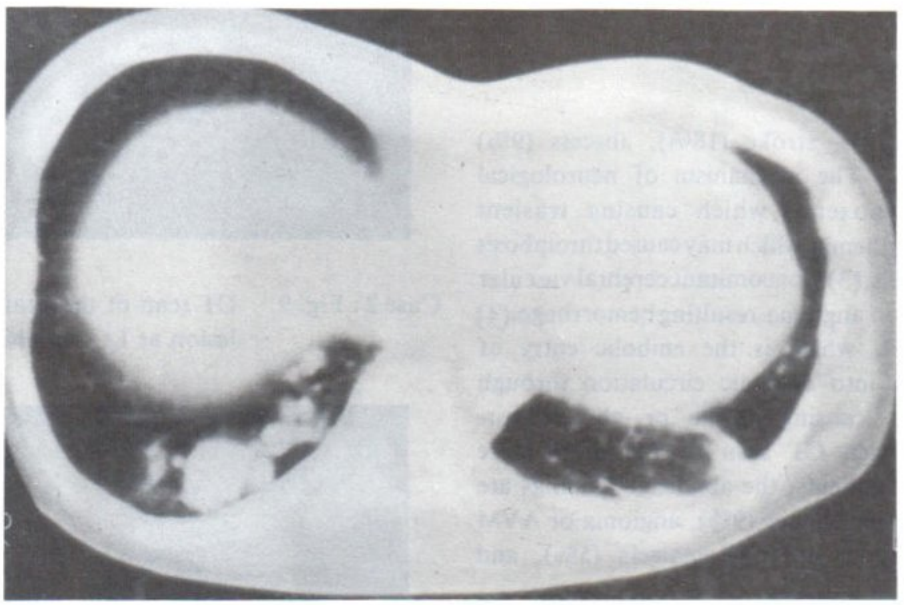

Fig. 6-7 CT scan of thorax revealed enlarged Rt. inferior pulmonary artery (Fig. 6) feeding the cluster of abnormal vessels at Rt. base (Fig. 7)

as pathologic direct communication between arterial & vanous vessels of the lungs. It caused by failure of maturation & regression of fetal splanchnic bed, with resultant dilatation & formation of thin-wall vascular sac.[4] The incidence in male & female patient is 1:1.5-1.9, with 10% diagnosed in childhood. It may be unrecognized until second or third decade.[22] It is unilateral in 75%, and single lesion in 64% of cases. The most common location is lower lobe (60%), and frequently located in the medial third of the lung.[4] The symptoms are likely to occur when the lesion is more than 2 cm in size or producing more than 25% shunt.[4] The triad of symptoms are cyanosis, clubbing of fingernails & polycythemia. The common pulmonary symptoms are dyspnea (71%), hemoptysis (13%), and hemothorax (9%).[27]

Some of the patients may present with neurological symptoms, as in our cases, with migraine as the leading neurological complaint (43%). The others are transient

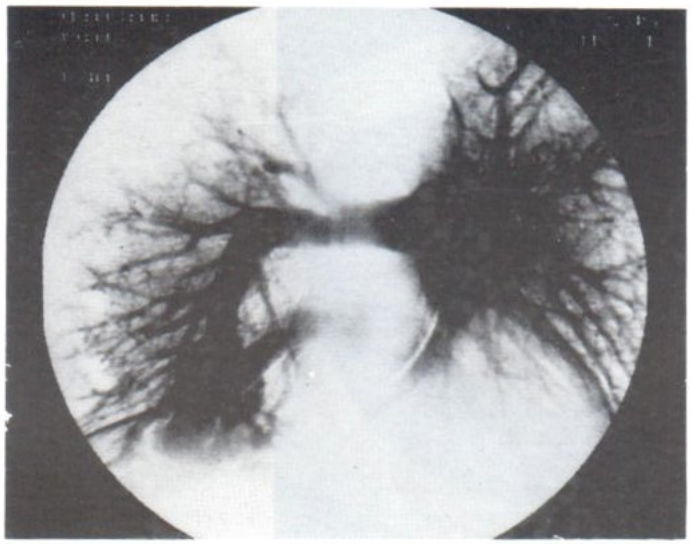

Case 1: Fig. 8 Digital subtraction pulmonary angiogram confirmed the CT findings, as well as demonstrating abnormally dilated vein draining into Lt. atrium.

ischemic attack (37%), stroke (18%), abscess (9%) and seizure (8%).[27] The mechanism of neurological deficits are (1) Hypoxemia, which causing trasient symptom (2) Polycythemia, which may caused thrombosis of intracranial vessels. (3) Concomitant cerebral vascular lesion i.e. AVM or angioma resulting hemorrhage. (4) Paradoxical emboli, which is the embolic entry of venous thrombosis into systemic circulation through right-to-left shunt, causing stroke or abscess formation.[8,15] And when CT scan of the brain were performed in these patients, the abnormal findings are stroke (36%), atrophic change (9%), angioma or AVM (5%), porencephaly or encephalomalacia (5%), and abscess (3%).[27]

There are three types of classification of PAVM; classified by the cause, angioarchitecture, or number & size. By the cause, there are congenital & acquired types. The congenital type is frequently associated with OWRD (33-60%), and 5% of this type associated with brain abscess.[4,8,19] The acquired type may be secondary to varying causes; trauma, surgery, infection, long standing hepatic cirrhosis, chronic inflammatory pulmonary disease, or metastasis such as thyroid carcinoma.[4,8,17]

Classification by its angioarchitecture consisted of the simple type (79%), which having single arterial feeder & single draining vein, and the vessel has bulbous and non-septated appearance; the complex type (21%), which having 2 arterial feeders and 2 draining veins, and the vessels have bulbous with internal septation; and lastly the mixed type.[17]

Classified by number & size composed of four types; (1) solitary type, which 36% associated with OWRD; (2) multiple, of varying size and (3) multiple of uniformed size, both types are 57-88% associated with OWRD; and (4) diffuse type or telangiectatic type.

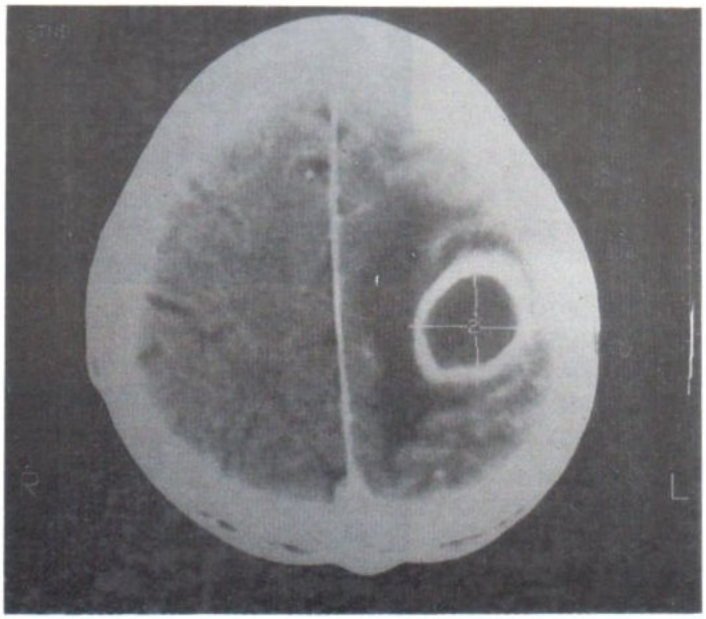

Case 2: Fig. 9 CT scan of the brain showed ring enhancing lesion at Lt. parietal area.

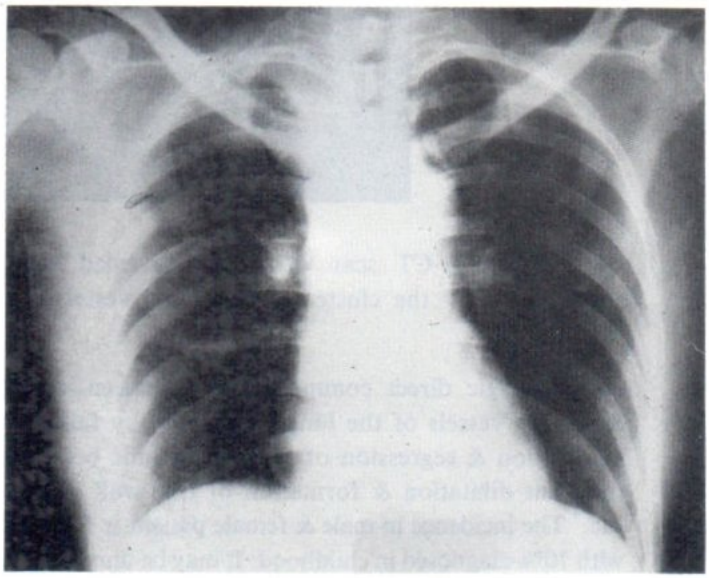

Case 2: Fig. 10 Chest film revealed Rt. paratracheal density & calcified nodule at Rt. hilar area. No abnormal vessel was demonstrated.

In conclusion, we have reported two cases of brain abscess with underlying pulmonary arteriovenous malformation. This association is relatively rare, as they are 9% of the patient with PAVM presenting with neurological deficits and 3% demonstrated by CT scan of the brain. However, this association should be borne in mind in the young patient with repeated neurological episodes or stroke in the young.

The author would like to express her sincere thank to the Associates Professor Saroj Wannaprug, Department of Radiology, Faculty of Medicine Siriraj Hospital for permission to report on the angiographic study of the first case. She also would like to express her thanks and gratitude to Wing Commander Napavadee Impoolthup of Phumipol Air Force Hospital for advices and support.

Case 2 :
Fig. 11.

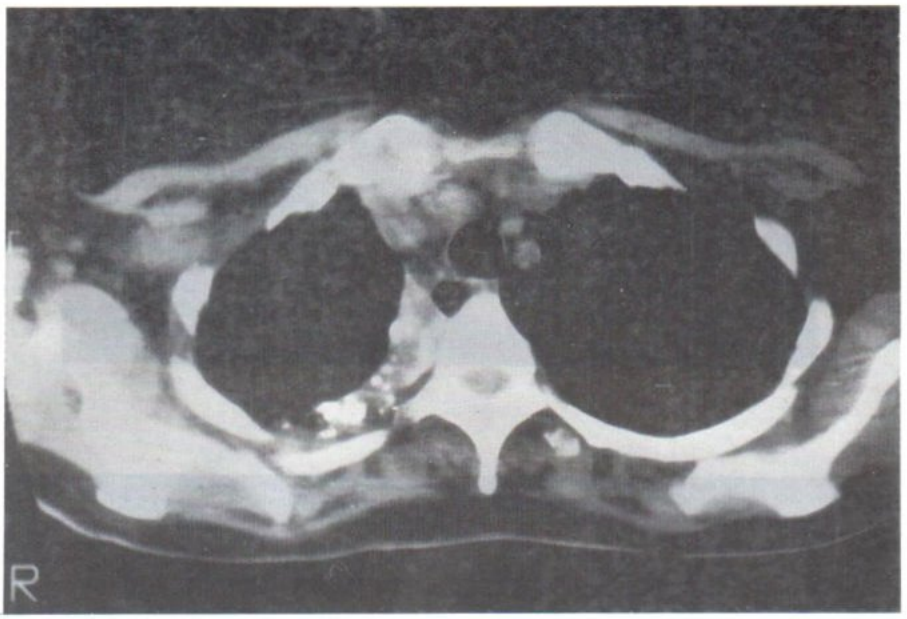

Case 2 :
Fig. 12.

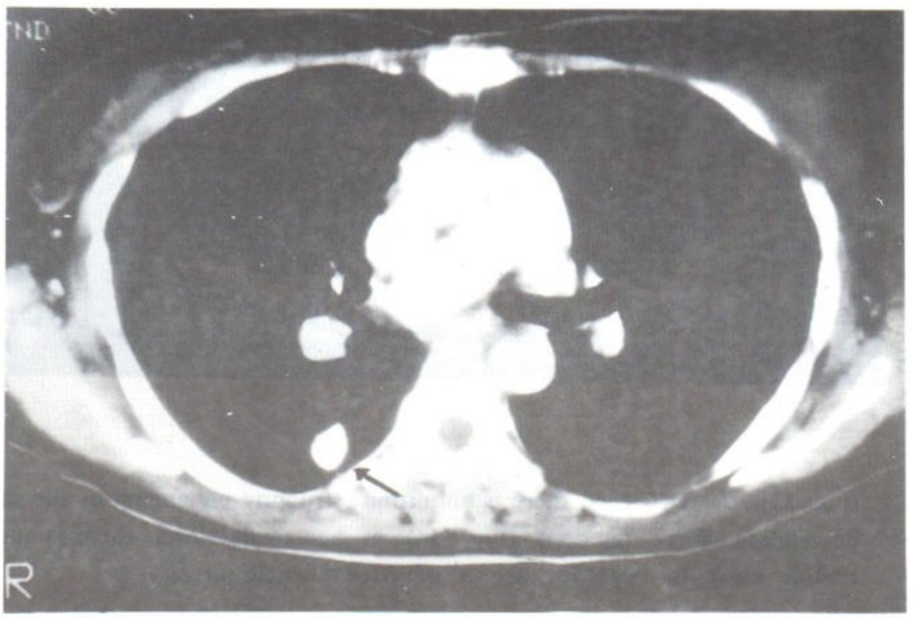

Fig. 11-12 CT scan of thorax; (Fig. 11) at upper lobe level revealing calcified atelectasis of RUL; (Fig. 12) at hilar level showing calcified nodule (arrow) situating in superior segment of RLL.

Case 2 :
Fig. 13.

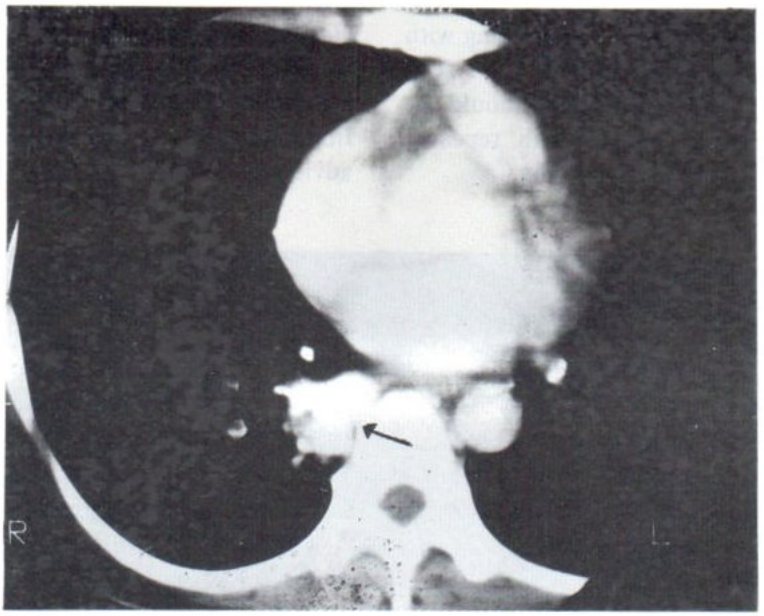

Case 2 :
Fig. 14.

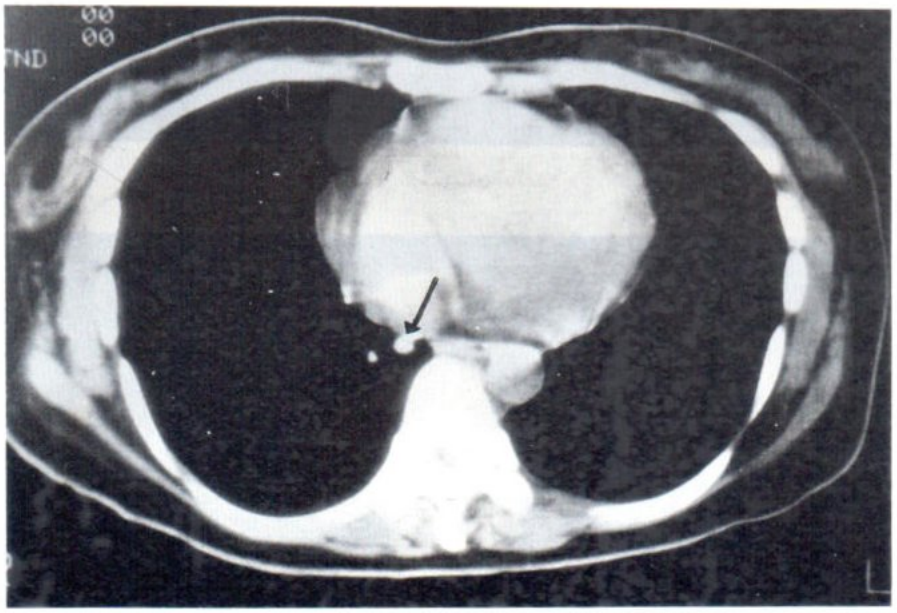

Fig. 13-14 (Fig. 13) At atrial level, there is abnormal structure enhancing as the same degree as descending aorta (arrow); (Fig. 14) at ventricular level, there is small enhancing nodule close to posterior aspect of Rt. ventricle (arrow).

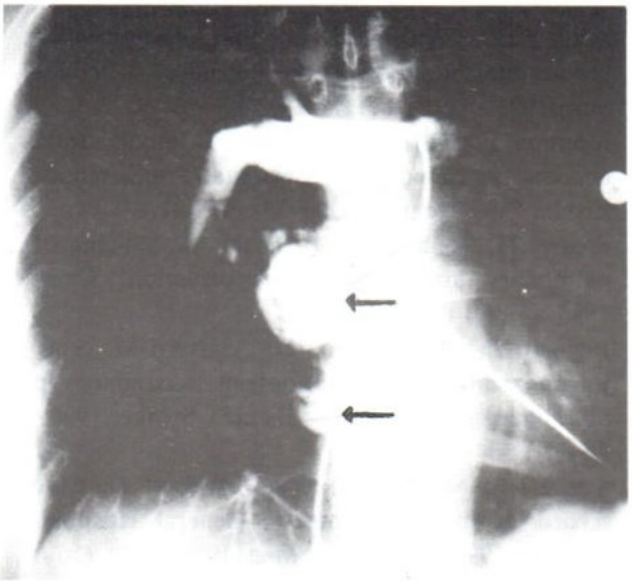

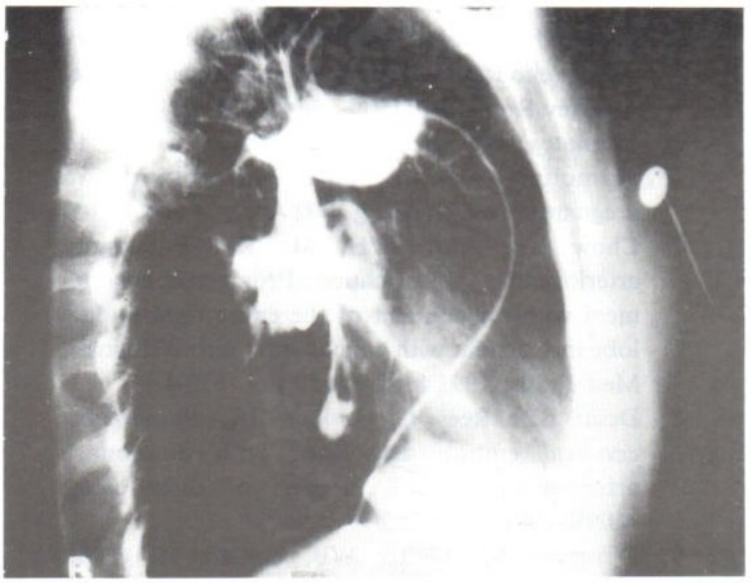

Case 2 : Fig. 15-16 Pulmonary angiogram revealed two foci of pulmonary AVM (arrows) in AP & lateral views.

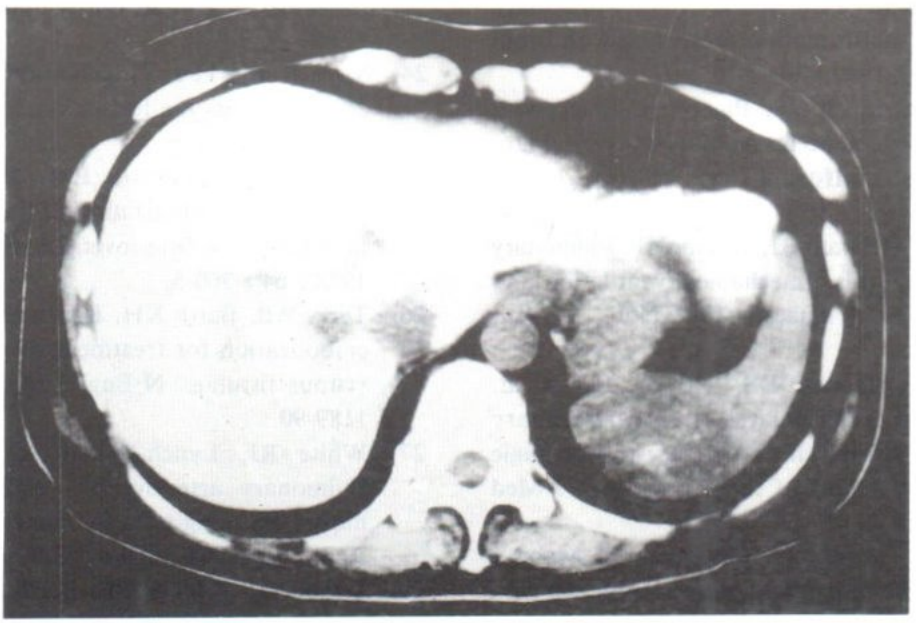

Case 2 : Fig. 17 Plain CT scan of upper abdomen revealed hemochromatosis of the liver parenchyma secondary to chronic hypoxia. A calcified mass-like lesion within posterior splenic tip was likely splenic hemangioma.

REFERENCES

1. Allen SW, Whitfield JM, Clarke DR, et al. Pulmonary arteriovenous malformation in the newborn : a familial case. Pediadr Cardiol 1993 Jan ; 14 (1) : 58-61.
2. Armitage JM, Fricker FJ, Kurland G, et al. Pediatric lung transplantation. The years 1985 to 1992 and the clinical trial of FK 506. J Thorac Cardiovasc Surg 1993 Feb ; 105 (2) : 337-45.
3. Armitage JM. Fricker FJ, Kurland g, et al. Pediatric lung transplantation : expanding indication, 1985 to 1993. J Heart Lung Transplant 1993 Nov-Dec ;12 (6 Pt 2) : S246-54.
4. Audenaert SM, Wood BP. Pulmonary arteriovenous fistula associated with Osler-Weber-Rendu Syndrome. AJDC 1990 ; 144 : 575-6.

5. Burke CM, Safai C, Nelson DP,et al.Pulmonary arteriovenous malformation : A critical update. Am Rev Respir Dis 1986 ; 134 : 334-9.
6. Chanatry BJ. Acute hemothorax owing to pulmonary arteriovenous malformation in pregnancy. Anesth Analg 1992 Apr ; 74 (4) : 613-5.
7. Chow LT, Chow WH, Ma KF. Pulmonary arteriovenous malformation. Progressive enlargement with replacement of the entire right middle lobe in a patient with concomitant mitral stenosis. Med J Aust 1993 May 3, 158 (9) : 632-4.
8. Desai SP, Rees C, Jinkins JR, Paradoxical cerebral emboli associated with pulmonary arteriovenous shunts : Report of three cases. AJNR 1991 ; 12 : 355-9.
9. Dinsmore BJ, Gefter WB, Hatabu H, et al. Pulmonary arteriovenous malformation : Diagnosis by gradient-refocused MR imaging. J comput Assist Tomogr 1990 ; 14 (6) : 918-23.
10. Dove AM, Fan LL, Wood BD. Pulmonary arteriovenous malformation presenting with brain abscess. AJDC 1990 ; 144 : 1045-7.
11. Duggan CJ, Grinnell VS, Pigott PC. Successful percutaneous baloon occlusion of a large pulmonary arteriovenous malformation. Thorax 1989 ; 44 : 76-7.
12. Friedman BC, McGrath BJ, Wlliams JF. Pulmonary arteriovenous fistula : mechanical ventilation and hypoxemia. Can J Anaesth 1992 Nov ; 39 (9) : 963-5.
13. Gelfand MS, Stephen DS, Howell El, et al. Brain abscess : Associated with pulmonary arteriovenous fistula and hereditary hemorrhagic telangiectasia : Report of three cases. Am J Med 1988 ; 85 : 718-20.
14. Laroche CM, Wells F, Shneerson J. Massive hemothorax due to enlarging arteriovenous fistula in pregnancy. Chest 1992 May ; 101 (5) : 1452-4.
15. Loscalzo J. Paradoxical embolism : Clinical presentation, diagnostic strategies, and therapeutic options. Am Heart J 1986 ; 112 (1) : 141-5.
16. Love BB, Biller J, Landas Sk, et al. Diagnosis of pulmonary arteriovenous malformation by ultrafast chest computed tomography in Rendu-Osler-Weber syndrome with cerebral ischemia-a case report. Angiology 1992 Jun ; 43 (6) : 522-8.
17. Lundell C, Finck E. Arteriovenous fistula originating from Rasmussen aneurysms. AJR 1983 ; 140 : 687-8.
18. Mitchell RO, Austin EH 3d. Pulmonary arteriovenous malformation in the neonates. J Pediatr Surg 1993 Dec ; 28 (12) : 1536-8.
19. Momma F, Ohara S, Ohyama T, et al. Brain abscess associated with congenital arteriovenous fistula. Surg Neurol 1990 ; 34 : 439-41.
20. Moser RJ, Tenholder MF. Diagnotic imaging of pulmonary arteriovenous malformation. Chest 1986 ; 89 (4) : 586-9.
21. Reguera JM, Colmenero JD, Guerrero M, et al. Paradoxical cerebral embolism secondary to pulmonary arteriovenous fistula. Stroke 1990 ; 21 (3) : 504-5.
22. Scully RE, Mark EJ, Mcneely WF, et al. Case record of the Massachusetts General Hospital, Case 16-1990. N Engl J Med 1990 ; 332 (16) : 1139-48.
23. Sisel RJ, Parker BM, Bahl OP. Cerebral symptoms in pulmonary arteriovenous fistula : A result of paradoxical emboli (7). Circulation 1970 Jan ; 123-8.
24. Stark P, Bjarke E. Noncommunicating pulmonary arteriovenous malformation. AJR 1990 ; 155 : 893-4.
25. Taylor BG, Cockerill EM, Manfredi F, et al. Therapeutic embolization of the pulmonary artery in pulmonary arteriovenous fistula. Am J Med 1978 ; 64 : 360-5.
26. Terry AB, Barth KH, Kaufman SL, et al. Balloon embolization for treatment of pulmonary arteriovenous fistulae. N Engl J Med 1980 ; 302 (21) : 1189-90.
27. White RI, Lynch-Nyhan A, Terry P, et al. Pulmonary arteriovenous malformation : Techniques and long-term outcome of embolotherapy. Radiology 1988 ; 169 : 663-9.
28. White RI, Mitchell SE, Barth KH, et al. Angioarchitecture of pulmonary arteriovenous malformation : An important consideration before embolotherapy. AJR 1983 ; 140 : 681-6.
29. Wood DJ, Krishnan K, Stocks P, et al. Catamenial haemoptysis : a rare cause. Thorax 1993 Oct ; 48 (10) : 1048-9.
30. Abrams HL, Cook PH. Abrams Angiography : Vascular & Interventional Radiology. Vol I, 3rd Ed. Boston : Little, Brown and Company, 1983 : 732-6, 2219-20.

EMBOLIZATION OF THE FIRST THREE SPINAL CORD AVM-CASES IN THAILAND

[1]Sirintara PONGPECH, [2]Suthisak SUTTHIPONGCHAI,

ABSTRACT

PURPOSE : To embolize the spinal cord arterio-venous malformation (SCAVM), by transarterial superselective microcatheterization and injection of N-butyl cyano-acrylate (NBCA) as the permanent embolic material; were performed under prompt anatomical analysis. PATIENTS; MATERIALS AND METHODS: Three patients with SCAVM were treated with NBCA embolization into the arterial feeders as close to the nidus or shunt as possible. Superselective catheterization with microcatheter in co-axial system technique was used. Immediate control post embolization angiogram were performed in all cases with pre and post embolization evaluation of signs and symptoms. RESULTS: All three SCAVMs were technically successful embolized with good anatomical post embolization controlled angiogram. Clinical signs and symptoms were improved without any complications in two patients. A patient got immediate complication of the weakness of upper extremities with remaining minor motor deficit of the right hand at 1 year follow up. CONCLUSION: Transarterial superselective embolization of the SCAVM using NBCA as permanent liquid embolic material; under prompt anatomical and hemodynamic analysis; has recently been one of the most appropriate and effective way for the treatment of SCAVM; which most of them are non surgical lesions.

Key Words **SCAVM,** spinal cord arterio-venous malformation, Embolization.

PATIENTS , MATERIALS AND METHODS .

PATIENT 1:

A 34 years old woman; presented with numbness of right arm since the age of nine. She also have had slightly progressive hyperesthesia of the same extremity during the last 6 years. Diagnosis was made with spinal MRI and angiogram to be SCAVM at C5-7 level which feeders were from both vertebral arteries and the veins drained both upward and downward. (Fig. 1-3).

The first embolization was performed 2 years ago into the right vertebral arterial feeder with the technique of co-axial superselective microcatheterization so that the tip of the microcathter was as close to as the nidus as possible; then the mixture of Histoacryl 1.5 ml. and lipiodal 0.6 ml. were injected into the nidus until a good filling was obtained. After that, approximately 50% of the vascularity in the nidus were disconnected as shown in Fig 4-6. Follow up angiogram study in 3 months showed that the residual nidus was still supplied by the left vertebral arterial feeder but the anterior spinal artery was also visualized in the same injection. (Fig 7). Dicision to perform second embolization had been made and again the same technique of catheterization was performed but this time with some difficulty to pass the microcatheter tip into the feeder

[1] Department of Radiology, Ramathibodi Hospital, Rama 6 Street, Bangkok 10400, Thailand.
[2] Department of Radiology, Siriraj Hospital, Bangkok.

far enough from the anterior spinal artery. During the glue injection (mixture of Histoacryl 1.5 ml. and lipiodol 0.4 ml.) the uncontrolable respiratory artifact in AP view was observed (Fig. 8). The controlled angiogram was performed immediately in which the complete occlusion of the nidus had been shown. (Fig. 9). Five minutes after that, the patient had got the motor deficit of both upper extreminities as

wrist extensor	grade II/V
Hand grip	grade II/V

Immediate treatment of the spinal shock was given. One day later, the neurological evaluation were upper extremities grade III/V except hand grip gr I-II/V

lower extremities grade II/V with foot drop

MRI C spine obtained and showed enlargement of the cervicle spinal cord with some increase SI in T2W image which were compatable with the spinal infarction.

After one year follow up, the patient gained normal motor power except the hand grip were still in grade III-IV/V. The rest of the motor weakness were all fully recovered. Physical therapy has still been continued.

PATIENT II

A 32 years old female; has had first symptoms 2 years ago during her pregnancy; with pain and numbness of the right frank that radiated down to her right leg and foot.

One year later; the symptoms increased with aggravation during walking and excrcise. Neurological examination revealed spastic of both lower extremities, Sensory loss below T10 level, Babinski upward right side with positive clonus was noted.

MRI and diagnostic angiography were performed. The studies revealed that there was the SCAVM locating at dorsal aspect of the conus medullaris with right L2 radiculo-pial artery as the main feeder (Fig. 10-13). Another small dural shunt or radicular AVM was accidentally found from right L3 injection. (Fig. 14) The anterior spinal artery was definitely found at left T10 injection. (Fig. 15)

Embolization was performed using the same technique that had been previously decribed except that the mixture of Histoacryl 1 ml. and Lipiodol 1.4 ml. had been used. This caused 75% of the vascularity in the nidus to disconnect (Fig. 16).

Immediately controlled angiogram had shown that there was total occlusion of the right L2 feeder and the good patency of the Adam-Kiewicz artery with minimally remained feeder (Fig. 16).

At one month follow up, the MRI and the clinical evaluation had shown no more spasticity of the lower extremities. However, the minimal extensor of right big toe weakness was remained without any pain or definite sensory abnormalities. The MRI showed that the glue cast and thrombosis had filled up about half of the nidus.

PATIENT III

A 13 year old boy presented with acute right subcostal pain following by the numbness of both feet which extended up to the umbilical level. The paraplegia had also occurred within a few hours after the beginning of other symptoms. At the hospital; neurological examination were

motor: lower extremities-paraplegia; flaccid tone
sensory: decrease from feet to T8 level; with sacral sparing

DTR: knee and ankle-0/0 both sides; clonus negative
MRI study revealed that there was an acute intramedullary hemorrhage from SCAVM at the level of T6-7 level. (Fig. 17). Diagnostic spinal angiogram was then performed which revealed that the SCAVM was located at the ventro-medial aspect of the cord with the right T8 radiculo-pial artery as the main feeder. (Fig. 18). The anterior spinal artery was identified by the left T10 injection. (Fig. 19-21).

Embolization was performed with the same previously mentioned technique but this time the mixture of Histoacryl 1 ml. and Lipiodol 1.4 ml. were used. About 70% of the vascularity in the nidus was disconnected. (Fig. 22-23).

At one month clinical follow up the improvement of the motor up to grade IV of all extremities was shown and the patient could have normal urination.

MATERIALS AND METHODS

All three patients with clinically suspected SCAVMs were diagnosed with MRI. The good quality subtraction spinal angiography had been performed. In this report; superselective distal catheterization was achieved by a 5F thin wall guiding catheter; spinal curve; and a variable stiffness microcatheter ≺ Minitorquer or Magic (BALT)≻. Superselective guide wire had also been used i.e. (Schnider 010). Permanent liquid embolic agent of NBCA was prepared using lipiodol to make variable mixture concentration and to increase the opacity during fluoroscopy. Therefore, the type of the mixture depended on the hemodynamics and the way to make the distal catheterization.

RESULTS

Among the three cases of SCAVMs in this study, two of them have got immediate clinical improvement even partial embolization achieved (50-70%) until 1 month follow up. The other one had also got the clinical improvement after the 1st session of partial embolization but she had still got neurological deficit after the attempt to get total occlusion in the 2nd session. At 1.5 year follow up she still have had handgrip muscle paresis Gr III.

DISCUSSION

Vascular malformation of the spine and spinal cord are considered to be an uncommon lesion, the incidence ranges from 3-16% of total spinal occupying lesion; and in relation to brain AVMs is 1:4 to 1:8. Treatment of the SCAVMs needs good understanding of the anatomy and hemodynamics; good diagnostic imaging quality and proper technique and materials. All SCAVMs symptomatic patients are indicated to be treated.

We have presented three cases of SCAVMs with endovascular treatment: transarterial superselective distal catheterization in co-axial system; with the use of permanent liquid agent which was known to yield definitive and stable results. There have been numerous previous reports on the use of other materials which usually led to incomplete and transient occlusion. Good analysis of the anatomy, especially the anterior spinal artery and the exact arterial feeders and hemodynamics, are needed in decision making for the treatment. Eventhough the total cure is still the ideal goal; but the partial treatment focused on the weak points would lead to clinical stabilization or improvement. One of our complication supports these hypothesis. Surgery should be reserved for the cases where embolization has failed in that a radiculo-medullary or radiculo-pial artery arises at the same level as the pathologic feeders or the superselective distal catheterization to the safety point is not possible. Alternatively stereotactic focused radiation might play role in the near future.

REFERENCES

1. Berenstein A, Lasjaunias P. Treatment of spine and spinal cord lesion in Surgical neuroangiography. Berlin. Springer-Verlags: 10-45.
2. Horton J, Latchaw R, Gold LH, Rang D Embolization of intramedullary arteriovenous malformations of the spinal cord AJNR 1986; 7: 113-118.
3. Garcia-Monaco R., Lasjaunias P Embolization of spinal AVMs and tumors. Current practice of intervention Radiology. Toronto, Decker: 1990; 154.-161.
4. Rodesch G, Lasjaunias. P Bereutein A. Interventional Neuro-radiology Embolization of Arteriovenous malformations of the spinal cord. Berlin Springer-Verlag, 1990: 135-150.

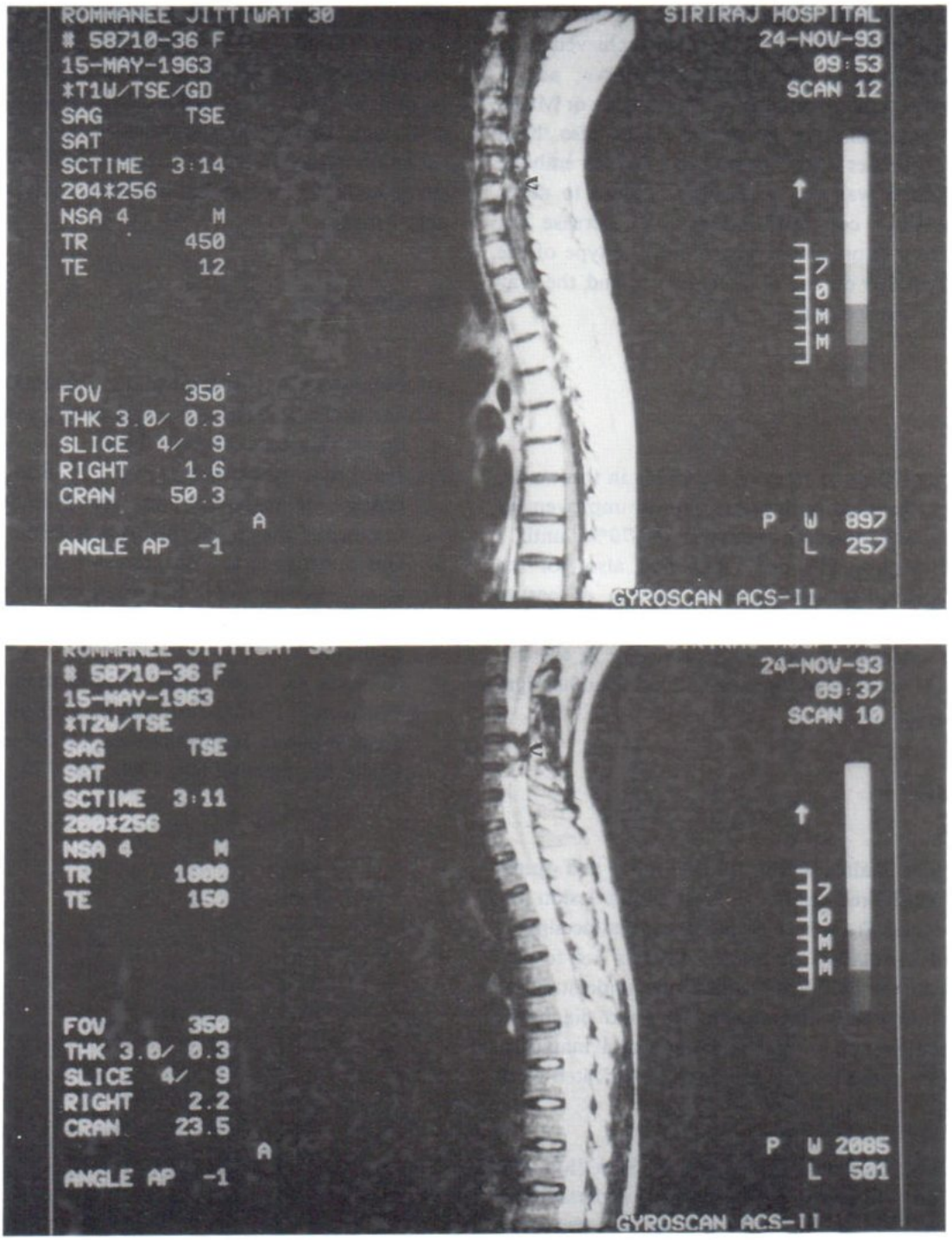

Fig. 1 (A-B) Sagittal MRI T1W, T2W image showed hemorrhage within the AVM lesion at level of C 5-7 (arrow).

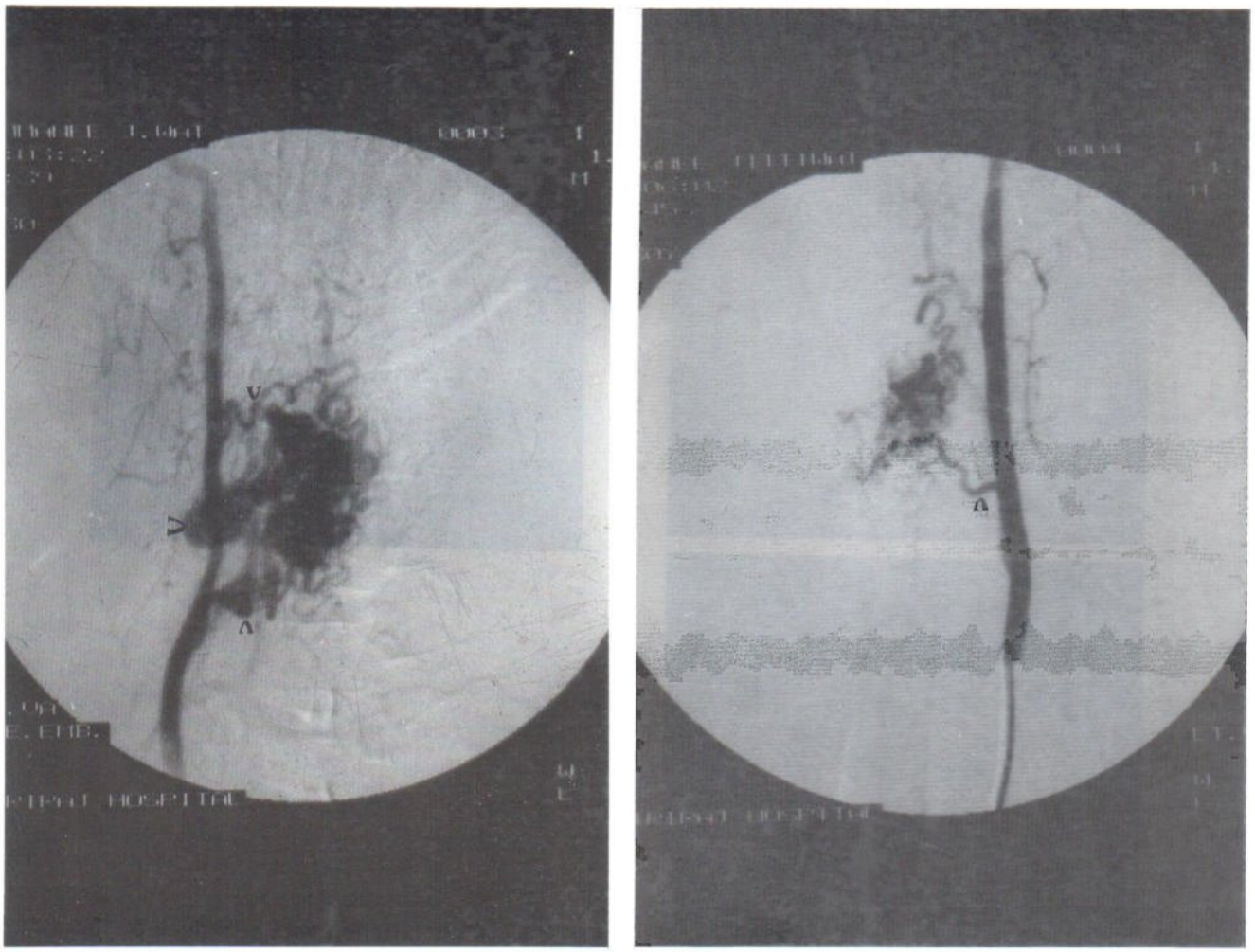

Fig. 2-3. RVA and LVA injection showed at least three feeders (arrows) to the nidus with venous pouches seen from the RVA injection (arrow head).

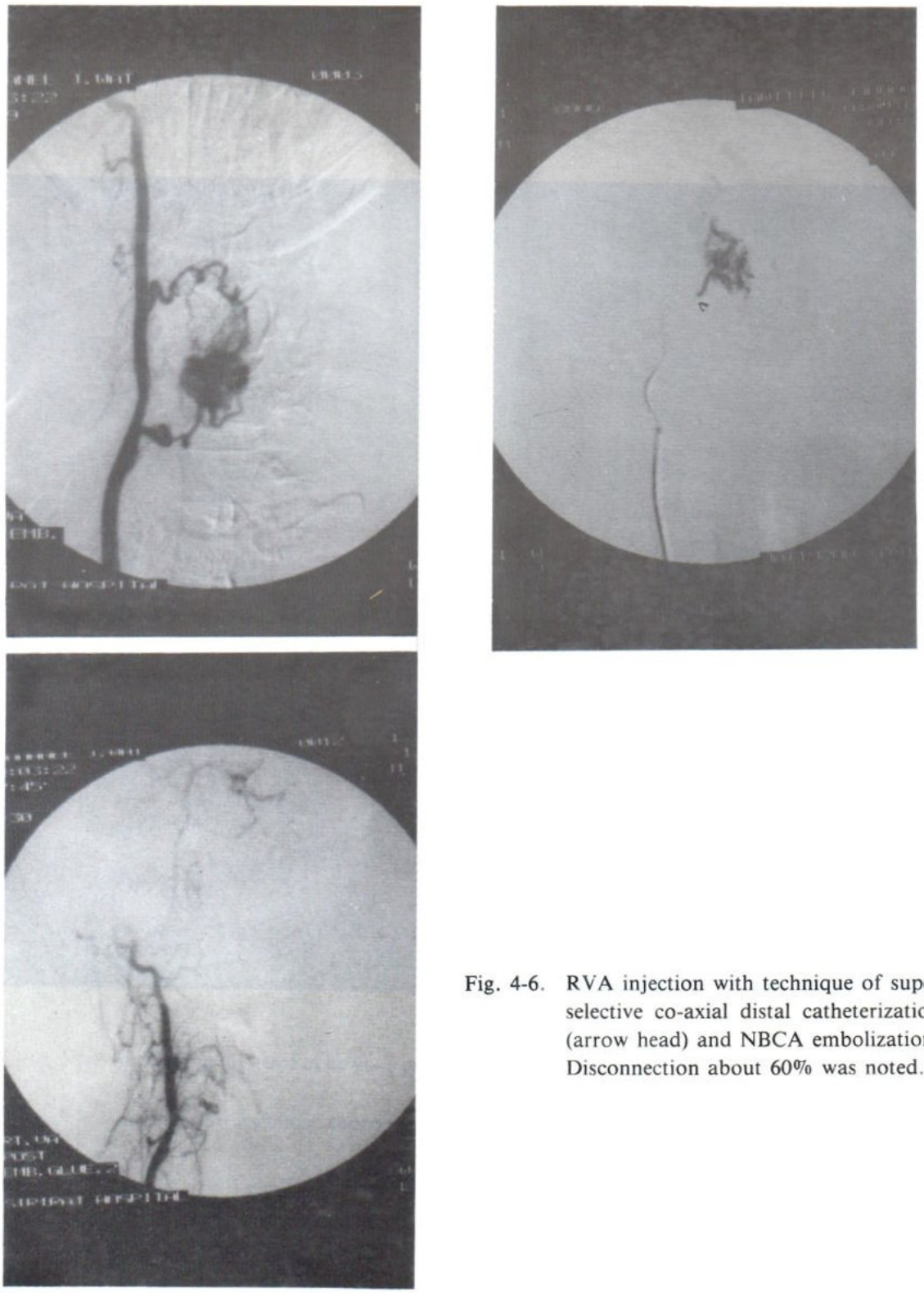

Fig. 4-6. RVA injection with technique of super selective co-axial distal catheterization (arrow head) and NBCA embolization. Disconnection about 60% was noted.

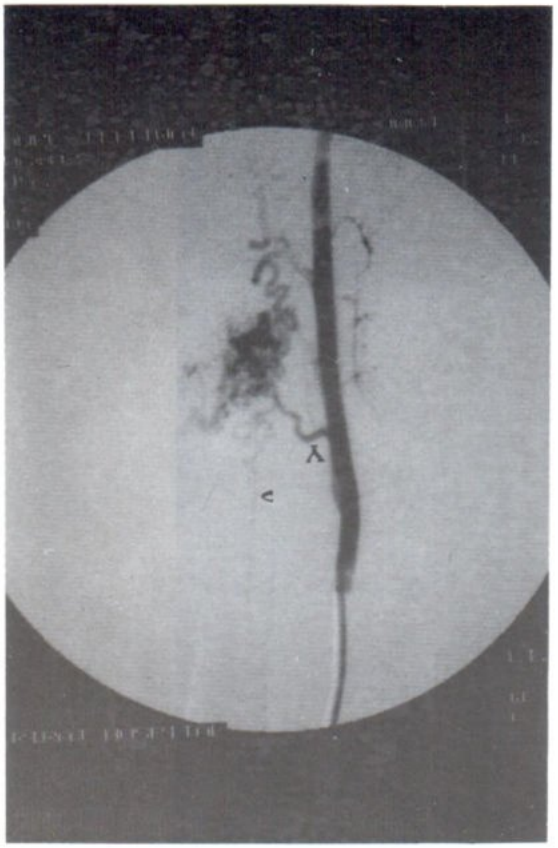

Fig. 7 LVA injection showed another feeder (arrow) with also the Anterior spinal artery visualized (arrow head)

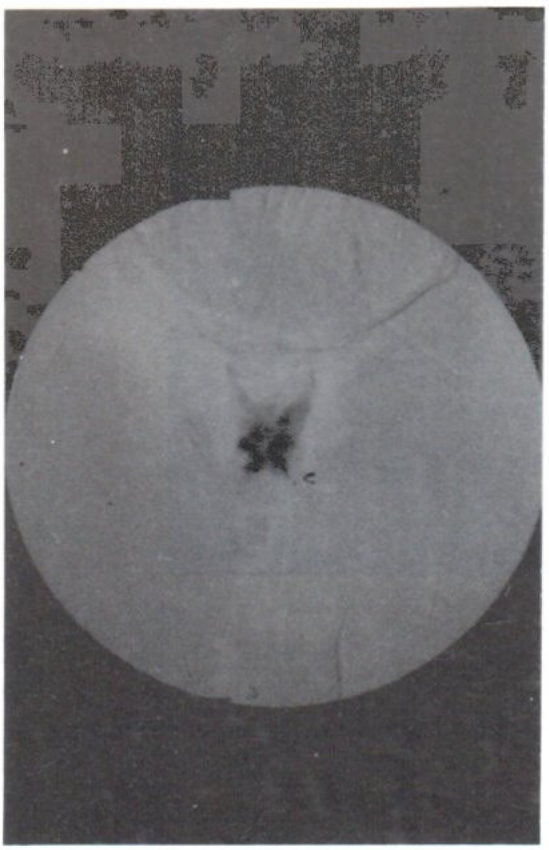

Fig. 8 During NBCA injection; uncontrolled respiratory and swollowing artifact occurred. Tip of the microcatheter was seen (arrow).

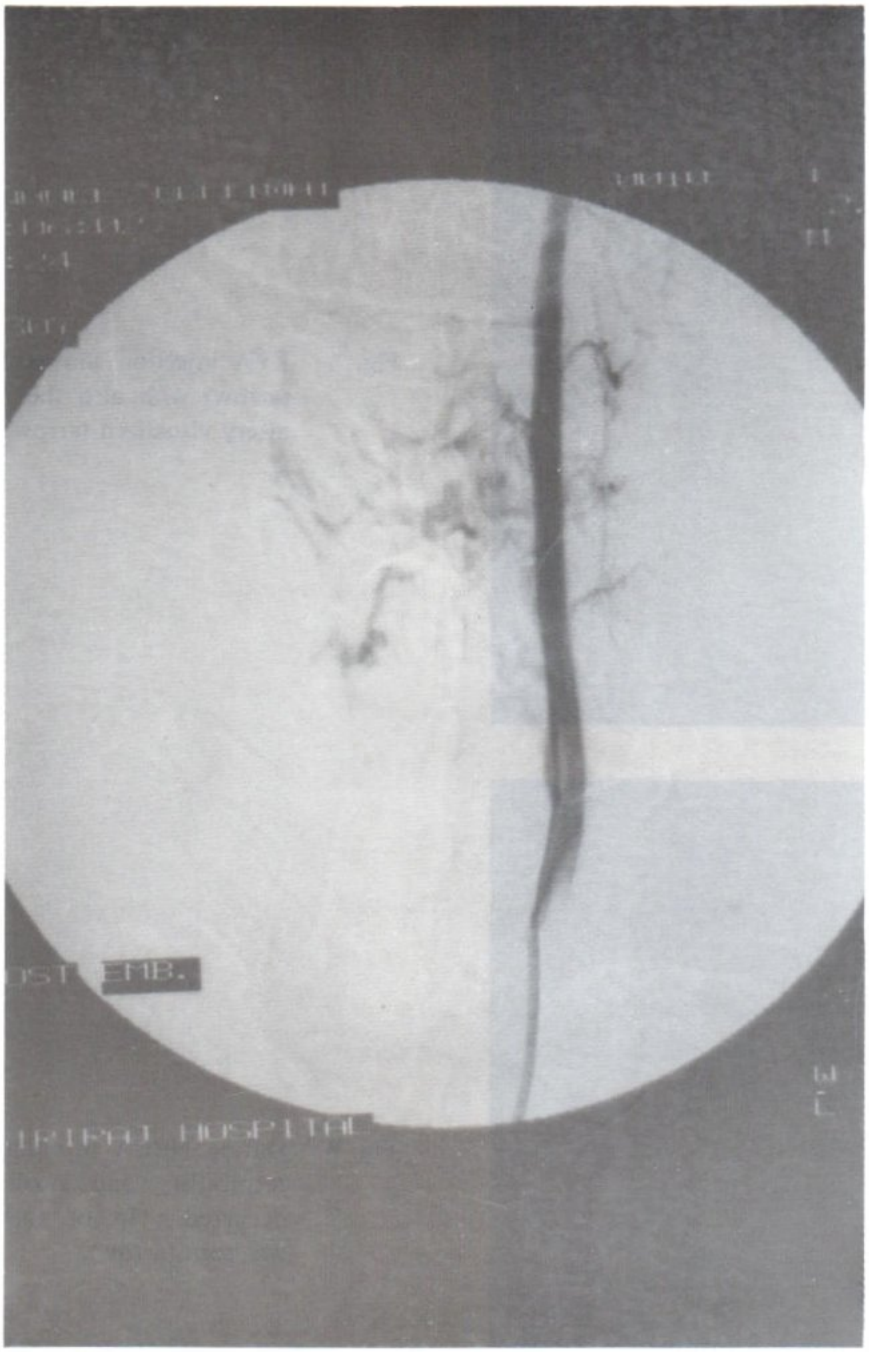

Fig. 9 LVA Post-Embolization showed complete occlusion of the nidus.

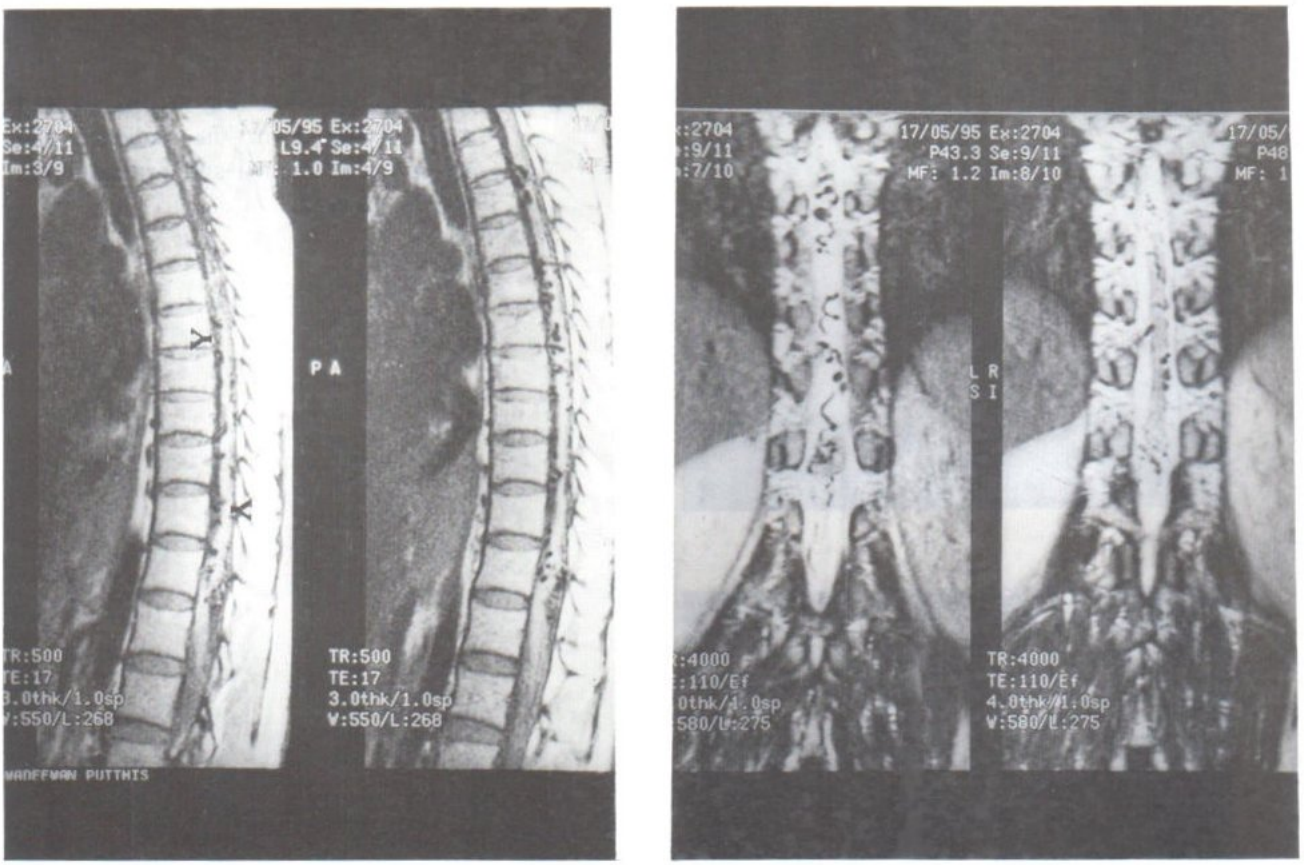

Fig. 10-11. MRI in sagittal and coronal view showed serpigenous flow void tubular structures along ventral and dorsal aspect of the cord down to conus medullaris (arrows).

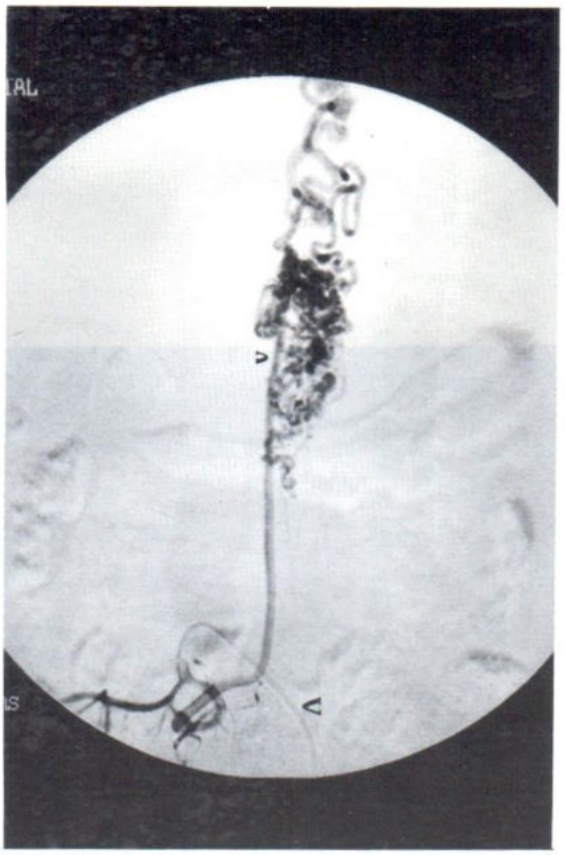

Fig. 12 Right L_2 injection (big arrow) showed main feeder from the radiculo pial artery (small arrow) and draining vein mainly upward.

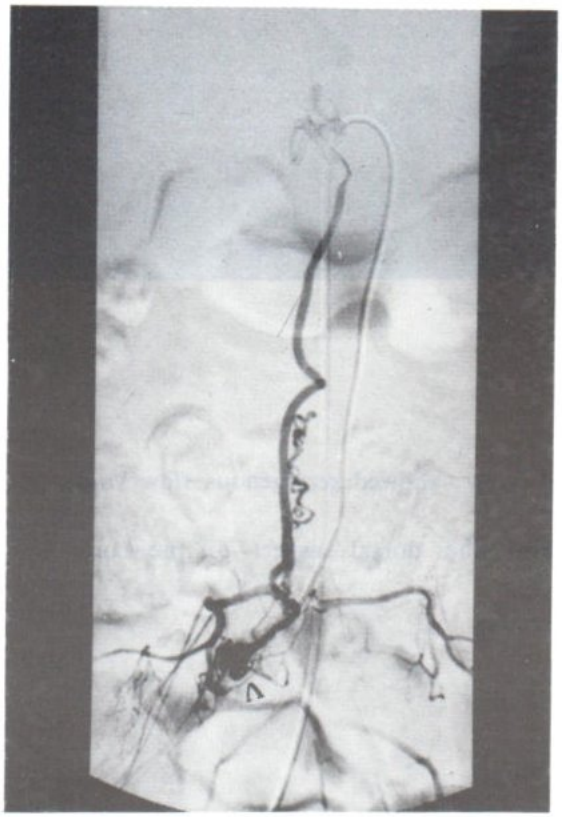

Fig. 13 Another small right L_3 radicular AVM (arrow) with also upward draining vein seen.

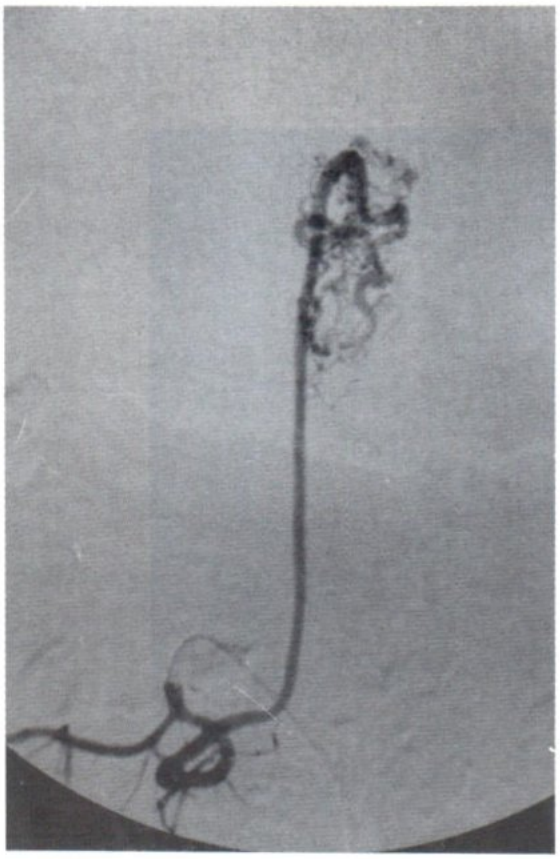

Fig. 14. Right L_3 superselectic injection during microcatheter place.

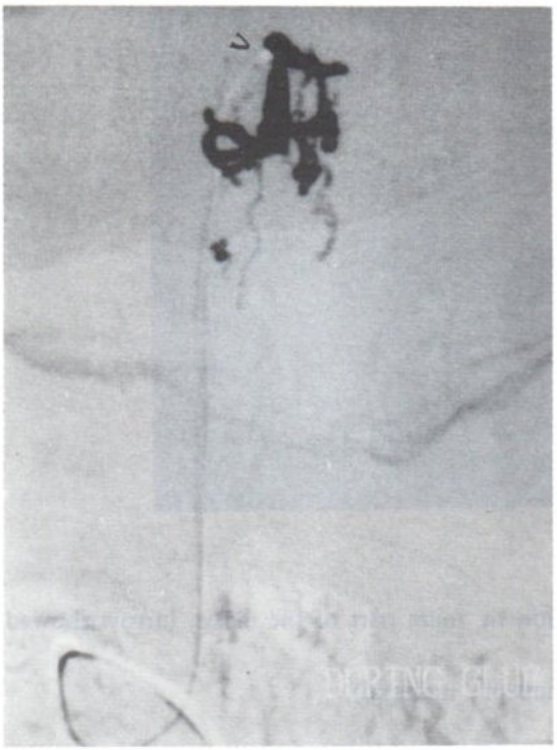

Fig. 15. During NBCA injection via Microcatheter tip (arrow) placed just above the nidus.

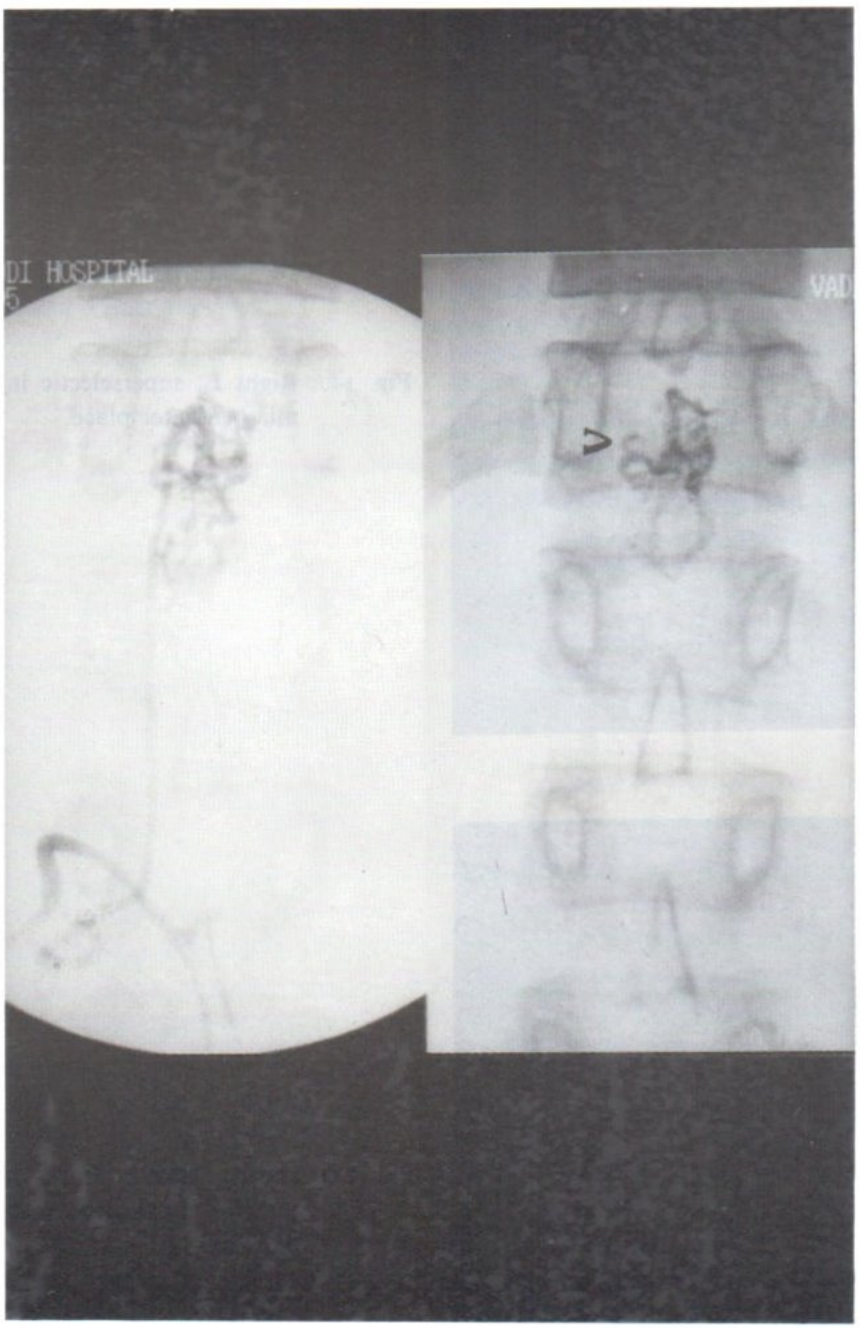

Fig. 16. Before and after NBCA deposition in main part of the nidus. (arrow showed opacity of the NBCA as permanent material).

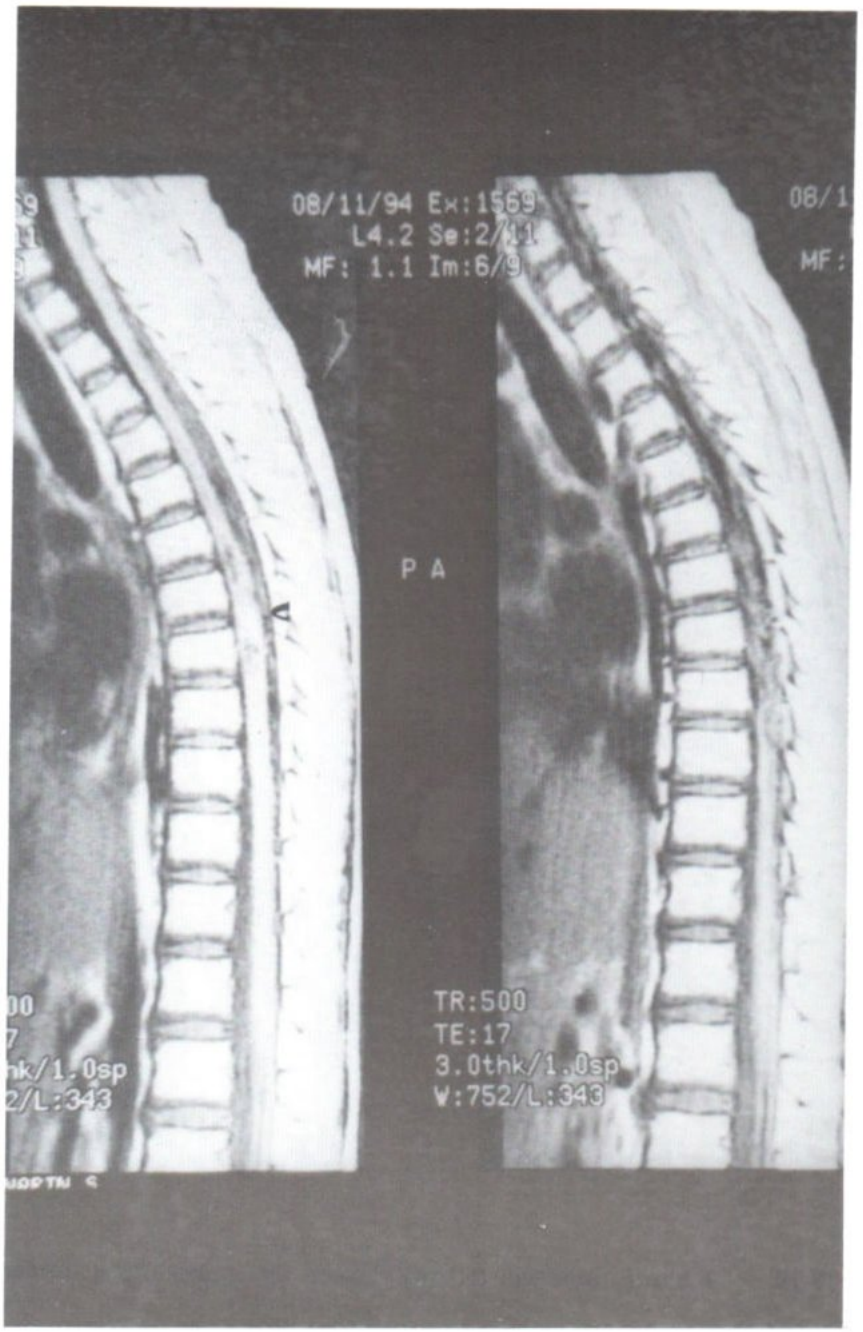

Fig. 17. MRI sagittal T1W showed hemorrhage within the cord at level of T_{6-7} (arrow) with dorsal tubular longitudinal flow void structures of draining veins.

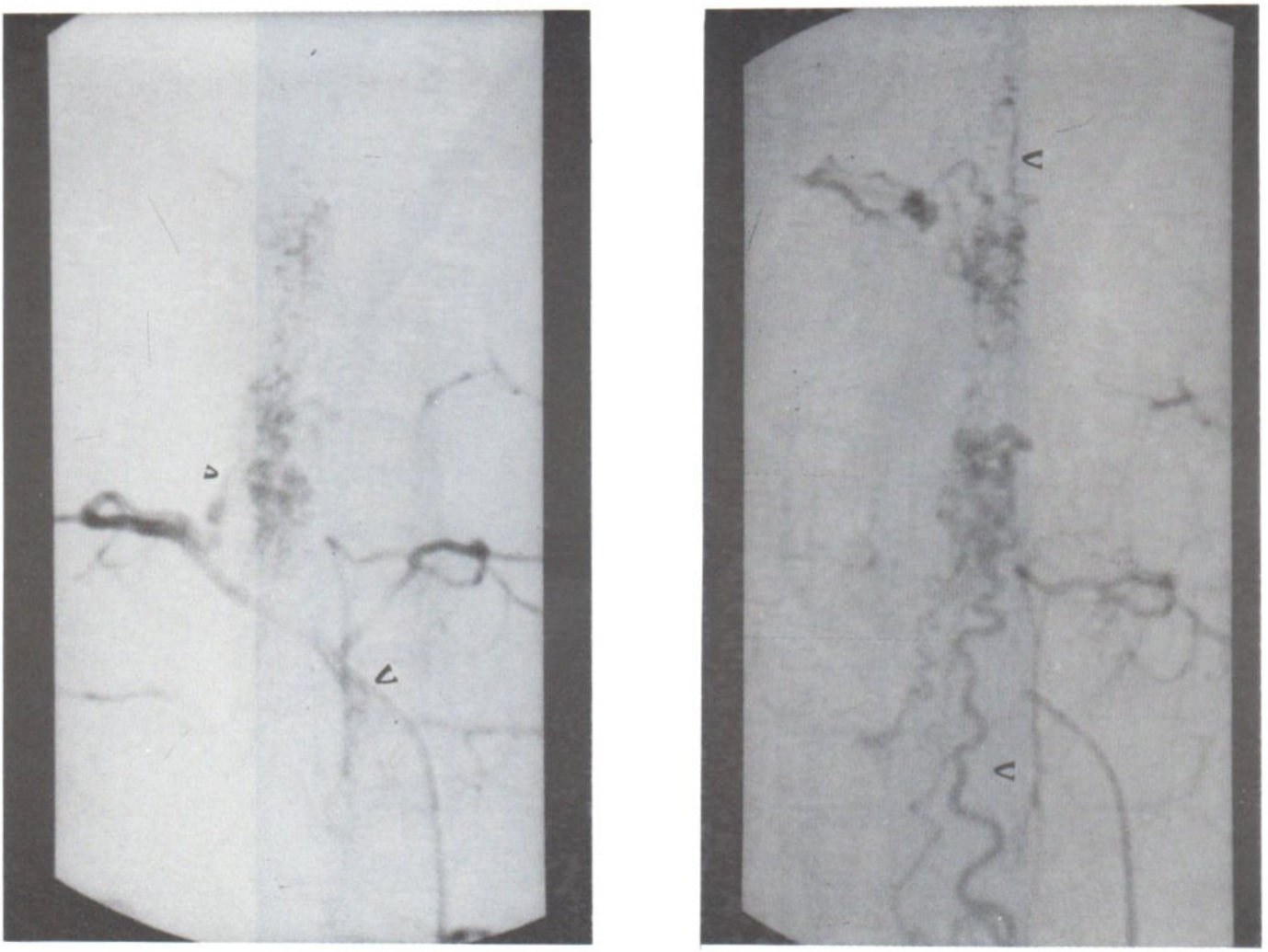

Fig. 18-19. Right T_8 injection (arrow) showed the radiculo-pial feeder (small arrow) to the nidus with both cephalad and caudad draining veins. (big arrow heads)

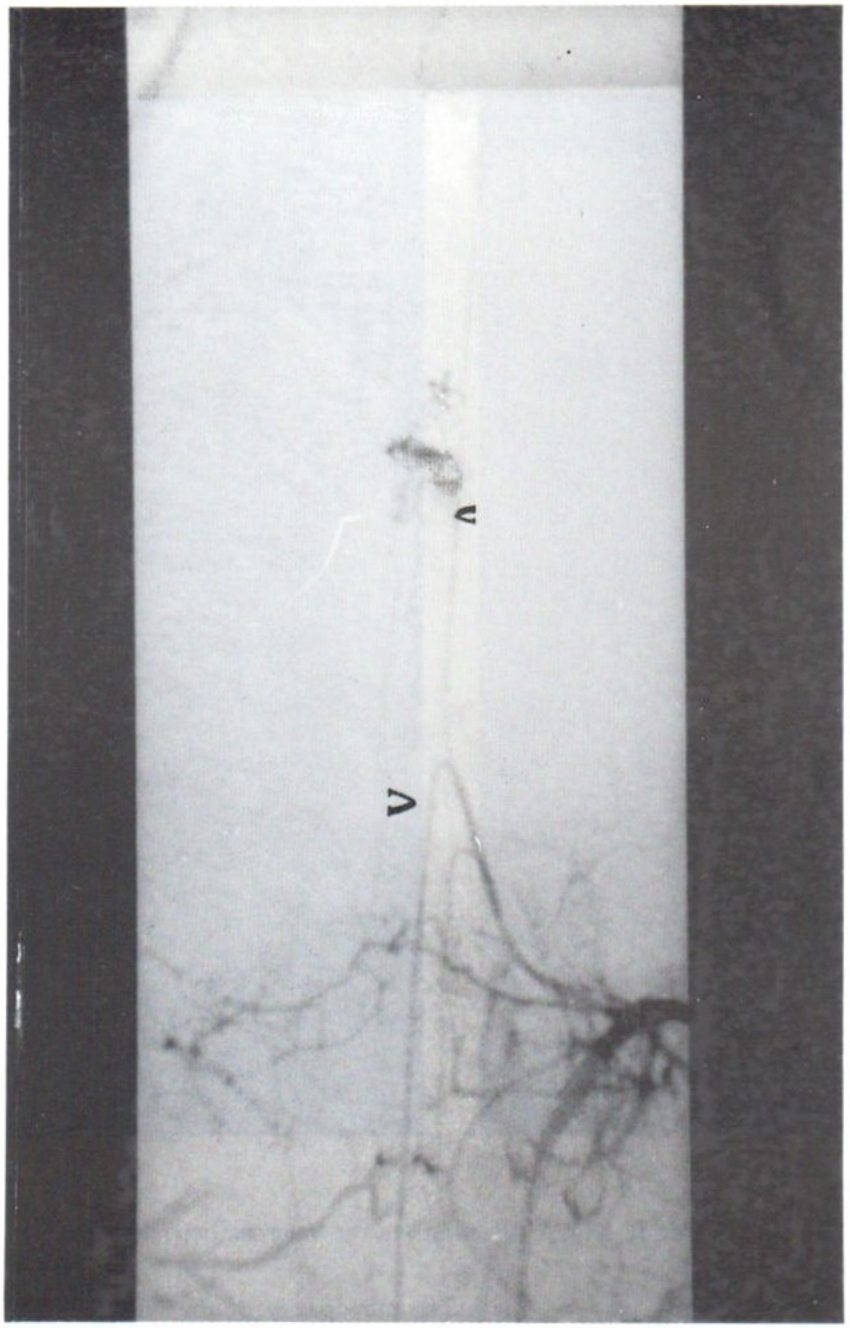

Fig. 20. The left T_{10} injection showed the anterior spinal artery (big arrow) with minimal feeders to the nidus too. (small arrowhead)

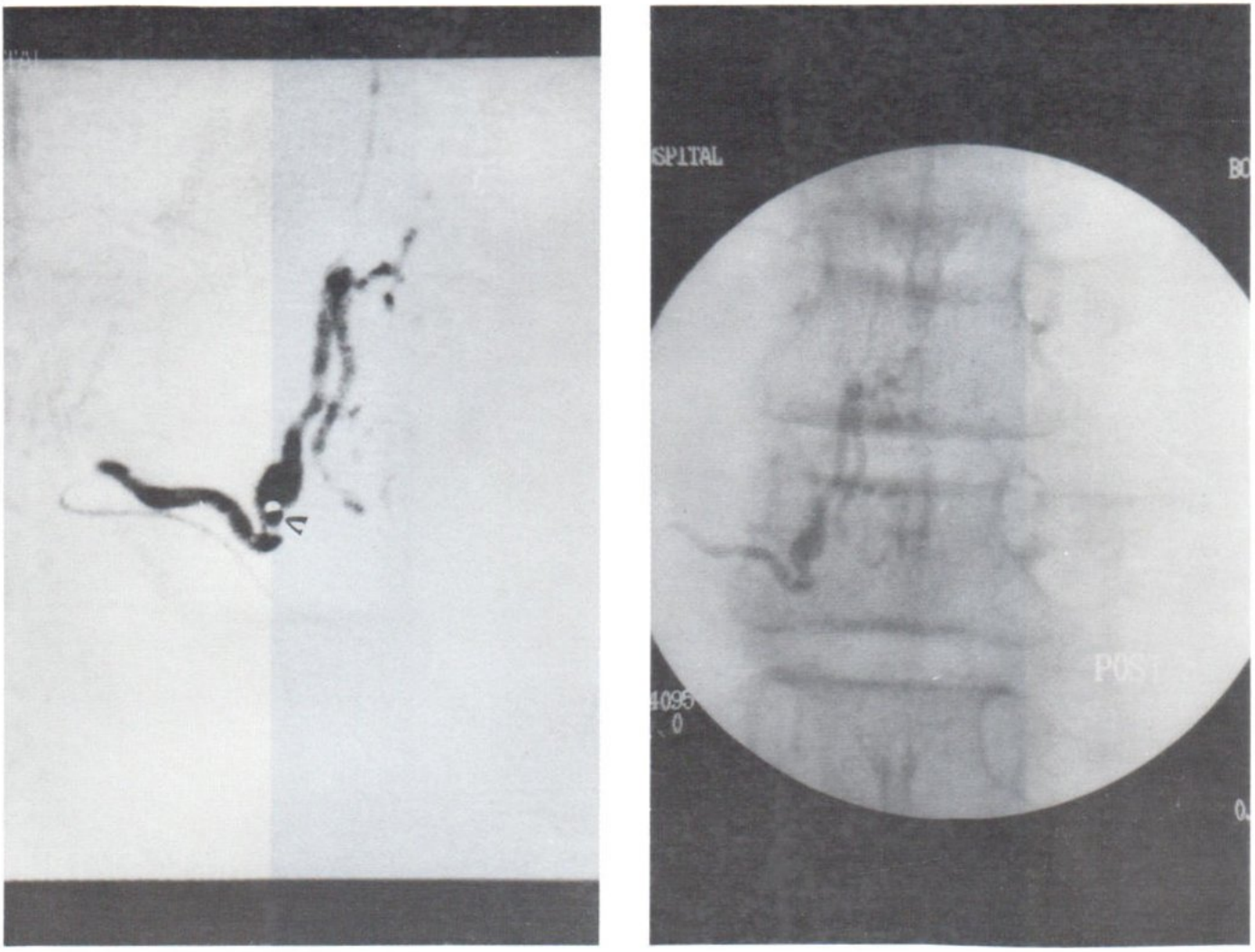

Fig. 21-22. During NBCA injection via the microcatheter tip (arrow) into part of the nidus and opacity of the NBCA after embolization.

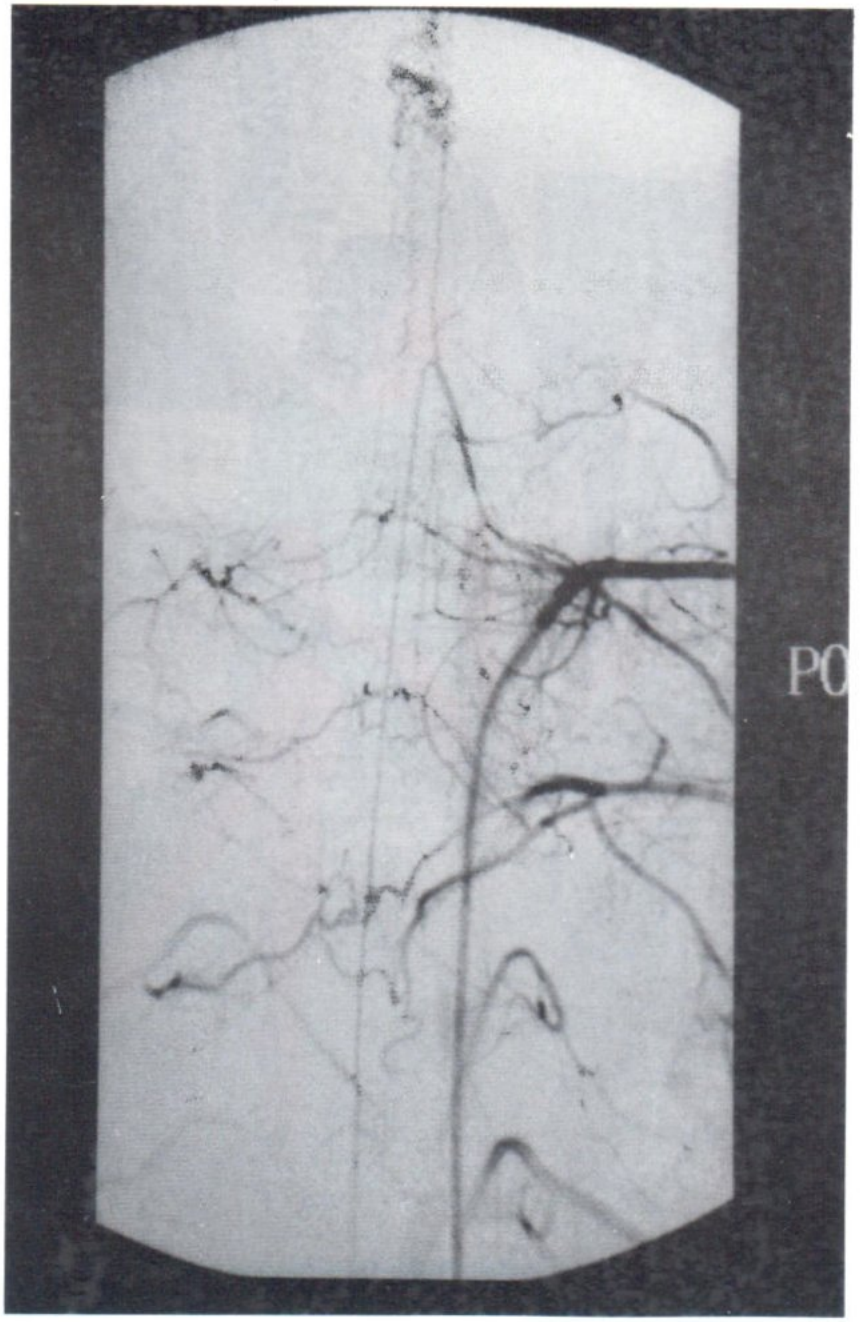

Fig. 23 Post Embolization immediate control left T_{10} injection showed good patency of the ASA with residual minimal feeder to the nidus.

Philips Medical Systems

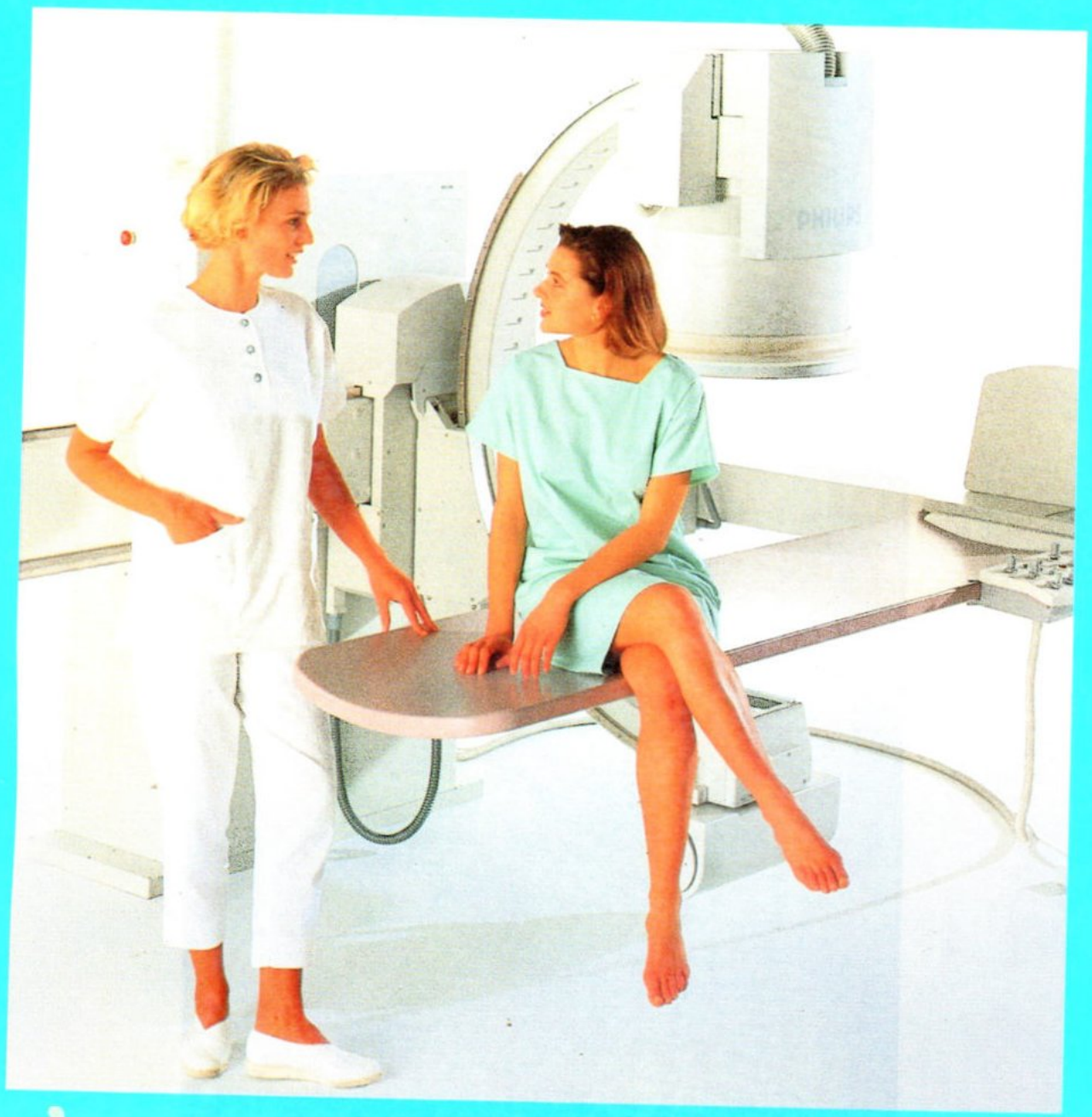

ร่วมสรรค์สิ่งที่ดีกว่า

Let's make things better.

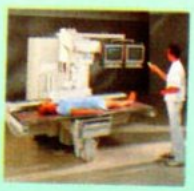

Multi DIAGNOST 3

The Multi DIAGNOST 3 is one of a new generation of remote-controlled systems, complementing the DIAGNOST 93 and DIAGNOST 96. All three systems have an attractive family look. With quality built-in, all were designed to be reliable, easy-to-use, efficient and provide digital image quality second to none.

Philips Medical Systems
Philips Electronics (Thailand) Ltd.
209/2 Sanpavut- Bangna Road Prakanong Bangkok 10260
Tel (662) 745-4090 Fax (662) 398-0792

PHILIPS

PHILIPS

PLUMMER-VINSON SYNDROME

Patchrin PEKANAN, Utaiwan SUTIART

ABSTRACT

Plummer-Vinson Syndrome or Paterson-Brown-Kelly syndrome denoted the association of dysphagia, angular stomatitis, and lingual abnormalities with iron deficiency anemia.[1] It is rarely seen in Thai population, especially nowadays. We report a case of this syndrome in a Thai patient.

CASE REPORT

A 41-year old female patient, admitted in 1991, had dysphagia especially for solid food for 3 days. She had mild intermittent similar symptom for 5 years. She felt easily tired for 2 years. Her hematocrit varied between 23% - 27%. Physical examination showed glossitis. Bone marrow biopsy was compatible with iron deficiency anemia. Barium swallowing study showed a web at the junction of the hypopharynx and the upper esophagus (Fig. 1). The anemic problem responsed well with blood transfusion and iron replacement. The dilatation of the obstructed part of the food pathway with esophagoscope showed no change in appearance of the web.

DISCUSSION

Most patients of Plummer-Vinson syndrome are middle-aged women. Clinical manifestations are (a) glossitis; mucosal changes in the mouth, pharynx, and proximal segment of the esophagus (webs, bands, mucosal folds) causing dysphagia; (b) simple hypochromic anemia; (c) achlorhydria; (d) other reported abnormalities: spoon-shaped fingernails, splenomegaly, association with Kartagener syndrome, postcricoid carcinoma.[2-8]

The dysphagia is due to the development of a mucosal web at the juncture of the hypopharynx and esophagus. Multiple webs may develop, usually extending from the anterior wall of the esophagus into the lumen. Occasionally, they may encircle the lumen, forming a cufflike structure. In other patients a stricture with or without a web may be found, drastically constricting the opening in the esophagus at the level of the cricoid cartilage. Relief of the dysphagia requires rupturing of the webs or dilatation of the stenosis, because repletion of the iron stores alone is not effective.[1]

Other gastrointestinal complaints, such as anorexia, pyrosis, flatulence, nausea, belching and constipation, are common in association with advanced iron deficiency anemia.[1]

The spleen is slightly enlarged in about 10 percent of patients with iron deficiency anemia. There are no specific pathologic changes in the organ, and the splenomegaly recedes with correction of the iron deficiency.[1]

Neuralgic pains, numbness, and tingling without objective neurologic abnormalities are reported by 15 to 30 percent of patients, and rarely iron deficiency anemia may lead to increased intracranial pressure, papilledema, and the clinical picture of pseudotumor cerebri.[1]

Department of Radiology, Ramathibodi Hospital, Rama 6 Street, Bangkok 10400, Thailand.

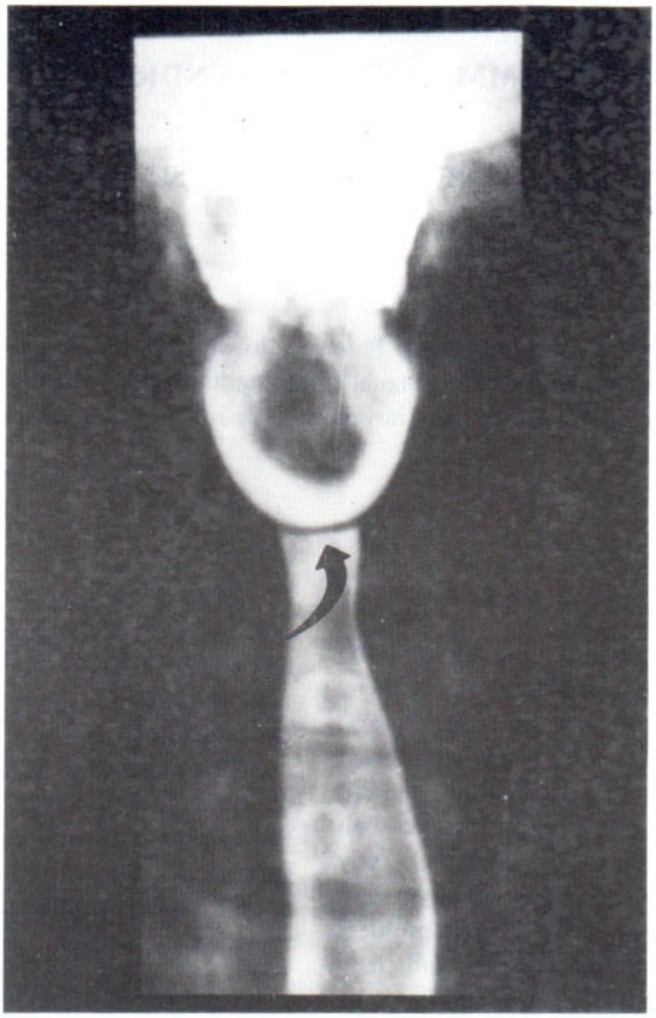

Fig. 1 AP view of the esophagogram revealed a circumferential web in a 41-years-old female patient with iron deficiency anemia.

REFERENCES

1. Kushner JP. Hypochromic anemias. In: Wyngaarden et al eds. Cecil, Textbook of Medicine. Philadelphia: W.B. Saunders, 1992: 843.
2. Taybi H. Radiology of syndromes, metabolic disorders, and skeletal dysplasias. Chicago: Year book medical publishers, 1990: 365.
3. Beitman RG, et al. Oral manifestations of gastrointestinal disease. Dig Dis Sci 1981; 26: 741.
4. Kelly AB. Spasm of the entrance to the esophagus. J Laryngol Otol 1919; 34: 285.
5. Miller G. Patterson-Kelly, Plummer-Vinson syndrome (letter). Dig Dis Sci 1980; 25: 813.
6. Nicoli F, et al. Radiologic and endoscopic diagnosis in Plummer-Vinson syndrome. Rays 1986; 11: 51.
7. Paterson DR.A clinical type of dysphagia. J Laryngol Otol 1919; 34: 289.
8. Plummer HS. Diffuse dilatation of the esophagus without anatomic stenosis (cardiospasm): A report of ninety-one cases. JAMA 1912; 58: 2013.
9. Todd NW Jr, et al. A patient with Kartagener and Paterson-Brown-Kelly syndromes. JAMA 1975; 234: 1248.
10. Vinson PP. Hysterical dysphagia. Minn Med 1922; 5: 107.

SPHERICAL PNEUMONIA IN AN ADULT PATIENT

Patchrin PEKANAN, Janjira JATCHAVALA.

ABSTRACT

Not all discrete mass lesions in the lung parenchyma are neoplastic. Sometines pneumonia consolidations are so round and discrete that they are mistaken for pulmonary neoplasm (1). This is the report case of a spherical pneumonia in an adult patient.

CASE REPORT

A 59-year-old female patient had chest pain, dry cough and high fever for one day. She smoked for 30 years. There was no history of hypertension, diabetes mellitus or tuberculosis. Physical examination showed decreased breath sound and crepitation at right mid lung field. She consumed a drug containing steroid to gain her weight. The temperature was 39 degree celsius. White blood cell count was 18400 with 92% PMN. The patient was treated with penicillin and the fever disappeared after 3 days of treatment. Hemoculture was negative for organisms.

PA chest film on the admission day (Fig.1) showed an ill defined border round-shaped mass lesion at right mid lung field. Small right pleural effusion was noted at the costophrenic sulcus. Right lateral view of the chest film (Fig.2), two days later shows an area of increased lung density at the superior segment of right lower lobe. The lesion was not seen as a mass in the figure 2 due to a response to treatment. Three weeks later, PA chest showed partial clearing of the lesion with evidence of an air bronchogram. The lesion was not seen as a mass anymore (Fig.3). The last PA chest film one month after admission, showed further clearing of the lesion (Fig.4).

DISCUSSION

The occurrence of well-circumscribed areas of inflammation simulating masses in adults has been described previously by Ackerman (2), Greenfield (3) and Swenson (4). Rose (5) reported 21 children-cases of spherical pneumonia simulating pulmonary and mediastinal masses in his 10-year-study. Pneumococci was the responsible pathogen in more than half of his cases. No other recognized pathogens were recovered in significant numbers. Thereapeutic response to penicillin within 48 hours was noted. Nasopharyngeal culture seemed to yield more benefit than the hemoculture, which was positive maximally only in 25% (6).

The radiographic presentation of pneumonia as a mass density in the lung could be explained by the studies of Roberson (7), Fraser and Wortz-man (8), and Recavarren (9). Under the influence of gravity, bacteria-laden fluid initially passes into the most dependent bronchus and then to the periphery of the lung. An acute inflammatory process with associated alveolar edema is disseminated centrifugally via intra-alveolar communications without regard for segmental boundaries. The dissemination process occurs largely through the communicating passages among the air spaces, the pores of Kohn, and the channels of Lambert. The consolidation characteristically begins at the periphery of the lung at the site of infection and progresses toward the hilus with a sharp line of demarcation generally existing between the advancing front of consolidated parenchyma and the unaffected lung adjacent to it. The rounded radiographic lesion was well developed on the first study, regardless of the time elapsed after the onset of symptoms, and cleared rapidly with treatment (5).

A pneumococcal orgin was postulated in the presented case on the basis of the clinical presentation and response to the antibiotic. The predominantly

Department of Radiology, Ramathibodi Hospital, Rama 6 Street, Bangkok 10400, Thailand.

posterior distribution of these lesions reported by Rose (5) and in this presented case, is as would be expected in pneumococcal pneumonais (10). It was only a clinical impression that the location of the lesion was related to the usual sleeping position of the patients. Recognition of the spherical pneumonias should help to eliminate the unnecessary diagnostic procedure for neoplastic work-up.

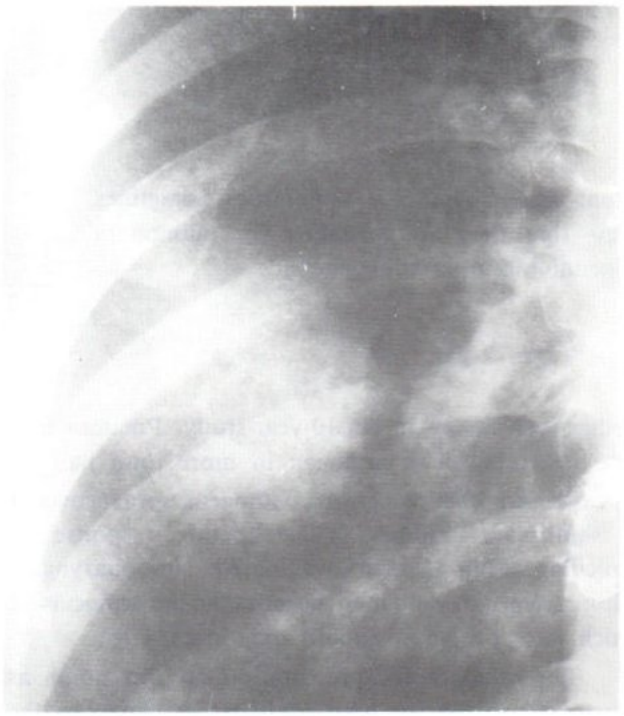

Fig.1 PA chest film on the admission day showed an ill defined border round shaped mass lesion at right mid lung.

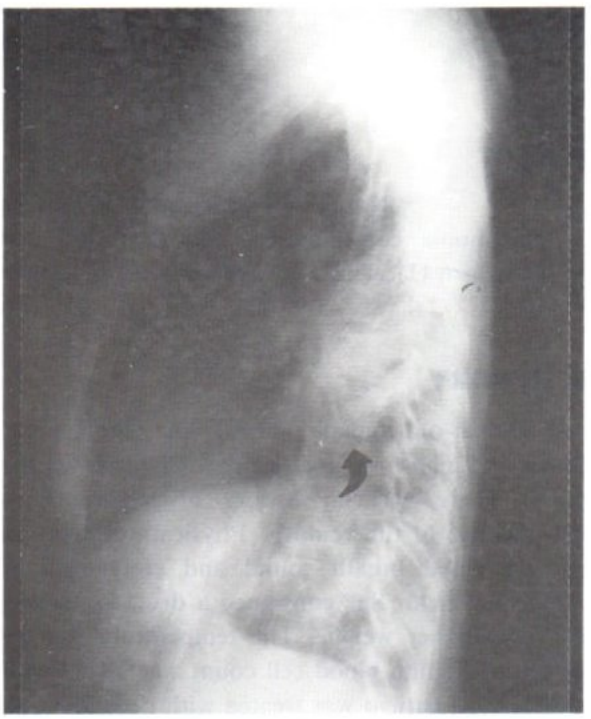

Fig.2 Right lateral view of the chest two days later showed an area of increased lung density at superior segment of right lower lobe.

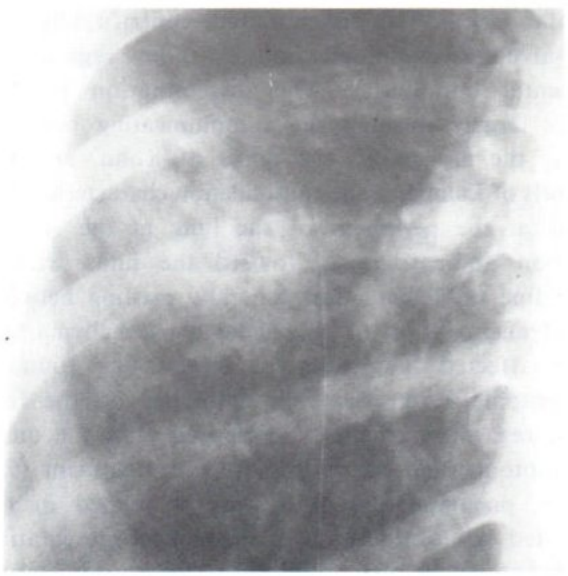

Fig.3 Three weeks later, PA chest film showed partial clearing of the lesion with small cavities and air bronchogram.

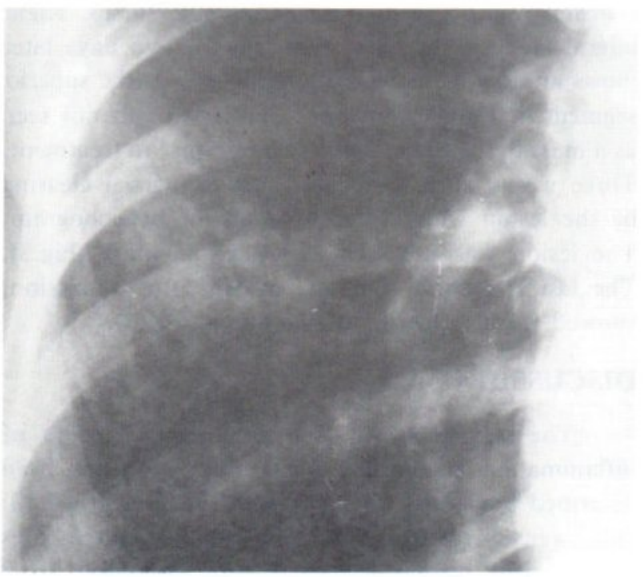

Fig.4 Further clearing of infiltration one month later was observed.

REFERENCES

1. Silverman FN, Kuhn JP. Caffey's pediatric x-ray diagnosis: an integrated imaging approach. St. Louis: Mosby, 1993.
2. Ackerman LV, Elliott GV, Alanis M. Localized organizing pneumonia: its resemblance to carcinoma. A review of its clinical, roentgenographic and pathologic features, Amer J Roentgen 1954; 71: 988-996.
3. Greenfield H, Gyepes MT. Oval-shaped consolidations simulating newgrowth of the lung. Amer J Roentgen 1964;91:125-131.
4. Swenson PC, Leaming RH. Chest lesions often confused roentgenographically with primary cancer of the lung. Amer J Roentgen 1950; 63: 629-645.
5. Rose RW, Ward BH. Spherical pneumonias in children simulating pulmonary and mediastinal masses. Radiology 1973;106:179-182.
6. Wyngaarden JB, Smith LH, Bennett JC. Cecil; Textbook of Medicine. Philadelphia: W.B.Saunders, 1992.
7. Robertson OH, Coggeshall LT, Terrell EE. Experimental pneumococcus lobar pneumonia in dog; pathogenesis. J Clin Invest 1993;12:467-493.
8. Fraser RG, Wortzman G. Acute pneumococcal lobar pneumonia:the significance of nonsegmental distribution. J Canad Ass Radiol 1959;10:37-46.
9. Recavarren S, Benton C, Gall EA. The pathology of acute alveolar disease of the lung. Seminars Roentgen 1967;2:22-32.
10. Fraser RG, Pare JAP. Diagnosis of diseases of the chest. An integrated study based on the abnormal roentgenogram, vol I. Philadelphia, Saunders, 1970,p289.

ด้วยความปรารถนาดี

จาก

บริษัท วรไทย เมดิคอล จำกัด

HOPE THAI MEDICAL CO.,LTD.

1054/7 ถ.นครไชยศรี เขตดุสิต กทม. 10300

โทร. 243-5268, 243-1791, 241-5371, 241-0620

แฟกซ์. 66-02-236-7693, 241-0620

ผู้แทนจำหน่าย

: COOK CATHETERS, GUIDE WIRES, NEEDLES

: COOK UROLOGY อุปกรณ์สำหรับศัลยกรรมระบบปัสสาวะ

: WILSON COOK อุปกรณ์สำหรับหน่วยระบบทางเดินอาหาร

: COOK CRITICAL CARE

: อุปกรณ์เอ็กซเรย์

: OKAMOTO CASSETTE & SCREEN

: KYOKKO INTENSIFYING SCEEN, เสื้อตะกั่ว

: MEDTRONIC PACEMAKER, HEART VALVE

: ULTRASOUND GEL CONDUCTIVITY

: ELECTRODE CREAM

: ฯลฯ

CHRONIC DISSEMINATED HISTOPLASMOSIS

Patchrin PEKANAN

ABSTRACT

Histoplasmosis is a disease of varied clinical and roentgenographic manifestations caused by the dimorphic fungi Histoplasma capsulatum and its variant H. duboisii. The former is much the more important organism of the two and exists in its mycelial form as a saprophyte in soil, and as an oval, 2-to 5-um yeast form in infected animals and humans (1).

A simple classification of histoplasmosis[1] is shown in the table 1.

A case of chronic disseminated histoplasmosis was presented and was considered rare in Thailand.

CASE REPORT

A 60-year-old male patient had chronic ulcer at the tongue for 2 months prior to the admission. PA chest film showed diffuse reticulonodular lesions in both lungs at the upper and middle zones and less at both lower zones (Fig.1). The patient was treated as a tuberculosis case without improvement. Sputum AFB was negative. Biopsy from the ulcer of the tongue showed positive Histoplasma capsulatum.The patient was responded to the Itraconazole which is an antifungal agent. Follow-up chest film 6 months (Fig.2) and three years later (Fig.3) showed slow clearing of the infiltration of both lungs.

DISCUSSION

Disseminated histoplasmosis is the less common form of histoplasmosis. It develops primarily in persons with defective host immunity, including infants with immature systems, compromised hosts, such as corticosteroid treated organ recipients and HIV infected persons, and individuals with either measurable defect or a highly selective defect, such as the failure of host lymphocytes to undergo in vitro blast transformation upon exposure to H. capsulatum antigen (2). The severity of the symptoms and signs of disseminated disease and the attendant histopathologic findings in a given patient mirror the level of immunocompetence of the individual. In patients with the mildest and most chronic forms of disseminated disease, well developed tuberculoid granulomas, typical of the response in normal hosts, can be found in reticuloendothelial tissues. In contrast, in patients with overwhelming multiorgan histoplasmosis superimposed on a severely immunocompromising condition, such as AIDS, the host response is suboptimal, with the pathologic findings consisting of large numbers of diffusely scattered macrophages filled with yeast forms and minimal or no granuloma formation.

Fever, chills, and other nonspecific constitutional symptoms predominate. Enlargement of the liver and spleen is common; less frequently, peripheral lymphadenopathy is present. Mucous membrane ulceration, especially of the oropharynx, occurs in about 25 to 75 per cent of patients with subacute disease. Laboratory clues may include anemia, leukopenia and thrombocytopenia as evidence of impaired bone marrow function or replacement of the marrow, elevated alkaline phosphatase levels, elevated erythrocyte sedimentation rate, and electrolyte abnormalities suggestive of adrenal insufficiency. Chest x-ray films may be normal or show findings suggestive of earlier primary infection or an intersititial pneumoitis consistent with hematogenous spread of infection. Unusual syndrome, including cardiac involvement

Department of Radiology, Ramathibodi Hospital, Rama 6 Street, Bangkok 10400, Thailand.

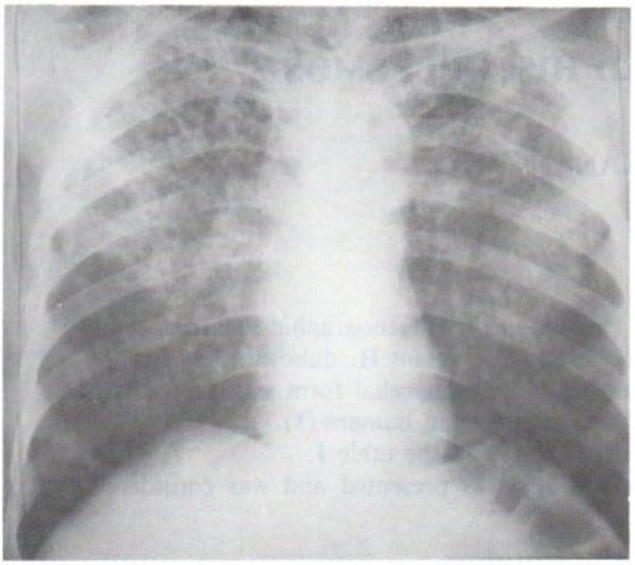

Fig.1 PA chest film on the admission day showed diffuse reticulonodular lesions in both lungs at upper and middle zones and less at both lower zones.

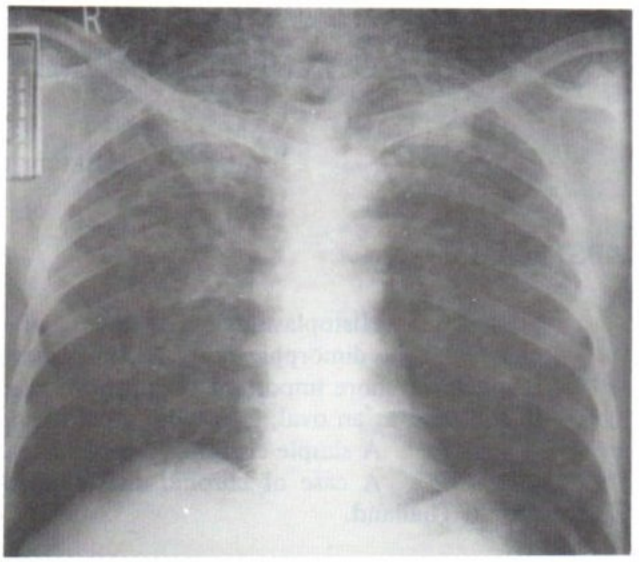

Fig.2 Partial clearing of pulmonary infiltration, 6 months post treatment for Histoplasmosis.

with culture-negative endocarditis associated with large emboli, gastrointestinal involvement with bleeding secondary to mucosal ulceration, or central nervous system involvement with chronic lymphocytic meningitis (3-6).

Chronic pulmonary histoplasmosis often occurs in men with underlying chronic obstructive pulmonary disease and resembles pulmonary tuberculosis in symptomatology and radiographic manifestations although this type of histoplasmosis tends to be milder and more indolent than that of tuberculosis. The pathogenesis and course of chronic pulmonary histoplasmosis are highly complex; pathologic studies indicate two basic lesions. An interstitial pneumonitis featuring mononuclear infiltration, periarteriolar inflammation, areas of infarctlike necrosism and few organisms is characteristic of the early lesion. The inflammatory process often surrounds apical emphysematous blebs and bullae. In contrast, the chronic lesion is manifested by organization of diseased tissue, with prominence of giant cells and progressive cavitation. Organisms are typically found in the necrotic lining or in surface exudate. In the thicker walled cavities, infection is persistent, with continuing necrosis, leading to progressive cavity enlargement. In 80 per cent of cases, the pneumonitis stage tends to resolve spontaneously over 2 to 3 months, with a small fibrotic residuum, whereas the cavitation stage, especially that associated with thick-walled cavities, tend to be relentlessly progressive, leading to destruction and diminution of lung parenchyma, fibrosis and respiratory insufficiency (1, 7-9).

The presented patient had ulcer of the tongue and interstitial process in the lungs. The patient had no prior pulmonary emphysema nor evidenced of defective immunity. The healing of the tongue ulcer was complete while the pulmonary infiltration resolved satisfactorily but slowly. The complete disappearance of the infiltration was not seen in this patient; he did not come for follow-up after the last film shown in fig.3

REFERENCES

1. Fraser RG, Pare JAP, Pare PD, Fraser RS, Genereux GP. Diagnosis of diseases of the chest. Philadelphia: W.B. Saunders Company, 1989.
2. Wyngaarden JB, Smith LH, Bennett JC, Cecil textbook of medicine. Philadelphia: W.B. Saunders Company, 1992.

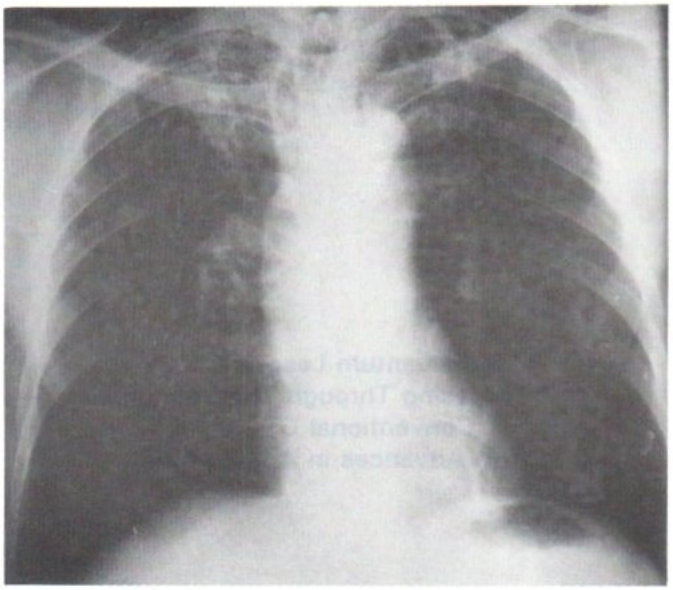

Fig.3 Incomplete clearing of the lesions after three years indicates slow process of clearing.

3. Wheat LJ. Diagnosis and management of histoplasmosis. Eur. J Clin Microbiol Infect Dis 1989;8:480.
4. Wheat LJ. Conolly-Stringfield PA, Baker RL. Disseminated histoplasmosis in the acquired immunodeficiency syndrome: Clinical findings, diagnosis, treatment and the review of the literature. Medicine (Baltimore) 1990;69:361.
5. Abilgaard WH Jr, Hargrove RH, Kalivas J, Histoplasma panniculitis. Arch Dermatol 1985; 121:914.
6. Cott GR, Smith TW, Hinthron DR, Primary cutaneous histoplasmosis in immunosuppressed patient. JAMA 1979;242:456.
7. Goodwin RA Jr. Des Prez. RM. Histoplasmosis. Am Rev Resp Dis 1978;117;929.
8. Goodwin RA Jr, Owens FT, Snell JD. Chronic pulmonary histoplasmosis. Medicine 1976;55:413.
9. Loewen DF, Prochnow JJ, Loosli CG. Chronic active pulmonary histoplasmosis with cavitation. A clinical and laboratory study of thirteen cases. Am J Med 1960;28:252.

TABLE 1. CLASSIFICATION OF HISTOPLASMOSIS

- Asymptomatic
- Symptomatic
  - Acute Histoplasmosis
    - Acute "flu-like" syndrome
    - Acute pulmonary histoplasmosis
    - Acute diffuse nodular disease (epidemic)
    - Histoplasmoma
    - Lymph node involvement
  - Chronic Histoplasmosis
    - Chronic pulmonary histoplasmosis
    - Mediastinal histoplasmosis
      - Pericarditis
      - Esophageal encroachment
      - Superior vena cava obstruction
      - Pulmonary arterial and venous obstruction
      - Tracheal and major airway encroachment
  - Disseminated Histoplasmosis
    - Acute
    - Subacute
    - Chronic

SIEMENS

บริษัท ซีเมนส์ จำกัด
Siemens Limited

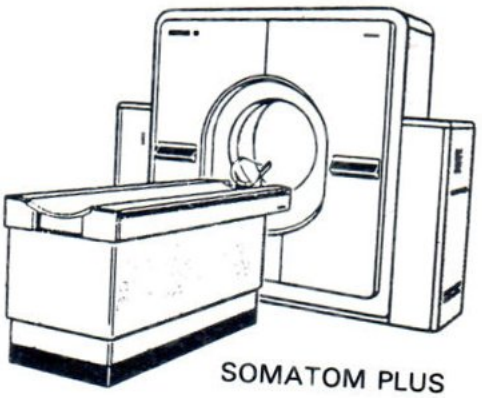

SOMATOM PLUS

*The Quantum Leap in CT
*Breaking Through The Boundaries of Conventional CT
*An Advances in Applications

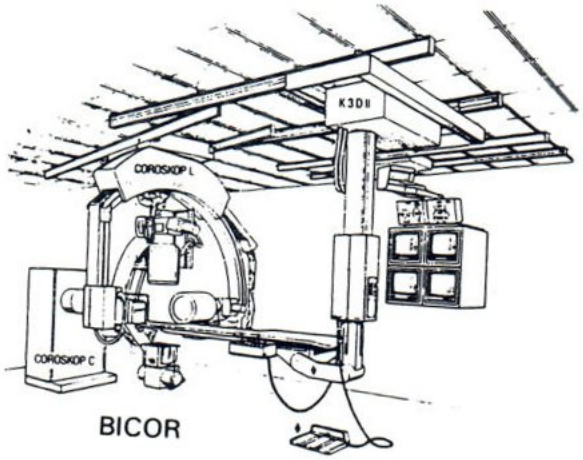

BICOR

The Superior System
for
Angio Cardiography
and
Angioplasty

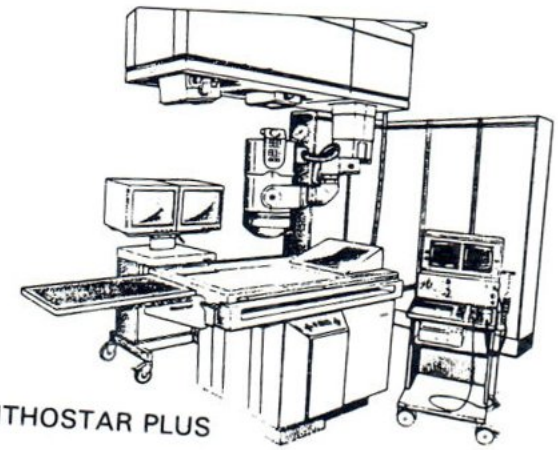

LITHOSTAR PLUS

The Universal Lithotripter for
all varieties of stone Therapy
in Urinary and Biliary treatment

บริษัท ซีเมนส์ จำกัด
แผนกวิศวกรรมการแพทย์
33 อาคาร ดร. เกอร์ฮาร์ด ลิงค์ ซอยเลิศนาวา
ถ.กรุงเทพกรีฑา แขวงหัวหมาก เขตบางกะปิ กรุงเทพฯ 10240
โทร. (662) 379-4333, 379-4455 โทรสาร (662) 379-4470

Siemens Limited
Medical Engineering Division,
33 Dr. Gerhard Link Building, Soi Lertnava,
Krungthepkreetha Road, Huamark, Bangkapi, Bangkok 10240
Tel. (662) 379-4333, 379-4455 Fax (662) 379-4470

PULMONARY NOCARDIOSIS: RADIOGRAPHIC FINDINGS IN HIV INFECTION AND OTHER COMPROMISED STATUSES.

Korkiat VIVITMONGKORNCHAI*
Sanan SIMARUK**

ABSTRACT

After the wide spread of HIV infection, in addition to the widely use of corticosteroid and other immunosuppressive therapy in many diseases as well as post organ transplantation, the incidence of pulmonary nocardiosis is significantly rising. Pulmonary manifestations in 11 cases of proved pulmonary nocardiosis and 7 cases of presumptive diagnosis of pulmonary nocardiosis are presented. The most pertinent radiographic abnormality is inhomogenous consolidation with multiple cavitary changes in both groups. Other radiographic abnormalities include pulmonary nodules, masses and reticulonodular infiltration. Pleural effusion and hilar lymphadenopathy are rarely seen. Pulmonary nocardiosis should be in the differential diagnosis if the above radiographic findings are observed in compromised patients and if sputum smear reveals weakly acid fast branching filamentous organisms, the diagnosis even be in highly suggestive. Prompt diagnosis and treatment may yield good clinical result even for these type of patients.

INTRODUCTION

In the past, pulmonary nocardiosis was considered to be an uncommon infection and usually encountered in patients who were on immunosuppressive therapy for their underlying diseases. Its occurence has significantly increasing especially after the beginning of HIV infection epidemic[1,2,3] and involution of organ transplantation.[4-8] Many studies in immunological aspect have pointed out that cell mediated immunity play an important role against nocardial infection.[4, 9-12] This can explain the marked out numbers of nocardial infections in immunocompromised patients. Descriptions of various pulmonary radiographic abnormalities caused by nocardial infection are presented with some speculations of findings to include for the differential diagnosis.

MATERIALS AND METHODS

From January 1991 to August 1993, there were 11 cases of culture proved pulmonary nocardiosis available for the study. Presumptive diagnosis of pulmonary nocardiosis in 7 cases based on the positive acid fast branching filamentous organisms on sputum smear with significant clinical and radiologic response to specific antibiotic for nocardia were also included. All medical records, bacteriologic reports and chest radiographs were retrospectively reviewed. Patients with extrapulmonary nocardiosis without pulmonary involvement were excluded.

RESULTS

The patients ranging in ages from 26 to 52 years, with the mean of 43 years. All patients were immunocompromised. Fourteen cases were men and all had positive HIV antibody. The remaining four cases were women who were in corticosteroid therapy for a long duration to control their underlying diseases, these included systemic lupus erythematosus for two, over – lapped syndrome and polymyositis for one case each.

Definite diagnosis of pulmonary nocardiosis was made in eleven cases, eight with HIV infection and the

* Department of Radiology, Faculty of Medicine, Chiangmai University.
** Department of Radiology, Faculty of Medicine, Chiangmai University.

remaining three with systemic lupus erythematosus, overlapped syndrome and polymyositis. All had positive culture, nine from sputum, one from bronchial biopsy and the other from pleural fluid. The remaining seven cases had positive acid fast branching filamentous organisms on sputum smear but negative on sputum culture. All 18 patients were treated with trimethoprim-sulfamethoxazole and significant clinical improvement with much regression of lesions, on the one month interval follow up chest film, were recognized. Eight cases had positive sputum smear and positive sputum culture. There were two cases of positive culture for nocardia from liver abscess, one had positive sputum culture and the other had positive sputum smear.

The most common clinical manifestations were fever and minimal productive cough. The other respiratory symptoms were mild dyspnea and less commonly, pleuritic chest pain. Duration of symptoms ranged from 3 days to 3 months, median duration was 3 weeks. In the HIV infected group, deterioration of general health (fatigue, anorexia and weight loss) was noted in seven cases, chronic intermittent diarrhea in two cases, oral thrush in two cases and skin lesion from Penicillium marneffei infection in one case. Concurrent right upper quadrant pain and tender due to nocardial liver abscesses were also noted in two cases of HIV infected patients.

The initial chest radiographic abnormalities were summarized in table 1.

The spectrum of radiographic abnormalities includes consolidation, nodule or mass with multiple cavitary changes in most of the patients in both groups, 64% and 86% respectively. (Fig. 1,2,3) The reticulonodular infiltration was seen but not as a sole manifestation. Frank abscess formation was presented in one case. (Fig. 4) Hilar lymphadenopathy and pleural effusion are seen in only one and two cases respectively. In case 10, progression of noncavitating nodule to cavitating mass and consolidations on the serial follow up films is noted. (Fig. 5) Later development of cavitations on follow up film was also observed in case 3. If both initial and follow up films were evaluated, the incidence of cavitary change is higher (82% and 86%). The most commonly radiographic pattern was inhomogenous consolidation in both groups (63% and 71%). More than one radiographic features were noted in four and three cases in both groups, respectively. Spontaneous pneumothorax on initial radiograph was observed in one case.

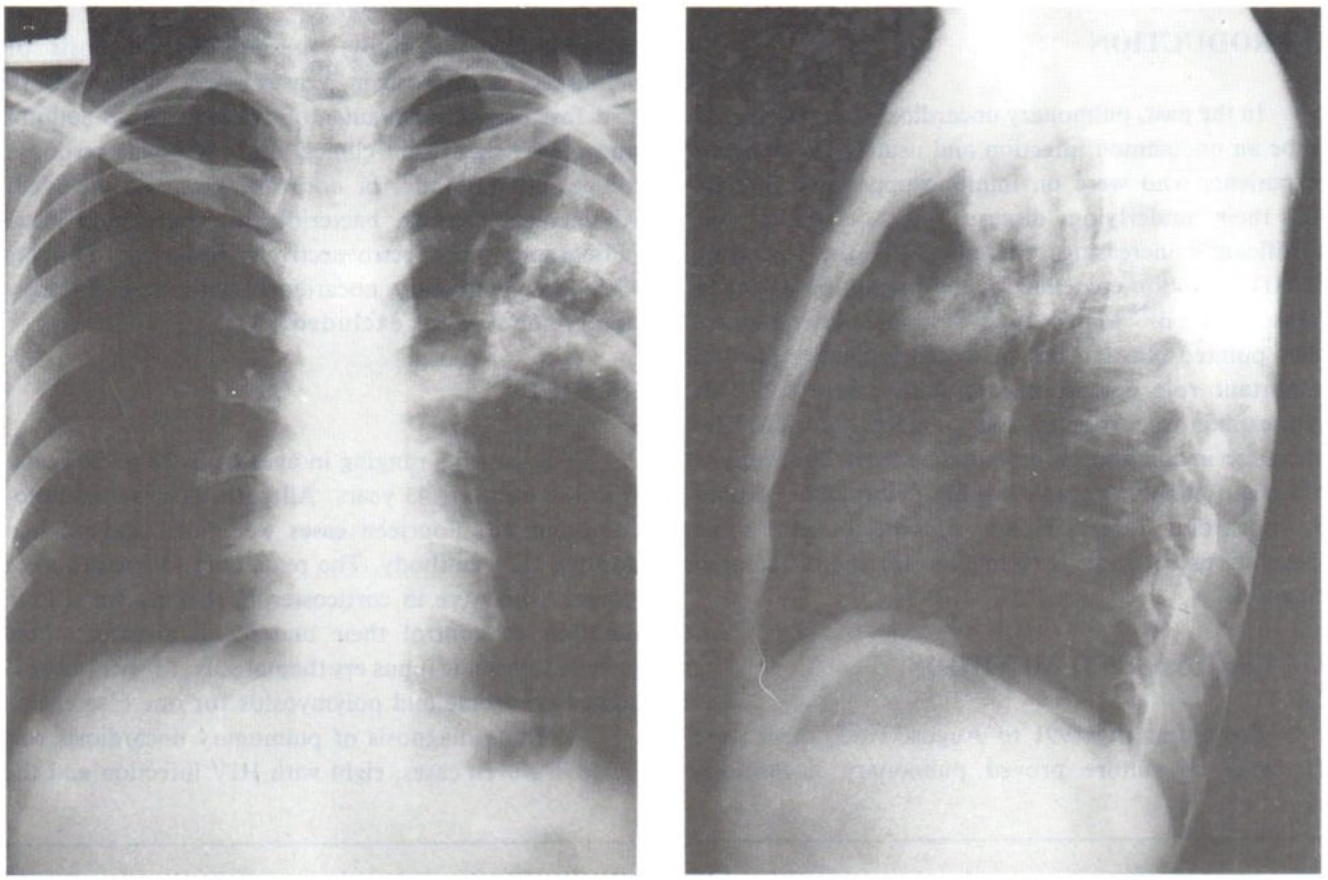

Fig. 1 Single inhomogenous consolidation at the anterior segment of LUL was noted. No lymphadenopathy nor pleural effusion.

DISCUSSION

In general, nocardial infection of the lung is not usually considered in patients presenting with clinical lower respiratory tract infection since its relatively low incidence as compared to pneumonias caused by other causative organisms. Although pulmonary nocardiosis can affected patients without concurrent disease or therapy,[13,16] most cases of pulmonary nocardiosis are encountered in patients who were treated for a long period with corticosteroid or other immunosuppressive drugs for their underlying diseases such as collagen vascular disease (particularly, systemic lupus erythematosus), chronic obstructive pulmonary disease, asthma, bronchiectasis, primary alveolar proteinosis, etc.[8,14,16-20] and antineoplastic agents for various malignant neoplasms.[11,16]

Recently, a significant number of nocardial infections is being diagnosed in a couple of patient groups. First, patients present with specific organ failure from other causes and was undergoing organ transplantation.[4-8] These patients must be on immunosuppressive therapy to prevent organ rejection and in turn increased susceptibility to opportunistic infections. Nocardial infection in cases post renal transplantation,[5,6,14,18] cardiac transplantation,[4] and hepatic transplantation[7] have been reported. The other group is that,the HIV infected patients.[1,2,3] It is known that HIV infection causes a gradual but irreversible depletion in number and functional destruction of T-helper lymphocytes. Postulated mechanisms include direct virus mediated lysis of infected cells and the induction of toxic substances that suppress or destroy T-helper lymphocytes. Progressive loss of T-helper lymphocytic function and number leads to opportunistic infections and certain types of neoplasms (Kaposi' sarcoma and B-cell lymphoma). The organisms that take advantage of T-lymphocytes defect are presented in Table 2, and common causes of pulmonary infection in AIDS patients are presented in Table 3.

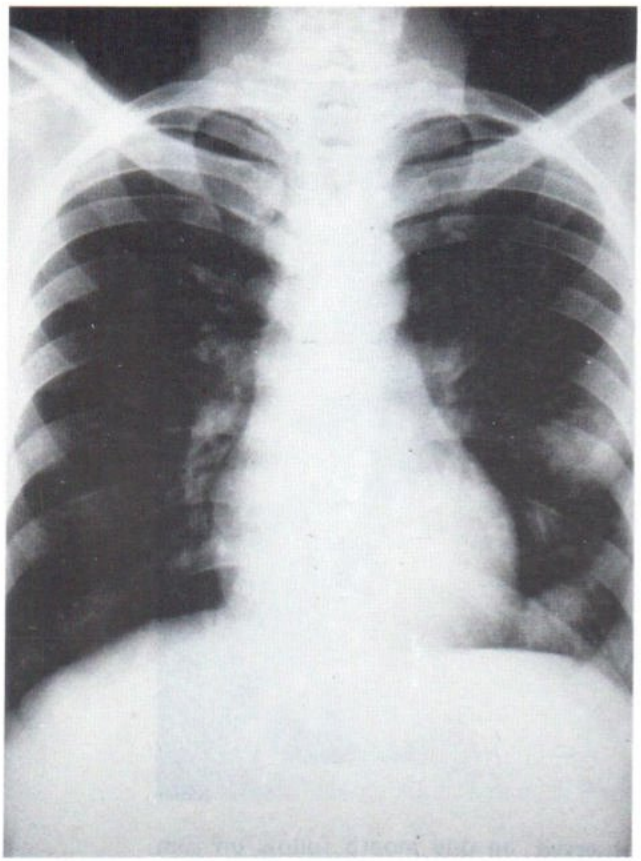

Fig. 2 A few cavitary nodules were noted at hilar region and left lower lung field.

Nocardia is a genus of aerobic actinomycetes and considered to be true bacteria rather than fungus.[10,14,16] Nocardia is native to soil.[14,16] The modes of infection are direct inoculation of the pathogen into skin during trauma or by inhalation into lungs.[16] Spectrum of disease is wide and nearly all organs can be affected by this pathogen.[10,19] Lung is the most frequently affected initial site of involvement.[6,12,19,22] N. asteroides is the most common pathogen for the majority of cases of pulmonary nocardiosis.[13,14,16] The clinical manifestation of pulmonary infection are included in fever, cough with or without mucoid or mucopurulent sputum, mild dyspnea and rarely pleuritic chest pain. These can be presented in either acute, subacute or chronic course.[14,15] Sometimes the patients may have no any symptoms at all.[12] Various extrapulmonary clinical manifestations of nocardiosis may also be presented

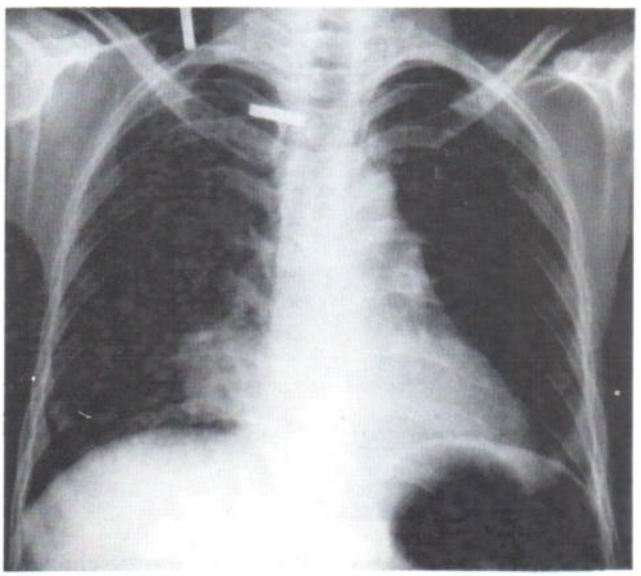

Fig. 3 Single cavitary mass lesion was noted on RML.

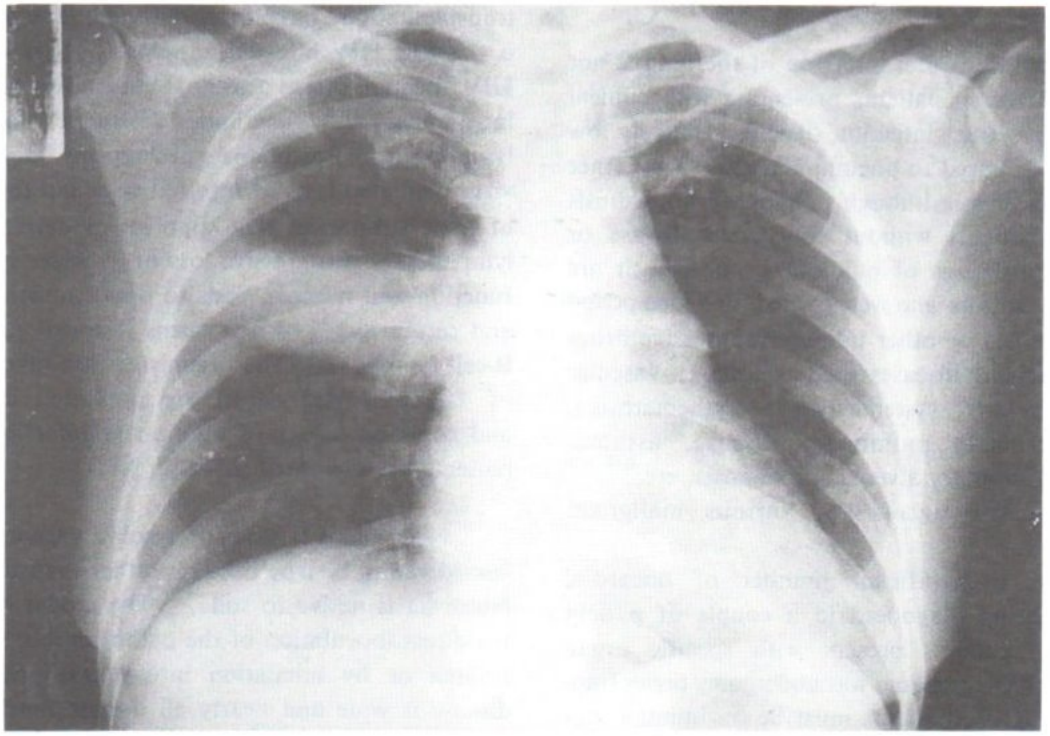

Fig. 4a A large abscess with air-fluid level was presented at RUL.

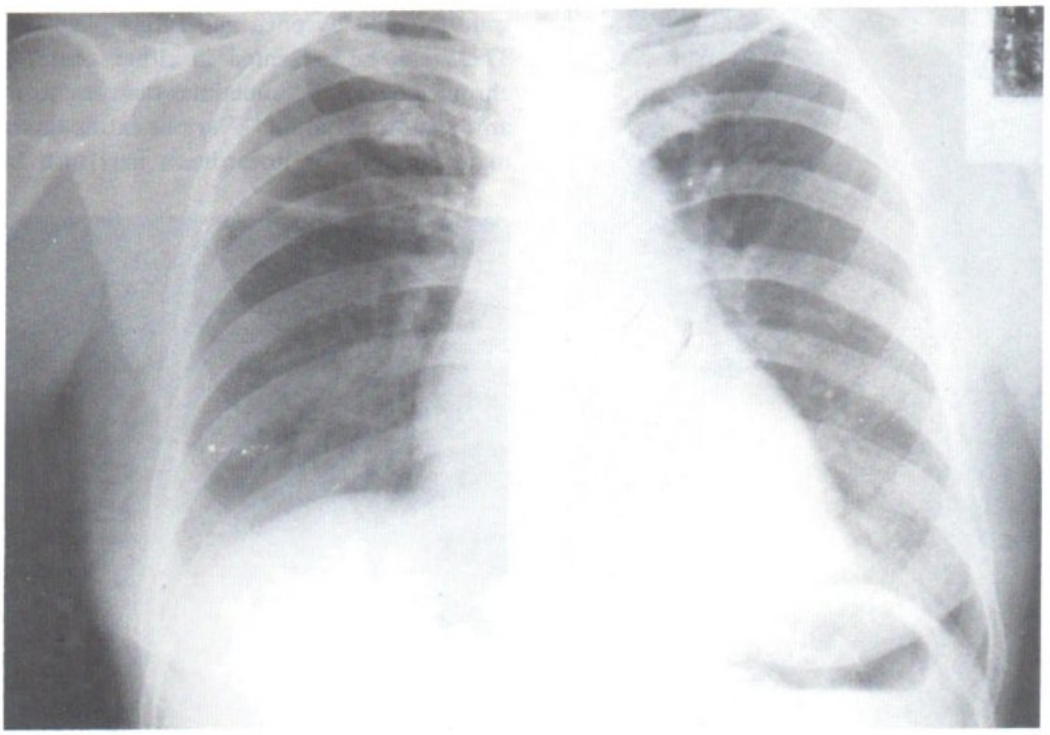

Fig. 4b Minimal residual fibrotic change was observed on one month follow up film after specific antibiotic treatment.

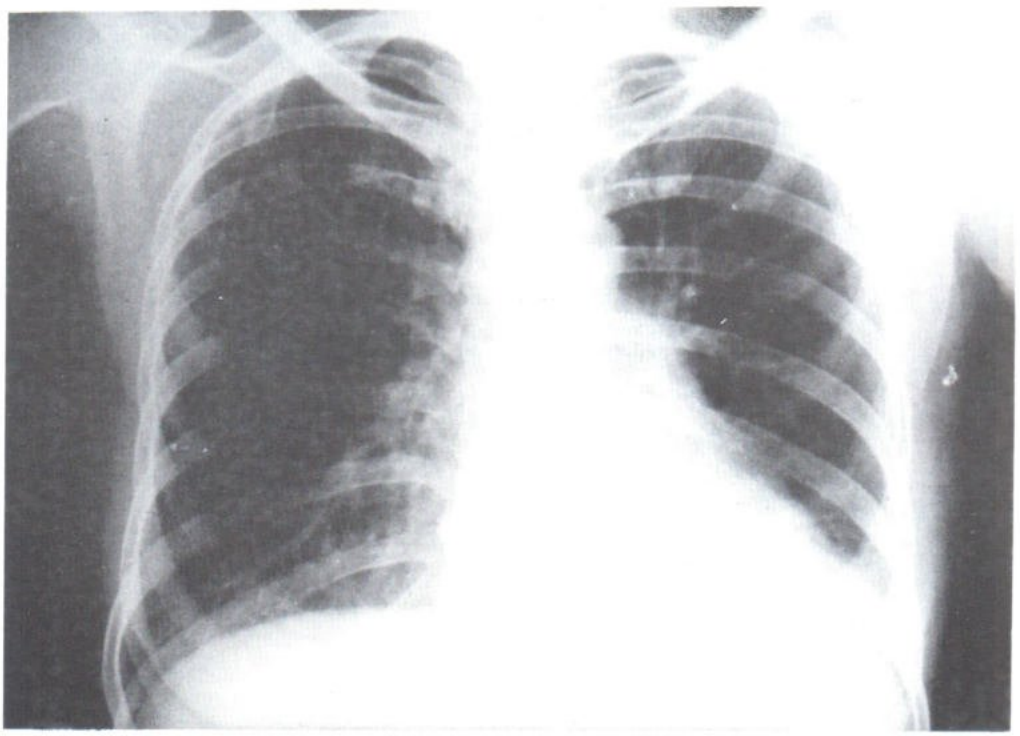

Fig. 5a Single pulmonary nodule at peripheral right mid lung field with early air space infiltration at bilateral basal lungs were noted on this initial film.

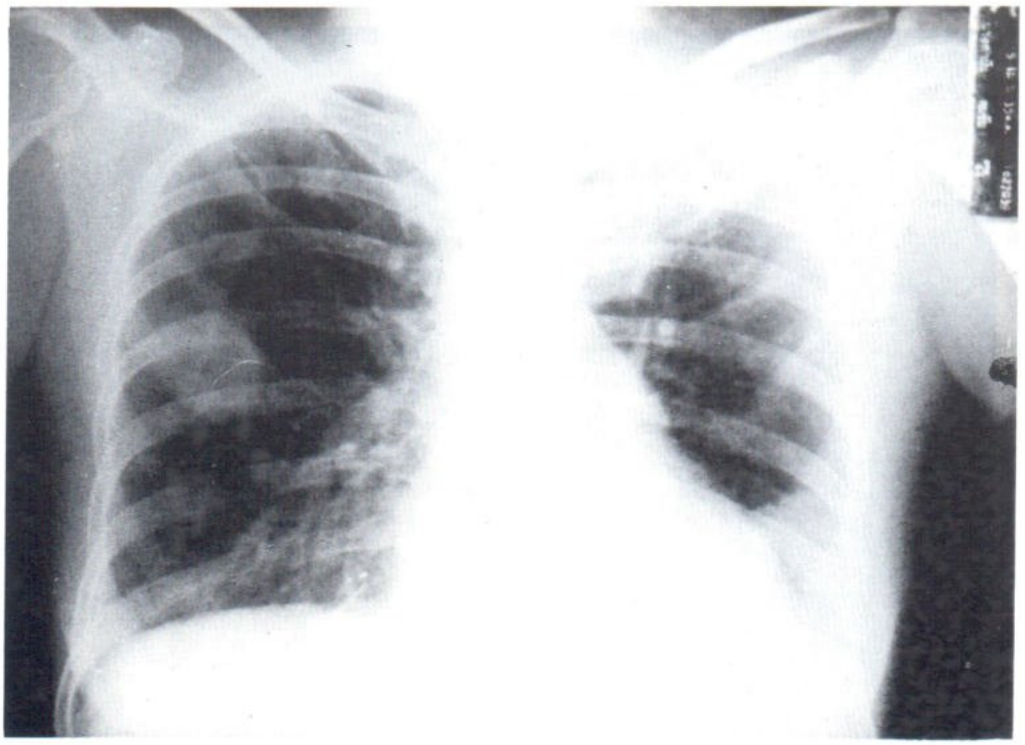

Fig. 5b Three weeks later; progression of previous lesions and development of new pulmonary mass at LUL and LLL. Left pleural effusion was also presented.

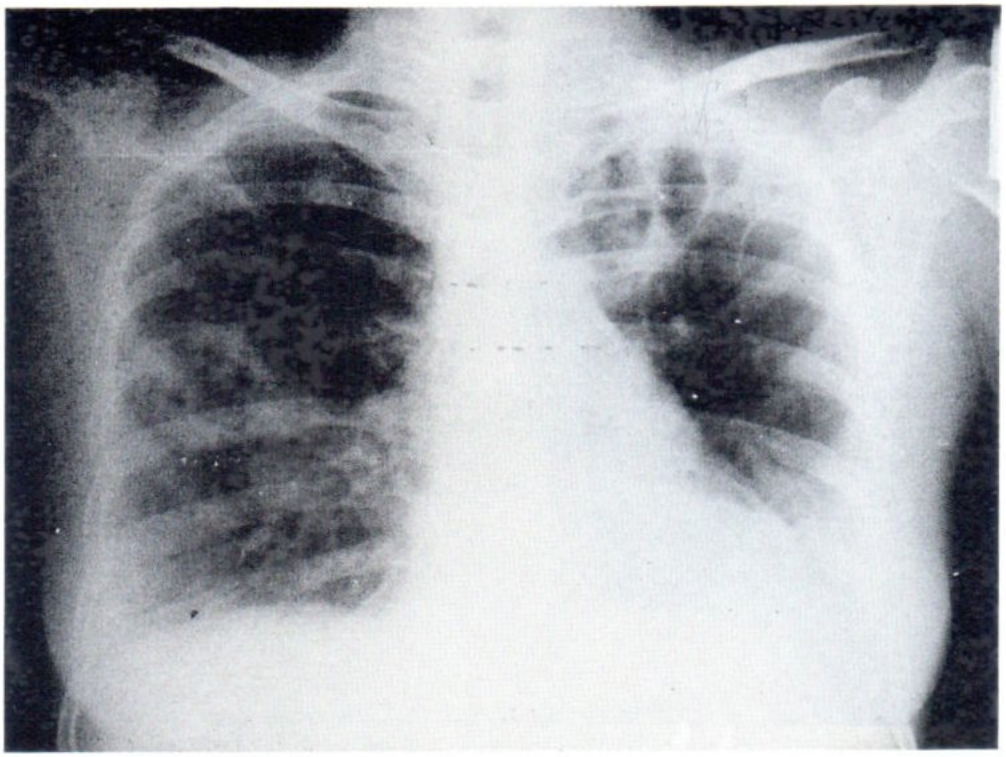

Fig. 5c One week later; cavitary changes of the pulmonary mass lesions were observed.

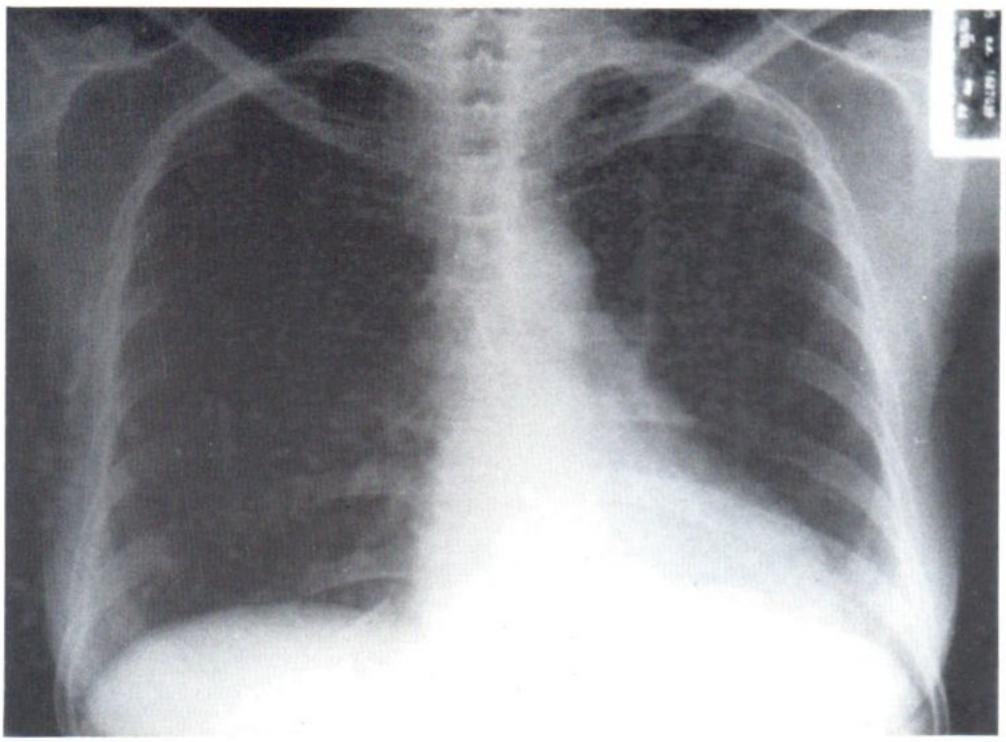

Fig. 5d Ten weeks follow up film after treatment shown only minimal residual fibrotic change at RML and LUL. Left pleural effusion was disappeared.

depend upon what organ is involved. Extrapulmonary manifestations of nocardiosis include skin lesion (especially subcutaneous abscess), liver abscess, brain abscess and abscess formation in any other organs.[10,11,15,19,22] Disseminated disease is not uncommon. The risk of metastatic infection did not seem to be related to patients' underlying immune status.[10,23] Poor prognostic factors in nocardiosis are (1) acute fulminant infection with an incubation period of less than 3 weeks. (2) Cushing's syndrome (3) central nervous system dissemination (4) those receiving corticosteroid or antineoplastic therapy.[10,14,22] Death by nocardial infection usually from sepsis, brain abscess and overwhelming pneumonia.[22]

Nocardial pulmonary infection can produce a variety of radiographic abnormalities.[1,9,10,11,13,17,18] Pulmonary consolidation in large area usually is the most common pattern in many previous reports.[1,13,14,15,17-19] Other radiographic patterns are solitary or multiple irregular masses or nodules, reticulonodular pattern, pleural effusion with or without pleural plaque, mediastinal or hilar lymphadenopathy. The frequency of cavitary lesions within the consolidated area or within the solitary nodules or masses are variable and range from 15-62%. The highest incidence of cavitation is in the series of pulmonary nocardiosis associated wih AIDS. Extension of pulmonary lesion into the pleural space with chest wall involvement occured in 8-10% of cases.[10,14] However, chest radiograph may appear normal despite sputum culture positive for nocardia. These patients usually have mild symptoms and recover without treatment. The saprophytic role of nocardia is still questionable.[11]

From our study, the consolidation (usually inhomogeneous rather than homogeneous in appearance) is also the most frequent pattern seen. Pulmonary nodules, masses or reticulonodular infiltrative pattern are commonly less seen. Multiple cavitary changes developed within the consolidation, nodules or masses either on initial or follow up radiographs are very pertinent character. They occur in higher percentage than previous reports.[1,13,14,17,18] Pleural effusion and hilar lymphadenopathy are often less seen. Solitary large abscess formation with air fluid level is seen in chest radiograph in only one case. Spontaneous pneumothorax presented in case of polymyositis could be due to the underlying disease itself or rupture of pre-existing subpleural bleb rather than the nocardiosis.

The morphology of nocardia is rather characteristically different from most of other bacteria, fungi and mycobacteria. Nocardia is seen as non-spore forming, filamentous Gram positive branching rod on usual sputum Gram stain and weakly acid fast branching filamentous organism on modified Ziehl-Neelsen staining method. The typical appearance of nocardia on sputum examination in combination with the compatible chest radiographic pattern in immunocompromised patients should suggest nocardial pulmonary infection and presumptive diagnosis can be made. Prompt and appropriate treatment should be initiated since therapeutic response is usually effective even in these compromised hosts. Although some other organisms of the family Actinomycetaceae have been reported to be positive with modified Ziehl-Neelsen staining method[23] but these occurance are not common. Moreover, nocardial infection of the lung is much common than the actinomycoses in the immunocompromised patients. However; sputum, pleural fluid, pus or any tissue preparations that are obtained should be sent for culture confirmation. Nocardia can grow on many kinds of culture media but isolation of nocardia is relatively difficult because it rerely grow on within the first 48 to 72 hours and the culture plates or tubes may have been discarded before any growth can be detected. In addition; there may be overgrowth of other more rapidly growing mouth flora which may interfere with the culture result.[12,14] Growth of nocardia usually require two or more weeks and suspecious nocardial infection should be informed upon request. False negative sputum culture may be as high as two third of all cases,[11] therefore; invasive procedure as tranbronchial biopsy, percutaneus needle aspiration or open lung biopsy may be required for definite tissue diagnosis.

As a radiologist, the consideration of pulmonary nocardiosis should be considered if the appearance of multiple cavitary changes are seen in the area of consolidation, nodules or masses with or without pleural effusion on chest radiograph of immunocompromised patients. Pulmonary tuberculosis or other atypical mycobacterial pneumonia, pyogenic pneumonia and unususal pattern of pneumocystis carinii pneumonia in HIV infected patients can also be presented in such radiographic patterns and should be included in the differential diagnosis.[24-27] In the same population of advancing age, single or multiple, cavitating or noncavitating nodule (s) or mass (es) with or without adjacent rib destruction should be differentiated from primary or metastatic lung cancer and histologic proof should be obtained.

ACKNOWLEDGEMENT

The authors are grateful to Mr. Somsak Wanwilairat and Mrs. Nantaka Pukanhapan for their excellent computerized secretorial work on the manuscript.

Table 1. INITIAL CHEST RADIOGRAPHIC ABNORMALITIES.

CASE	UNDERLYING DISEASE	CONSOLI-DATION (S)	NODULE (S)	MASS (ES)	R N.	CAVI-TIES	ABSCESS	HILAR LN.	PLEURAL EFFUSION
1.	HIV infection	+ (I,S)	+ (M)	—	—	+	—	+	—
2.	HIV infection	+ (I,S)	—	—	+	—	—	—	—
3.	HIV infection	+ (H,S)	—	—	—	—	—	—	—
4.	HIV infection	—	—	+ (S)	—	+	—	—	—
5.	HIV infection	+ (I,S)	—	—	—	+	—	—	—
6.	HIV infection	+ (I,S)	—	—	—	+	—	—	—
7.	HIV infection	+ (I,S)	—	—	—	+	—	—	—
8.	HIV infection	+ (I,S)	—	—	—	+	—	—	+ (U)
*9.	polymyositis	+ (I,M)	+	—	+	+	—	—	—
10.	overlapped syndrome	—	+ (S)	—	+	—	—	—	—
11.	SLE	—	—	—	—	—	+	—	—
	TOTAL	8	3	1	3	7	1	1	1
12.	HIV infection	+ (H,S)	—	—	+	—	—	—	—
13.	HIV infection	+ (I,S)	+ (M)	—	—	+	—	—	—
14.	HIV infection	+ (I,M)	—	—	—	+	—	—	—
15.	HIV infection	—	+ (M)	—	—	+	—	—	—
16.	HIV infection	+ (I,M)	+ (M)	—	—	+	—	—	+ (B)
17.	HIV infection	+ (I,M)	—	—	—	+	—	—	—
18.	SLE	+ (I,S)	—	+ (M)	—	+	—	—	—
	TOTAL	6	3	1	1	6	0	0	1

CASE 1-11 = definite pulmonary nocardiosis,
CASE 12-18 = presumptive pulmonary nocardiosis
RN. = Reticulonodular infiltration, HILAR LN. = Hilar lymphadenopathy
I = inhomogeneous, H = homogeneous, S = single area, M = more than one area
U = unilateral, B = bilateral
* = spontaneous right pneumothorax with parital right lung volume loss.

TABLE 2. INFECTIOUS COMPLICATION OF AIDS : ORGANISMS THAT TAKE ADVANTAGE OF T-CELLS DEFECTS

BACTERIA	FUNGI	VIRUSES	PARASITES
M. Tuberculosis M. avium intracellulae Salmonella Legionella Nocardia Listeria	Candida albicans Cryptococcus neoformans Histoplasma capsulatum Coccidioides immitis	Cytomegalovirus Herpes simplex virus JC virus ? adenovirus	Pneumocystis carinii Cryptosporidia Isospora belli

TABLE 3. CAUSES OF PULMONARY INFECTION IN AIDS PATIENTS

ORGANISMS TAKING ADVANTAGE OF T-CELL DEFECT	ORGANISMS TAKING ADVANTAGE OF B-CELL DEFECT	OTHER ORGANISM
Pneumocystis carinii Cytomegalovirus M. tuberculosis Legionella Nocardia asteroides ? M. avium intracellularae ? Adenovirus	Streptococcus pneumoniae Hemophilus influenza	Staphylococcus aureus Gr. B streptococcus Branhamella catarrhalis

REFERENCES

1. Kramer MR, Uttamchandani RB. The radiographic appearance of pulmonary nocardiosis associated with AIDS. Chest 1990; 98: 382-5.
2. Rodrigez JL, Barrio JI, Pitchenik AE. Pulmonary nocardiosis in the AIDS: diagnosis with bronchoalveolar lavage and treatment with non-sulphur containing drugs. Chest 1986; 90: 912-4.
3. Holtz HA, Larvey DP, Kapila R. Actinomycosis infection in the AIDS. Ann Intern Med 1985; 102: 203-5.
4. Krick JA, Stinson EB, Reminton JS. Nocardial infection in heart transplant patients. Ann Intern Med 1975; 82: 18-26.
5. Wilson JP, Turner HR, Kirchner KA, Chapman SW. Nocardial infection in renal transplant recipients. Medicine 1989; 68: 38-57.
6. Hellyar AG. Experience with Nocardia asteroides in renal transplant recipients. J Hosp Infect 1988; 12: 19-27.
7. Raby N, Forbes G, Wiliums R. Nocardial infection in patients with liver transplants or chronic liver disease: radiologic findings. Radiology 1990; 174: 713-6.
8. Simpson GL, Stinson EB, Eggar MJ, Reminton JS. Nocardial infection in the immuno compromised host: a detailed study in a defined population. Rev Infect Dis 1981; 3: 492-507.
9. Deem RL, Doughty FA, Beamen BL. Immunologically specific directed lymphocytic-mediated killing of Nocardia asteroides. J 2401-2406.
10. Curry WA. Human nocardiasis: a clinical review with selected case reports. Arch Intern Med 1980; 140: 818-26.
11. Young LS, Armstrong D, Blevins A, Lieberman P. Nocardia asteroides infection complicating neoplastic disease. Am J Med 1971; 50: 356-67.
12. Willium dm, Krick JA, Reminton JS. Pulmonary infection in the compromised host. Am Rev Resp Dis 1976; 114: 359-394/593-627.
13. Feigin DS. Nocardiosis of the lung: chest radiographic finding in 21 cases. Radiology 1986; 159: 9-14.
14. Wongthim S, Charoenlap P, Udompanich V, Punthumchinda K, Suwanagool P. Pulmonary nocardiosis in Chulalongkorn Hospital. J Med Assoc Thai 1991; 74 (5): 271-7.
15. George RB, Penn RL, Kinasewitz GT. Mycobacterial, fungal, actinomycotic, and nocardial infections of the pleura. Clin Chest Med 1985; 6: 63-75.
16. Beamen BL, Burnside J, Edwards B, Causey W. Nocardial infections in the United States, 1972-1974. J Infect Dis 1976; 134: 286-9.
17. Grossman CB, Bragg DG, Armstrong D. Roentgen manifestations of pulmonary nocardiosis. Radiology 1970; 96: 325-30.
18. Balikian JP, Herman PG, Kopit S. Pulmonary nocardiosis. Radiology 1978; 126: 569-73.
19. Murray JF, Finegold SM, Froman S, Will DW. The changing spectrum of nocardiosis. Am Rev Respir Dis 1961; 83: 317-30.
20. Andriole VT, Ballas M, Wilson GL. The association of nocardiosis and pulmonary alveolar proteinosis: a case study. Ann Intern Med 1964; 60: 266-75.
21. Gold JWM. Pulmonary effects of AIDS, infectious complications. Clin Chest Med 1988; 9: 377-86.
22. Presant CA, Wiernik PH, Serpick AA. Factors affecting survival in nocardiosis. Am Rev Respir Dis 1973; 108: 1444-8.
23. Robbay SJ, Vickery AL. Tinctorial and morphologic properties distinguishing actinomycosis and nocardiosis. New Eng J Med 1970; 282: 593-6.
24. Kuhlman JE, Fishman EK, Hruban RH, Knowles M, Zerhouni EA, Siegelman SS. Diseases of the chest in AIDS: CT diagnosis. Radiographics 1989; 9: 827-57.
25. Kuhlman JE, Deutsch JH, Fishman EK, Siegelman SS. CT features of thoracic mycobacterial disease. Radiographics 1990; 10: 413-31.
26. Amorosa JK, Nahass RG, Nosher JL, Goeke DJ. Radiologic distinction of pyogenic pulmonary infection from Pneumocystic carinii pneumonia in AIDS patients, Radiology 1990; 175: 721-4.
27. Klein JS, Warnock M, Webb RW, Gamsu G. Cavitating and noncavitating granulomas in AIDS patients with PCP. AJR 1989; 152: 753-4.

The Change is Here

Professional artist donna krin Korkes, using X-ray images as the basis for her artwork, brings a new perspective to interpreting medical images. This painting, called "Double Exposure," is derived from various X-ray images. To see the work of this New Jersey-based artist, stop by the 3M booth.

No developer. No fixer. No wet processor. No wet chemistry maintenance. No wet processor downtime. No wet chemistry purchase costs. No wet processor/ chemistry drift. No plumbing. No darkroom. No wet chemistry fumes. No wet chemistry disposal costs.

3M DryView Laser Imaging Scores a Big Hit

The early reviews are in, and the new 3M DryView Laser Imaging System is scoring big hits in the radiology department. And 3M DryView 8700 Laser Imagers are available now.

Abbott Northwestern (Minneapolis, Minn.), HealthEast St. John's Hospital (Maplewood, Minn.), Baystate Medical Center (Springfield, Mass.), the University of Michigan (Ann Arbor, Mich.), the University of Arizona (Tucson, Ariz.), Kaiser Healthcare (Parma, Ohio), Mayo Clinic (Scottsdale, Ariz.) and Memphis Regional Hospital (Memphis, Tenn.) were the first hospitals in the U.S. to use the new 3M DryView Laser Imaging System. As of press time, hospitals around the world are lining up to install 3M DryView Laser Imagers.

"3M DryView systems create a new paradigm in radiology" says Jim List, administrative director of radiology for Abbott Northwestern Hospital. "For us, the real sizzle from 3M DryView Laser Imagers isn't just the elimination of wet chemistry, but in enabling entirely new ways to help us deliver better service to patients. Because 3M DryView systems aren't tied down to plumbing, drains and all the components that are needed for 'wet' laser imagers, they give us a whole new dimension for innovation in the radiology department."

"I'm very pleased with the quality of 3M DryView Laser Imaging Systems," says Dr. Doug Yock, radiologist and MRI director at Abbott Northwestern. "The 3M DryView images are as good or better than those from 'wet' laser systems, while the mechanical simplicity of 3M DryView systems provide major advantages for siting and operation."

If you're looking for change from the costs and inconveniences of traditional "wet" processing systems or from the lower quality from other output options, stop by Booth 6340 and take a look at the 3M DryView Laser Imaging Systems.

It All Adds Up for 3M DryView Laser Imaging

If you're thinking about whether the switch to a 3M DryView Laser Imager can cut your imaging costs, please stop by Booth 6340 and ask us to show you the 3M DryView Interactive Cost Evaluation program. It's a computerized evaluation that can help you identify cost areas and how 3M DryView Laser Imaging Systems can save you money.

The 3M DryView Interactive Cost Evaluation program considers wet-chemistry operating costs, wet-chemistry capital costs and other factors and compares these with operating and capital costs for 3M DryView systems to produce a customized analysis based on information you supply.

If you want to know how much you can save by switching to a 3M DryView Laser Imaging System, stop by our booth and ask us about the 3M DryView Interactive Cost Evaluation program.

Stop by 3M booth 6340

For more information about these or any other 3M products and services, stop by our RSNA booth # 6340 in the North Building at McCormick Place, Chicago. Or call your local 3M representative, authorized 3M distributor or the 3M Health Care Customer Helpline at 1-800-228-3957, ext. 7-1332.

What to Look for from 3M

- 3M™ Dry View™ Laser Imaging Systems are here now! This revolution in diagnostic-quality laser imaging changes virtually everything about the process, except the image.
- The 3M™ Dry View™ 8300 Laser Imager will offer the convenience of wet-chemistry free processing in a desk-top size laser imager for 8 by 10-inch film.
- The 3M™ Dry View™ 8700 Laser Imager offers all the features of our popular 3M Laser Imagers for 14 by 17-inch film, without the chemicals.
- The 3M™ Dry View™ 8800 Multi-Input Manager offers flexible printing options from up to eight modalities to the 3M Dry View 8700 Laser Imager, a 3M™ 969 HQ Laser Imager, or a combination of both.
- The 3M™ Dry View™ Interactive Cost Evaluation program — a computerized evaluation that will show you what you can expect to save by switching to 3M Dry View Laser Imaging Systems.
- Conventional solutions for chest imaging with the 3M™ Chest System.
- The new 3M™ Trimatic™ Modular Advanced Processing System — a compact, light-weight system that's ideal where space is limited.
- A tribute to 100 years of radiology — a time capsule from Radiology Centennial, Inc. and 3M that will bring greetings from RSNA 95 to the radiology community in the year 2095.

3M Health Care

MALIGNANT INFANTILE OSTEOPETROSIS: ROENTGENOGRAPHIC DIAGNOSIS

Sudee CHOMDEJ

ABSTRACT

Osteopetrosis is the condition of increased bone density or sclerotic bone. Albers-Schoenberg disease was described as the infantile malignant osteopetrosis based on the disorders of clinical course, radiographic and genetic transmission.[2]

Osteopetrosis was classified as the generalized skeletal dysplasia[3], autosomal recessive of probably deficiency of carbonic anhydrase II with functional defect of the osteoclast resulted in nondestruction of calcified matrix during growth. This causes obliteration of marrow space in the medullary cavities and replaced by excessive calcified matrix. The thickened solid spongiosa causes little blood formation space or obliteration of marrow space within the skeletal portion.

The dysplasia presented in infantile period with anemia, hepatosplenomegaly, recurrent infection, and failure to thrive. Blindness may develop early due to narrowing of the optic canals and other cranial foramina by excessive osteopetrosis. Hydrocephalus may develop due to narrowing of the foramen magnum.

The diagnosis by radiographic examination of the skeleton reveals marked sclerosis of the skeletal structure, as dense as marble bones or osteopetrosis. The bones of osteopetrosis are made up largely of calcified cartilage and are brittle rather than strong, the fracture is not uncommonly frequent. The hematological presentation is protracted hypoplastic anemia, thrombocytopenia and reinfection.

The early dysplasia in infancy is the enlarged metaphysis resembling rickets. The failure of underconstriction of the metaphysodiaphysis or funneralization is found in long bones with the presence of alternating transverse lucency in the sclerosis. The course is early fatal due to depletion of hematopoiesis in bone marrow. The treatment was initiated by bone marrow transplantation with some favorable result.[9-11]

INTRODUCTION

Osteopetrosis is a complex disease of at least four different types. These have very distinct clinical, radiologic, and histopathologic features.[1] It is the condition of increased bone density or sclerotic bone,[2] inherited both by autosomal dominant and recessive ones.

A case report of a 5-months-old boy with malignant type (precocious, congenital or infantile type) of osteopetrosis was presented with plain roentgenographic images.

CASE REPORT

A 5 months old boy had recurrent upper respiratory tract infection for one month. He had anemia, enlarged abdomen and a hard lump at the chest wall. He breathed loudly. He was the product of normal labor and was full term. The other two siblings were healthy and there was no familial history of similar illnesses. The child appeared well-nourished and had received a normal course of immunization.

He was found to have hepatosplenomegaly. He was anemic (Hb 8 gm%), leukocytosis (WBC 23000,

Department of Radiology, Chulalongkorn University Hospital, Henry Dunant Street, Bangkok, Thailand.

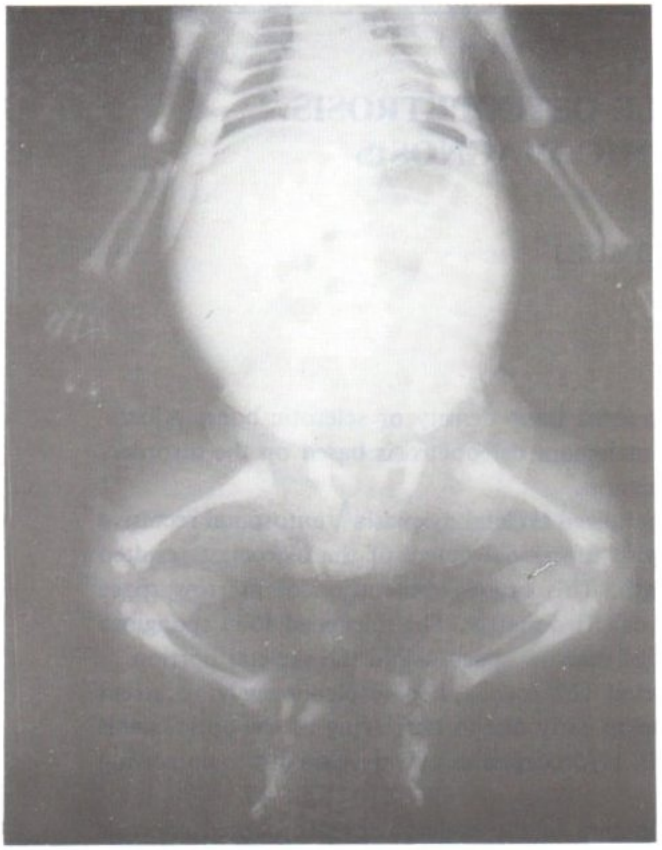

Fig.1: Humanogram including the long bone of upper and lower limbs, spine, ribs and pelvis reveals the increased bone density as sclerosis of the entire bone with obliteration of normal marrow cavity, sclerosis involved the epiphysis, spine and tarsal bone. The sclerotic bone in bone is seen in the pelvic bone, talus, calcaneum, and short bones of the hand and feet. The healing fracture with periosteal new bone as the result of brittle osteopetrosis presented at metaphyso-diaphyseal region of proximal and distal parts of femurs, tibia, humeri, radius and ulna.

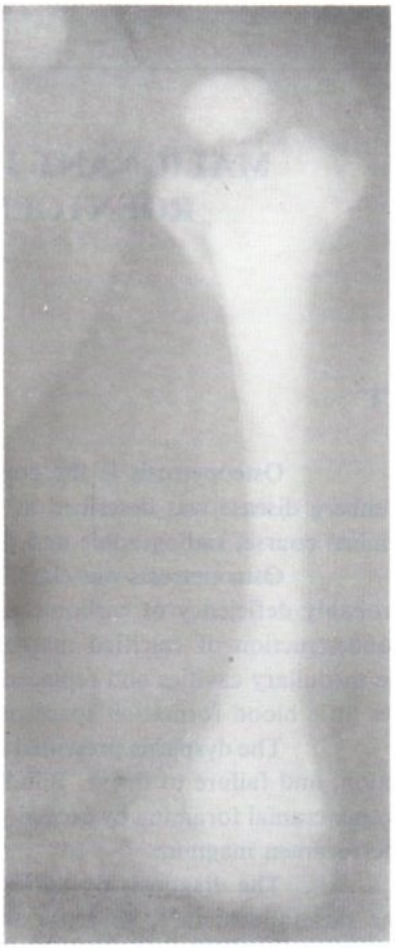

Fig.2: Long bone of left femur revealed the characteristic bone changes of infantile malignant osteopetrosis. The sclerotic clubbing enlarged and fraying metaphyseal end with sclerotic diaphysis and obliteration of normal medullary marrow cavity is noted. The periosteal reaction was disclosed at the metaphyso-diaphyseal region which indicated the healing fracture of the fragile bone disorder. The epiphysis was sclerotic which was the opposite finding seen in ricket.

PMN 29 Band 2, blast 1, promyelocyte 1, metamyelocyte 2, Eos 8, L 49, atypical L8), NRBC was 21/100 RBC, the reticulocyte count was 8% polychromasia 1+.RBC morphology was of hypochromic normocytic pattern and the platelet count was 48000. The LFT, UA and the stool examination was within normal limit. The BUN and creatinine ratio was 5.4 to 0.11. The blood picture was defined as leukoerythroblastosis. The TORCH and VDRL titer were negative. The bone marrow biopsy was obtained from the metaphysis of the tibia and revealed myelofibrosis.

The roentgenographic study of the skull, long bones, spine and flat cuboid bones revealed generalized bony sclerosis with obliteration of the marrow space (Fig.1,2). The metaphyseal ends of the long bones were enlarged and clubbed, having fraying appearance. The long bones of the limbs, were affected. The anterior end of the ribs had the rachitic rosary pictures (Fig.3). The striking findings are the sclerosis of the diaphysis or shafts of the long bones with obliteration of the normal medullary cavity. The fracture of the metaphysis was present with evidence of healing process by the periosteal new bone reaction at the metaphysodiaphyseal region of the proximal femurs. The epiphysis were sclerotic which was in opposite to the findings in ricket. The vertebral bodies and the

small bones of the tarsal bones were also sclerotic (Fig.4). The similar involvement of the skull, and orbits were seen (Fig.5).

DISCUSSION

Infantile malignant osteopetrosis is a rare autosomal recessive disorder characterized by the presentation of diseases in the infancy. It occurs as the result of the osteoclastic functional defect. There is generalized osteopetrosis or dense sclerosis of the bones of the calvarium, spine, long and short small bones. The obliteration of the marrow cavity in the bone is characteristic which results in the profound anemia, hepatosplenomegaly, myelofibrosis or leukemia as were noted in this case. Most patients of the reported cases presented with anemia, bleeding tendency, susceptible infection of the upper respiratory tract or of skin due to the functional defect of the osteoclast.[3,4,5]

The metaphyseal dysplasia is seen as enlarged metaphyses, clubbing and fraying; the sclerosis is less, compared with the denser sclerotic diaphysis. The epiphysis is also sclerotic. These abnormalities are definitely not similar to what is seen in ricket. In ricket, the metaphysis is osteoporotic though the fraying and cupping appearance is present. The diaphysis and epiphysis is osteoporotic and the diaphysis may have the picture of osteomalacia. Congenital metastaes of neuroblastoma and syphilis would be in the differential diagnosis.

The defect of the osteoclast is responsible for the under constriction of the tubular bone at the metaphysodiaphyseal part. The sclerotic bone is fragile and the fracture is noted at the metaphysis with the periosteal new bone formation. The appearance of the dense bone in the bone is mostly observed in the small bones and in the epiphysis of the mandible and iliac bone. The rachitic rosary noted in this case was shown at the anterior end of the ribs of the enlarged metaphysis with sclerosis[2,6].

The thickening of the bone at the cranial foramens causes the regional neurological deficit such as blindness, hearing loss and facial palsy. The thick calvarium later would present as the hair on end on radiographic film, MRI and CT scan with the perpendicular striation of the active marrow. The thickening of the paranasal sinuses was reported and appeared as the poor or nonpneumatized air sinuses, including small nasal cavities, which might be responsible for recurrence of the upper respiratory tract infection.

The dense orbits and skull base are quite unique for this entity. The bone marrow scintigraphy of the cranium revealed extensive marrow activity in the expanded bone marrow cavity.

Hydrocephalus, brain stem compression and the obstruction of the CSF flow is caused by impingement at the foramen magnum, demonstrated clearly by MR and CT imaging in osteopetrosis[6,7,8].

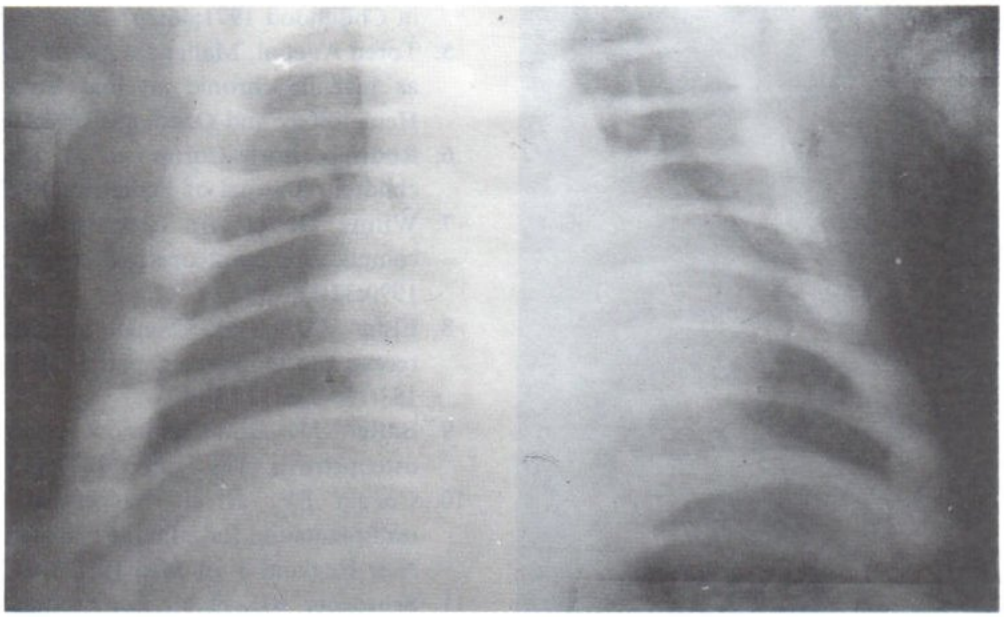

Fig.3: Dense rachitic rosary of the anterior end of the ribs is seen at the lateral part of thoracic cage, as the dense enlarged metaphysis of the sclerotic ribs. The thoracic spine was osteopetrotic.

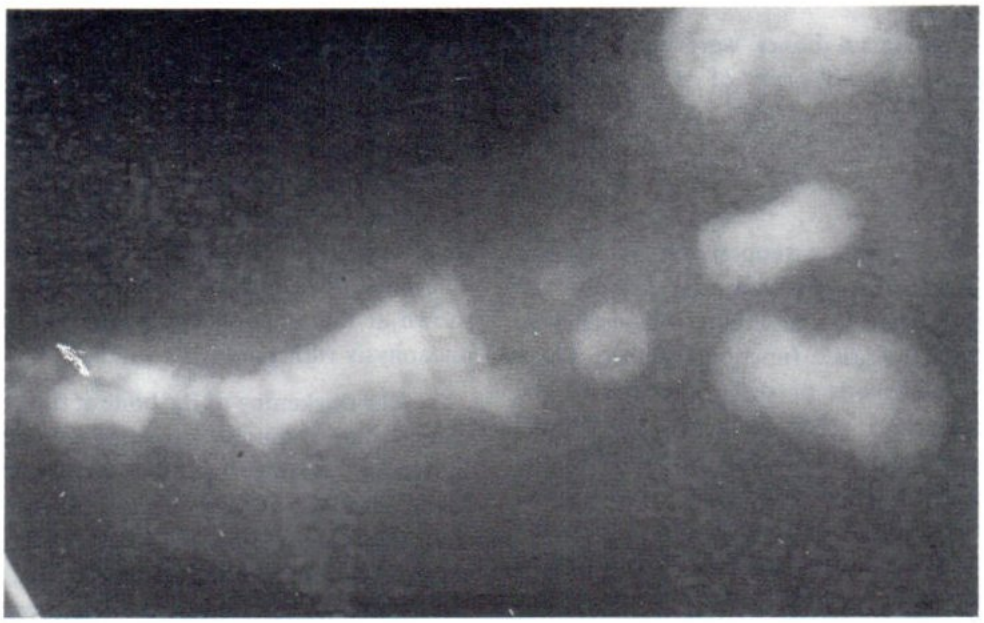

Fig.4: The sclerotic bone in bone revealed at the Talus, calcaneum and metatarsal bones.

The infantile malignant osteopetrosis shows the malignant course of the disease. It has extremely poor prognosis, the patients died in early childhood. The recent treatment was successful in the aspect of remission of the hematologic abnormalities and decreased bone abnormalities by bone marrow transplantation.[9,10,11]

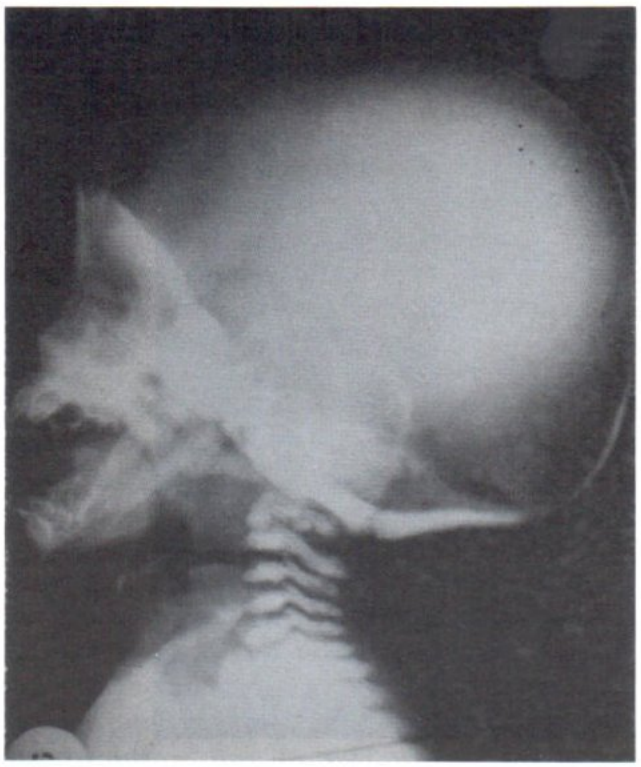

Fig.5: Lateral view of the skull revealed the marked sclerosis of the skull base, occipital bone, orbits, mandible and cervical spine.

REFERENCES

1. Resnick, Niwayama. Diagnosis of bone and joint disorders. Philadelphia:W.B.Saunders Company, 1988:3478-3483.
2. Silverman F, Kuhn JP. Caffey's pediatric X-ray diagnosis. ST Louis: Mosby, 1993:1533-1687.
3. Lenhard S, al. Defective osteoclast differentiation and function in the osteopetrotic (os) rabbit. Americal Journal of Anatomy 1990;188:438-44.
4. Yu JS, et al. Osteopetrosis. Archives of Disease in Childhood 1971;46:257-263.
5. Toren A, et al. Malignant osteopetrosis manifested as juvenile chronic myeloid leukemia. Pediatric Hematology and Oncology 1993;10:187-9.
6. Rodrigo Loria-Cortes et al. Osteopetrosis in children. Journal of Pediatrics 1977;91:43-47.
7. Wilms G, et al. Cerebrovascular occlusive complication in osteopetrosis major. Neuroradiology 1990;32:511-3.
8. Elster AD, et al. Cranial imaging in autosomal recessive osteopetrosis, part I, II. Radiology 1992; 183:129-135:137-144.
9. Ballet JJ. Bone marrow transplantation in osteopetrosis. The Lancet 1077;1137.
10. Coccia PF, et al. Successful bone marrow transplantation for infantile malignant osteopetrosis. New England J of Med 1980;302:701-708.
11. Schroeder RE, et al. Longitudinal follow up of malignant osteopetrosis by skeletal radiographs and restriction fragment fragment length polymorphism analysis after bone marrow transplantation. Pediatrics 1992;90:986-989.

ABDOMINAL ACTINOMYCOSIS

Patchrin PEKANAN, Thitiporn RANGSITPOL

ABSTRACT

Two cases of abdominal actinomycosis was presented. In one case, the disease involved ileocecum and appendix of a 35-year-old man. Plain film and ultrasonography was suggestive of localized inflammation of the ileocecal area and not specific. In another case, the disease involved left ovary with fistula tract to the anterior abdominal wall. CT scan showed left ovarian mass and soft tissue lesion at anterior parietal peritoneal cavity and muscle of right anterior lower abdominal wall.

INTRODUCTION

Actinomycosis is a chronic, progressive, suppurative disease characterized by formation of multiple abscesses, draining sinuses, abundant granulation and dense fibrous tissue. The appearance of sulfur granules in the lesions, sinus walls or discharges of involved tissues is characteristic (1).

Two cases of abdominal actinomycosis were shown; the lesion involved ileocecal area and the appendix in one case and ovary in another case.

CASE REPORTS

CASE 1

A 35-year-old man, a labor-worker in Bangkok, admitted to Ramathibodi hospital due to right lower quadrant colicky pain for one day. Watery diarrhea was noted for five times. He also had high fever for 12 days prior to the admission. A mass was palpated at right lower quadrant with signs of peritonitis in this region. Leukocytosis was present with PMN predomination. Ruptured appendicitis was suspected and he was explored. Plain films of the abdomen (Fig.1) showed localized rigidity of the bowel loop of terminal ileum and proximal right colon with short air fluid levels. Intraperitoneal free fluid was noted. Ultrasonography at right lower quadrant (Fig.2) showed thickened bowel wall and surrounding fatty infiltration with fluid. At operation, 500 cc of serosanguinous fluid was found. There was hyperemia of the terminal ileum, mass at cecum, necrosis of the mesocolon and retroperitoneal area. Fibrin and old hemorrhage was observed. Enlarged nodes were not detected. At pathological examination revealed ulceration of the mucosa of the terminal ileum. Ileocecal valve was markedly swelling. The lumen of the appendix was severely narrow. Intact folds of the cecum and mild swelling of the mucosa was detected. Fibrin coating at serosal surface of the resected bowel was seen. A mass, size 3-4 cm in diameter was seen at mesocolon of the ascending colon; cut surface showed soft yellowish, gray and tan friable tissue with hemorrhagic and necrotic foci. Actinomycosis was suggested, though organisms were not identified by GMS. The patient recovered well.

CASE 2

A 26-year-old woman from Yasothorn province (North-eastern part of Thailand), observed a foul smell, bloody greenish discharge from the palpated mass at right lower abdomen for one day. She had chronic lower abdominal pain for 3 months. A 10-cm mass at left adnexa was found by the Gynecologist one month ago. Right lower abdominal pain and palpable mass was observed for 5 days. There was a low grade fever. Twenty-weeks-sized suprapubic mass was noted

PMN = Polymorphonuclear

Department of Radiology, Ramathibodi Hospital, Rama 6 Street, Bangkok 10400, Thailand.

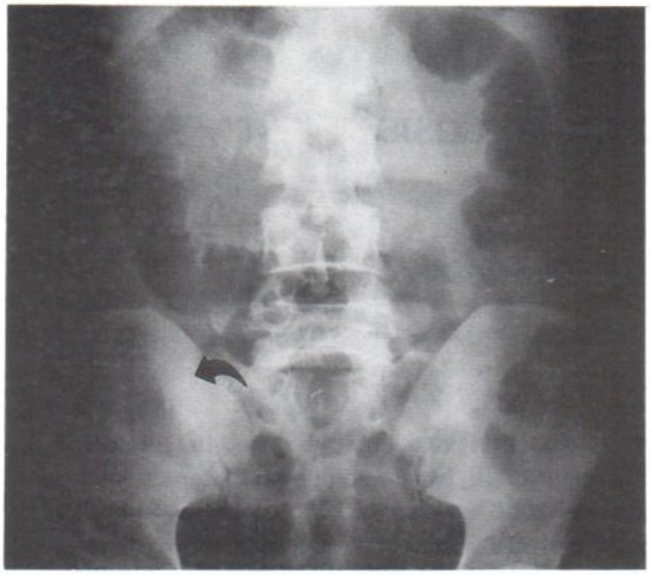

Fig.1 Case 1. Localized rigidity of the terminal ileum at RLQ by plain film

with nodular surface and local cellutitis. A complexed mass was noted by ultrasonography at right lower quadrant, (Fig.3). CT scan showed a solid mass at left adnexa with small cystic areas. Left ovary could not be identified well (Fig.4). An ovoid shape soft tissue lesion was shown at left paramedian anterior intraperitoneal cavity, attached to the parietal peritoneum and was at just anterior to the urinary bladder. An infiltrative border soft tissue lesion was detected at muscle plane of right lower anterior abdominal wall, at mid and lower iliac wing level (Fig.4).

At surgery, left ovary was slightly enlarged, filled with pus. A fistular tract was noted at right side of the abdominal wall connecting to the intraabdominal cavity. Adhesion was present with the omentum and jejunum. At gross examination, the left ovary contained solid,grey-whitish mass in the entire ovary. Section of the left ovary was compatible with actinomycosis.

DISCUSSION

Abdominal actinomycosis was first described by Bradshaw (2) in 1846. Bolinger (3) demonstrated that a fungus was the primary infective agent in 1877. Actinomyces was derived from the Greek works for ray and fungus, due to the appearance of the filaments radiating from a central tangled mass. Israel (4) noted granules from material, containing mycelia in 1878. Studies of cell wall components resulted in classification of Actinomyces as a bacterium, distinct from the fungi (5,7).

The Actinomyces organism is a fastidious, gram positive, non-spore forming microaerophilic or obligate anaerobe that varies in growth pattern and is somewhat difficult to isolate. Successful isolation requires culture of multiple samples of purulent material in enriched media under anerobic conditions with carbon dioxide, and an adequate time for growth (1,8,9).

There are at least six different species of bacteria which can cause actinomycosis in humans (9,12). Actinomyces israelii, Actinomyces propionicus, Arachnia propionica (13,15). Actinomyces naeslundii

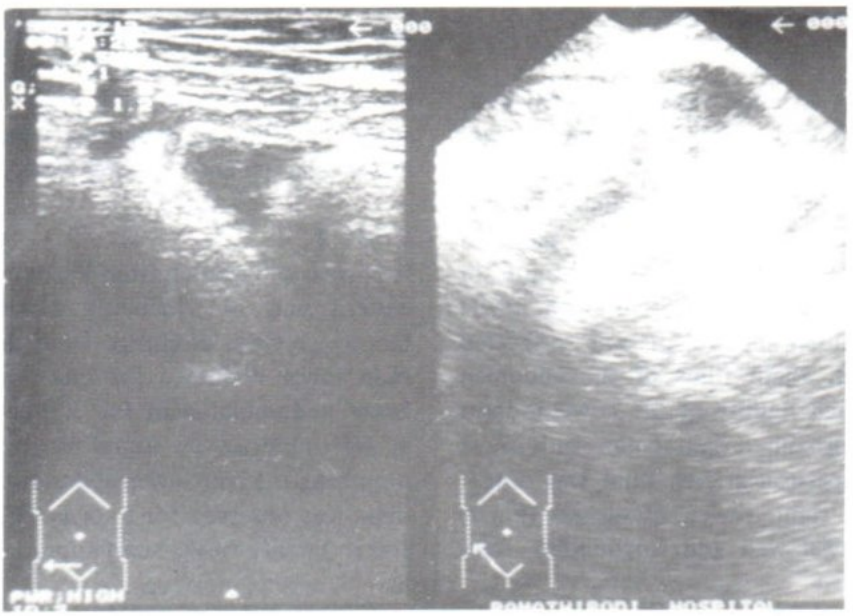

Fig.2 Case 1. Fluid collection at RLQ and around bowel loop, was seen at ultrasonographic examination.

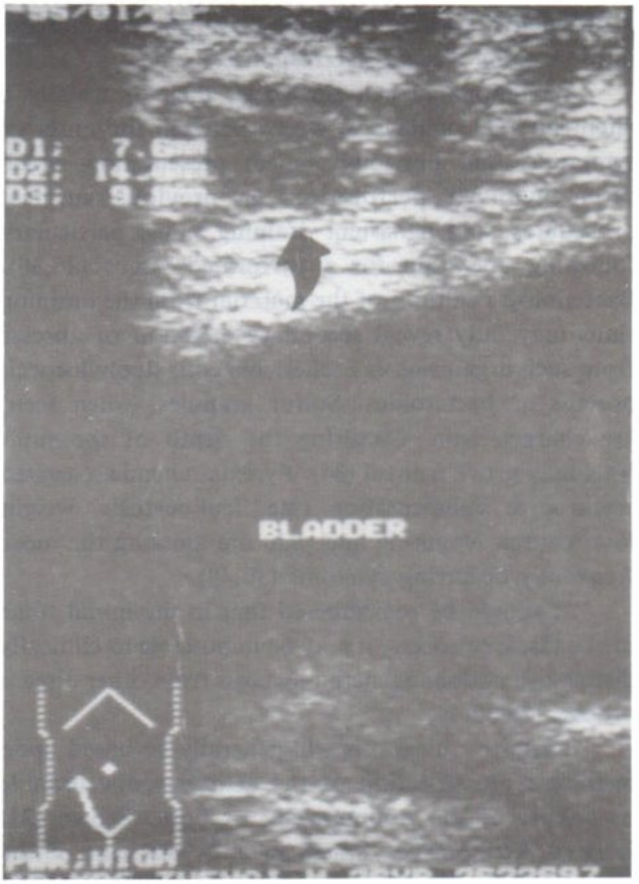

Fig. 3A. Case II. Low echoic right anterior abdominal wall lesion, at ultrasonogram.

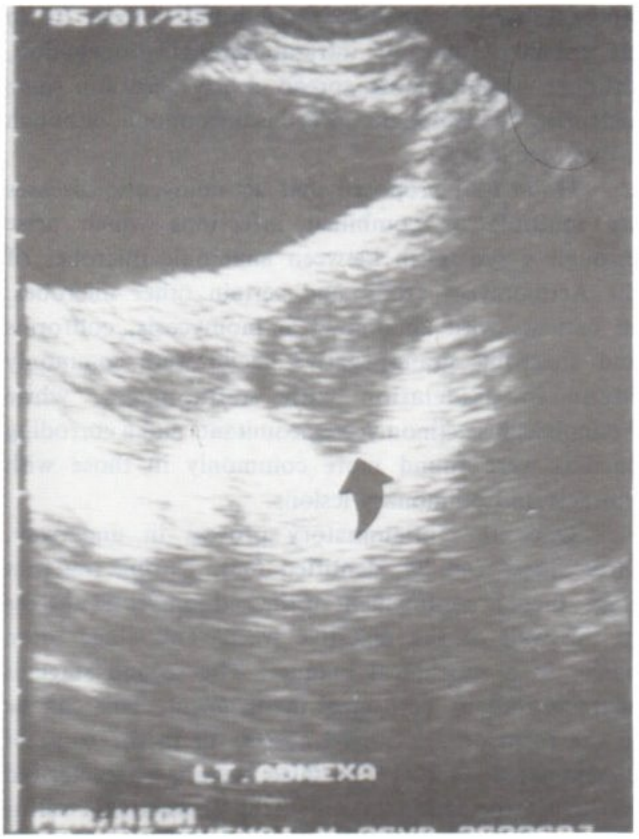

Fig. 3B. Enlarged left ovary with solid lesion at posterior part, at sonography

(16,17), Actinomyces viscosus (18), Actinomyces eriksonii, Bifidobacterium (11), and Actinomyces odontolyticus (19,20).

Although the low percentage of recovery of Actinomyces organisms by culture, and the high percentage of no growth in culture is generally conceded (12), it is also contended that in order to obtain more fruitful yield, close cooperation between the attending physician and the microbiologist is required (9,15).

Actinomycosis has a world-wide distribution and is present with equal frequency in city and rural dwellers. There is no discernible sex predilection, although males are more frequently infected than females (8). Most instances occur in adolescents and middle-aged individuals.

The frequency with which abdominal actinomycosis occurs as compared with the cervicofacial and thoracic forms of the disease is varied. In some studies, it ranks first (22,23), in others third (22,24-26) and in most second (24,26,27).

The incidence of actinomycosis is difficult to estimate. It would appear that the principal reasons for difficulty lie in the fact that clinical suspicion of the disease is generally low, difficulties are encountered in obtaining bacteriologic cultures, the response of the microorganisms to penicillin is exquisite and Actinomyces israelii is indigenous to the oral cavity and as such, simple recovery does not necessarily establish the diagnosis.

It is accepted that the Actinomyces organism is a normal, frequently found inhabitant of the oral cavity and tonsillar crypts (11). Infestation of the gastrointestinal tract appears to come primarily from Actinomyces in the oral cavity (28,29).

Abdominal actiomycosis shows a predilection for the right iliac fossa and has frequently followed operations for acute appendicitis or drainage of abscesses in this region. The appendix is by far the most common intra-abdominal organ involved (22,24). This is followed with much lesser involvement of the colon (30), stomach (31), liver (32), gallbladder (33), pancreas (34), small bowel (35), anorectal region (38), pelvis (37), abdominal wall (38), and other less common sites (39,40). Most instances show involvement of a single organ. Disseminated intra-abdominal actinomycosis is less common (21,41). With the introduction of intrauterine contraceptive devices, a number of instances of pelvic actinomycosis have been reported (42,43,44).

Once the organisms have penetrated through the mucosal barrier, spread by continuity appear as to the primary route of intra-abdominal propagation, although hematogenous spread clearly occurs in some instances. The lymphatic spread is uncommon, although it does occur (46).

Holm (46) proposed that actinomycotic diseases are multiple or combined infections which arise through a synergism between anaerobic microbes of the Actinomyces group and certain other microbes. In patients with abdominal actinomycosis, coliforms and anaerobic gram-negative bacilli were commonly found in association with Actinomyces, while Actinobacillus actinomycetemcomitants and a corroding bacillus were found more commonly in those with thoracic and pulmonary lesions.

Once the inflammatory process in underway, three stages can be identified (35). During the first stage, there is confinement of the actinomycotic abscess to the wall of the digestive tract. This stage often passes in a subclinical manner. The second stage is characterized by peritoneal involvement. This can be in the form of a localized abscess or in the form of disseminated disease. The third stage is characterized by fistula formation in which the charactristic sulfur granules are often noted.

The actinomycotic abscess without formation of fistula is generally typified by single or multiple abscess or by indurated masses with hard fibrous walls and soft central loculations containing white or yellow pus.

Minsker and Yegorova (47) demonstrated that the inflammatory response to Actinomyces began during the first hours after inoculation and comprised three stages. The first stage was characterized by a nonspecific exudative inflammatory response, the second stage by a productive specific inflammatory response and the third stage by a regressive response.

In abdominal actinomycosis, there is usually a latent interval of days to weeks between the onset of symptoms and previous clinical presentation which often involved perforation or previous surgical procedures, and persistent draining sinus, particulary following operation for a perforated viscus (26,30). Bacteriologic cultures of the material from the draining sinus may only reveal secondary infection of abscess from such organisms as Escherichia coli, staphylococci, proteus or bacteroides. Sulfur granules, when seen, are characteristic. Culturing the depth of the sinus tract may prove fruitful (34). Pyrexia, anemia, elevated erythrocyte sedimentation rate, leukocytosis, weight loss, nausea, vomiting and pain are amoung the more frequently occurring symtoms (30,48).

It should be remembered that in the initial stage of the disease process, it may be impossible to clinically distinguish abdominal actinomycosis from other disease process (26,35,49).

Definitive diagnosis will generally be based upon histologic identification of the actinomycotic granule or culture of the Actinomyces, or both. Brown (21) isolated Actinomyces israelii in a 24 per cent of the instances cultured. There was no growth in about 46 per cent of the cultures and the remaining cultures grew other bacteria or unidentified organisms.

In the abdominal form of actinomycosis, the majority of reported instances have become evident several weeks or even months after an acute episode of perforated gastrointestinal disease, such as acute appendicitis, perforated colonic diverticulitis, perforated peptic ulcer or acute ulcerative disease of the intestinal tract, or after trauma, including operations. However,

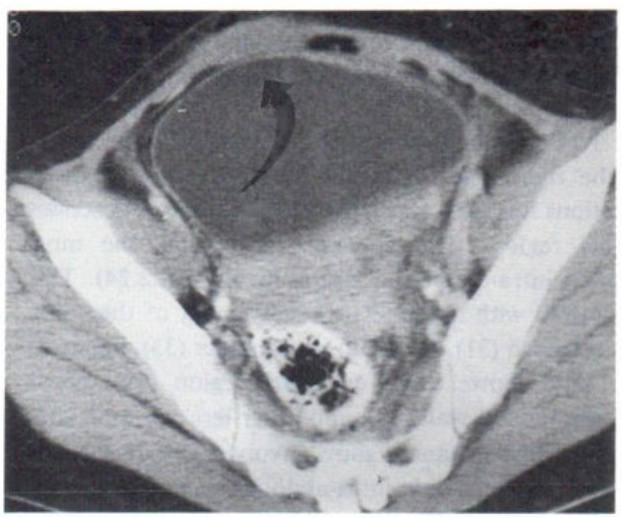

Fig.4A. Case II Right anterior abdominal wall lesion, at CT scan

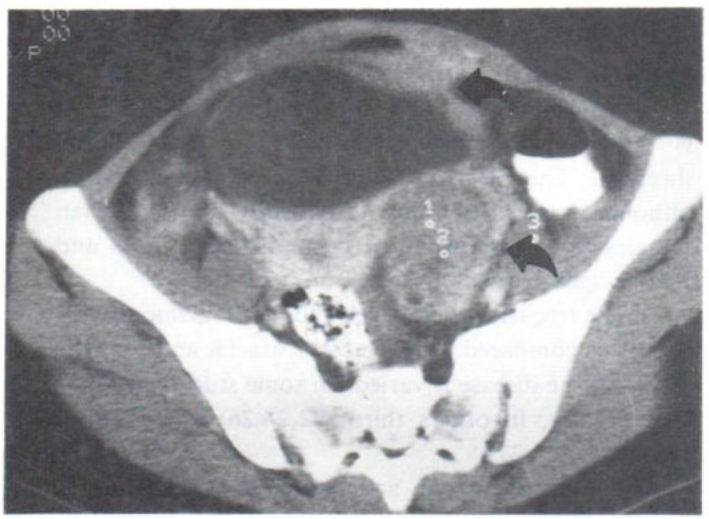

Fig.4B. Left ovarian lesion, at CT scan

in many patients no antecedent disease or operation has been noted (21). Actinomyces organisms are best thought of as opportunist pathogens, although the conditions predisposing to infection are not always apparent. A more frequent association of antecedent disease or trauma, or both, generally noted in the cervicofacial or thoracic forms of actinomycosis. A number of patients with thoracic actinomycosis have pre-existing chronic bronchitis, emphysema, chronic pneumonitis, aspiration or infarction (21).

Our first case mimicked acute appendicitis and the disease was at stage two and the second case was at stage three. Imaging diagnosis of these two cases alone could not lead to the proper diagnosis due to the nonspecificity of the findings. Fistula tract could occur in other chronic infections such as tuberculosis, Crohn's disease, fungal infection, and in malignant process.

REFERENCES

1. Berardu RS. Abdominal actinomycosis. Surgery, Gynecology & Obstetrics 1979;149:257-266.
2. Idem. Visceral actinomycosis. Br.Med J 1949; 2:1311.
3. Bollinger O. Ueber sine neue Pilzkrankheit beim Rinde. Centralb f.d. med. Wissensch, Berl 1877; 15:481.
4. Israel J. Neue Beobactungen auf dem Gebiete der Mykosen des Menschen. Virchow Arch Pathol Anat. Berlin 1878;74:15.
5. Cummins CS. The chemical composition of cell walls of actinomycetes and its taxonomic application. Ann Inst. Pasteur, 1962;103:385
6. Idem. Chemical composition and antigenic structure of cell mass of Corynebactrium, Mycobacterium, Nocardia, Actinomyces and Arthrobacter. J Gen Microbiop 1963;28:35.
7. Cummins CS, Harris H. Studies on the cell wall composition and taxonomy of Actinomycetales and related groups.J Gen Microbiop 1958:18:173.
8. Conant MF, Smith DT, Bajer RD and Callaway JL. Actinomycosis. In:Manual of clinical Mycology, 3rd ed., chapt i,ppl-37. Philadelphia: W.B. Saunders Co., 1971.
9. Dowell VR, Sonnenwirth AC. Gram-positive nonsporeforming anaerobic bacilli. In:Manual of Clinical Microbiology 2nd ed, chap 42, pp 396-401. Washington, D.C.:Am Soc Microbiologists, 1974.
10. Bowden GH, Hardie JM. Commensal and pathogenic Actinomyces species in man. Soc Appl Bacteruik Symposium Series, London, 1973:2:227.
11. Lerner PI. Susceptibility of pathogenic Actinomycetes to antimicrobial compounds. Antimicrob Agents Chemother 1974;5:302.
12. Wallace RJ, Jr. Musher DM. Actinomycosis; an update. Int J Dermatol 1977;16:185.
13. Abe PM, Majeski JA, Stauffer LR. Histological changes observed in Arachnia propionica infection of mice. J Surg Res 1978;25:174.
14. Brock DN, Georg LK, Brown Jm, Hicklin ND. Actinomycosis caused by Arachnia propionica; report of 11 cases. Am J Clin Pathol, 1973;59:96.
15. Georg LK, Roberstad GW, Brinkman SA. A new pathogenic Actinomyces species. J Infect Dis 1965; 115:88.
16. Salkin IF, Gordon MA. Pathogenicity of Actinomyces naeslundii. Chest 1974;66:467.
17. Varkey B, Kurup PV. Pathogenicity of Actinomyces naeslundii. Chest 1974;66:467.
18. Gutschik E. Endocarditis caused by Actinomyces Viscosus. Scand J Infect Dis 1976;8:271.
19. Guillon JP, Durieux R, Dublanchet A, Chevrier L. Actinomyces odontolyticus; premiere etude realisee en France, CR Acad Sci, Paris 1977; 285:1161.
20. Morris JF, Kilbourn P. Systemic actinomycosis caused by Actinomyces odontolyticus. Ann Intern Med 1974;81:700.
21. Brofwn JR. Human actinomycosis; a study of 181 subjects. Hum Pathol 1973;4:319.
22. Harvey JC, Cantrell JR, Fisher AM. Actinomycosis; its recognition and treatment. Ann Intern Med 1957;46:868.
23. Weed LA, Baggenstoss AH. Actinomycosis; a pathologic and bactriologic study of twenty-one fatal case. Am J Clin Pathol 1949;19:201.
24. Davis MIJ. Analysis of forty-six cases of actinomycosis with special reference to its etiology. Am J Surg 1941;52:447.
25. Pulverer G. Problem of human actinomycosis. Postepy Hig Med Dosw 1974;28:253.
26. Copy VZ. Actinomycosis. London: Oxford University Press, 1938.
27. Eastridge CE, Orather JR, Hughes FA, Jr. Actinomycosis; a 24-year-experience. South Med J 1972;65-839.
28. Kolouch F, Peltier LF. Actinomycosis. Surgery 1946;20:401.
29. Spilsbury BW, Johnstone FRC. The clinical course of actinomycotic infections; a report of 14 cases. Can J Surg 1962;5:33.
30. Davies M, Deddie NC. Abdominal actinomycosis. Br J Surg 1972;60:18.

31. Cajal SRY, DeLaPena M, Campo C. Actinomycosis gastrica Intramural; observaciones anatomoclinicas sobre un caso y revision de la literatura. Rev Enfern Apar Dig 1977:50:445.
32. Golematis B, Hatzitheofilou C, Melissas J. Liver actinomycosis. Am J Gastroenterol 1976;65:148.
33. Marrie T. Stiver HG, Molgat A. Actinomycosis of the gallbladder. Can J Surg 1977;20:147.
34. Jelen M, Drak AJ, Korolewicz W, Wadowski R. Diagnostic difficulties in an atypical case of actinomycosis of the abdominal cavity. Patol Pol 1977;28:227.
35. Mousseau PA, Mousseau-Brodu MC.L' actinomycose abdominale. J Chir, Paris 1973;106:565.
36. Brewer NS, Soencer RJ, Nichols DR. Primary anorectal actinomycosis. JAMA 1974;228:1379.
37. Chakrabarty D, Wessely Z. Ovarian actinomycosis. N.Y. Stage J Med 1978;5:806.
38. Minocha VR, Sharma MM, Nair SK. Primary actinomycosis of the abdominal wall. Aust N Z J Surg 1975;45:66.
39. Anscombe AR, Hofmeyer J. Peranal actinomycosis complicating pilonidal sinus. Br J Surg 1954;41:666.
40. Crosse JEW, Soderdahl DW, Schamber DJ. Renal actinomycosis. Urology 1976;8:309.
41. Legum LL, Greer KE, Glessner SF. Disseminated actinomycosis. Sougth Med J 1978;71:463.
42. Barnham M, Burton AC, Copland P. Pelvic actinomycosis associated with IUD Br Med J 1978; 1:719.
43. Csapo Z, Csomor S, Zambo Z. Ovarian actinomycosis developed during the use of a plastic intrauterine contraceptive device. Acta chir Acad Sci Hung 1977;18:149.
44. Luff RD, Gupta PK, Spence MR, Frost JK. Pelvic actinomycosis and the intrauterine contraceptive device; a cytohistomorphologic study. Am J Clin Pathol 1978;69:581.
45. Spilbury BW, Johnstone FRC. The Clinical course of actinomycotic infections; a report of 14 cases. Can J Surg 1962;5.33.
46. Holm P. Studies on the aetiology of human actinomycosis-I, the other "microbes" of actinomycosis and their importance. Acta Pathol Microbiol Scand, 1950;27:736.
47. Minsker OB, Yegorova TP. Studies on histogenesis of actinomycosis. Mykosen 1974;17:303.
48. Putman HC, Dockerty MB, Waugh JM. Abdominal actinomycosis; an analysis of 122 cases. Surgery 1950;28:781.
49. Brongden CJ. Actinomycosis of the gastrointestinal tract; a study of fourteen cases. J Lab Clin 1922; 8:180.

LARGE SEBACEOUS CYST AT THE BUTTOCK

Patchrin PEKANAN, Thitiporn RANGSITPOL, Chitchanok TUNTIWIWAT

ABSTRACT

Sebaceous cyst or epidermal cyst, epidermal inclusion cyst and epidermoid cyst is an epithelial cyst of the skin due to proliferation of surface epidermal cells within the corium, arising from occluded pilosebaceous follicles and containing a laminated, cheesy, oderiferous keratious epithelium (1). We present a case of large buttock sebaceous cyst with imaging of plain film and ultrasonography.

CASE REPORT

A 40-year-old male patient had a mass at left buttock for 5 years. The mass was soft to firm and was not tender. The mass had grown in size slowly. Plain film at left buttock region showed both ill and well defined borders, soft tissue density mass (Fig. 1). The mass did not produce any bone changes. Ultrasonography of the mass showed a well defined border mass, with homogeneous low echoic pattern and diffuse scattered uniformed hyperechoic internal echo. There was no posterior enhancement or acoustic shadowing (Fig. 2). Aspiration of the content revealed cheesy material and the whole mass was totally removed. The mass was proved to be sebaceous cyst.

DISCUSSION

Sebaceous cysts are usually asymptomatic unless they grow or become infected. There were few reports on imaging findings in this pathology outside the central nervous system except lesions at the breasts and testicles. In the breast, the lesions are sharply defined and of high rediographic density. Sonographically, the masses are hypoechoic, very well defined and have scattered low-level internal echoes with posterior acoustic enhancement (2). In the testicles, the lesions had variable sonographic characteristics (3,4). They have been described as sharply circumscribed lesions within the testicular parenchyma. The cyst was usually an encapsulated round or oval lesion 1-3 cm in diameter. The echogenicity of the lesions may be low, high or mixed. Sonograms may show a mass with a "target" appearance (a central area of increased echogenicity surrounded by a sonolucent zone), a sharply defined mass with hyperechoic margins representing a rim of calcification, or a well defined, solid mass with an echogenic rim and high intensity echoes throughout (5). Malvica (6) reported an unusual sonographic findings of epidermoid cyst of the testicle. It showed a relatively hypoechoic mass. Echoes within the mass had a lamellar, swirling configuration similar to the cross section of an onion. Alternating rings of dense echogenicity and sonolucency were present. Echogenicity was most prominent in the central portion of the lesion. The outermost band was relatively sonolucent. The lesions was well circumscribed and surrounded by normal testicular parenchyma.

Yasumoto (7) reported two cases of epidemoid cysts at the left submandible and right lower lip. The border of both lesions were smooth. The internal echo level was echogenic, the echo was coarse and hemogeneous. Posterior echo was no change or slightly enhanced.

There was no report of large sebaceous cyst by imaging at the buttock area as shown in our case.

REFERENCES

1. Friel JP. ed Dorland's illustrated medical dictionary, Tokys: Saunders international edition, 1982: 388.
2. Mendelson EB. Breast Sonography. In: Rumack Cm, et al ed. Diagnostic ultrasound. St.Louis: Mosby Year Book. 1991:559-560.

Department of Radiology, Ramathibodi Hospital, Rama 6 Street, Bangkok 10400, Thailand.

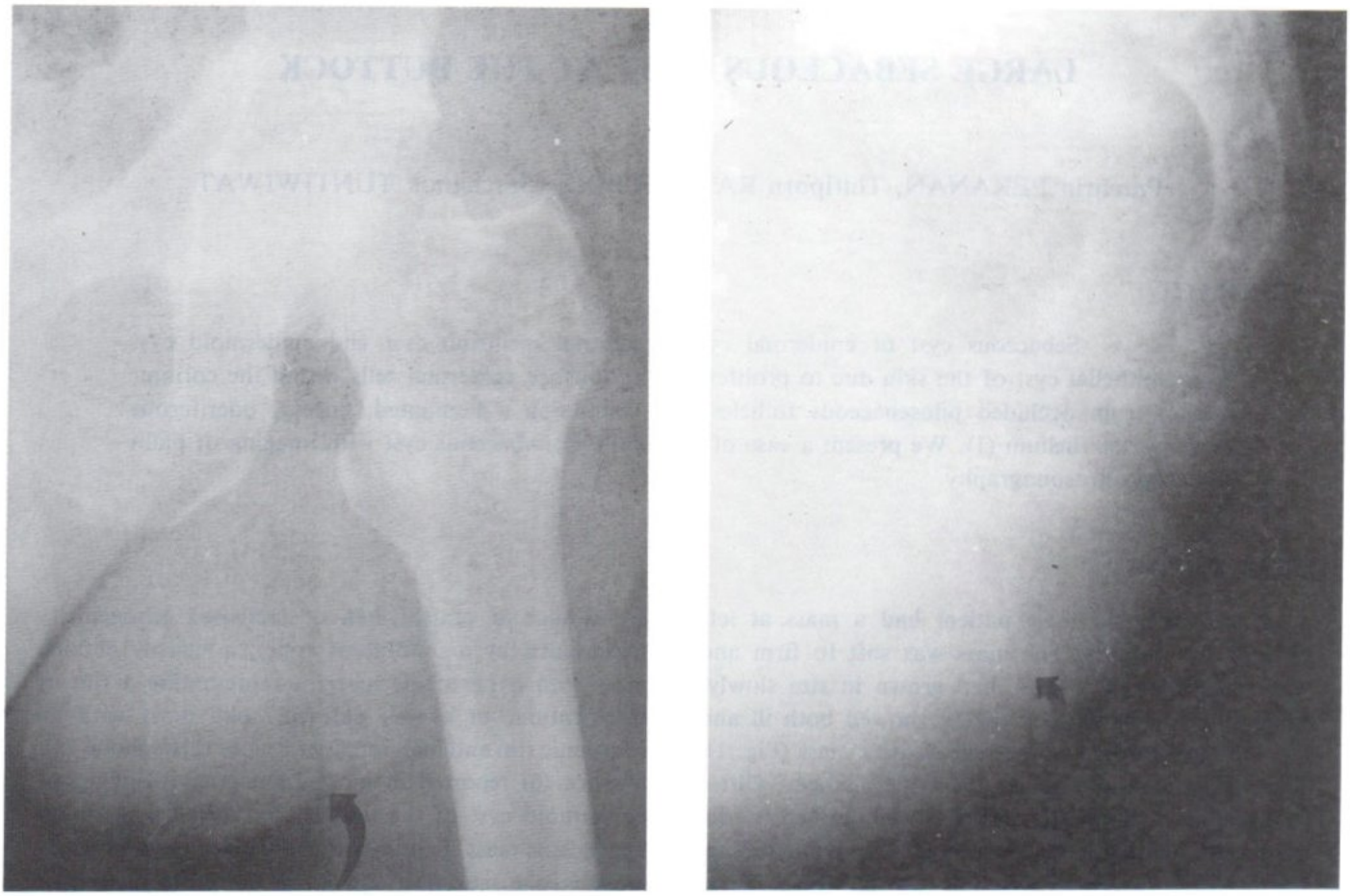

Fig.1 A,B Ap and lateral views of the buttock showed both ill and well defined border-soft tissue density mass. The mass did not produce bony changes.

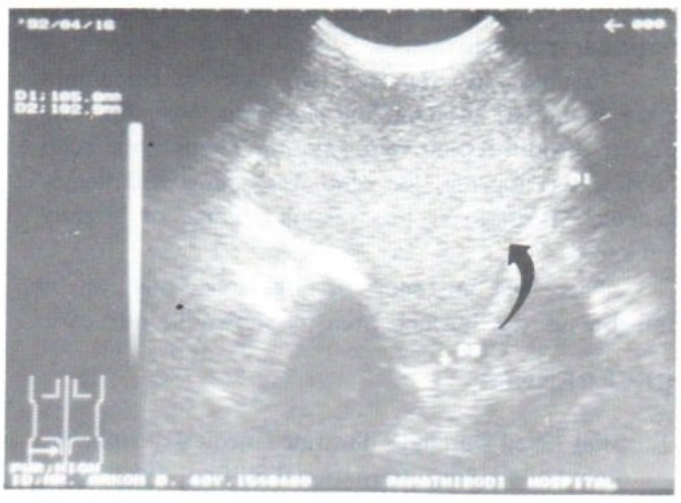

Fig. 2 Ultrasonography of the mass showed a well defined border mass, with homogeneously low echoic pattern and diffuse scattered uniformed hyperechoic internal echo. There is lack of posterior enhancement or acoustic shadow.

3. Maxwell AJ,Mamtora H. Sonographic appearance of epidermoid cyst of the testis. JCU 1990;18:188-190.
4. Bahnson RR, Slasky BS, Ernstoff MC, Banner BF. Sonographic characteristics of epidemoid cysts of testicle. Urology 1990;35:508-510.
5. Cohen EL, Mandel E, Goodman JD, Carr L, Feigin G, Dikman S. Epidermoid cyst of the testicle. Urology 1984;23-69-81.
6. Malvica RP. Epidermoid cyst of the testicle: an unusual sonographic finding. AJR 1993;160: 1047-1048.
7. Yasumoto M, Shibuya H. Gomi N, Kasuga T. Ultrasonographic appearance of dermoid and epidermoid cysts in the head and neck. JCU 1991; 19:455-461.

METASTASIS TO THE BREAST FROM EXTRAMAMMARY MALIGNANCIES: MAMMOGRAPHIC FEATURES

Malai MUTTARAK, M.D.,* Angsana NIMMONRAT, M.D.,*
Suwalee POJCHAMARNWIPUTH, M.D.,* Benjaporn CHAIWUN, M.D.**

ABSTRACT

Metastatic tumors to the breast from extramammary malignancies are unusual. We present 3 cases of such lesions. Two cases were in females with one primary each from the ovary and lung, and one in a male with primary lung carcinoma. The incidence, pathology and radiographic findings of such metastatic lesions are reviewed.

INTRODUCTION

Metastatic tumors to the breast are unusual especially from extramammary malignancies. The autopsy incidence varies from 1.7% to 6.6%.[1-3] Many of the reported examples in the literature are based on clinical rather than radiographic evaluation.[4] We report our experience in 3 cases of breast masses in patients with known extramammary malignancies and emphasize the importance of recognizing the mamographic distinctions between metastasis and primary breast carcinoma.

CASE REPORTS

Case 1.

A 41-year-old woman presented with lumps in her right breast, axilla and flank. She had a 10-year history of ovarian carcinoma. Mammogram showed multiple densely calcified masses in the right axilla and the right breast (Fig 1). CT scans revealed calcified masses in the right breast and in the subcutaneous tissues over the right flank (Fig 2). ^{99m}Tc-MDP (methylene diphosphonate) bone scan demonstrated abnormal activity in the same areas. Biopsy of the right breast mass revealed papillary adenocarcinoma consistent with a metastatic neoplasm of ovarian origin.

Case 2.

A 50-year-old woman with a known history of squamous cell carcinoma of the left lung, presented with multiple masses in both breasts and the abdomen. Mammogram showed very dense breasts with multiple ill-defined mass(Fig 3) which on sonography appeared as well defined hypoechoic masses (Fig 4). Fine needle aspiration demonstrated squamous cell carcinoma.

Case 3

A 46-year-old man presented with lumps in his left breast. A chest radiograph showed a mass in the right upper lobe. Mammography revealed a well circumscribled mass occupying nearly the entired left breast (Fig 5). Excisional biopsy revealed metastatic squamous cell carcinoma.

DISCUSSION

Metastasis to the breast may occur by two distinct routes: lymphatic and blood-borne.[4] Lymphatic metastasis is the more common and usually occurs from primary carcinoma of the opposite breast. Metastases from extramammary malignancies are usually the result of hematogenous spread with the

* Department of Radiology,
** Department of Pathology, Faculty of Medicine, Chiang Mai University, Chiang Mai 50200 THAILAND.

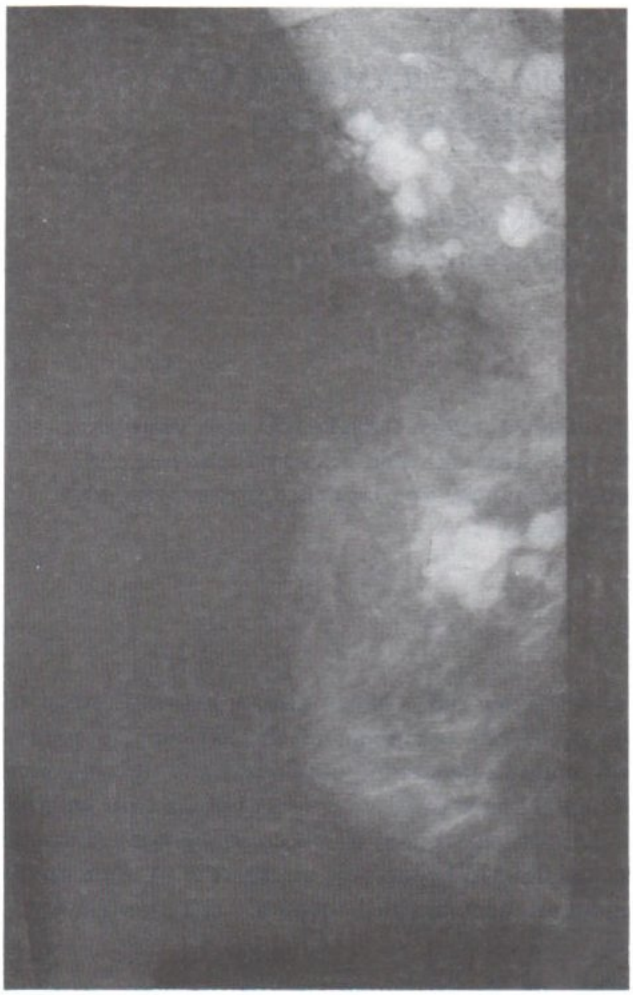

Fig 1. Mediolateral oblique mammogram of the right breast showing multiple calcified nodules in the axilla and upper quadrant of the breast.

three most common sites of origin being lymphoma/leukemia, melanoma, and lung cancer. Spreading from the ovaries, soft tissue sarcoma, the GI and GU tracts have also been reported.[5] Metastatic tumor to the male breast is very rare but has been reported in a number of instances, primarily from the prostate.[6-8]

The metatstastic foci appear on mammograms as discrete nodules, ususally solitary, and less often multiple, with a predilection for the upper outer quadrant. Axillary node involvement is frequently encountered. Calcification is very infrequent except for rare instances of metastases from ovarian carcinoma. Most metastatic nodules cannot be differentiated from benign nodules such as cysts or fibroadenomas or from well circumscribed breast cancers such as medullary or mucinous tumors. A disinct spiculated mass or microcalfication indicates the presence of an unrelated primary breast lesion rather than metastases.[3-5,9]

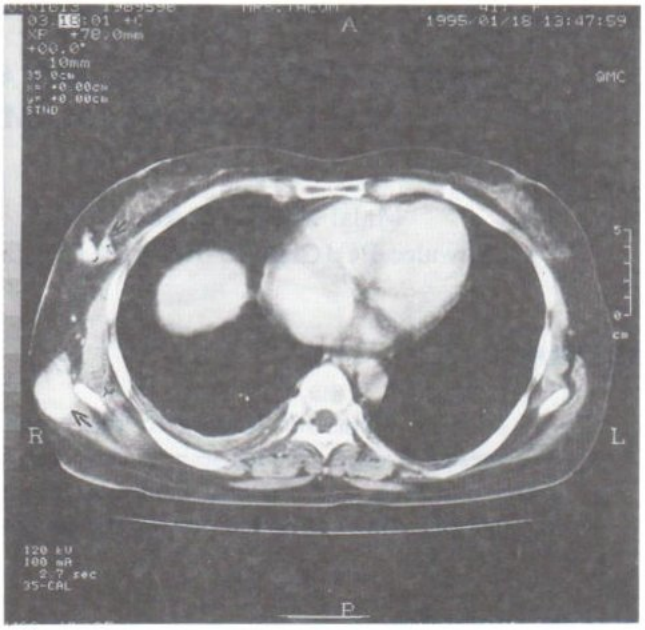

Fig 2. CT scan of the chest showing calcified nodules in the tail of the right breast and subcutaneous tissue (arrows).

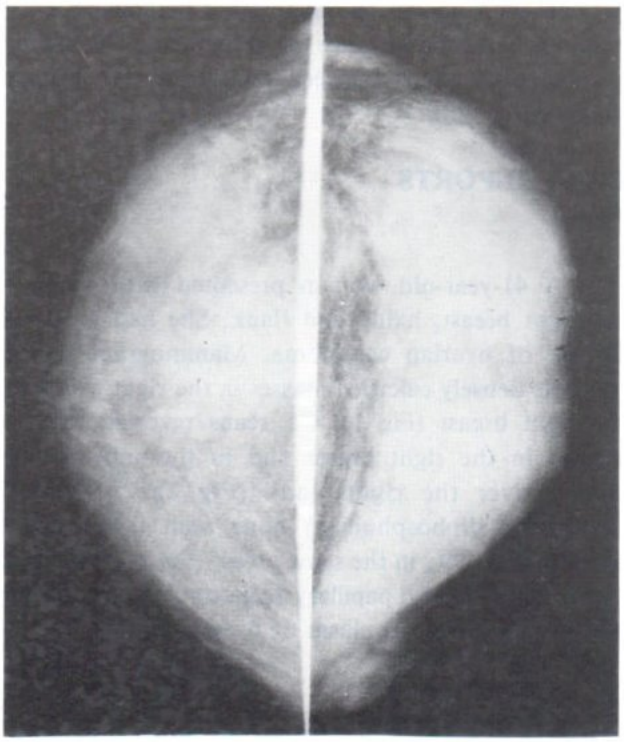

Fig 3. Craniocaudal mammograms of both breasts showing dense breasts and multiple ill-defined masses.

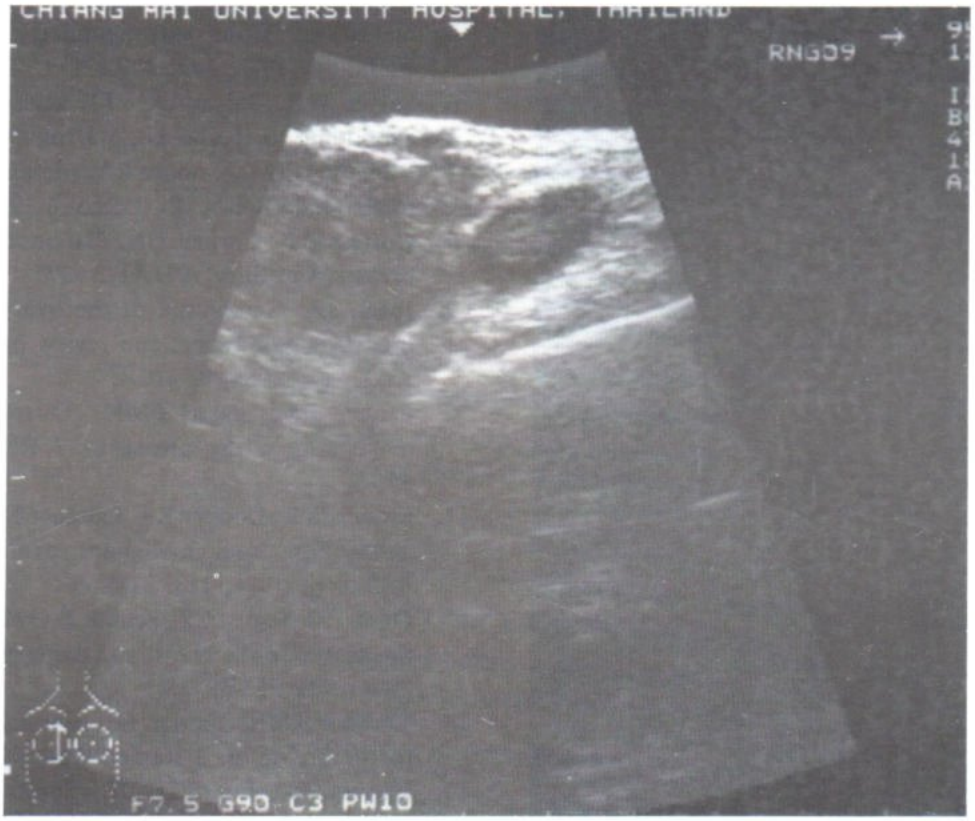

Fig 4. Ultrasound of the right breast showing multiple well defined low echoic masses.

The mammographic appearance of calcified metastases from primary ovarian papillary cystadenocarcinoma was first described in 1974 by Royen et al[10] and Moncada et al.[11] In 1991, Duda et al[12] reported a patient with a papillary serous adenocarcinoma with metastasis to the right breast, axillary lymph node, and subcutaneous tissues. This report describes the mammographic findings and special immunohistochemical stains with CA-125 of the tumor. Our patient in case 1 shows calcified metastases not only from mammograms but in ^{99m}Tc-MDP bone scintigraphy. The localized uptake of ^{99m}Tc-MDP in the breast can be found in normal breasts as well as in those with benign and malignant disease. Marked local radionuclide uptake has been reported in primary osteosarcoma of the breast.[13,14]

Case 2 has a very dense breasts and metastatic nodules were hardly seen on mammogram but were well delinated by ultrasonography. Multiple fibroadenomas cannot be excluded solely on the basis of the ultrasonographic findings. However, fibroadenoma usually occurs in younger woman and less often multiple.[15]

Breast enlargement in Case 3 can be either gynecomastia or metastasis as gynecomastia may be associated with lung carcinoma. Mammograms showed a well circumscribed mass in contrast to gynecomastia. Primary male breast cancer can exhibit the typical features of female breast cancer but may also show as a well-difined mass.[16] Therefore, differentiation between primary and secondary breast cancer in male is not possible.

ACKNOWLEDGEMENT

We express our appreciation to Dr. Ezekied Freed, (Northridge Medical Center, LA, U.S.A.) for reviewing the manuscript.

REFERENCES

1. Sandison AT. Metastatic tumors in the breast. Br J Surg 1959; 47: 54-8.
2. Hajdu SI, Urbon JA. Cancers metastasis to the breast. Cancer 1972; 29: 1691-6.
3. Toombs BD, Kalisher L. Metastatic disease to the breast: Clinical, pathologic, and radiographic features. AJR 1977; 129: 673-6.
4. Paulus DD, Libshitz HI, Metastasis to the breast. Radiol Clin North Am. 1982; 20: 561-7.

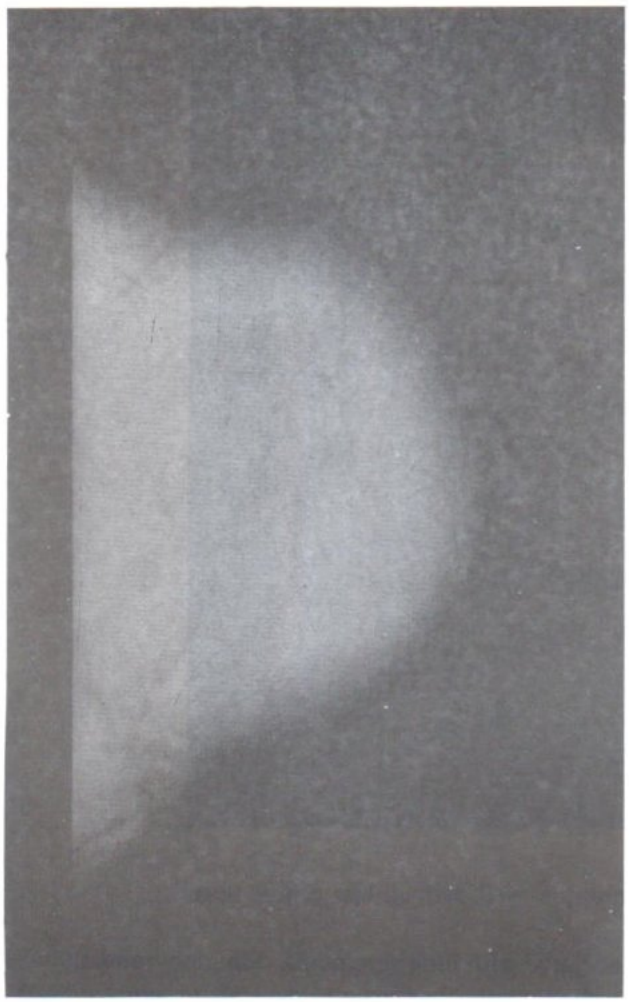

Fig 5. Lateral mammogram of the left breast showing a well circumscribed dense mass occupying nearly entire breast.

5 Bohman LG, Bassett LW, Gold RH, et al. Breast metastases from extramammary malignancies. Radiology 1982; 144: 309-12.

6. Salyer WR, Salyer DC. Metastases of prostatic carcinoma to the breast. J Urol 1973; 109671-5.

7. Ramamurthy L, Cooper RA, Metastatic carcinoma to the male breast. Br J Radiol 1991; 64: 277-8.

8. Cortese AF, Cornell GN. Carcinoma of the male breast. Ann Sury 1971; 173: 275.

9. Ibach JR. Carcinoma of the ovary metastatic to breast: A case report and review of the literature. Arch Surg 1964; 8: 410-4.

10. Royen PM, Ziter FMH. Ovarian carcinoma metastatic to the breast Br J Radiol 1974; 47: 356-7.

11. Moncada R, Cooper RA, Garces M, et al. Calcified metastases from malignant ovarian neoplasm. Radiology 1974; 113: 31-5.

12. Duda RB August CZ, Schink J. Ovarian carcinoma metastatic to the breast and axillary node. Surgery 1991; 110: 552-6.

13. Thomas AMK, Nathan Be. Primary osteosarcoma of the breast. Br J Radiol 1984; 57: 762-4.

14. Harvey JA, Fondriest JE, Smith MM. Densely calcified breast mass. Invest Radiol 1994; 29: 516-8.

15. Fornage BD, Lorigan JG, Andry E. Fibroadenoma of the breast: Sonographic appearance. Radiology 1989; 17: 671-5.

16. Cooper RA, Gunter BA, Ramamurthy L. Mammography in men. Radiology 1994; 191: 651-6.

DUPLEX COLLECTING SYSTEM WITH ECTOPIC URETEROCOELE A CASE REPORT OF INTRAUTERINE DIAGNOSIS BY ULTRASOUND

Pannee HORSAKUL, M.D.

ABSTRACT

A demonstrating case of intrauterine diagnosis of duplex collecting system and ectopic ureterocoele is reported. Early surgical intervention by removal of the dysplastic kidney, its dilated ureter and ectopic ureterocoele can prevent obstruction of the contralateral ureteric orifice and the ipsilateral lower ureter by the ectopic ureterocoele. Comparison and follow up of ultrasound before and after delivery, intravenous pyelogram at 3-month-old, operative and pathological findings are also shown.

INTRODUCTION

Findings of a tortuous tubular fluid-filled structure extended from cystic mass in the upper pole of kidney to the bladder with another thin wall cystic mass in the bladder are suggestive findings of duplex collecting system and ectopic ureterocoele. Absence of gas in the fetal bowel and the limitation of fetal movement in the uterine cavity make sonographic tracing of the entire ureteric course from kidney to bladder performed during intrauterine life easier than performed after delivery. Early surgical intervention by removal of the dysplastic kidney, its dilated ureter and ectopic ureterocoele can prevent obstruction of the contralateral ureteric orifice and the ipsilateral ureter from ectopic ureterocoele.

CASE REPORT

A 31-year-old, G2P1 pregnant woman with a history of uterine atony in the previous pregnancy was first seen in a private clinic for antenatal care. There was a discrepancy of gestational age (GA) estimated from last menstrual period (LMP) and from fundal height. Sonography was performed and revealed a single female breech presentation fetus. Average estimated gestational age from many parameters was 30 weeks 4 day ± 23 days. The amount of amniotic fluid was normal. There was a large cystic mass about 3 × 4 cm in the upper pole of the right kidney. Dilated tortuous fluid filled structure extended from the cyst to the bladder was noted. Minimal separation of the right lower pole and the left renal central echo were also observed. Ureters from these 2 parts were not dilated. Another thin wall cystic mass about 2 × 2 cm in the bladder was seen (FIG 1,2.3,) Duplex collecting system of right kidney with ectopic ureterocoele and mild left hydronephrosis were diagnosed for the foetus.

Elective caesarean section was performed at 39 weeks. Single female baby with good apgar score was delivered. Birth weight was 2.800 gm. Sonography performed 2 days after delivery showed no change in size of the ectopic ureterocoele and the upper system of right kidney. Mild degree of hydronephrosis in the left kidney and the lower system of right kidney remained unchanged. Right lower system ureter and left ureter could not be seen in the entire of their course as the fetal bowel gas made them obscured (Fig 4)

Surgeon suggested that operative treatment for the baby should be done after 1 month. 3 months later the baby was presented with urinary tract infection. Intravenous pyelogram was done after medical treatment of urinary tract infection, and showed nonvisualization of the upper pole

Department of Radiology, Songkhla Hospital, Songkhla, Thailand.
G2P1 = Gravid 2, Para 1.

of the right duplex collecting system. The lower collecting system of the right kidney was mild hydronephrotic and was displaced downward and laterally. Delayed excretion of left kidney with marked dilatation of the left renal pyelocalyceal system and the entire left ureter were evidenced. Large well defined filling defect in the right side of the bladder caused by ectopic ureterocoele was seen. (Fig 5, 6)

Ultrasound performed 1 day after intravenous pyelogram showed markedly increase in severity of the left hydronephrosis with no change of the ectopic ureterocoele and both collecting systems of the right kidney as compare to the findings performed at birth. (Fig 7, 8)

Cystoscope revealed right accessory orifice with normal bladder mucosa. Right upper pole nephrectomy and dissection of its ureter were done at 4-month-old. Pathological specimens showed a large hydronephrotic kidney about 3 × 3 × 3 cm with chronic pyelitis changes and a hydronephrotic ureter about 12 × 0.6 cm with chronic ureteritis changes. The baby was in a satisfactory condition as seen in the next 3 months follow up.

DISCUSSION

Duplex collecting system and ectopic ureterocoele defines as conditions with double renal pyelocalyceal systems and duplication of the ureters which are separated throughout their course on ipsilateral side. The ureter from the caudal renal pelvis enters the vesicular trigone in the normal position but the orifice of the ureter derived from the cephalic pelvis enters caudal to it. The ectopic ureteral orifice may open into the urinary or genital tract. When the opening located anywhere along the trigone to the vesical neck, it is unlikely to cause symptoms, but if the openings located distally to the visical neck, they can cause clinical symptoms from obstruction, reflux and incontinence. When obstruction occurs, the dilated ureter which passes into the wall of the bladder from the region of the normal uretero-vesicular orifice to the bladder neck produces a large herniation within the bladder which has been called ectopic ureterocoele. The size may vary from a small bulge of 1-2 centimetres in diameter to a lesion that may almost fill the bladder. The outer surface is vesical epithelium and the inner is ureteral epithelium, between them is a thin layer of muscle and collagen. Large ectopic ureterocoele may obstruct ipsilateral lower pole ureteric orifice and sometimes is large and

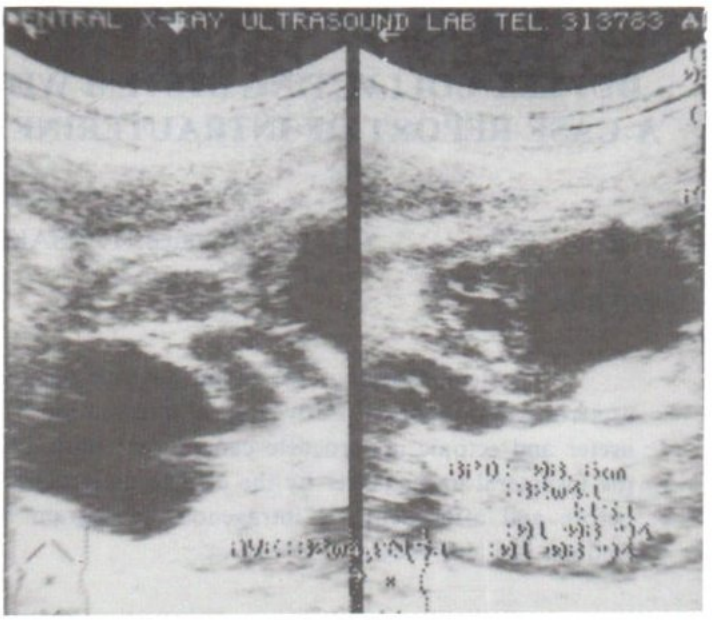

Fig 1. Right: there is a cystic mass about 3 × 4 cm. in the upper pole of right kidney. Left: Dilated tortuous ureter extends from this cystic mass to the bladder.

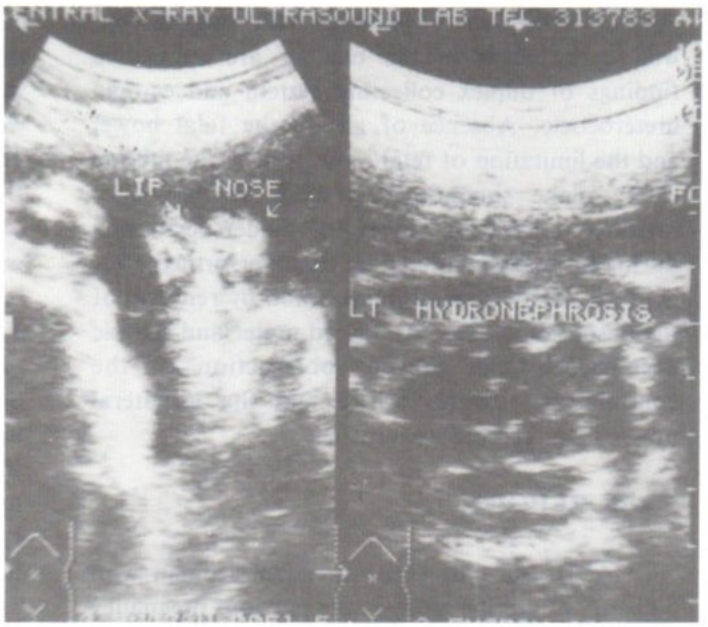

Fig 2. Right: Minimal left hydronephrosis.

tense enough to obstruct the ureteric orifice of the contralateral side as well. In addition, reflux into the lower pole ureter of a duplex system is not uncommon. In girls, the usual sites for an ectopic orifice are the bladder neck, urethra, vagina,uterus and cervix. In males ectopic ureters usually drain into prostatic urethra, prostatic utricle, seminal vesicle, vas deferens or ejaculatory duct.[2] Sonography

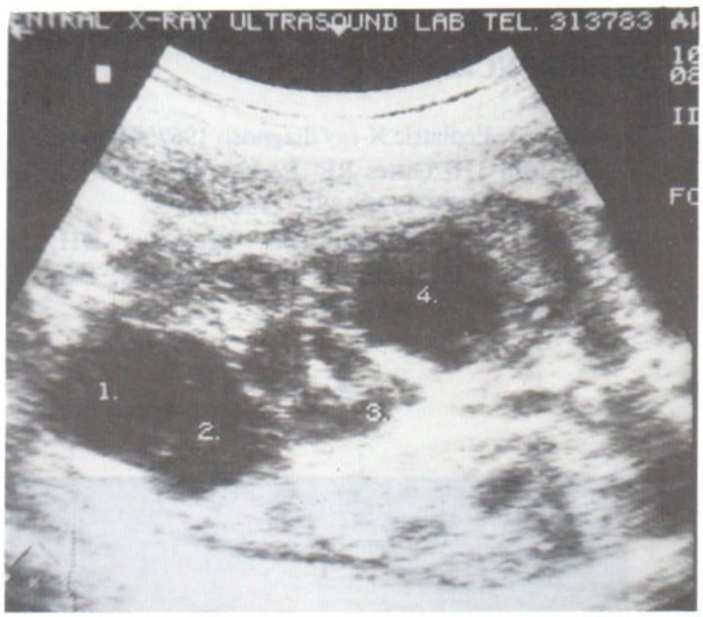

Fig 3. Ectopic ureterocoele about 2 × 2 cm. located at the bladder outline rather than in the center of the bladder. 1 = ectopic ureterocoele 2 = bladder 3 = tortuous dilated right upper system ureter 4 = hydronephrosis of the upper system of right kidney.

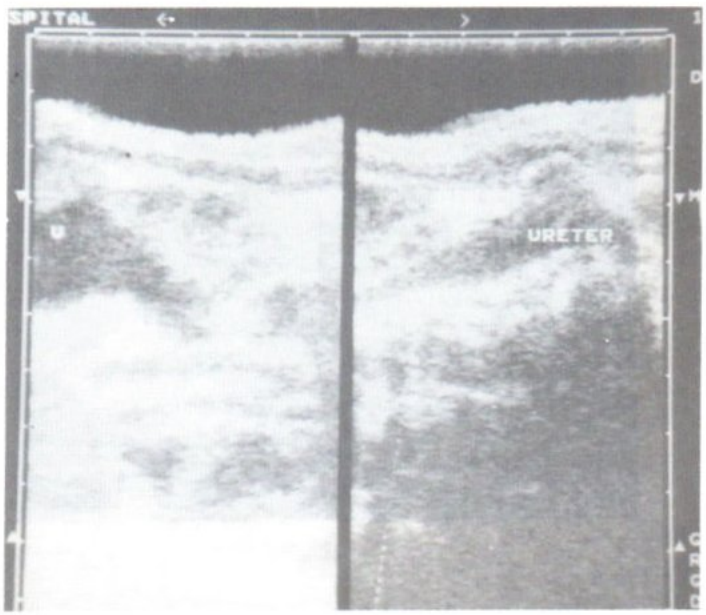

Fig 4. Ultrasound 1 day after delivery showed hydronephrosis of right upper system and tortuous dilated ureter, inability to demonstrate the entire ureter due to obscuring by th fetal bowel gas. U = upper system of right kidney L = lower system of right kidney.

performed during intrauterine is easier than performing after delivery as there is no interference from fetal bowel gas and limitation of fetal movement in uterine cavity. A tortuous fluid filled structure which touchs the fetal spine, originating from the renal pelvis and extending into retrovesicular position distinguished a dilated ureter from fluid filled bowel.[3] A dilated upper pole with a normal lower pole intrarenal collecting system indicates an obstructed duplex collecting system. A thin walled cystic mass in the bladder suggests ectopic ureterocoele. The usual radiographic findings is a nonvisualizing or poorly visualizing upper pole of a duplex system that may be massively hydronephrotic. The upper system displaces the lower pole downward and outward. The calyces of the lower system are fewer in number than in the normal kidney. In addition the lower pelvis and the upper portion of its ureter may be displaced further from the spine than the normal side. Nonopaque filling defect of varying size in bladder from ectopic ureterocoele is usually off center and always appears on the bladder outline rather than as a complete circle within the bladder shadow.[2] No specific prenatal intervention is necessary especially when there is normal amount of amniotic fluid which indicates normal renal function.[3] The portion of kidney drained by the ectopic ureter is almost dysplastic, and management usually requires surgery after delivery. The usual treatment for an ectopic ureter associated with a poorly visualizing or nonvisualizing upper pole of a renal duplication is partial nephrectomy and ureterectomy.[2]

Ectopic ureterocoele may occurs in a single collecting system, usually in males 80% is associated with duplicated collecting system. Ectopic ureter appears commonly in females, varying from 2-12 times more than in males. Approximately 10% of ectopic ureterocoele is bilateral. Ectopic ureterocoele is one of the more serious anomalies of the urinary tract in infancy and childhood. Serious urinary tract symptoms usually occur in the first year of life. The patient often presents during the first few month of life with symptoms of urinary tract infection or failure to thrive. Because of no fetal bowel gas and limitation of fetal movement in utero, sonographic evaluation of kidney and the entire ureter can be done easier than performed after delivery. Early diagnosis and early surgical intervention can prevent damaged of contralateral system and ipsilateral lower ureter from large ectopic ureterocoele compression and from infection.

ACKNOWLEDGEMENTS

I would like to thank Dr. Punya sanguancheur, the hospital administrator, for his permission to report the case.

REFERENCES

1. Caffey J, Pediatric X-ray diagnosis 1967; 640-644.
2. Harrison JH, Gittes RF, Perlmutter Ad, et al, Urology. 1979; 1376-1381, 1756-1779.
3. Nyberg DA, Mahony BS, Pretorius DH, Diagnostic ultrasound of fetal anomalies. Text and atlas. 1990; 445-451.

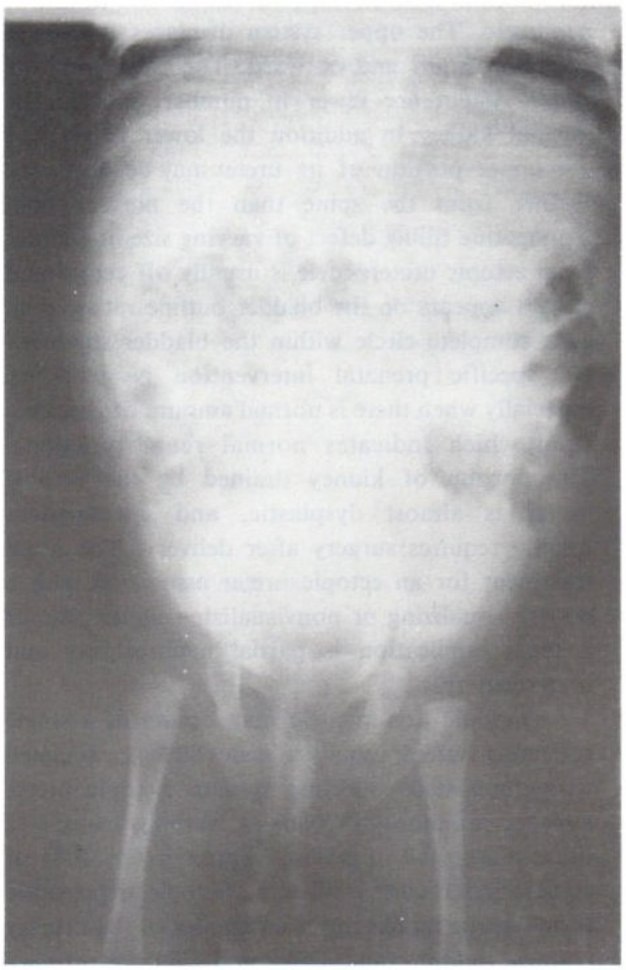

Fig 5.

IVP at 3-month-old. Minimal dilatation of the lower system of right kidney which was displaced downward and laterally. Delayed function of left kidney with filling defect in the bladder from ectopic ureterocoele.

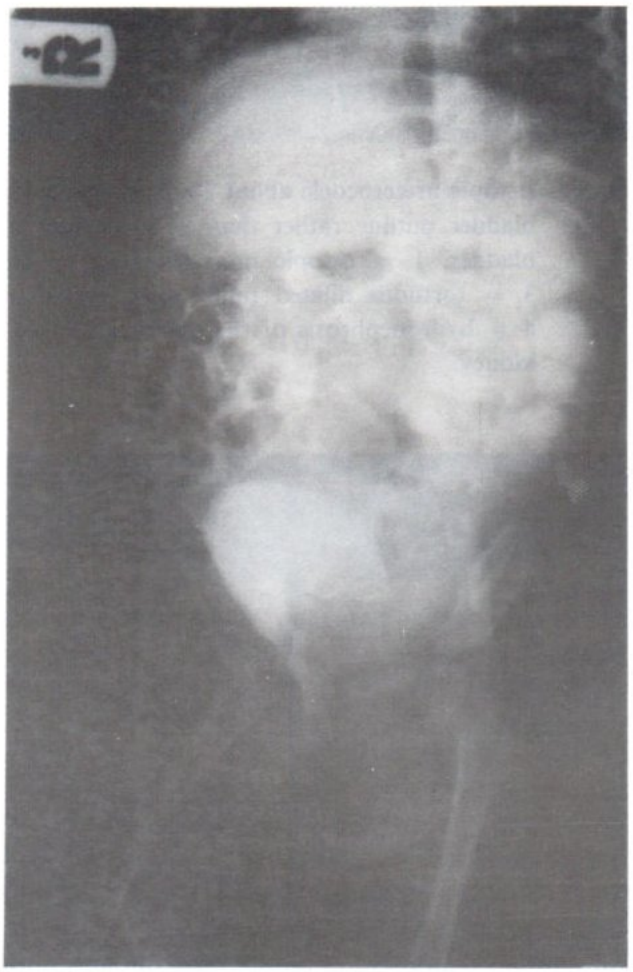

Fig 6.

Progression of left hydronephrosis.

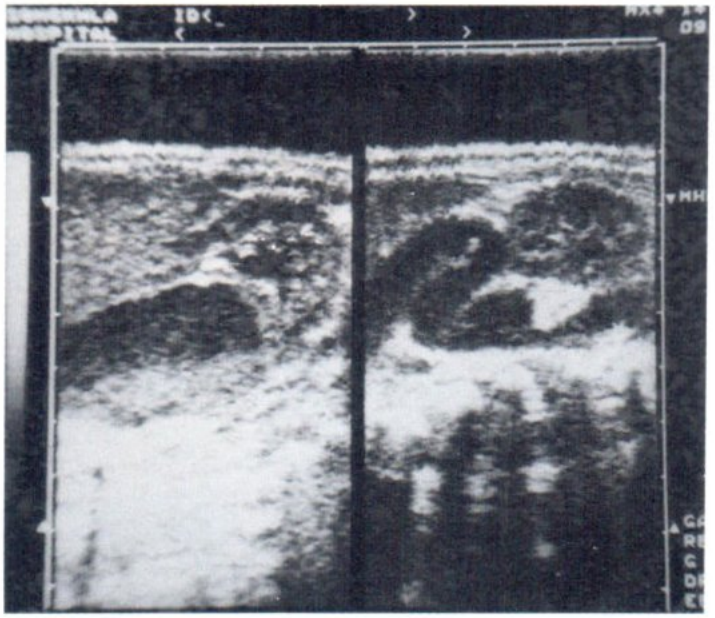

Fig 7. Ultrasound at 3-month-old showed no change of right duplex kidney.

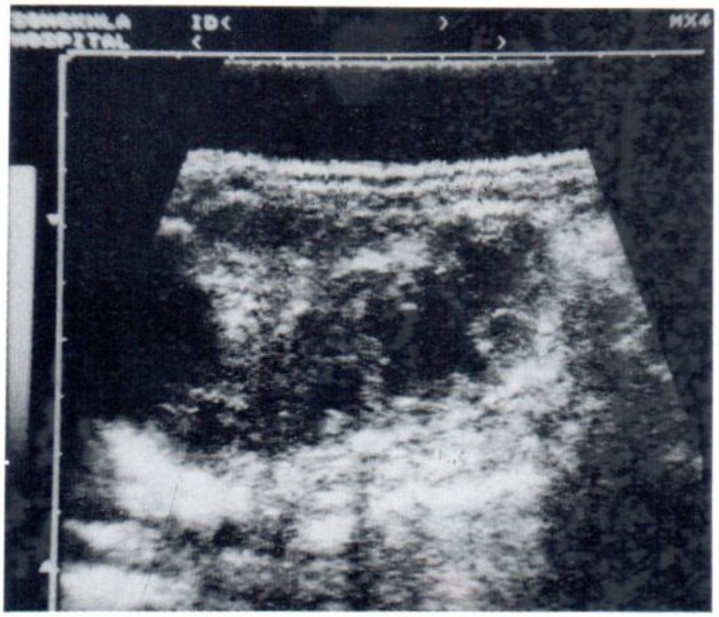

Fig 8. Ultrasound at 3-month-old showed increase in severity of left hydronephrosis as compare to the finding at birth.

SHIMADZU

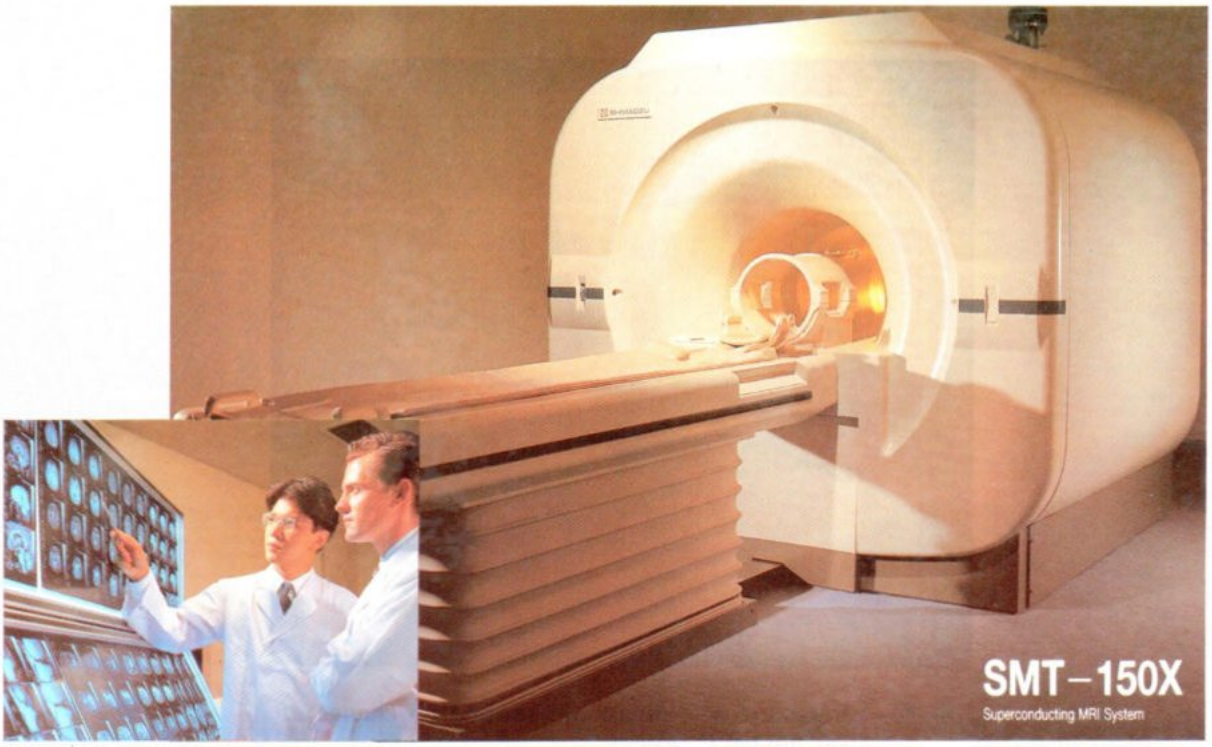

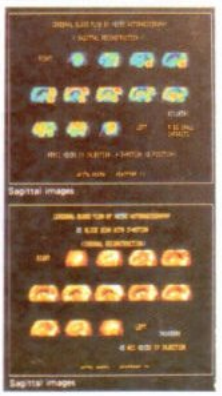

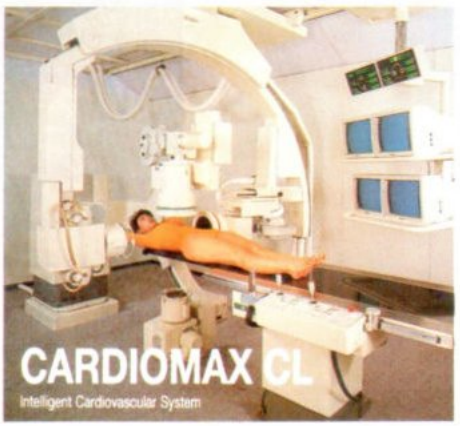

SOLE DISTRIBUTOR :

INTERNATIONAL COSMETICS CO., LTD.

757/10 Soi Pradoo 1, Sathupradit Road, Yannawa, Bangkok. 10120

Tel. 2949541, 2940294 (Ext. 264, 273) Telefax : 2949541

A case report : EXTRAHEPATIC BILIARY CYSTADNOCARCINOMA ARISING FROM COMMON HEPATIC DUCT.

Korkiat VIVITMONGKORNCHAI*
Pim HANDAGOON**
Nirush LERTPRASERTSUKE***

ABSTRACT

A case of extrahepatic biliary cystadenocarcinoma arising from the common hepatic duct is reported. The sonographic, CT and ERCP appearances correlated well with the pathological findings. The typical imaging characteristics of biliary cystadenoma and cystadenocarcinoma especially the sonography and CT can lead one to the correct preoperative diagnosis even the tumor arising from the extrahepatic bile duct.

INTRODUCTION

Cystadenoma and cystadenocarcinoma are rare cystic tumors of biliary origin. They comprise of less than 5% of intrahepatic cystic lesions.[1,2,3] Biliary cystadenoma and cystadenocarcinoma may arise either from intrahepatic or extrahepatic bile duct as well as the gall bladder. However, most of them are located entirely within the liver.[1,3,4] Characteristic sonographic and computerized tomographic findings of intrahepatic biliary cystadenoma and cystadenocarcinoma were described as multiloculated or less often as uniloculated cystic mass lesion.[2,3,6.7,8] We report further on the typical imaging appearances of extrahepatic biliary cystadenocarcinoma arising totally from the common hepatic bile duct without contiguous intrahepatic bile duct component.

CASE REPORT

A 42-year-old female patient presented with epigastric discomfort and mild intermittent jaundice for about 4-month duration. A large non-tender mass with firm to hard consistency was palpable in the right upper quadrant. No ascites nor palpable lymph nodes was revealed through physical examination. The hematogram and urine analysis were within normal limits. Minimal elevation of both direct bilirubin and total bilirubin as well as serum amylase were noted but the liver enzymes and alkaline phosphatase were within the normal ranges.

Ultrasonography revealed a large, well-defined mass arising from common hepatic duct. It composed of multiple cystic spaces separated by septa. Several cysts contained internal echoes. Focal nodular thickening of septa was noted. The lesion caused proximal ducts dilatation and compressed upon the gall bladder. (Fig. 1 a, b)

CT confirmed the presence of a well encapsulated multiloculated cystic mass with variable attenuation values in the common hepatic duct causing proximal bile ducts dilatation. A coarse calcification was seen eccentrically within the wall. Nodular thickening of septa with enhancement of the septa and wall of the mass lesion was also observed. No other intrahepatic lesion, ascites or enlarged lymph nodes was detected. (Fig. 2 a, B)

ERCP demonstrated a large ovoid shape filling defect in the common hepatic duct with dilatation of both main intrahepatic ducts. The gall bladder was not opacified. (Fig. 3)

At laparotomy, a multiloculated cystic mass arising from the common hepatic duct was seen compressing the nearby gall bladder. Complete excision of the mass, cholecystectomy and hepaticojejunostomy were done. The patient recovered well after surgical treatment.

* Department of Radiology (Resident)
** Department of Radiology
*** Department of Pathology
Faculty of Medicine, Chiangmai University.

ERCP
E = Endoscopic
R = Retrograde
CP = Cholangiopancreatography

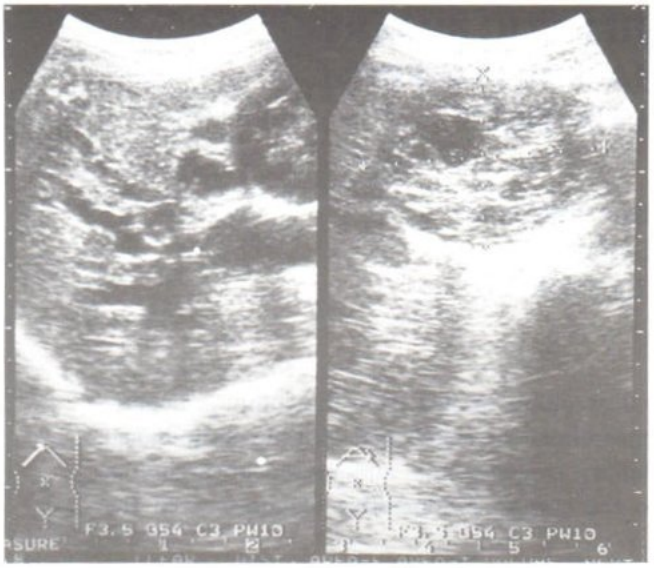

Fig. 1a . A large multiloculated mixed echoic mass was demonstrated with intrahepatic duct dilatation.

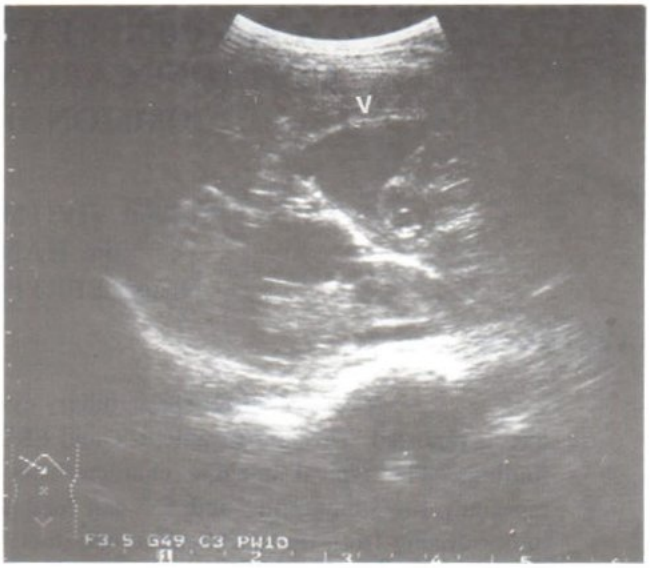

Fig. 1b . The mass was clearly seen arising from common hepatic duct (arrow).

Grossly, the common hepatic duct was remarkably dilated. There was a large solid-cystic mass with nodulated free surface, 6 × 4 × 4 cm, arised from the lateroposterior wall. The residual mucosa was smooth in comparison to the tumor surface where focal hemorrhage was observed. (Fig. 4a) Cut sections showed a multiloculated lesion with abundant mucinous content and irregular fibrous septa. (Fig. 4b) Microscopically, there were numerous clefts and cystic spaces lined by mucin-producing high columnar epithelium which were occasionally pseudostratified. (Fig 5a) Pleomorphic nuclei with dysorientation and mitotic figures were frequent in the micropapillae and abortive tubules. (Fig 5b) Notably, small cysts with low columnar epithelia and hyperchromatic nuclei were observed in the fibrous septa and fibrotic wall of the hepatic duct. They were interpreted as stromal invasion. Calcification within the luminal mucin was focally observed. Neither vascular invasion nor distant metastases were seen.

DISCUSSION

Biliary cystadenoma and cystadenocarcinoma are rare, being slow growing tumors of biliary tract. They are assumed to be developed originally from aberrant hamartomatous bile ducts or ectopic rests of embryonic gall bladder.[1,4,8] They occur predominantly in middle aged women, with ages ranging from 19 to 71 years.[2,3,4] Most patients presented with epigastric discomfort and mass in right upper quadrant or epigastrium with or without fever and intermittent jaundice.[1,3,7] The mass is usually large at presentation.

The ultrasound appearance of cystadenoma and cystadenocarcinoma is of oval, cystic, anechoic mass with multiple septa. The cystic spaces occasionally have internal echoes suggesting infection or hemorrhage.[3,6,7] The mural nodules and papillary projections were seen arising from the walls and septae. These findings were commonly noted in biliary cystadenocarcinoma[1,4,5] but they could not be used as the indication of malignancy since they also have been described in benign cystadenoma as well.[2,3,5,5,6,7]

The CT of biliary cystadenoma and cystadenocarcinoma reveal multiloculated cystic areas with attenuation value ranging from 0 to 30 Hounsfield Units.[3,6,10] The variation of attenuation is due to various contents such as serous fluid, mucin, pus or cholesterol.[3,5,10] Enhancement of internal septations with intravenous contrast administration was also described.[3,7] Sonography is more sensitive than CT in the detection of septa in a cystic lesion. CT may detect calcifications in these lesions.[5,9] The presence of solid nodular masses or coarse calcifications along the wall or septa in a multilocular cystic mass suggested a more likely diagnosis of biliary cystadenocarcinoma.[1,4,5]

The sonographic and CT findings in our case are correlated well with the previous description of biliary cystadenocarcinoma even though it arises from the common hepatic duct. The other tumors which may arise from the extrahepatic bile duct such as choledochal cyst with or without malignant change,[11,12] hepatocellular carcinoma[13] and cholangiocarcinoma[14,15]

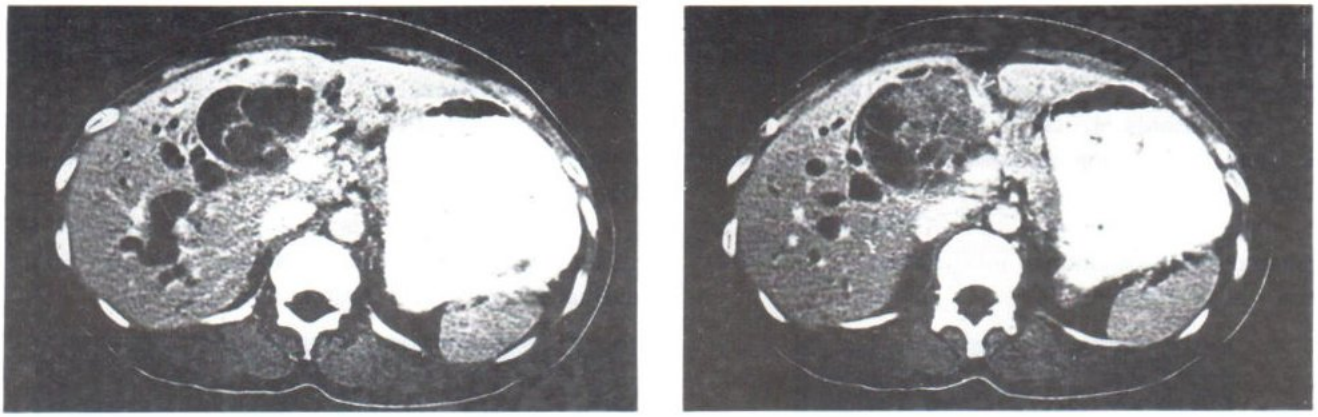

Fig. 2a . Axial CT showed a multiloculated cystic mass with variable attenuation contents, nodular thickening of septa and a coarse calcification (arrow) in the common hepatic duct. Intrahepatic duct dilatation was also noted.

were not presented as this multiloculated cystic character. Complete surgical removal of the tumor is the treatment of choice since this can relieve the biliary obstruction and patient's symptoms.[1,7] Most importantly, it provides histologic confirmation of benign or malignant nature that cannot be relied on the imaging characters.[5,6] Histologically, biliary cystadenomas appear well encapsulated and are composed of numerous cystic spaces lined with a single layer cuboid or columnar nonciliated, mucin-secreting epithelium. The cyst wall contains epithelium of biliary tract origin with a capsule of mesenchymal tissue.[1,4] Evidence of stromal invasion indicates malignancy.[4]

In conclusion, our case confirms that sonography and CT can accurately demonstrate the internal morphologic features characteristic of cystic biliary neoplasm even arising in the common hepatic duct.

ACKNOWLEDGEMENTS

The authors gratefully acknowledge Professor Sanan Simaluk for his valuable suggestion and review of the manuscript.

REFERENCES

1. Ishak KG, Willi GW, Gummins SD, et al. Biliary cytadenoma and cystadenocarcinoma report of 14 cases and review of literature. *Cancer* 1977; 38: 322-8.

2. Forrest ME, Cho KJ, Shilds JJ, Wicks JD, et al. Biliary cystadenomas: Sonographic-angographic-pathologic correlations *AJR* 1980; 135: 723-7.

3. Hodgson T, Fox S, Bayjoo P. Case report: Extra-hepatic biliary cystadenoma in Association with Adenomyomatosis of the Gall-bladder. *Clin Radiol* 1991; 43: 210-2.

4. Wheeler DA, Edmondson HA. Cystadenoma and mesenchymal stroma (CMS) in the liver and bile ducts. *Cancer* 1985; 56: 1434-45.

5. Korobkin M, Stephens DH, Lee JKT, et al. Biliary cystadenoma and cystadenocarcinoma: CT and Sonographic Findings. *AJR* 1989; 153: 507-11.

6. Choi Bl, Lim JE, Han MC, et al. Biliary cystadenoma and cystadenocarcinoma: CT and sonographic findings. *Radiology* 1989; 171: 57-61.

7. Frick MP, Feinberg SB. Biliary cystadenoma. *AJR* 1982; 139: 393-5.

8. Stanley J, Vujic I, Schabel SI, et al. Evaluation of biliary cystadenoma and cystadenocarcinoma. *Gastrointest Radiol* 1983; 8: 245-8.

9. Federle MP, Fily RA, Moss AA. Cystic hepatic neoplasm. *AJR* 1981; 136: 345-8.

10. Genkins SM, Tueker JA, Seigler HF, et al. Case report-biliary cystadenoma with mesenchymal stroma: CT and angiographic appearances. *JCAT* 1988; 12: 527-9.

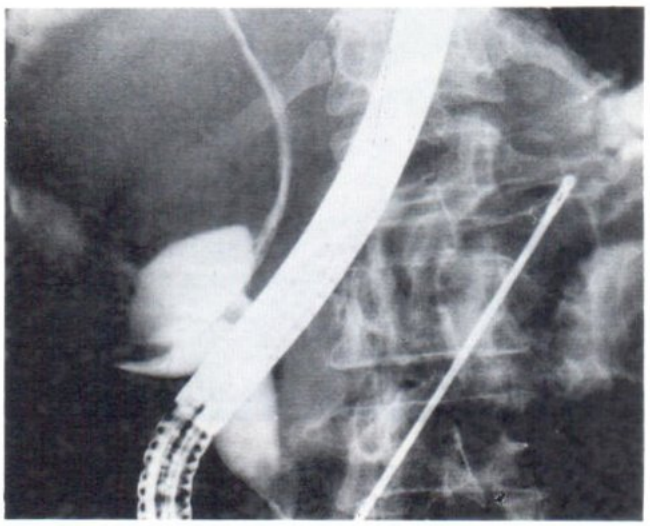

Fig. 3 ERCP demonstrated a large ovoid filling defect in the common hepatic duct.

11. Hagen G, Kolmaniskog F. Radiologic approach to bile duct cysts in adults. *Acta Radiol* 1992; 33: 240-4.

12. Yoshida H, Itai Y, Minami M, et al. Biliary malignancies occuring in choledochol cysts. *Radiology* 1989; 173: 389-92.

13. Park CM, Cha IH, Chung KB, et al. Hepatocellular carcinoma in extrahepatic bile duct. *Acta Radiol* 1991; 31: 34-6.

14. Mittelstaedt CA, et al. *General Ultrasound*. Churchill livingstone in. 1992. 344-52.

15. Haaaga JR, Alfidi RT, et al. *Computed tomography of the whole body*. The C.V. Mosby company 1988. 2nd ed. 898-903.

16. Cheung YK, Chan FL, Leong LLY, et al. Biliary cystadenoma and cystadenocarcinoma: Some unusual features. *Clin Radiol* 1991; 43: 183-5.

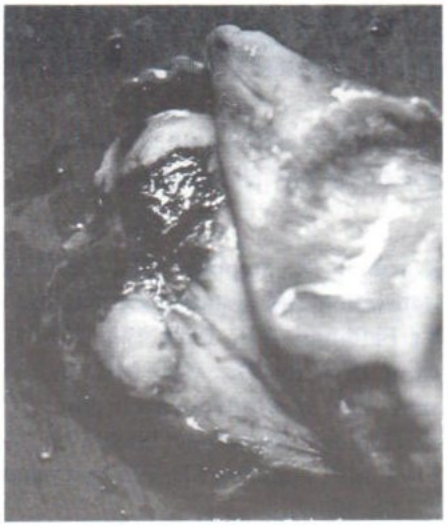

Fig. 4a. The tumor mass with nodulated surface and large area of hemorrhage arised from lateral wall of the common hepatic duct.

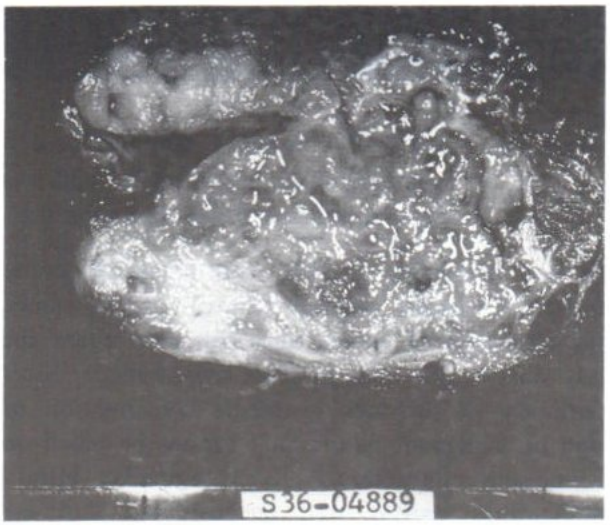

Fig. 4b. The cut section disclosed multiloculation filled with mucin and separated by various thickness of septa.

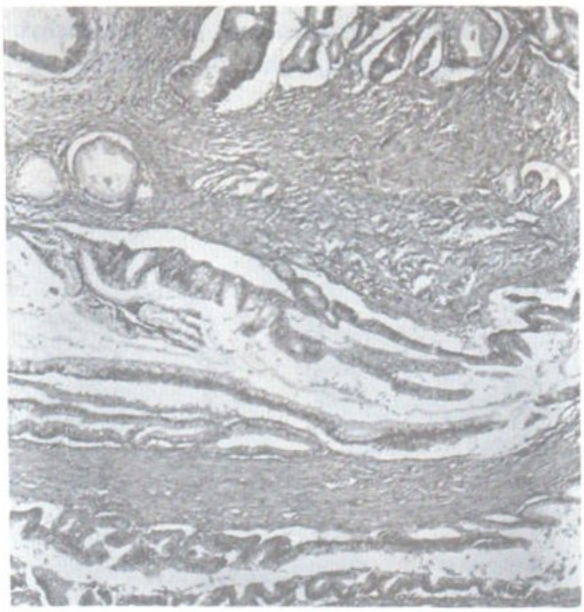

Fig 5a, b: Microscopically, the tumor mass consisted of abortive and well-formed tubular structures with stroma invasion. Formation of micropapillae with bizzare and dysorientated nuclei were prominent.

OSTEOSARCOMA : A STUDY OF 100 CASES.

Lucksana POCHANUGOOL, Kesanee KUHATONG,
Tasanee LAYANGKUL, Daungjai SANGTHAWAN, Suporn ONSANIT

ABSTRACT

One hundred cases of osteosarcoma were studied clinically, pathologically and treated with preoperative intraarterial chemotherapy with or without preoperative irradiation and followed by surgery. Prophylactic lung irradiation was administered for every case after surgery. Sixty two patients belonged to Enneking's stage IIB and 11 cases were in stage III. The acturial three years survival rate of 25 cases was 48 percent.

INTRODUCTION

Osteosarcoma is the most common primary malignant bone tumor in Thailand. The incidence was 39.9 percent of all malignant bone tumor or comprised of 2.2 percent of all cancer cases in the year 1992 and 1.01 percent in 1993 in Ramathibodi Hospital.[1-3] Before 1986, osteosarcomas of the long bone, in the Faculty of Medicine, Ramathibodi Hospital, were treated exclusively by amputation, adjuvant chemotherapy while radiation were aimed at palliative treatment for advanced and affordable cases.[4] However, the results were poor, all cases died within the first 2 years. In the light of the effectiveness of adjuvant chemotherapy for osteosarcoma; as reported in Western countries, our institute pioneered the multidisciplinary treatment of osteosarcoma in this country when our program commenced in 1986. They were adapted partly to suit our socioeconomic conditions.[5-12] Local irradiation treatment including prophylactic lung irradiation was adjuncted with the purpose of enhancing the chemotherapeutic response.[13-15]

MATERIALS AND METHODS

From January 1988 to January 1994, 100 cases of osteosarcoma were enrolled in the study. There were 52 males and 48 female patients. The age of the patients ranged from 7 to 45 years old. Sixty four percent was in the second decade. Twenty one patients were belonged to the third decade and 10 were below ten and only 5 cases had the age over 30 (Fig. 1). Fifty nine patients presented with pain and 31 cases experienced pain after some kinds of trauma. Every patients had visited physicians at least two times before the diagnosis of osteosarcoma was given. They were diagnosed as sprain in 82 cases with 5 osteomyelitis and 4 tendinitis. Lump only was detected in 10 cases, the other 31 cases had lump followed by pain one or two weeks later (Fig 2A, B). Twenty patients had pathological fracture prior to the diagnosis, mostly belonged to the telangiectatic subtype. There were 60 osteoblastic, 19 chondroblastic, 13 telangiectatic and 8 fibroblastic subtype. Primary skeletal distributions were 49 femur, 24 tibia, 10 humerus 6 fibula, 2 pelvis and others as shown in Fig 3. The roentgenographic appearence were mostly osteolytic (Fig. 4A, B).

The treatment started after routine blood test including erythrocyte sedimentation rate (ESR), serum alkaline phosphatase (AP), and lactic acid dehydrogenase (LDH). The roentgenologic study included plain film of primary lesion and chest, linear or computerized tomogram of the lung and computerized scan of the primary tumor for the diagnosis of any soft tissue extension and intramedullary metastasis (Fig. 5). Bone scintigraphy was also requested for detecting skip metastasis and metastatic disease outside the bone.

Department of Radiology, Faculty of Medicine, Ramathibodi Hospital.

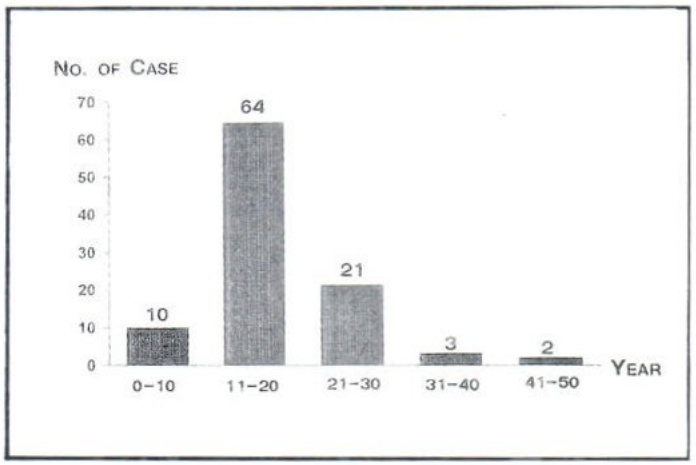

Fig. 1 Age at diagnosis for 100 cases of osteosarcoma.

All these patients were randomized to different arms of the study as shown in figure 6. Chemotherapy was repeated every 3 weeks if WBC was normal, total WBC $\geq$3000/ul or total PMN $\geq$ 1500/ul for 8 courses. Most of the patients received 4 courses of intraarterial chemotherapy followed by 4 intravenous routes after surgery, concomittant with prophylactic whole lung irradiation (Fig. 7). Total treatment time was about 32-52 weeks according to WBC and clinical status. Patients who also received methyl progesterone acetate (MPA) seemed to have shorter treatment time.

In the group of patients who were randomized to receive radiation to the affected primary tumor, the radiation treatment began on the next day after the last intraarterial chemotherapy. Treatment was done by Co-60 teletherapy or 6 MV linear accelerator. A total dose of 30 Gy in 10 fractions over 12 days was given using two opposed fields with the doses specified at midplane. Radiation port included only primary bone disease, abnormal vessels, and also intramedullary extension. No safety margin was given due to the concept that microscopic disease could be destroyed by intraarterial chemotherapy and to preserve normal tissue as much as possible especially in the limb salvage group. Two to 4 weeks after radiation, the patients were reevaluated to decide on limb salvage surgery or amputation. After surgery, the specimens were reveiwed to plan for further treatment (Fig. 8A, B). If tumor necrosis in the surgical specimens was less than 80 percent, the patient with limb salvage was advised to have amputation. Patients with poor tumor response had to receive a change in the chemotherapeutic regimens. For prophylactic whole lung irradiation, each lung was irradiated 150 cGy every other day to the total dose of 2550 cGy to each lung at midline depth without correction for the lung inhomogeneity, concurrented with intravenous chemotherapy.

RESULTS

For the total cases of one hundred, 27 cases refused treatment and continued to have traditional medicine. Sixteen patients had incomplete treatment, twelve of them returned to the hospital again with either lung metastases or severe progression of primary tumor. All were dead within the next other year after diagnosis. Other 11 cases terminated from either lung or bony metastases, 4-24 months after initial visit. Limb salvage surgery after preoperative intraarterial chemotherapy with or without radiation was performed in 22 cases. Other 19 patients underwent amputation or disarti-

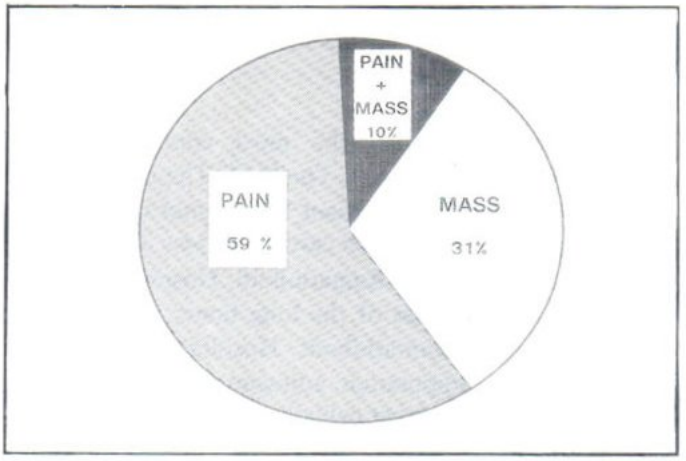

Fig. 2A Presenting symptom of 100 cases of osteosarcoma.

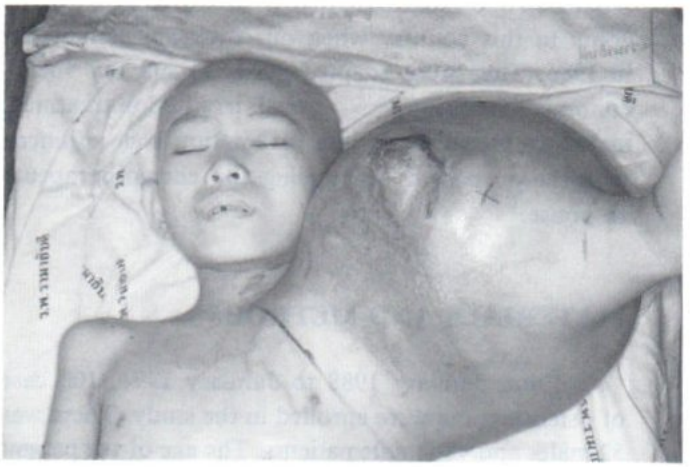

Fig. 2B One boy with a very huge shoulder mass, he was disarticulated with all his 15 axillary nodes negative for osteosarcoma.

culation. The rest of 5 patients, received incomplete treatment at the time of evaluation due to severe neutropenia and poor general condition.[4,16-20]

There were 25 cases who were followed up for longer than 3 years (15 limb salvage, 10 amputated cases). Three years survival rate was 48%, three of them had lived longer than 5 years now.

For the cost of treatment, excluding professional fee, was 125,000 baht or about US$ 5000 per case.

DISCUSSION

In this study we had approximately the same incidence between male and female patients. Peak incidence was in the second and third decade of life which was the period of very high bony activity. The first diagnosis was mostly that of sprain, osteomyelitis or tendinitis. Very few patients were diagnosed to be osteosarcoma at the first visit, so definitive treatment was delayed in almost every case. Early X-ray of the primary site would be of much help for early detection of osteosarcoma. Other cause of treatment delay was refusal to have amputation of the limb. The patients and their parents tried to seek other chances including traditional medicine, and most of them returned to have treatment after metastases has already established. Limb salvage procedure was the other chance to comfort the patient and their parents. This study, therefore, suggested that adjuvant chemoradiotherapy and limb salvage benefit patients in terms of quality of life and disease free survival. The outcome shown in our study was satisfactory; it was observed that disease-free survival, especially in the limb-salvage group, was better than historical control. Cost of the entire treatment was approximately 125,000 baht (US$ 5000) per case, which might be considered appropriate for the economic status of Thai patients. It is therefore advocated that limb-salvage procedure with preoperative intraarterial chemotherapy and radiotherapy be the treatment of choice for early cases of osteosarcoma in this country. Overall significance in terms of cure rate, however, awaits further follow up.

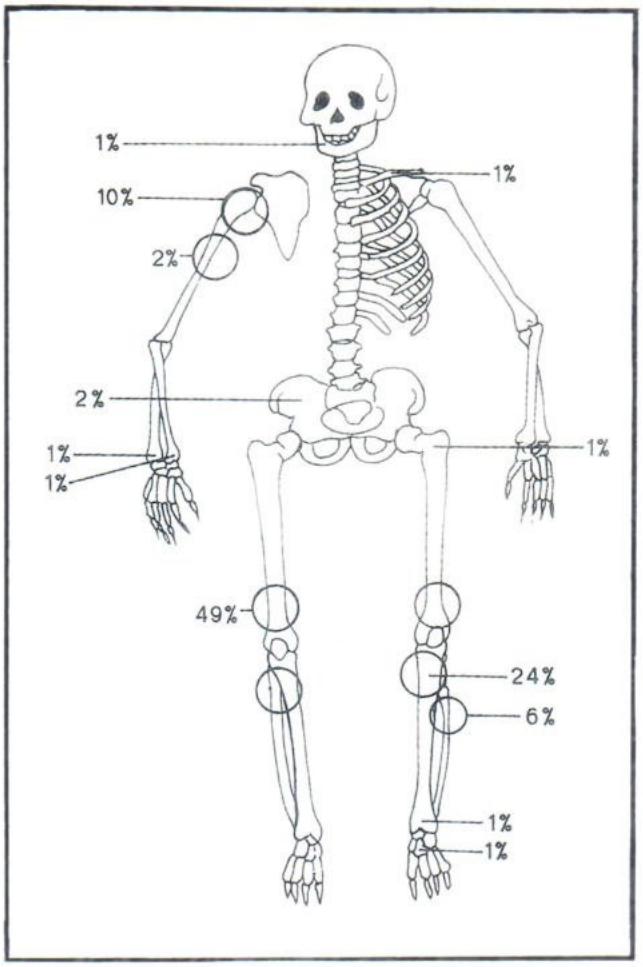

Fig. 3 Location of the primary lesion.

REFERENCES

1. Pongkripetch M, Sirikulchayanonta V. Analysis of bone tumors in Ramathibodi Hospital, Thailand during 1977-1986: study of 652 cases. J Med Assoc Thai 1989; 72: 621-8.
2. Ramathibodi Cancer Registry. Annual report 1992: Faculty of Medicine, Ramathibodi Hospital, Mahidol University.
3. Ramathibodi Cancer Registry. Anual report 1993: Faculty of Medicine, Ramathibodi Hospital, Mahidol University.
4. Pochanugool L, Nontasul S, Subhadharaphandou T et al. Multidisciplinary "Limb salvage" treatment of osteosarcoma. J Med Assoc Thai 1991; 74: 404-11.
5. Jaffe N, Frei E III, Traggis D, Bishop Y. Adjuvant methotrexate and citrovarum factor treatment of osteogenic sarcoma. N Engl J Med 1974; 291: 994-7.
6. Jaffe N. Advances in the management of malignant bone tumors in children and adolescents. Ped Clin North Amer 1985; 32: 801-10.
7. Goorin AM, Abelson HT, Frei III E. Osteosarcoma: Fifteen Years later. N Engl J Med 1985; 313: 1637-42.

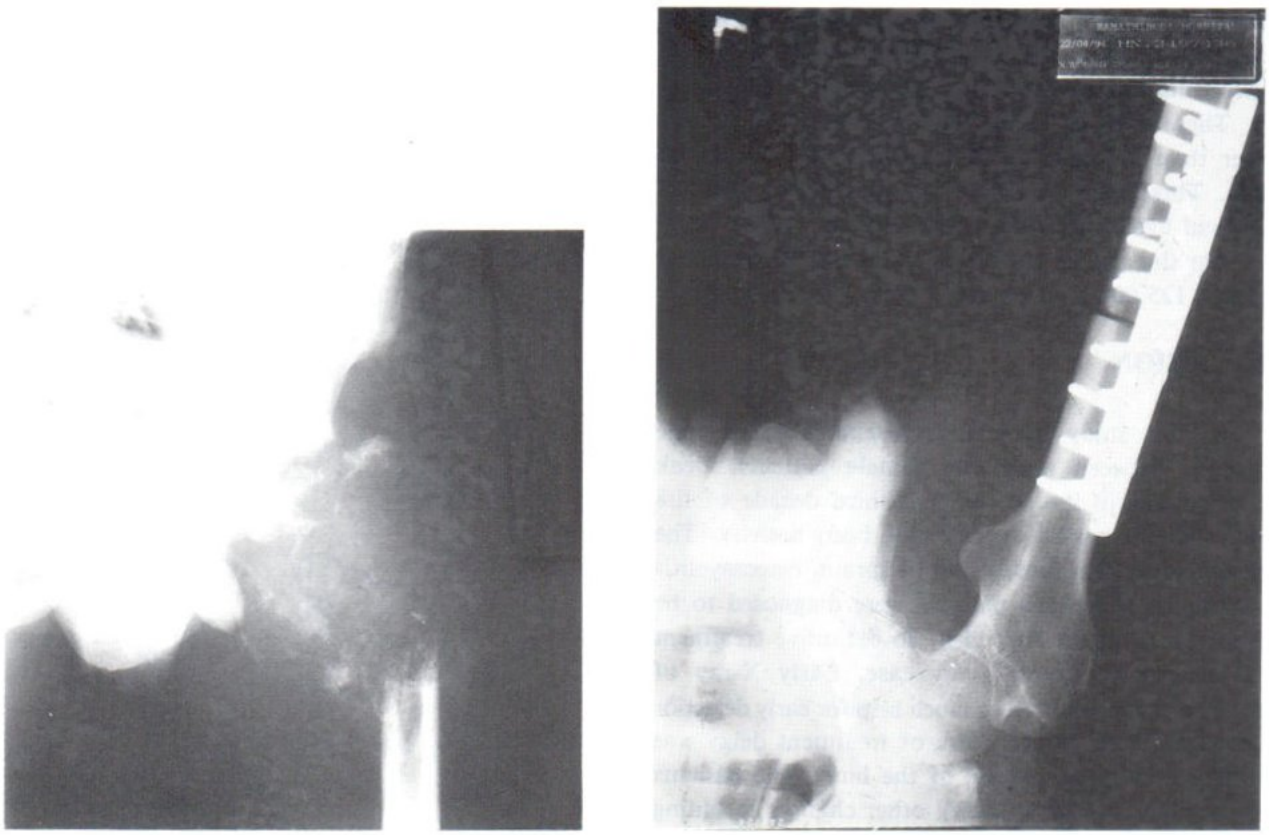

Fig. 4A,B Plain film of a patient with upper femur lesion, he was undergone preoperative chemotherapy with limb salvage surgery.

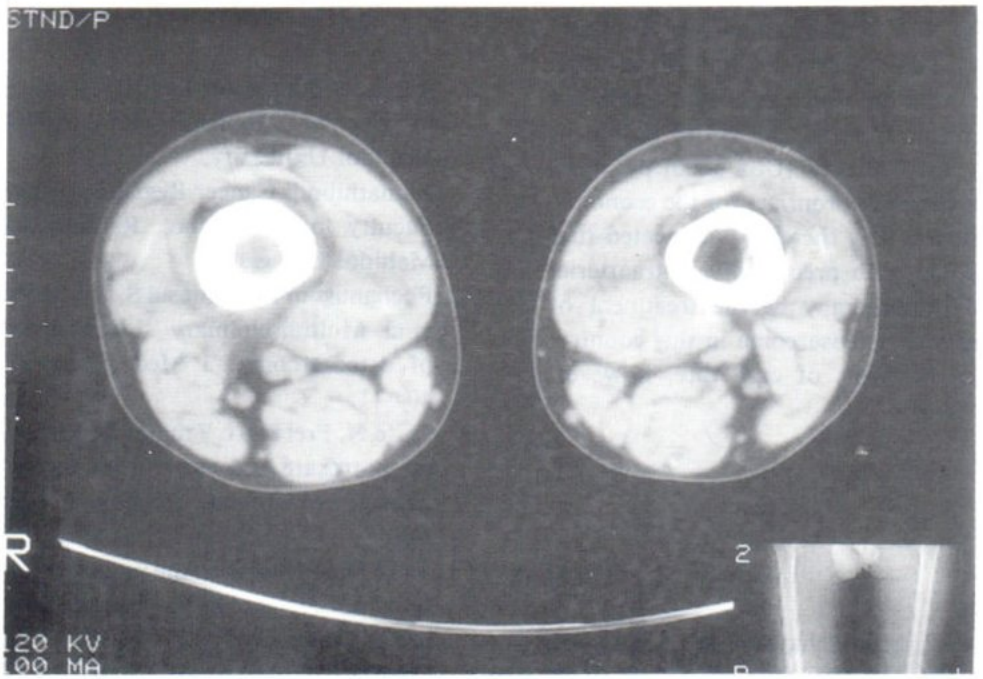

Fig. 5 Computer tomography of the bone showed intramedullary extension, in some patient the extension was 13-19 cms from the primary lesion.

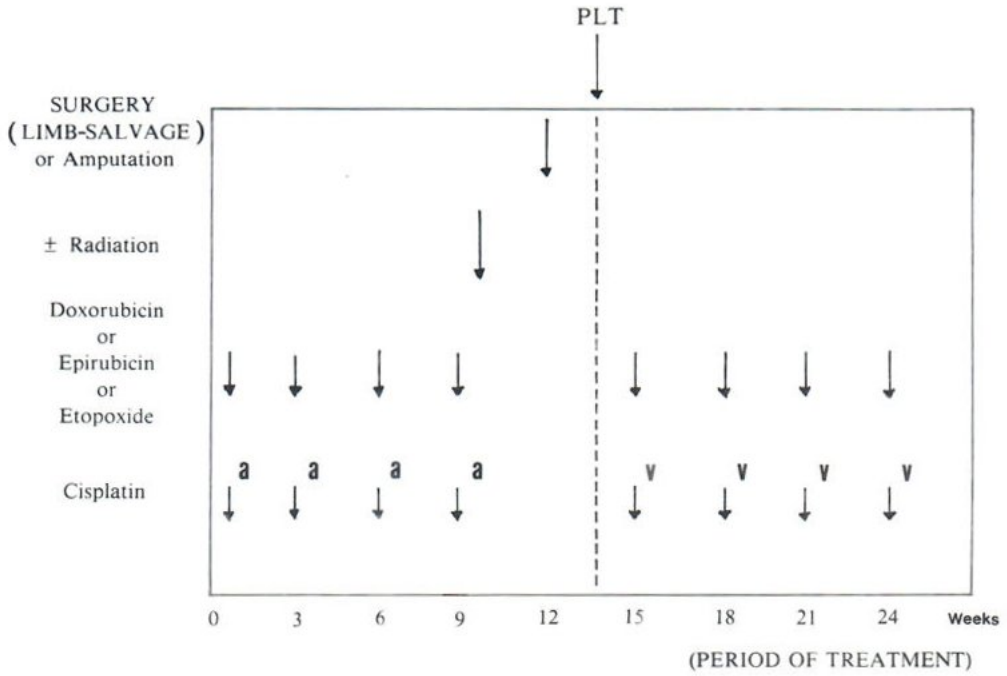

Fig. 6 Schedule of adjuvant treatment : PLI = prophylactic lung irradiation.

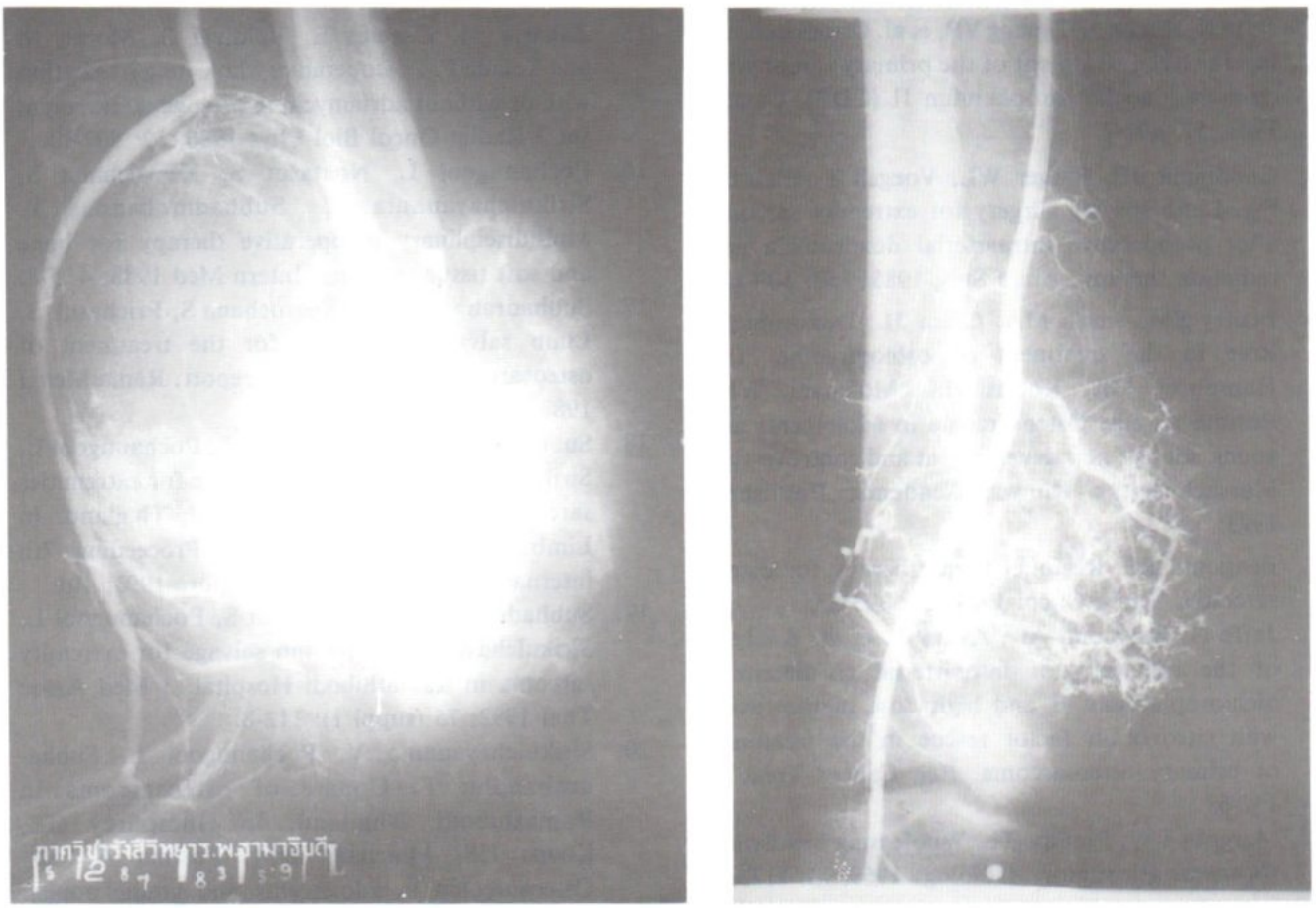

Fig. 7A,B Intraarterial cisplatin after femoral angiography.

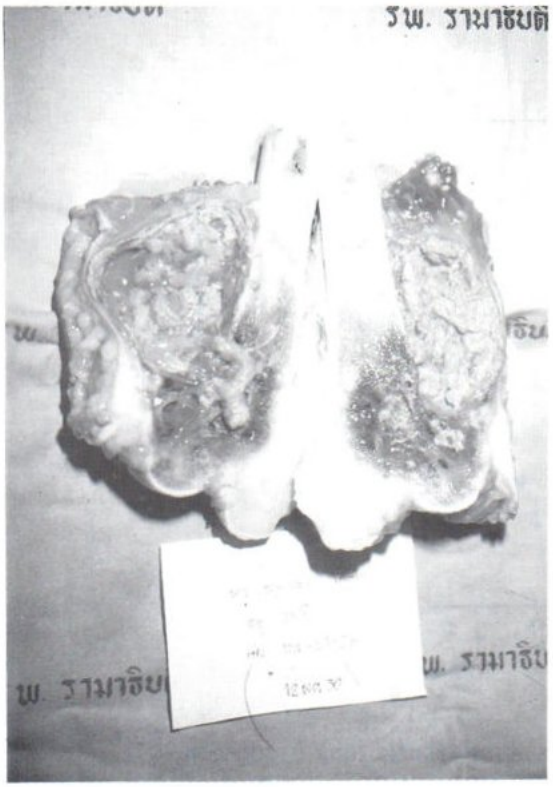

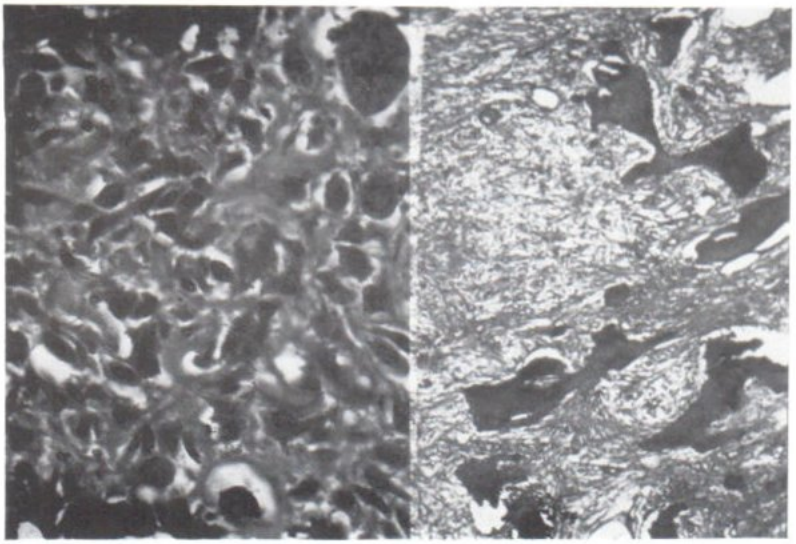

Fig. 8A,B Surgical specimen with 100% tumor necrosis in a female patient of 29 years old.

8. Jaffe N, Knapp J, Chuang VP, et al. Osteosarcoma: Intra-arterial treatment of the primary tumor with cis-diammine-dichloroplatinum II (CDP). Cancer 1983; 51: 402-7.
9. Goodnight JE, Barger WL, Voegeli T, Blaisdell FA. Limb sparing surgery for extremity sarcoma after preoperative intraarterial doxorubicin and radiation therapy. Am J Surg 1985; 150: 109-13.
10. Blaney SM, Smith MA. Grem JL. Doxorubicin: Role in the treatment of osteosarcoma. In : Humphrey GR, Koops HS, Molenaar WM, Postma A, eds. Osteosarcoma in adolescents and young adults : new development and controversies. Massachusetts : Kluwer Academic Publishers 1993: 55-73.
11. Benjamin RS. Regional chemotherapy for osteosarcoma. Semin Oncol 1989; 16: 323-27.
12. Jaffe N, Raymond AK, Ayala A. et al. Analysis of the efficiency of intraarterial cis-diammine dichloroplatinum II and high dose methotrexate with citrovorum factor rescue in the treatment of primary osteosarcoma. Reg Cancer Treat 2: 157-63.
13. Margolis LW, Phillips TL. Whole lung irradiation for metastatic tumor. Radiology 1969; 93: 1173-9.
14. Rubin P. The radiographic expression of radiotherapeutic injury. Semin Roentgenol 1974; 9: 5-13.
15. Zaharia M, Caceres E, Valdivia S, Moran M and Tejada F. Postoperative whole lung irradiation with or without adriamycin in osteogenic sarcoma. Int J Radiat Oncol Biol Phys 1986; 12: 907-10.
16. Pochanugool L, Nontasut S, Keorochana S, Sirikuichayananta V, Subhadhrabandhu T. Multidisciplinary preoperative therapy for bone and soft tissue sarcoma. Intern Med 1988; 4: 5-8.
17. Subhadrabandhu T, Kearochana S, Prichasuk S. Limb salvage procedure for the treatment of osteosarcoma : a preliminary report. Rama Med J 1988; 11: 104-10.
18. Subhadrabandhu T, Nontasut S, Pochanugool L, Sirikulchayananta V. Limb salvage for extremities sarcoma in Ramathibodi Hospital, Thailand. In Limb salvage, current trends. Proceeding 7th international symposium. Singapore 1993; 101.
19. Subhadrabandhu T, Nontasut S, Pochanugool L, Sirikulchayananta V. Limb salvage for extremity sarcoma in Ramathibodi Hospital. J Med Assoc Thai 1992; 75 (suppl 1): 112-8.
20. Sirikulchayananta V, Pochanugool L, Subhadrabandhu T. Update of osteosarcoma in Ramathibodi, Thailand. In Humphrey GB, Koops HS, Molenaar WM, Postma A, eds. Osteosarcoma in adolescents and young adults: new development and controversies. Massachusetts: Kluwer Academic Publishers 1993; 371-4.

RADIATION RESPONSE OF PULMONARY METASTATIC OSTEOSARCOMA

Lucksana POCHANUGOOL, Chirapha TANNANONTA,
Daungjai SANGTHAWAN, Suporn ONSANIT.

ABSTRACT

Pulmonary metastatic osteosarcoma still has fatal outcome in the Eastern country due to the low socioeconomic problem. Many of the patients cannot afford chemotherapy. Radiation treatment combined with chemotherapy has shown to be a very good response with some survivors. This study showed the benefit of the irradiation combined with chemotherapy over chemotherapy alone in 5 cases of pulmonary metastatic disease,the other 4 acted as a good adjuvant. Only one case, the lung nodule increased in size after radiation and chemotherapy but the pleural effusion has been controlled.

INTRODUCTION

The overall survival rate among patients with osteosarcoma has improved dramatically in the past decade partly due to the improved outcome of treatment of patients with pulmonary relapse. Gross metastatic disease in the lung was detected at diagnosis in 10-20 percent of all patients with osteosarcoma in the first presentation.[1] Eight percent of relapses occur in the lung alone and 90 percent of relapses occur within the first two years of initial diagnosis. During the past decade the universally poor 5 year survival rates, which range from 0 to 30%, have stimulated the active role to combat pulmonary spreading.[2] Treatment of pulmonary metastasis includes chemotherapy and aggressive resection of the tumor but very limited use of pulmonary irradiation. Whole lung irradiation has been used extensively in the treatment of pulmonary metastases from various malignant tumor, with an extremely radiosensitive nature such as Ewing's and Wilm's tumor.[3] In the cases of osteosarcoma, elective whole lung irradiation of 15 Gy in 12 days showed no significant differences in either survival or postponing the appearing of metastasis.[4] Therefore, pulmonary irradiation was not found to be of value as an adjuvant measure in the treatment of pulmonary metastatic osteosarcoma.

The purpose of this study was to emphasize the adjuvant role of radiation in controlling pulmonary metastasis and leading to increase chance for cure.

MATERIALS AND METHODS

Multidisciplinary preoperative therapy was a new approach of osteosarcoma in Faculty of Medicine, Ramathibodi Hospital. The treatment consisted of preoperative intraarterial infusion of cisplatin combined with intravenous chemotherapy, with or without local irradiation, surgery and prophylactic whole lung irradiation.[5-10]

From the total 125 cases of osteosarcoma, 10 cases of osteosarcoma with pulmonary metastases, admitted to Ramathibodi Hospital between March 1986 to March 1995, were treated with irradiation and chemo-therapy. All patients received 23.40-35.00 Gy (100-180 cGy daily, 5 fractions per week) to the affected whole lung with or without booster dose of 18-30 Gy at the pulmonary nodules. In the cases of bilateral lung disease, the worse lung was irradiated and the effectiveness of the adjuvant chemotherapy

Department of Radiology, Faculty of Medicine, Ramathibodi Hospital

was determined by the response of the other non irradiated lung. The criteria for selecting the lung for irradiation included number of nodules and size of the metastasis. The treatment were given by using two parallel opposing fields with Cobalt-60 teletherapy or from 6 MeV linear accelerator with mid line depth without lung inhomogeneity correction. All patients received additional cisplatin 100-120 mg/m^2 IV infusion during the irradiation treatment every 3 weeks combined with either doxorubicin, epirubicin, etoposide or bleomycin, cyclosphosphamide and dactinomycin, according to the whole group randomization.

There were 2 female and 2 male patients with unilateral lung disease. The other female and 5 males had bilateral metastases. (Table 1). The mean age of the patients was 17.03 ± 7.7 with the range of 4 to 29 years old. The main criteria for evaluating the effectiveness of adjuvant lung irradiation was the disappearance or reduction in size of the pulmonary nodule or pleural effusion.

RESULTS

Among 10 patients, one 26 years old female survives for more than 43 months after initial diagnosis of the disease and gave birth to a healthy baby girl weight 3015 gms. Her lung lesion disappeared with asymptomatic mild irradiation effect at her right middle lung field (Fig. 1-2). All other 8 patients showed very good radiation responses. All pulmonary nodules in the irradiated lung dissolved or disappeared in contrast with the controlled unirradiated lung. All but one of the patients with bilateral diseases, the lung nodules in the unirradiated lung increased in size even they were on chemotherapy (Fig. 3-5). One girl who still survived for more than 17 months now, had one calcified lung nodule which was proved to be negative on lung resection, but another nodule was positive and she was continued on chemotherapy.

Only one 16 years old boy had increased in size of the pulmonary nodule in the previous irradiated thoracotomized lung, but the pleural effusion was under controlled. He returned to school with a very good health, even his lung still had pulmonary nodule and he was continued on chemotherapy but the regimen was changed from cisplatin combined with epirubicin to ifosfamide added to cisplatin. The status of the

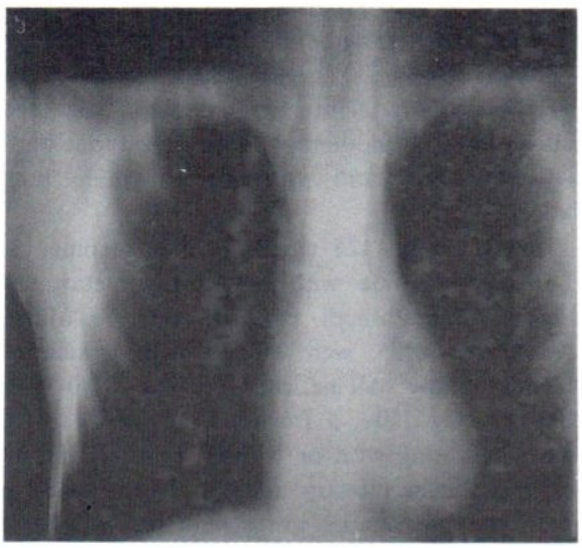

Fig 1 Tomogram of the chest showed nodular lesion in the right lower lobe, differentiated from the nipple shadow.

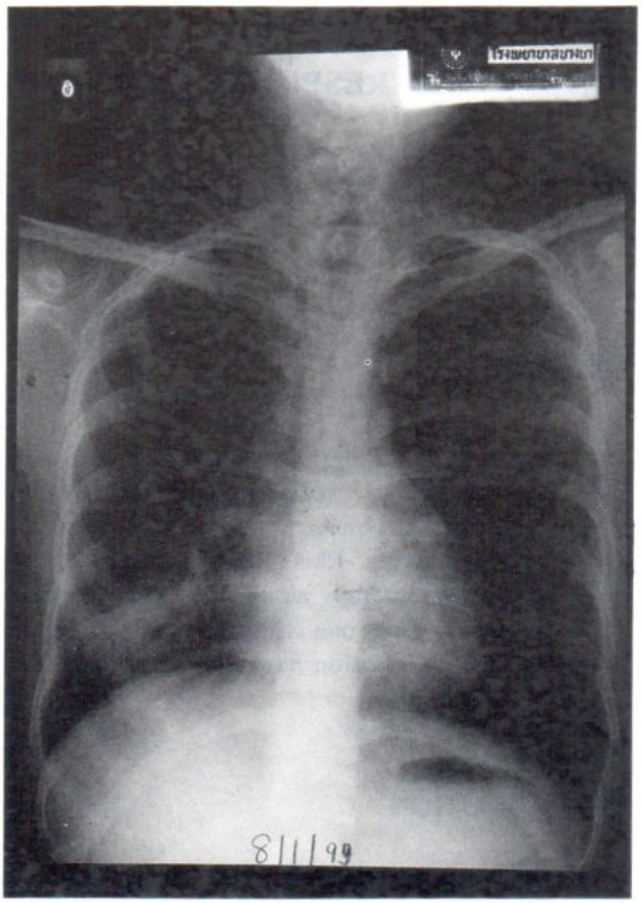

Fig 2 Plain film of the chest in the same patient after 4350 cGy local irradiation combined with chemotherapy. The nodule was disappeared with asymptomatic radiation infiltration.

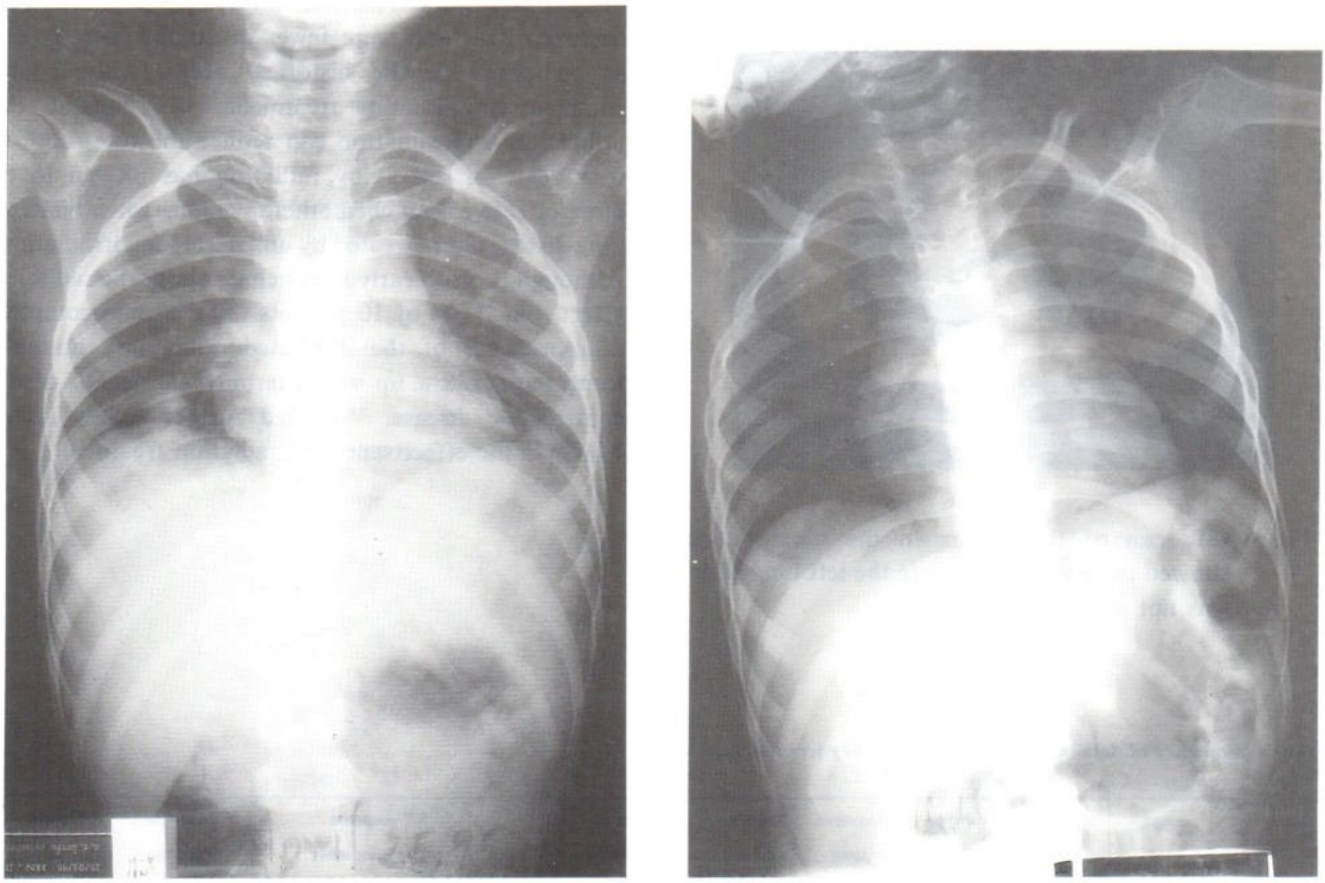

Fig 3-4 Plain film of the chest before and after irradiation of 2520 cGy at the right lung field combined with chemotherapy.

patients was shown in Table 2, among these 10 cases, 2 patients developed bony disease, one with bone and spinal cord lesion, another had stump recurrence.

DISCUSSION

Metastases which were detectable on the chest x-ray, have a diameter of at least 6-10 mm. and contain 10^8 or more tumor cells.[11] Experience has shown that these metastases can seldom, if ever, be completely destroyed by radiation even in a much higher dose. Apart from the specific radiosensitivity of the certain tumor, a chance of cure by radiation is also depended on the number of viable tumor cells. Observation and calculations by Breur and Abbatucci had shown that the radiosensitivity of osteosarcoma is sufficient to eradicate tumor nodule of 10^5 cells with a dose of 20 Gy over 10 days, that is, the maxinum dose which was tolerable for both lungs. So prophylactic lung irradiation may play important role to prevent lung metastasis.[11-15] In the cases of fullblown pulmonary metastasis, patients receiving chemotherapy combined with aggressive resection of the tumor survived for more than 41% in Western country.[1] but in Eastern country even in Thailand, there were no survivor left. Aggressive lung irradiation adjuncted with chemotherapy, may control pulmonary metastasis. From March 1986 to March 1995 a total of 125 cases of osteosarcoma were treated in Ramathibodi Hospital. There were 49 lung metastases in this study 39 cases had already terminated with other 5 still survived with disease. The rest of the patients were lost to follow up and suspected to be dead due to far advanced diseases. Only 2 patients were still survived without disease detectable 79^+ and 43^+ months after treatment. One was treated by chemotherapy alone, the other by combined chemotherapy and radiation. The other 9 cases were excluded in this study.

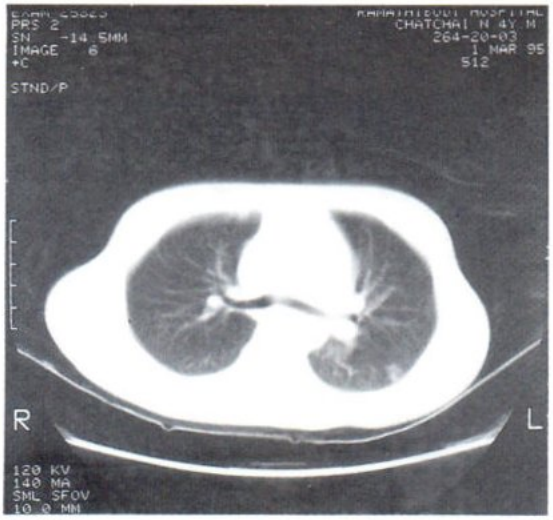

Fig 5 CT scan of the thorax in the same patient showed pulmonary nodule in the left lung which was not radiated.

Jaffe et al. suggested that pulmonary metastases in patients who received adjuvant chemotherapy occurred later and were fewer in number per patient as compared to the historical group without any comment on radiation treatment.[1] In Thailand, the utilization of irradiation can reduce the total cost of treatment. In this study, radiation has proven to be more effective than chemotherapy alone when bilateral lung diseases were treated by unilateral lung irradiation. Although it is too early to conclude about the radiation effect, but 9 out of 10 patients (90.0%) had complete disappearance of the irradiated pulmonary nodules. Long term follow up will determine the length of the controllable disease. We need further follow up to conclude the effectiveness of radiation treatment.

Table 1 Summary of data on 10 cases of pulmonary irradiation.

case	sex	age	site	subtype	Involved lung		chemo-therapy	dose of irradiation cGy		RT response of the lung mass			survival 1 mos	Course of disease
					Rt	Lt		1°	booster dose	disappeared	decreased	increased		
1	F	26	fibula	osteo-blastic	/		epi	2550	1800	X			43+	survive
2	F	14	fibula	chondro-blastic	/		VP-16	2550			X		17+	second bone
3	F	16	tibia	chondro-blastic	/	/	epi + BCD	3500		X			16	loss
4	M	17	femur	osteo-blastic		/	epi + BCD	2550	3000	X			15	bone, cord
5	M	14	tibia	fibroblastic	/	/	doxo	2550	-	X			12	loss
6	M	12	tibia	osteo-blastic	/	/	epi	2520	-	X			7+	jaw other lung progressed
7	M	29	femur	MFH variant	/	/	epi	2550		X			8+	stump recur other lung progressed
8	M	23	femur	osteo-blastic	/	/	epi	2340	-	X			5+	stab'e
9	M	4	femur	chondro-blastic	/	/	epi	2520	-	X			4+	other lung progressed
10	M	16	tibia	telangiec-tasis	/		epi	2520				X	3+	stable

Epi = epirubicin, doxo = doxorubicin, BCD = bleomycin – cyclophosphamide + dactinomycin.

Table 2 Status of the diseases

Metastasis	
bone	2
bone + cord	1
stump recur	1

REFERENCES

1. Goorin AM, Abelson HT, Frei III E. Osteosarcoma: Fifteen Years Later. N Eng J Med 1985; 313: 1637-42.
2. Price CHG, Jeffree GM. Metastatic spread of osteosarcoma. Br J Cancer 1973; 28: 515-23.
3. Margolis LW, Phillips TL. Whole lung irradiation for metastatic tumor. Radiology 1969; 93: 1173-9.
4. Rab GT, Ivins JC, Childs DS, Cupps RE Pritchard DJ. Elective whole lung irradiation in the treatment of osteogenic sarcoma. Cancer 1976; 38: 939-42.
5. Pochanugool L, Nontasut S, Subhadrabandhu T et al. Multidisciplinary "Limb salvage" treatment of osteosarcoma. J Med Assoc Thai 1991; 74: 404-11.
6. Pochanugool L, Nontasut S, Keorochana S, Sirikulchayananta V, Ratanatharathorn V, Subhadrabandhu T. Multidisciplinary pre-operative therapy for bone and soft tissue sarcoma. Intern Med 1988; 4: 5-8.
7. Subhadraphandhu T, Kearochana S, Prichasuk S. Limb salvage procedure for the treatment of osteosarcoma : a preliminary report. Rama Med J 1988; 11: 104-10.
8. Subhadrabandhu T, Nontasut S, Pochanugool L, Sirikulchayananta V. Limb salvage for extremities sarcoma in Ramathibodi Hospital, Thailand. In Limb salvage, current trends. Proceeding 7th international symposium. Singapore 1993: 101.
9. Sirikulchayananta V, Pochanugool L, Subhadrabandhu T. Update of osteosarcoma in Ramathibodi, Thailand In Humphrey GB, Koops HS, Molenaar WM, Postma A, eds. Osteosarcoma in adolescents and young adults : new developments and controversies. Massachusetts : Kluwer Academic Publishers 1993: 371-4.
10. Subhadrabandhu T, Nontasut S, Pochanugool L, Sirikulchayananta V. Limb salvage for extremity sarcoma in Ramathibodi Hospital. J Med Assoc Thai 1992; 75 (suppl 1): 112-8.
11. Burgers JMV, Van Glabberke M, Busson A, et al. Osteosarcoma of the limbs. Report of the EORTC SIOP 63 Trial 20781 Investigating the value of adjuvant treatment with chemotherapy and or prophylactic lung irradiation. Cancer 1988; 61: 1024-31.
12. Burgers JMV. Experience of the EORTC radiotherapy chemotherapy group in osteosarcoma trial. In : Humphrey GB, Koops HS, Molenaar WM, Postma A, eds. Osteosarcoma in adolescents and Young adults : new developments and controversies. Massachusetts : Kluwer Academic Publishers 1993: 173-5.
13. Breur K, Cohen P, Schweisguth O, Hart AMM. Irradiation of the lungs as an adjuvant therapy in the treatment of osteosarcoma of the limbs. An E.O.R.T.C. randomized study. Europ J Cancer 1978; 14: 461-71.
14. French bone tumor study group. Age and dose of chemotherapy as major prognostic factors in a trial of adjuvant therapy of osteosarcoma combining two alternating drug combinations and early prophylactic lung irradiation. Cancer 1988; 61: 1304-11.
15. Zaharia M, Caceres E, Valdiria S, Moran M, Tejada F. Postoperative whole lung irradiation with or without adriamycin in osteogenic sarcoma. Int J Radiat Oncol Biol Phys 1986; 12: 907-10.

ผู้นำเทคโนโลยีด้านเครื่องมือแพทย์

O.R.System

UROLOGY

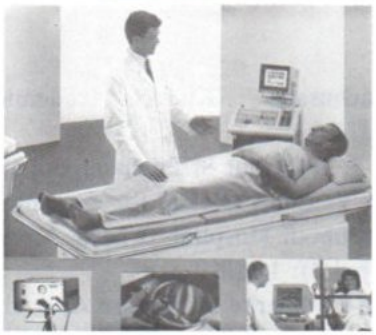

E E N T.

RADIOLOGY

O. P. D.

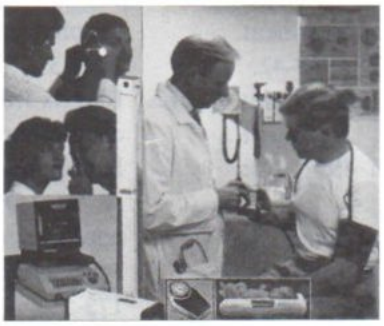

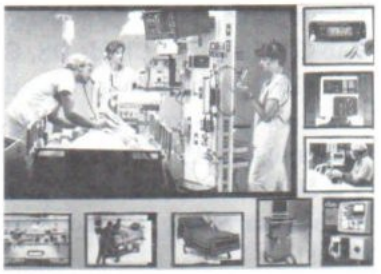

E . R .

I. C. U.

PERINATAL

supreme PRODUCTS CO.,LTD.

บริษัท สุพรีม โพรดักส์ จำกัด

163/81-82 PRAPINKLAO ROAD, BANGKOK 10700 THAILAND.

TEL.434-0040,434-0050 SERVICE DEPT.434-0060 FAX.433-3971

IRIDIUM-192 WAX MOULD THERAPY FOR THE TREATMENT OF SUPERFICIAL TUMOR OF THE FLOOR OF MOUTH.

PATTARANUTAPORN P.*
CHANSILPA Y.*
PANICHIVALAK A.**

ABSTRACT

Two cases of superficial tumor of the floor of mouth with T_{1-2} N_0 M_x lesions were treated with radiation therapy by surface mould technique. The brachytherpy source was HDR-Ir.[192] One case was treated with brachytherapy alone with a dose of 32.5 Gy in 5 weeks. One fraction of 6.5 Gy per week was given for 5 fractions in order to avoid a repeated course of external irradiation. This patient had received a previous treatment for laryngeal cancer 7 years ago by external radiation with a late radiation reaction of the skin in the neck region. The other patient was treated with 6.5 Gy per fraction, 2 fractions with 1 week interval, prior to 50 Gy of external irradiation in 5 weeks. The result were complete response without any complication. The technique was simple, reproducible and safe for the treatment of carcinoma of the floor of mouth and might be used for other tumors in the oral cavity.

INTRODUCTION

Brachytherapy is one of the two main methods of irradiation technique, performed by placing the radionuclide sources closed to or within the tumor. Its main advantage is the ablity to deliver a high dose at the tumor area without excessive irradiation to the surrounding structures. The tumor of skin, esophagus, nasopharynx and cervix are the major sites that can be treated by this procedure with various radionuclides such as Ra-226, Cs 137 and Co-60 by various methods of brachytherapy : Intracavitary insertion, Interstitial implantation and surface mould.[1-8] Among these techniques, mould therapy is the most proper for any superficial tumor that can be easily approached, such as skin, vulva, vaginal canal and oral cavity, and easy to make the negative mould that can be fitted to the anatomy of the treatment sites.

In this report, two patients with the superficial tumor of the floor of mouth were treated by mould therapy with two different ways for curative intent. The wax moulds were individually made. The procedure was evaluated. The result and complication were observed.

CASE REPORT

Case no. I

A 67 years old male patient developed a second primary cancer at the floor of mouth after 66 Gy of postoperative irradiation for laryngeal cancer 7 years ago. (figure 1) The pathological section was proved to be squamous cell carcinoma. Because of medical contra-indication for surgery, the patient was planned to be treated radically by irradiation. Because of the late sequelae of the skin and subcutaneous tissue from the previous radiation therapy in the neck region, brachytherapy was the main treatment for this patient.

The individual wax mould of lower jaw and floor of mouth was made for the stable fixation of the applicators. (Figure 2) The procedure for making mould is

1. The 0.5 cm thick wax was made by melting wax at 55°C and left it to be cool.
2. The wax was imprinted on the floor of mouth while it is cool but still soft.
3. Three grooves were done on the upper surface of the mould along the position of the lesion that was imprinted on the mould.

* Radiation Oncology Div., Dept. of Radiology Faculty of Medicine, Siriraj Hosp., Mahidol University.
** Radiotherapy Sec., Radiology Unit, Vajira Hospital.

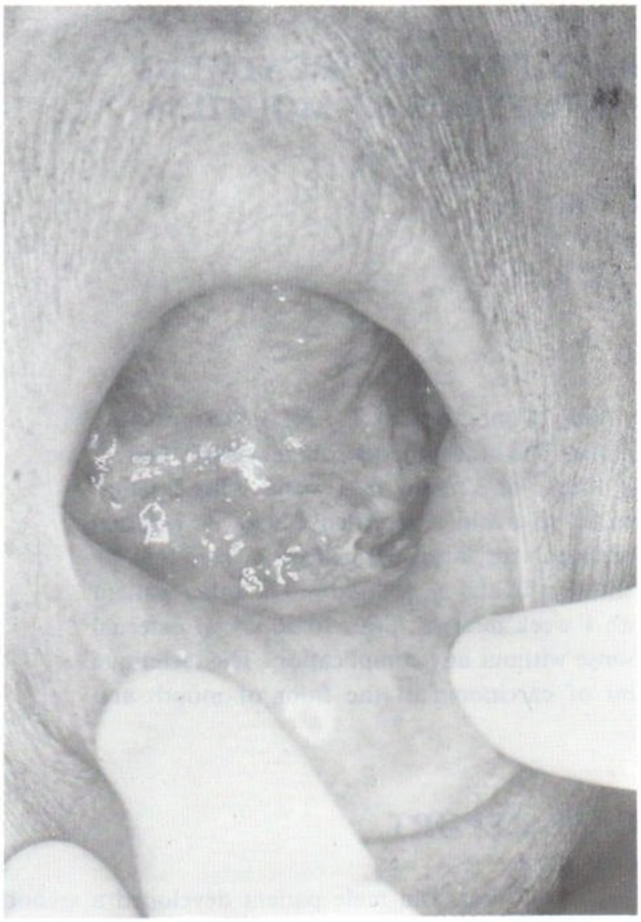

Fig. 1 The superficial ulcer at the floor of mouth.

4. Three plastic catheters were placed in the grooves and fixed by pouring the melted wax about 1 cm thick for seperation of the tongue and palate, and imprint the upper surface of mould by placing the mould in position.

5. Local anesthesia was given by xylocaine spray and the surgical clip was placed at the edge of the tumor. The wax mould was held in the mouth (Figure 3) and the simulation film was taken with the dummy in the catheters for treatment planing in order to locate the dwelling positions of the Ir-192 source (Figure 4).

The radiation dose of 6.5 Gy was prescribed at 1 cm beneath the mucosal surface and 1 cm around the tumor margin shown by surgical clip. Five fractions of mould therapy was given once a week for 5 weeks. With the TDF formula, the total tumor dose is equivalent to 5000 cGy of external radiation.[14]

Case no. II

A 52 years old male patient was diagnosed to be T_1 N_0 M_0 carcinoma of the floor of mouth. Because the lesion was bordered line T_1 or T_2, he was then treated as a T_2 lesion. The treatment was started with 2 times of mould therapy with the same technique and dosage as in the first patient to the primary lesion, and then after, the external irradiation of 50 Gy was given to the primary and the regional lymph nodes. The patient received 13 Gy by mould therapy and 50 Gy by external radiation to the primary tumour.

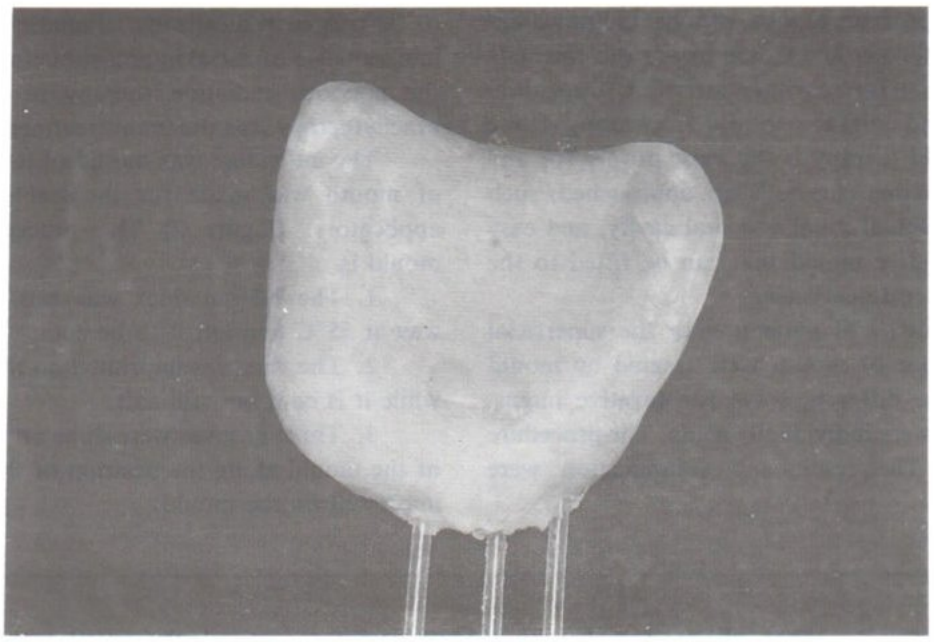

Fig. 2 The wax mould with three catheters.

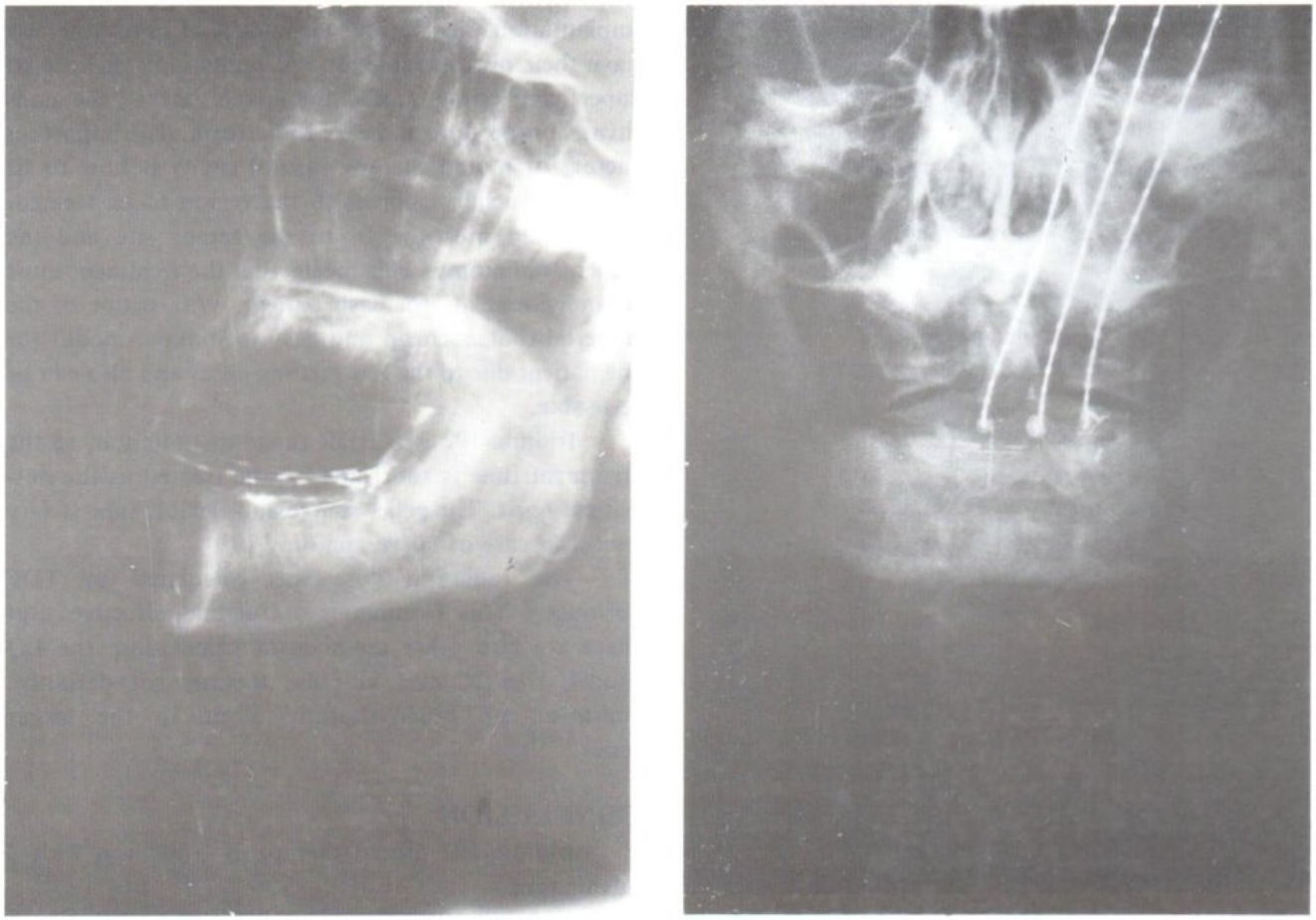

Fig. 4 The simulation films

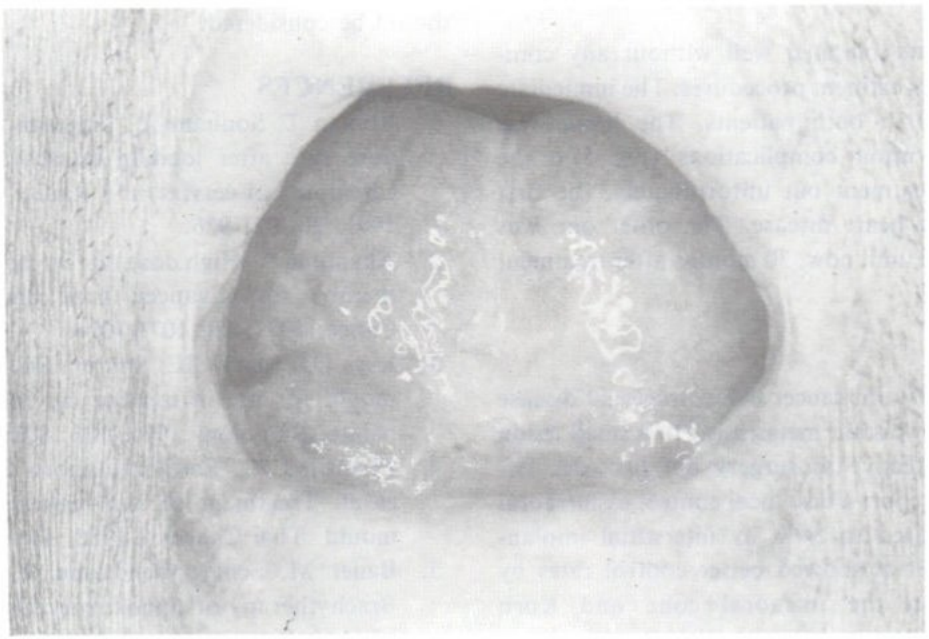

Fig. 5 After completion of treatment

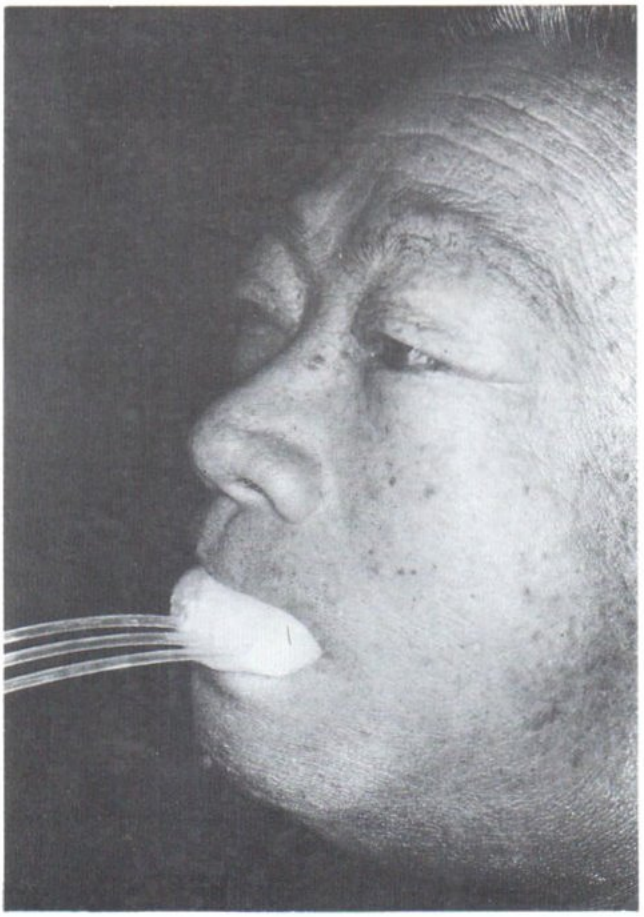

Fig. 3 The wax mould in position.

RESULT

The 2 patients tolerated well without any complication from the treatment procedures. The immediate results were good in both patients. The lesion was still well control without complications (Fig. 5) in the first year after treatment but unfortunately, the first patient died from heart disease. The other one was still well controlled until now, 30 months after treatment with no morbidity.

DISCUSSION

The nature of oral cancer is loco-regional disease with only 7-15% of distant metastasis.[9] In a small lesion, radiation is as effective as surgery but provides less morbidity. Wang report a best local control by intraoral cone, 86% compared to 54% by interstitial implantation.[10-11] Akine et al showed better control rates by implantation than the intraoral cone and Korb reported no difference between these two procedures.[12,13] There were a great number of patients with head and neck cancer treated by brachytherapy in Institut Gustave Rouss.[15] Two hundred and six patients with carcinoma of floor of mouth were treated by implantation. The various techniques of brachytherapy have their own advantages and limitations. In case of superficial lesion, mould therapy is one of the non-invasive procedure and easy to perform. The important factor for mould therapy in oral cavity is how to fit the radionuclides sources to the region to be treated. The mould must be fit to the tumor site and the patient's anatomy. This means that the treatment must be individualizd for each patient. Wax is one of the material that is cheap and easy to make a mould for the patient due to the low melting point and also can be re-usable.

Iridium-192 is a HDR range of radiation, so the treatment time is short and can be treated as the out-patient basis. The pellet source and flexible tube is very useful in case of curve anatomy.

The radiation dose was calculated by TDF formula.[14] This formula is useful and effective. But there are also other methods of calculation, the LQ model, that is used in pulse therapy for definitive radiation by brachytherapy alone in the larger lesion.[14,16-18]

CONCLUSION

Iridium-192 mould therapy is a method with 3 advantages.

1. It is easy to perform and reproducible.
2. It is safe for the personels and patients.
3. It can be used as a booster or main treatment in early stage of floor of mouth carcinoma

Further study for radiation dose and schedule should be considered.

REFERENCES

1. Roman T, Souhami L, Freeman CR, et al. High dose rate after loading intracavitary therapy in carcinoma of cervix. Int J Radiat Oncol Biol Phys 1991; 20: 921-926.
2. Akanuma A. High dose rate intracavitary radiation therapy for advanced head and neck tumors. Cancer 1977; 40: 1071-1076.
3. Keys DJ, Marks JE, Sharma SC. An Iridium-192 mould for use in treating carcinoma of the soft palate. Radiology 1979; 133: 802-803.
4. Chansilpa Y, Pattaranutaporn P, Attakorn P, et al. Treatment of skin cancer with Cobalt-60 mould. Thai Cancer J. 1988; 14: 68-73.
5. Bauer M, Schulz-Wendtland R, Fritz P, et al. Brachytherapy of tumor recurrences in the region of the pharynx and oral cavity by means of a remote-controlled after loading technique. B.J.R. 1987; 60: 477-480.

6. Karolis C, Reay-Young PS, Walsh, et al. Silicone plesiotherapy moulds. Int J Radiat Oncol Biol Phys 1983; 9: 569-573.
7. Joslin CAF, Liversage WE, Ramsey NW. High dose rate treatment moulds by after loading techniques. B.J.R. 1969; 42: 108-112.
8. Kitchen G, Dalton AE, Pope BP, et al. A surface applicator for basal cell carcinoma of the right pinna.: A case report. Activity Selectron Brachytherapy Journal 1991; 5: 140-141.
9. Merio OR, Lindberg RD, Fletcher GH. An analysis of distant metastasis from squamous cell carcinoma of the upper respiratory and digestive tract. Cancer 1977; 40: 145-151.
10. Wang CC. Radiotherapeutic Management and results of T_1 N_0, T_2 N_0 carcinoma of the oral tongue : Evaluation of boost technique. Int J Radiat Oncol Biol Phys 1989; 17: 287-291.
11. Wang CC. How essential is interstitial radiation therapy to the curability of head and neck cancer. J Radiat Oncol Biol Phys 1990; 18: 1529-1530.
12. Akine Y, Tokita N, Ogino T, et al. Stage 1-11 carcinoma of the anterior two-thirds of the tongue treated with different modalities : A retrospective analysis of 244 patients. Radiotherapy & Oncology 1991; 21: 24-28.
13. Korb LJ, Spaulding CA, Constable WC. The role of definitive radiation therapy in squamous cell carcinoma of the oral tongue. Cancer 1991; 67: 2733-2737.
14. Orton CG, F Ellis. A simplication in the used of the NSD concept in practical radiotherapy. B.J.R. 1973; 46: 529-537.
15. Gerbaulet A, Haie-Meder C, Marsiglia H, et al. Role of Brachytherapy in Head & Neck cancer : Institut Gustave-Roussy Experience with 1140 Patients. in : Brachytherapy from Radium to optimization. Mould RF (ed) Veenman Drukkers, Wageningen, the Netherlands. 1994: 101-120.
16. Fowler JF. The linear-quadratic formula and progress in fractionated radiotherapy. A review. B.J.R. 1989; 62: 679-694.
17. Dale RG. The aplication of the linear-quadratic dose-effect equation to fractionated and protracted radiotherapy. B.J.R. 1985; 58: 515-528.
18. Barendson GW. Dose fractionation, dose rate and isoeffect relationships for normal tissue response. J Radiat Oncol Biol Phys 1982; 8: 1981-1987.

Our new laser imager reviews films before you do

The new 3M Model 969 HQ Laser Imager doesn't perform diagnoses. But it does review images before you see them. If the quality doesn't meet your preset requirements, it makes the necessary adjustments — automatically.

This revolutionary Automatic Image Quality Control System from 3M ensures that each film meets your expectations the first time, every time. It frees your staff from the time-consuming task of monitoring and adjusting the printing process. And it provides radiologists with the image quality and consistency they need to perform fast, accurate diagnoses.

The 3M Model 969 HQ Laser Imager is the first to offer Automatic Image Quality Control. But that shouldn't surprise anyone. After 20 years of industry leadership, the medical imaging world expects "firsts" from 3M.

For a more detailed review of the new 3M Model 969 HQ Laser Imager, call the 3M THAILAND LIMITED

3M THAILAND LIMITED

159 Sermmit Tower 12th Floor, Sukhumvit 21, Bangkok 10110
Tel: 2608577 (50 lines), 5790023 ext. 301
Fax: 2617535, 5614052

3M *Innovation*

In Touch with Tomorrow

TOSHIBA

GLOBAL IMAGING ■ MEDICAL SYSTEMS

Helical Scanner

Xvision

XVISION: IT'S POWERFUL. IT'S FLEXIBLE. IT'S SMALL. IT'S THE CT OF THE FUTURE.

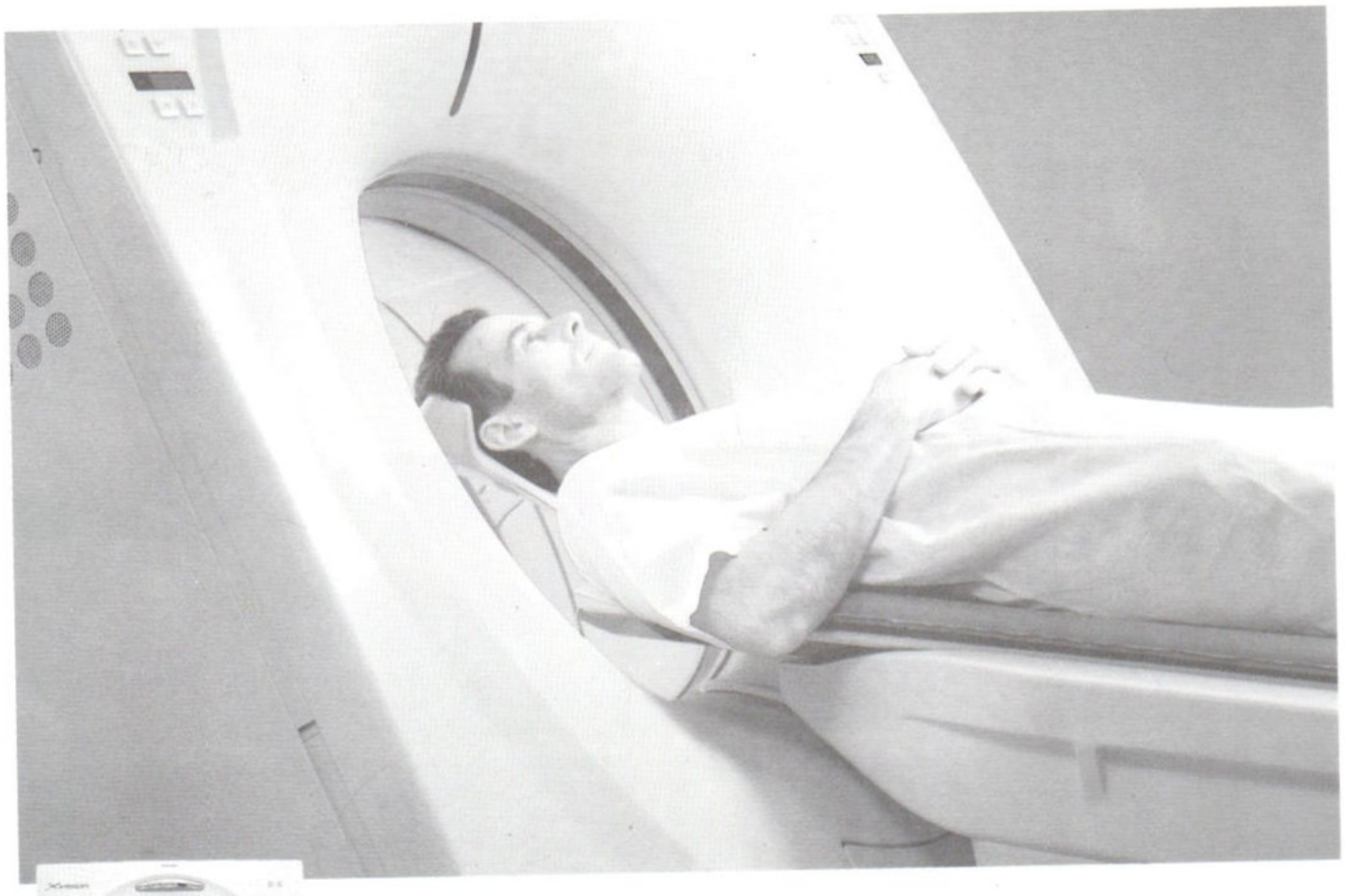

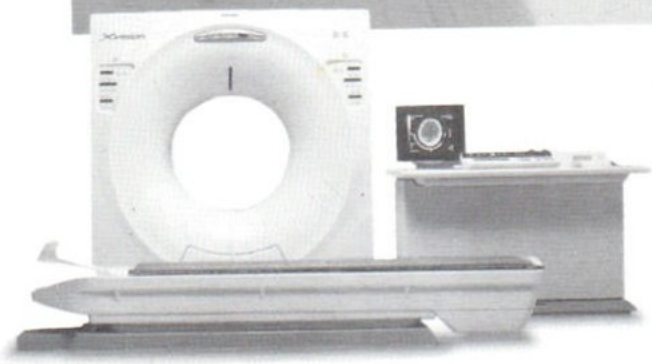

Toshiba introduces the Xvision, a highly compact, flexible, fast and efficient CT scanner that employs the unique Helical Scan™ system. This system makes it possible to complete a scan in a mere 1.5 seconds in routine examinations. Image quality is excellent, and speed, flexibility and efficiency are outstanding features of this scanner, so that high patient throughput can be achieved over a wide range of examinations.

CMC BIOTECH

CMC BIOTECH CO.,LTD.

1433 Soi 3/3 Muban Town-in-Town Ladphrao 94 Road, Bangkapi Bangkok 10310 Tel. 530-4995-6, 559-3261-2 Fax: (662) 539-6903

Southern Branch

306 Prachayindee Road, Khorhong Haadyai Songkhla 90110 Tel. (074) 356259, Handphone 01-9359703 Pagephone 151, 152 call 341790

North Eastern Branch

301/155 Muban Khon Kaen Villa, Mittrapab Road, Amphur Muang, Khon Kaen 40000 Tel. (043) 246210, 244729, Handphone 01-9283082 Pagephone 151, 152 call 341787